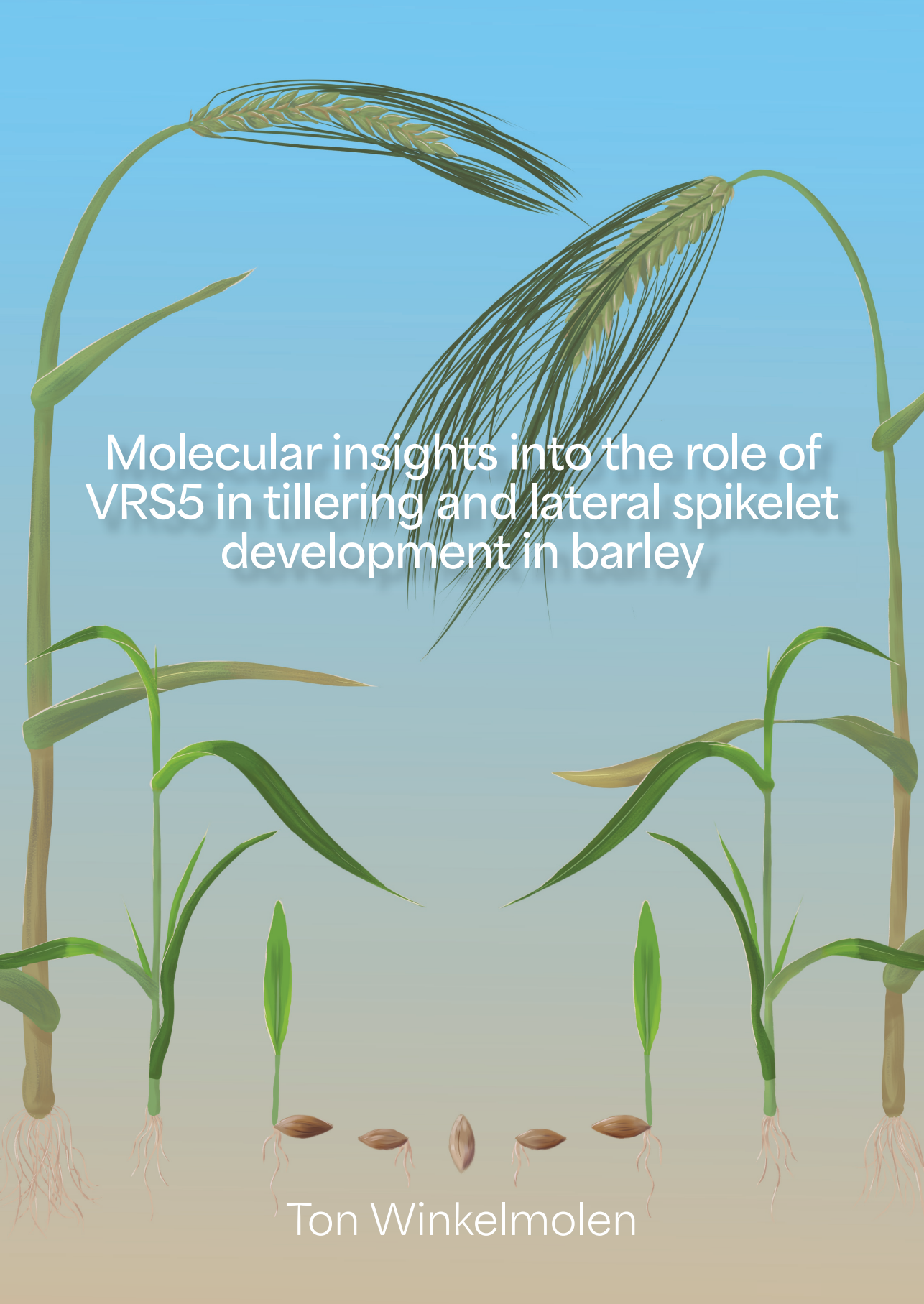


Molecular insights into the role of VRS5 in tillering and lateral spikelet development in barley

Ton Winkelmolen

Propositions

1. Recent technological advances make it possible to perform fundamental research directly on crops
   (this thesis)

2. There is more breeding potential in modification of cis-regulatory elements than in modification of protein coding sequences
   (this thesis)

3. Publishing a new reference genome without providing identifier mapping to previous versions is a violation of FAIR data principles

4. Conceptual understanding is essential to perform efficient research

5. The social media algorithms are causing a new form of pillarization

6. Sporting competitively helps in multiple ways to better cope with setbacks

Propositions belonging to the PhD Thesis, entitled

Molecular insights into the role of VRS5 in tillering and lateral spikelet development in barley

Ton Winkelmolen

Wageningen, 12 June 2026

Molecular insights into the role of VRS5 in tillering and lateral spikelet development in barley

Ton Winkelmolen

Thesis committee

Promotor
Prof. Dr Richard G.H. Immink
Professor in Cell and Developmental Biology
Wageningen University & Research

Co-promotor
Dr G. Wilma van Esse
Assistant Professor in Molecular Biology
Wageningen University & Research

Other members
Prof. Dr Dolf Weijers, Wageningen University & Research
Dr Laura Dixon, IPK Gatersleben, Germany
Dr Maike E. Stam, University of Amsterdam
Prof. Dr Mark G.M. Aarts, Wageningen University & Research

This research was conducted under the auspices of the Graduate School Experimental Plant Sciences

Molecular insights into the role of VRS5 in tillering and lateral spikelet development in barley

Ton Winkelmolen

Thesis
submitted in fulfilment of the requirements for the degree of doctor
at Wageningen University
by the authority of the Rector Magnificus,
Prof. Dr C. Kroeze,
in the presence of the
Thesis Committee appointed by the Academic Board
to be defended in public
on Friday 12 June 2026
at 3.30 p.m. in the Omnia Auditorium.

Ton Winkelmolen

Molecular insights into the role of VRS5 in tillering and lateral spikelet development in barley, 206 pages.

PhD Thesis, Wageningen University, Wageningen, the Netherlands (2026)
With references, with summary in English
https://doi.org/10.18174/681744

Contents

Chapter 1 **8**
General Introduction

Chapter 2 **26**
VULGARE ROW-TYPE SIX 5 binds to the promoter of tillering and floral homeotic genes to regulate their expression

Chapter 3 **66**
A novel VRS5 variant untangles pleiotropic effects on barley tillering and row-type

Chapter 4 **104**
SOC1-Like acts downstream of VRS1 and VRS5 in lateral spikelet development

Chapter 5 **130**
An Extension of the Golden Gate Toolkit for CRISPR-Cas9 Mutagenesis in Barley: Improved Cloning Efficiency, sgRNA design, and editing efficiency

Chapter 6 **148**
General Discussion

Reference List **162**

Appendices
Summary 194
Nederlandse Samenvatting 196
Acknowledgments 198
Education statement 202
About the author 204



Chapter

1

General introduction

Plants have developed a wide range of architectural adaptations during evolution in order to spread and survive in different environments. Plants are mostly indeterminate, as they have multiple growth axils with meristematic tissue. Whether these meristems grow, stay dormant or undergo fate changes, gives an infinite number of architectural options. Due to this indeterminate nature, plants were able to adapt to their habitat by changing meristem outgrowth or organ formation and patterning (Chomicki et al., 2017; Sussex & Kerk, 2001). Better adapted plants were able to survive environmental challenges and propagate. Through evolution different plant species gained specific architectural traits to survive their habitat (Joshi, 2023). To prevent against herbivory for example, some plants have adapted spines or thorns. In dry environments some plants developed waxy leaves to reduce water loss or deeper roots to reach water better. Some plants that are living in wet and swampy environments have special air tissue to provide gas exchange in submerged plant parts. As a consequence, plant architecture is immensely diverse across the plant kingdom. Variation in plant architecture did not only arise from evolutionary adaptation, but was also targeted during crop domestication. Perhaps one of the most famous examples of such adaptation is modern maize, which was domesticated from the wild ancestor teosinte about 9,000 years ago in what is now known as southern Mexico (Matsuoka et al., 2002; van Heerwaarden et al., 2011). The primary progenitor is *Zea mays* subspecies *parviglumis*, which shares the closest genetic relationship with modern maize (Iltis, 1983). The transformation from the progenitor to maize involved drastic changes in plant architecture, especially in the development of a non-shattering cob, larger, exposed kernels, and a reduced number of branches (J. Doebley, 2004; Matsuoka et al., 2002; R.-L. Wang et al., 1999). Also in other cereal crops like rice, wheat and barley, plant architectural traits were targeted during domestication (Meyer & Purugganan, 2013). In wild cereals, mature seeds naturally fall off to aid seed dispersal. Domesticated varieties carry loss-of-function mutations in *BRITTLE RACHIS 1 (BTR1)* and/or *BRITTLE RACHIS 2 (BTR2)*, causing the inflorescence and seeds to remain intact during ripening (Jin et al., 2008; Konishi et al., 2006; Lin et al., 2012; Pourkheirandish et al., 2015). This shift was a fundamental change in cereal domestication, especially for barley and wheat, allowing for more efficient harvest. Other traits that were targeted during the domestication of cereals include: photoperiod insensitivity and flowering time modulation (Faure et al., 2012; Turner et al., 2005); vernalization requirement (Saisho et al., 2011; Trevaskis et al., 2003); altered inflorescence architecture (Komatsuda et al., 2007; Ramsay et al., 2011), and changed branching patterns and synchrony (Meyer &

Purugganan, 2013). To date, these traits are still of key interest when breeding for yield optimization. However, yield is a complex trait that depends on different components such as the grain number and weight, grain size and number of tillers. These traits are interconnected; changing one often impacts the other, either directly or indirectly, which makes yield optimization difficult. Understanding how yield components are regulated genetically and molecularly can increase the efficiency and speed of breeding. Here, I will first describe cereal plant architecture in more detail, followed by how vegetative branching and inflorescence architecture are regulated.

Cereal plant architecture

During the vegetative phase of cereal development, leaves are initiated by the shoot apical meristem (SAM). When the meristem is still vegetative it is at the ground level with very little space between the internodes; a structure known as the crown. The SAM coordinates the formation of all above ground organs such as leaves, axillary meristems (AM), internodes, and eventually the inflorescence. In the axil of each leaf, typically a single AM is formed, which develops into a tiller bud. These buds can grow out into tillers (**Figure 1**). Each tiller resembles a miniature version of the main shoot, capable of producing its own leaves, AMs, stem, and inflorescence. The earliest tillers develop from the axils of the lower leaves, and subsequent tillers emerge. The AMs of primary tillers can also form new tillers, contributing to the overall branching architecture of the plant. This way, the number of tillers can grow rapidly during development. Therefore, the actual outgrowth of a tiller bud into a tiller is tightly regulated, which I will explain in more detail later in this chapter.

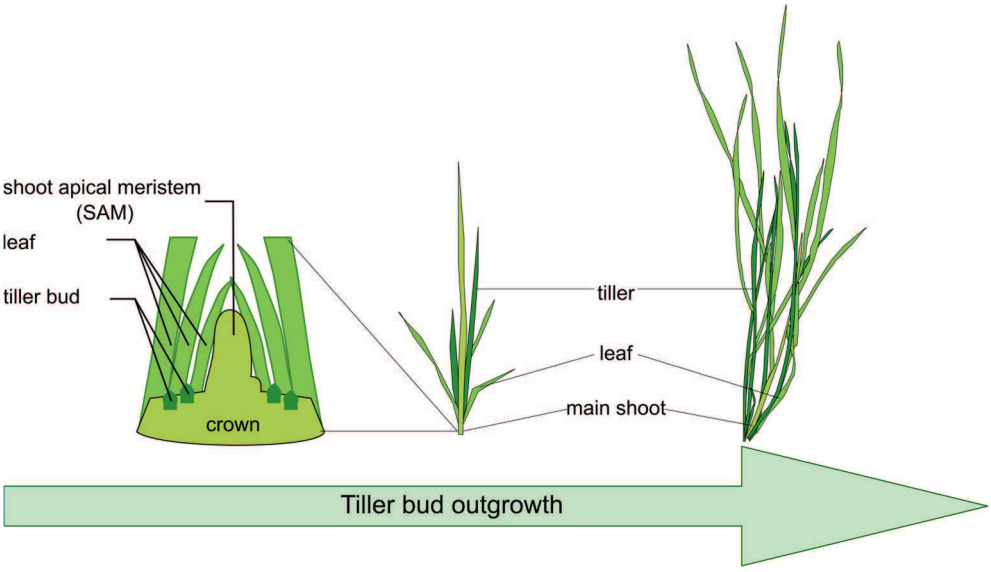


Figure 1: Tiller bud outgrowth in cereals. In the vegetative state, the shoot apical meristem (SAM) produces only leaves, with very little space between the internodes. In the leaf axils, axillary meristems are formed that develop into tiller buds. These buds can grow out into tillers, resulting in the overall branching phenotype of the plant.

As the plant matures, a developmental transition from the vegetative to the reproductive phase occurs. The SAM changes identity and becomes an inflorescence meristem (IM), initiating the formation of the inflorescence. From this point onwards, the IM starts moving upwards through the shoot, by elongation of internodes. The tiller buds that form within the leaf axils while the IM is moving upwards do not develop into tillers anymore, while already formed tiller buds at the crown can still develop into tillers (Miralles & Richards, 2000). Each tiller on a plant has its own apical meristem, meaning that each tiller has the potential to form an inflorescence. Differences in inflorescence architecture are controlled by the maintenance and determinacy of the meristems and primordia formed in time and place. Each meristem transition is tightly controlled, which means that at each transition, an altered regulation can have architectural effects. Thanks to this, there is a massive variation in inflorescence architecture within cereals (Koppolu & Schnurbusch, 2019; C. Wang et al., 2021; Y. Zhang, Shen, Shi, et al., 2024). In inflorescences like the rice panicle and maize tassel, branch meristems (BMs) are initiated from the IM (**Figure 2**). From the BMs, spikelet meristems (SMs) are initiated. Each SM can form one or multiple floret meristems (FMs), which, upon pollination, can eventually develop and form grains. In wheat and barley inflorescences, called spikes, no BMs are formed, but SMs initiate directly from the IM (**Figure 2**). For barley specifically, a triple spikelet meristem (TSM) is formed, containing three SMs: a central spikelet meristem (CSM) and two lateral spikelet meristems (LSM). These SMs each form one FM. In two-rowed barley, only the central spikelet develops into a fertile flower, whereas in six-rowed barley, all three spikelets develop into a fertile flower, producing a denser spike.

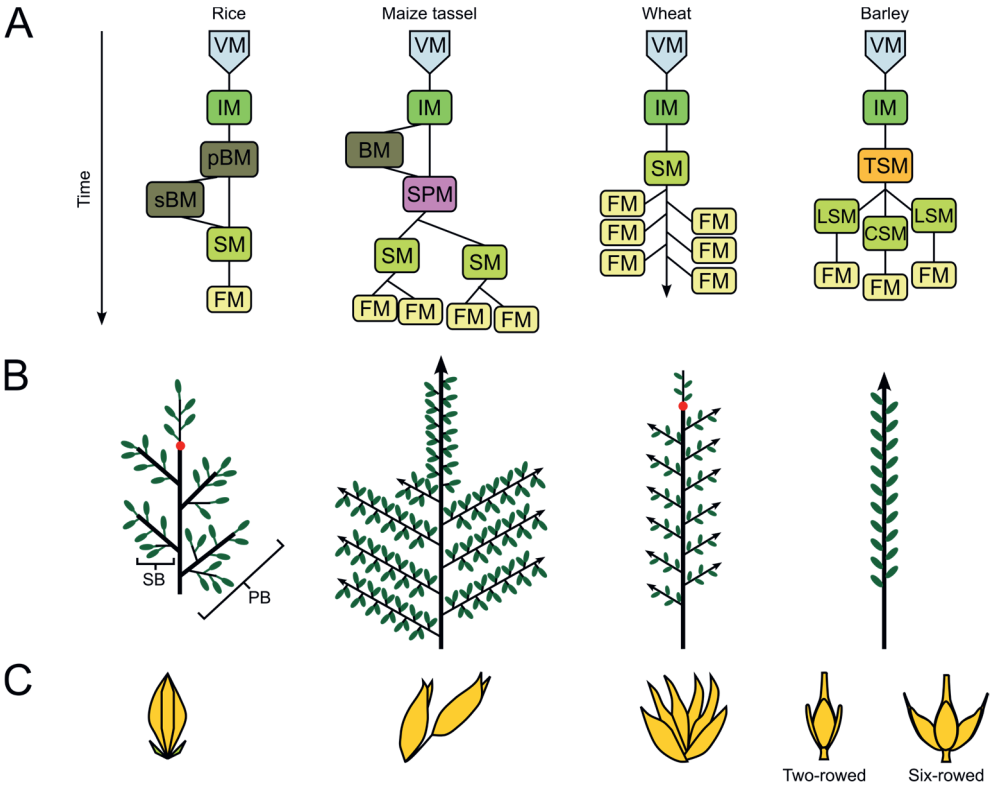


Figure 2: Cereal inflorescence architecture. A) Modular overview of cereal inflorescence development. During floral transition the vegetative meristem (VM) transitions into an inflorescence meristem (IM). Over time, floral meristems (FM) form along the IM. In the rice panicle and maize tassel branch meristems (BM) are formed, in rice creating both primary and secondary branch meristems (pBM, sBM). Along these, spikelet meristems (SM) and eventually FMs are formed. In the maize tassel along the BM, spikelet pair meristems (SPM) are formed consisting of two SMs, which each form two FMs. In wheat, the SMs are indeterminate, meaning they produce multiple FMs. In barley, a triple spikelet meristem (TSM) is formed, consisting of three SMs: one central spikelet meristem (CSM), and two lateral spikelet meristems (LSM). Each of these form a FM. B) Drawing of cereal inflorescences, with in rice the primary branches (PB) and secondary branches (SB). C) Drawing of rice spikelet, maize tassel spikelet pair, wheat spikelet, and barley spikelet triplet. In two-rowed barley cultivars only the central spikelet develops into a fertile flower. In six-rowed cultivars also the lateral spikelets develop into fertile flowers. *Figure is adapted from Koppulu & Schnurbusch, 2019.*

Genetic regulation of tiller bud formation

As described above, the number of tillers is determined by the frequency of leaf initiation and hence, of AMs between the formed leaves and their stem, and the subsequent bud development and outgrowth. There are multiple genetic loci studied that directly regulate AM initiation and tiller bud formation and thus directly limit tiller number, resulting in no or just a few tillers.

Known mutants in cereals that inhibit or abolish AM initiation are *cul2* in barley and *moc1* in rice (Babb & Muehlbauer, 2003; X. Li et al., 2003). In those plants, no tiller buds are formed in the leaf axils during plant development. In the *moc1* mutant in rice, no AMs are formed at all, whereas in *cul2* mutants, some meristematic tissue is formed in the leaf axils, but that does not develop into a bud. The underlying gene for the *cul2* mutants has not been characterized thus far. For *moc1*, the underlying gene belongs to the GRAS protein family, and is homologous to *Arabidopsis LATERAL SUPPRESSOR (LAS).* In the *las* mutant and the tomato *lateral suppressor (ls)* mutant, axillary meristem formation is abolished (Greb et al., 2003; Schumacher et al., 1999).

Some less severe phenotypes are observed in plants that only produce primary tillers, but no secondary tillers, due to the lack of formation of secondary tiller buds. The barley mutant *low number of tillers (lnt1)* shows a reduction in tillers caused by a mutation in the *JuBel2* gene, which translates into a protein that is part of the BELL-family of homeodomain transcription factors (Dabbert et al., 2010). *JuBel2* is homologous to *Arabidopsis BELLRINGER (BLR)*. *Absent lower laterals (als)* shows a similar phenotype to *lnt1,* but no underlying candidate gene has been characterized thus far (Dabbert et al., 2009). Another low tillering mutant in barley is *cul4*, of which the underlying gene transcribes a BTB-ankyrin protein (Tavakol et al., 2015). How these underlying genes inhibit AM initiation and thus tillering has not been shown thus far.

Regulation of tiller bud outgrowth

The next step in tiller development, assuming the axillary meristems are initiated and the bud is formed, is the actual outgrowth of the bud. This process is regulated on multiple levels by internal and external signals, making it a multifaceted complex trait. Examples of external factors influencing the outgrowth of tiller buds are light quality, nutrient availability, and drought (Bakht et al., 2000; Chaturvedi et al., 1981; Skinner & Simmons, 1993).

Phytohormonal regulation of tiller bud outgrowth

Internal perception and signaling of these external factors is usually orchestrated by phytohormones, which in turn can regulate tiller bud outgrowth (Y. Liu et al., 2011). Phytohormones are thus important internal signals and disruption on this level of regulation can lead to altered timing of bud outgrowth, a reduction, or an increase in the number of tillers, but usually not as severe as in the mutants described above. One of the phytohormones inhibiting axillary bud outgrowth is auxin. Auxin is produced in the shoot apex and the leaves, and is actively transported downwards by auxin efflux carriers (Zažímalová et al., 2010). Because of this so-called polar auxin transport, outgrowth of tillers is inhibited (Agusti & Greb, 2013). This phenomenon is called apical dominance and is conserved throughout many plant species (Beveridge et al., 2023). Although this response is not only regulated by auxin, but also strigolactones (SL) and sucrose (Beveridge et al., 2023; Cao et al., 2023; Nahas et al., 2024), the role of auxin is important. This is also the case in barley, where removal of the shoot apex resulted in more tillering, while injection of auxin inhibited this response. Furthermore, application of auxin inhibits tillering, while inhibiting the transport of auxin has the opposite effect (Leopold, 1949). That means that genetic modification of auxin synthesis, transport, and signaling also affects tillering. This can be seen in the barley *hnt1* and *htd* mutants, which were mapped to the same locus, and show an increased number of tillers, hypothesized to be caused by inhibition of polar auxin transport (Hua et al., 2020; Ye et al., 2019). Similarly, homologous genes in rice, *NARROW LEAF1 (NAL1)* and *PLANT ARCHITECTURE AND YIELD 1 (PAY1),* affect tillering, as *nal1* mutants show increased tillering and overexpression of *PAY1* shows decreased number of tillers (Qi et al., 2008; Zhao et al., 2015). If the bioactive form of auxin (IAA) is inactivated above-ground, which is the case in the gain-of-function mutant *tld1-D* in rice, the number of tillers is increased (S.-W. Zhang et al., 2009).

Other hormones can interact with this network by regulating auxin transport. This is the case for SL, which can regulate polar auxin transport by directly modulating the expression and localization of auxin efflux carriers, PINs, in the plasma membrane (Shinohara et al., 2013; J. Zhang et al., 2020). In line with this, mutations in SL biosynthesis genes in barley lead to an increase in tillering (H. Wang et al., 2018). Also, mutations in the SL receptor D14 give an increase in tiller number (Arite et al., 2009; Kelly et al., 2025). Upstream of SLs, Abscisic acid (ABA) can regulate SLs, as increased ABA accumulation inhibits SL biosynthesis (H. Wang et al., 2018).

Opposite to auxin, cytokinin can increase the bud outgrowth in barley (SHARIF & DALE, 1980). Normally, cytokinin levels are regulated, amongst others, by degrading cytokinin by cytokinin dehydrogenase (CKX). Mutations in *HvCKX1* cause an increased number of tillers, which is in line with an increased cytokinin accumulation (Holubová et al., 2018).

Indirect factors influencing tiller bud outgrowth

Next to phytohormones and transcription factors that directly regulate axillary branching, there are also genes known to indirectly play a role in the number of tillers a barley plant will produce. For example, genes that alter the plastochron, the time between the initiation of sequential leaf primordia, influence the number of tillers. *Many noded dwarf (mnd)* mutants show an altered plastochron with a highly increased number of leaves and tillers (Hibara et al., 2021; Mascher et al., 2014; Walla et al., 2020). Tiller bud outgrowth usually stops shortly after the floral transition, when shoot elongation begins and the floral meristem is pushed upwards in the plant (Miralles & Richards, 2000). Therefore, alleles altering the duration of the vegetative phase, and subsequently the timing of shoot elongation, influence the number of tillers a plant produces. That means that changes in the expression or function of *VRN1, VRN2, PPD-H1,* and *HvCEN,* regulating the duration of the vegetative phase, alter the number of tillers indirectly (Alqudah et al., 2016; Bi et al., 2019; Fernández-Calleja et al., 2021; Karsai et al., 2006).

TB1/BRC1: A key transcription factor in regulating axillary branching

An important regulator of axillary branching in many species is the class II TCP transcription factor BRC1 and its orthologs in dicots, and the similar gene *TB1* and its orthologs in monocots (J. Doebley et al., 1995; Gao et al., 2016; González-Grandío et al., 2013; Kebrom et al., 2006; Martín-Trillo et al., 2011; Ramsay et al., 2011; Takeda et al., 2003). *In Arabidopsis* and maize, it was shown that BRC1 and TB1 directly target ABA biosynthesis and signalling genes in the tiller buds in order to regulate tillering (Dong et al., 2019; Gonzalez-Grandio et al., 2017; van Es et al., 2024). Next to that, the *TB1* ortholog in rice regulates tillering through interaction with MADS57, and in that way regulates the expression of the SL receptor D14 (L. Chen et al., 2018; S. Guo et al., 2013). This shows that BRC1 and TB1 regulate tillering by regulating hormonal signals important for axillary bud outgrowth. Expression of *BRC1* and *TB1* orthologs is highly increased under shade (González-Grandío et al., 2013; Kebrom et al., 2006; Kumar et al., 2021; H. Wang et al., 2022). This makes it an important transcriptional player in the shade avoidance response, where apical dominance is increased under shading,

leading to repressed axillary branching. This mechanism is highly conserved as orthologs of BRC1 in dicots, like tomato (Martín-Trillo et al., 2011), and TB1 in monocots, like rice (Takeda et al., 2003), all regulate axillary branching and apical dominance. Also, the barley ortholog of *TB1, VRS5,* regulates tillering and its expression is increased under shade (Ramsay et al., 2011; H. Wang et al., 2022).

Overall, tillering can be altered by several internal and external signals, either directly or indirectly, making it a very complex trait. Understanding how it is regulated and what other factors are involved is thus crucial and valuable information for plant breeders.

Genetic regulation of inflorescence development

Each tiller on a plant has its own apical meristem, meaning that each tiller has the potential to form an inflorescence and thus can bear grains. Just like tillering, many processes regulate the development and architecture of the inflorescence.

The transition from a vegetative to an inflorescence meristem is a process that is conserved across plant species. This transition is determined by the competition of florigens and anti-florigens. FLOWERING LOCUS T (FT) activates this transition, while TERMINAL FLOWER1 (TFL1)/CENTRORADIALIS (CEN) represses it. After transition, TFL1/CEN maintains the IM identity, in a negative feedback loop with AP1/FUL and AP2 (Y. Zhang, Shen, Shi, et al., 2024). *tfl1* mutants flower thus early and terminate the inflorescence after just one or a few flowers (Shannon & Meeks-Wagner, 1991). In barley, mutation of the *TFL1* ortholog, *HvCEN,* also leads to early flowering, but the inflorescence stays indeterminate (Bi et al., 2019). Not only is the floral transition accelerated, but also the subsequent determination of the inflorescence is, leading to a shortened inflorescence with fewer spikelets (Bi et al., 2019). Mutations in an *AP2-like* gene in barley, *INTERMEDIUM-M*, result in a very short, terminal spike, caused by a lack of inflorescence meristem indeterminacy (Zhong et al., 2021). Also, in other cereals, mutations or overexpression of *FT/TFL1, AP1/FUL*, or *AP2* genes lead to changes in inflorescence size and determinacy (Chuck et al., 2008; Danilevskaya et al., 2010; Lee & An, 2012; C. Li et al., 2019; Nakagawa et al., 2002; Simons et al., 2006). As described before, changes in the timing of the floral transition not only have an influence on the inflorescence but also indirectly on the number of tillers a plant produces, showing that these traits are linked.

Regulation of barley spike development

During the development of the inflorescence, BMs and/or SMs are formed along the IM (**Figure 2**). In *Triticeae*, like wheat and barley, normally no BMs are formed, meaning that the inflorescence develops along one main axis (**Figure 2**). The formation of BMs in the barley spike is genetically inhibited, and changes in these regulators can therefore lead to a branched spike. Barley mutants that show a branched spike are the *compositum 1* (*com1)* and *compositum 2 (com2)* mutants (**Figure 3**). These mutants lose the SM identity for some SMs at the bottom of the spike, reverting them to IMs. COM1, also known as TEOSINTE BRANCHED2 (TB2), and BRANCHED AND INDETERMINATE SPIKELET 1 (BDI1), is a class II TCP transcription factor that promotes SM identity and therefore represses inflorescence branching (de Souza Moraes et al., 2022; Poursarebani et al., 2020; Y. Shang et al., 2020). COMPOSITUM2 (COM2) is an AP2-ERF transcription factor that has a conserved function in inhibiting spike branching in barley and wheat (Poursarebani et al., 2015). Also, in other grasses, this function is conserved and mutations cause a higher degree of inflorescence branching in maize, rice, and *Brachypodium* (Chuck et al., 2002; Derbyshire & Byrne, 2013; Komatsu et al., 2003). Genetically upstream of both *COM1* and *COM2* is *VULGARE ROW-TYPE SIX 4 (VRS4)* (Koppolu et al., 2013; Poursarebani et al., 2015). *Vrs4* mutants can form a BM instead of an SM.

Row-type

The barley inflorescence is normally indeterminate and unbranched, so the inflorescence develops along one main axis. Along that axis, triple spikelet meristems (TSM) are formed in a zigzag pattern. The TSM consists of three individual SMs, of which each SM can form one FM in a determinate way. Each triple spikelet meristem consists of one central spikelet and two lateral spikelets (**Figure 2, Figure 3**). Each spikelet has the potential to develop into a fertile floret and eventually into a grain. The development of the lateral spikelets differs, even between elite barley lines. This difference is the main architectural difference within the barley inflorescence and is called row-type. In two-rowed barley, the development of the lateral spikelets is repressed, so only the central spikelets develop into a grain, whereas in six-rowed barley, both the central and lateral spikelets develop into fertile florets and can form grains (**Figure 2, Figure 3**). The inhibition of lateral spikelet development is genetically regulated, and thus far, five *VULGARE ROW-TYPE SIX (VRS)* genes have been identified: *VRS1, VRS2, VRS3, VRS4, and VRS5*. Loss of function of one or more of these leads to the development of fertile lateral spikelets to differing extents. Thus far, *VRS1* is genetically the most downstream gene regulating lateral spikelet development,

and genetically under the control of the upstream regulators VRS3, VRS4, and VRS5 (van Esse et al., 2017)(**Figure 3**). Both VRS3 and VRS4 regulate the expression of *VRS1* and *VRS5* (Bull et al., 2017; van Esse et al., 2017). *VRS1, VRS3, VRS4*, and V*RS5* are thus part of the same genetic pathway, whereas *VRS2* is not.

VRS1 translates to a HOMEODOMAIN LEUCINE ZIPPER (HD-ZIP) transcription factor, and is highly expressed in the lateral spikelet primordia specifically during inflorescence development (Komatsuda et al., 2007). *VRS2* encodes a SHORT INTERNODES (SHI) transcription factor regulating hormonal patterning in the spike (Youssef, Eggert, et al., 2017). Compared to the other *VRS* genes, loss of function of *vrs2*, leads to a weaker phenotype: developed lateral spikelets, but mostly limited to the lower part of the spike (Youssef, Eggert, et al., 2017). VRS3 is a histone demethylase, so it is hypothesized to regulate lateral spikelet development indirectly by changing the chromatin state (Bull et al., 2017; van Esse et al., 2017). *VRS4* encodes a LOB domain transcription factor. Loss of function of *VRS4* leads to a six-rowed spike, but also gives rise to some additional spikelets caused by a loss of spikelet determinacy (Koppolu et al., 2013)(**Figure 3**).

VRS5 regulates lateral spikelet development and tiller bud outgrowth

VRS5, also known as *INTERMEDIUM-C*, is the ortholog of maize *TB1*, and homolog of *Arabidopsis BRC1*, both known for their crucial function in inhibiting axillary branching (J. Doebley et al., 1995; González-Grandío et al., 2013). Loss of function *vrs5* shows developed fertile lateral spikelets, but not awned; this is the so-called *intermedium* spike phenotype, which is between two-rowed and six-rowed (Ramsay et al., 2011). *VRS5* is thus not only important for regulating row-type, but also tillering (**Figure 4**). In line with this, *vrs5* mutants show, next to fertile lateral spikelets, also an increase in the number of tillers early in development (Liller et al., 2015; Ramsay et al., 2011; Zwirek et al., 2019).

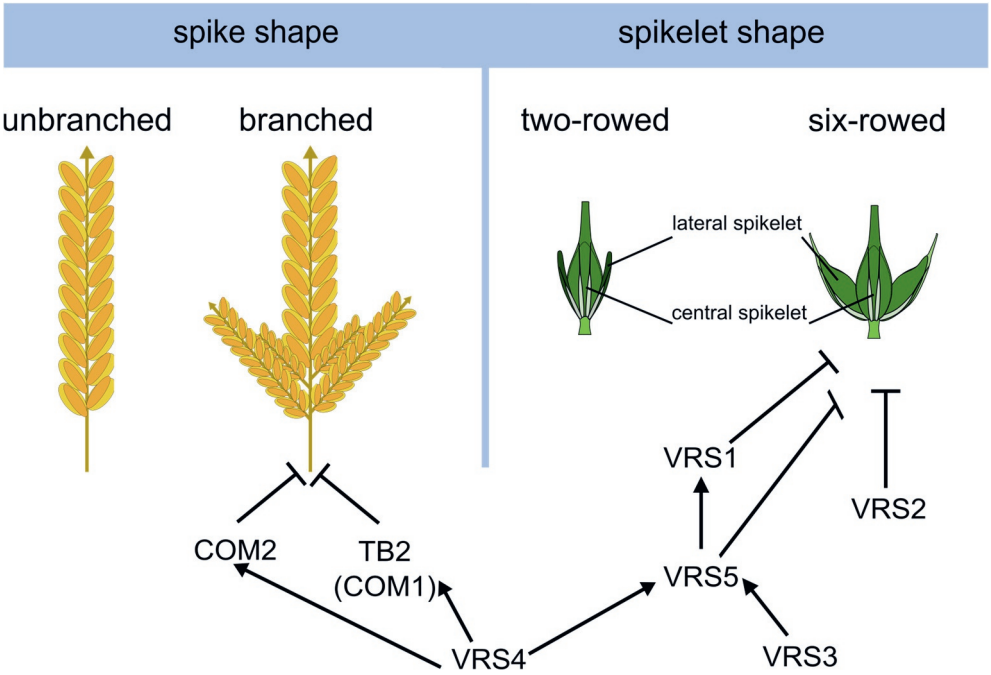


Figure 3: Regulatory network of barley spike architecture: Barley normally has an unbranched spike, mainly caused by COM2 and TB2 (COM1) that inhibit spike branching. Expression of *COM2* and *TB2* is regulated by VRS4. VRS4 is also part of the VRS network that regulates lateral spikelet development. Expression of *VRS5* and *VRS1* is reduced in *vrs4* and *vrs3* mutants, while in *vrs5* mutants, only the expression of *VRS1* is reduced. VRS2 inhibits lateral spikelet development as well, but its expression is not dependent on the other VRS genes.

Although the mutant phenotype of *vrs5* is characterized and some genetic interactions with VRS5 are known, it remains unclear how VRS5 functions at the molecular level. Previous studies in maize and *Arabidopsis* have identified direct downstream targets of TB1 and BRC1 in axillary buds, showing some conserved targets in ABA synthesis and signaling amongst others (Dong et al., 2019; Gonzalez-Grandio et al., 2017; van Es et al., 2024). This conservation might suggest similar direct targets for VRS5 in regulating axillary branching, but direct VRS5 targets in regulating lateral spikelet development are unknown. Next to that, it is known that TCP transcription factors can interact with other TCP transcription factors and bind DNA together (Viola et al., 2011). Also VRS5 can heterodimerize with other class II TCP transcription factors, including TB2 (de Souza Moraes et al., 2022). What the implications of VRS5 heterodimerization with other TCP transcription factors are, and if they can bind DNA as a heterodimer, remains to be investigated.

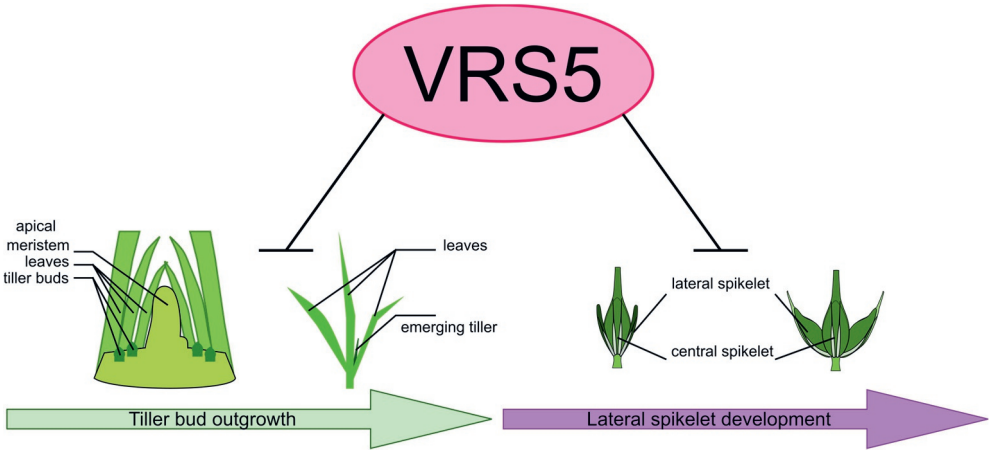


Figure 4: VRS5 regulates both tiller outgrowth and lateral spikelet development

Outline of this thesis

Understanding both tillering and lateral spikelet development on a molecular level is crucial to develop strategies to untangle these traits. Therefore, VRS5 is the gene of interest in this thesis as it is the key player in regulating both these traits (**Figure 4**). Using different strategies, I aim to provide molecular insights in the role of VRS5 on both tillering and lateral spikelet development.

As a transcription factor, VRS5 directly binds DNA and can regulate downstream targets. I hypothesize that during tillering and lateral spikelet development a different set of genes is targeted. Knowing these targets might give new candidate genes regulating tillering or lateral spikelet development. In **Chapter 2**, we aim to identify these direct downstream targets of VRS5. Using DNA affinity purification followed by sequencing (DAP-seq), the genome-wide binding sites of VRS5 are identified. Using RNA-seq of wild-type and *vrs5* mutants, genes differentially expressed by VRS5 in different developmental stages during tillering and inflorescence development are identified. Genes both bound by VRS5 and differentially expressed are classified as *bona fide* direct targets of VRS5.

We discovered that *VRS5* can produce two different transcripts, potentially resulting in two different protein isoforms. In **Chapter 3**, we wanted to know if these protein isoforms are functionally different. Using CRISPR, plant lines that can only form one of these isoforms are made that show phenotypical differences compared to full knockouts of *vrs5*. Furthermore, we aimed to understand the underlying molecular causes of the different isoform functions and hence, phenotypical differences. By looking at the interaction of the different VRS5 isoforms with another closely related TCP, TB2, and DNA, we found differences for the two isoforms in DNA binding as a heterodimer.

One of the found direct targets of VRS5 was *VRS1*, thus far the most downstream gene in the regulation of lateral spikelet development. Despite its crucial role in regulating lateral spikelet development, the molecular mode of action of VRS1 remains unclear. In **Chapter 4**, we aim to understand which genes are targeted by VRS1 in this regulation. We identified the direct downstream targets of VRS1 using a combination of DAP-seq and RNA-seq. Using CRISPR, we knocked out one of its targets, *SOC1-like*, and identified its role in lateral spikelet development. Next to that, we show that mutations in this target are selected during barley domestication.

Experiments in this thesis involved the creation of CRISPR mediated mutations. This can be a limiting factor during research because of low transformation and/or editing efficiencies. In **Chapter 5**, we show how we improved several aspects of CRISPR editing in barley using a combination of previously published methods, resulting in a highly increased editing efficiency.

In **Chapter 6**, I discuss the major findings and integrate them into the current state of the art in this field of science.



Chapter 2

VULGARE ROW-TYPE SIX 5 binds to the promoter of tillering and floral homeotic genes to regulate their expression

Ton Winkelmolen
Pierangela Colleoni
Matthew J. Moscou
Parastoo Hoseinzadeh
Klaus Oldach
Ralf-Christian Schmidt
Richard G. H. Immink
G. Wilma van Esse

Published in: *Plant Physiology* (2025): 198 (4), kiaf309
https://academic.oup.com/plphys/article/198/4/kiaf309/8204445

Abstract

Variation in shoot architecture, or tillering, is an important adaptive trait targeted during the domestication of crops. A well-known regulatory factor in shoot architecture is TEOSINTE BRANCHED 1 (TB1). TB1 and its orthologs have a conserved function in integrating environmental signals to regulate axillary branching, or tillering in cereals. The barley (*Hordeum vulgare*) ortholog of *TB1*, *VULGARE ROW-TYPE SIX 5* (*VRS5*), regulates tillering and is involved in regulating row-type by inhibiting lateral spikelet development. These discoveries predominantly come from genetic studies; however, how VRS5 regulates these processes on a molecular level remains largely unknown. By combining transcriptome analysis between the *vrs5* mutant and the wild type at different developmental stages and DAP-sequencing to locate the genome-wide DNA binding sites of VRS5, we identified bona fide targets of VRS5. We found that VRS5 targets abscisic acid- related genes, potentially to inhibit tillering in a conserved way. Later, in inflorescence development, VRS5 also targets row-type gene *VRS1* and several known floral development genes, such as MIKCc- type MADS-box genes. This study identifies several significant genes for mutational analysis, representing a selection of bona fide targets that will contribute to a deeper understanding of the VRS5 network and its role in shaping barley development.

Introduction

Variation in shoot architecture is one of the most important adaptive traits that have been targeted during crop domestication (J. F. Doebley et al., 2006). In cereals like barley and wheat (*Triticum aestivum*), the aboveground architecture is determined by the number of branches, called tillers, and inflorescence (spike) architecture (Dixon et al., 2022). Tillers are formed during vegetative growth of the shoot apical meristem, which produces successive leaves with (vegetative) axillary meristems (AM) in the leaf axil. The regulation of tillering usually happens after AM initiation, where the developing AM can enter a stage of dormancy as a bud (Hussien et al., 2014; Riaz et al., 2023; Q. Shang et al., 2021). The trigger to develop a bud into a tiller, or to remain dormant, depends on both internal and external cues (Dixon et al., 2022; Shaaf et al., 2019; H. Wang et al., 2018).

One of the key players that is involved in the control of bud outgrowth is TEOSINTE BRANCHED 1 (TB1). TB1 orthologs have been targeted during domestication for their impact on plant architecture and development (Clark et al., 2004; Martín-Trillo et al., 2011; R.-L. Wang et al., 1999). In maize (*Zea mais)* for example, increased expression of *ZmTB1* contributes to a complete suppression of the lateral tillers and increased crop yield (J. Doebley et al., 1995; A. Studer et al., 2011). TB1 is a member of the TEOSINTE BRANCHED 1/CINCINNATA/PROLIFERATING CELL FACTOR (TCP) family. TCP family members regulate gene expression through DNA binding and act as transcriptional regulators. Recent studies in maize indicate that at the molecular level TB1 directly regulates genes involved in hormone signaling, including abscisic acid (ABA), gibberellic acid (GA), and jasmonate (JA), and sugar signaling (Dong et al., 2019).

Besides its function in the control of tiller outgrowth, TB1 plays an additional role in orchestrating spike architecture in the *Triticeae*. In wheat, high levels of *TaTB-D1* result in reduced expression of meristem identity genes, thereby promoting paired spikelet formation (Dixon et al., 2018). In barley, the *TB1* ortholog, *VULGARE ROW-TYPE SIX 5* (*VRS5*), which is also known as *INTERMEDIUM-C* (*INT-C*), impacts not only tiller development, but also represses lateral spikelet development. When compared to wild-type lines, *vrs5 (int-c)* mutants exhibit an increased tiller number at early developmental stages and developed lateral florets of the triple spikelet meristem, leading to a six-rowed spike phenotype in contrast to a two-rowed spike in wild-type barley (Liller et al., 2015; Ramsay et al., 2011; Zwirek et al., 2019). In two-rowed cultivars, the formation of lemma and carpel primordia stagnates in the lateral florets, making them infertile, which means the lateral florets do not form a grain. In contrast, carpel primordia are formed and fully developing in *vrs5* mutants, making them fertile, which means

the lateral florets do develop into grains (Zwirek et al., 2019). Taken together, functional VRS5 in two-rowed cultivars, prevents the formation of carpel primordia in the lateral spikelets. In line with the mode of action of VRS5 in tiller and lateral spikelet development, *VRS5* is expressed in the tiller buds and the lateral spikelet primordia of developing inflorescences (Thiel et al., 2021; H. Wang et al., 2022).

Despite the key role of VRS5 in orchestrating tillering and lateral spikelet development in barley, the molecular mode of action remains poorly understood. To gain a better understanding of the regulatory network by which VRS5 controls both tiller and inflorescence development, we have profiled transcriptional changes associated with altered development in the *vrs5* mutant. This comprehensive analysis enabled us to define the *vrs5*-related transcriptional changes over development. In combination with a genome-wide transcription factor (TF) binding site mapping using DNA affinity purification (DAP-seq), we identified *bona fide* VRS5 targets. Amongst these *bona fide* targets are floral homeotic and meristem identity genes. In addition, our transcriptional profiling combined with DAP-seq using VRS5 as bait, reveals an evolutionarily conserved and divergent role of VRS5 in the regulation of tiller and grain development. Taken together, this study shows a comprehensive view of the core molecular network downstream of VRS5 and provides candidate genes that can be exploited in the regulation of tillering and inflorescence architecture in cereals.

Results

VRS5 regulates both tillering and row-type

Previous mutant analysis revealed a role for *VRS5* in tillering and in determination of the row-type in the spikelet (Liller et al., 2015; Ramsay et al., 2011; H. Wang et al., 2022). Significant differences in tillering between *vrs5* and Bowman were observed already early in development (**Figure 1A-B, Figure S1A**), corroborating previous reports (Liller et al., 2015; Ramsay et al., 2011; H. Wang et al., 2022; Zwirek et al., 2019) . To identify genes regulated by **VRS5**, we performed a transcriptome analysis on shoot apexes of WT (*Bowman*) and ***vrs5*** (*int-c.5*) mutants at four distinct developmental stages. This approach enabled us to investigate the role of **VRS5** across early and later stages of development, including tiller bud outgrowth and inflorescence development. The vegetative apex (VA) and transition apex (TA), were sampled as two early developmental stages (**Figure 1B**). These samples include the entire crown, which comprises of the (vegetative) meristem and tiller buds. To identify differentially regulated genes early in spikelet and floral organ development we isolated RNA for transcriptome profiling from developing inflorescences at the triple mound (TM), and lemma and stamen primordia stage (LP/SP), respectively. At these stages, the central and lateral floret primordia are initiated, and the first floral organ primordia are formed (**Figure 1B, Figure S1B**).

From the generated transcriptomes, principal component analysis (PCA) of all expressed transcripts showed that developmental stage (PC1) and the genotype (PC2) contribute the most to the observed variation (**Figure S2**). To gain further insight into the differentially expressed genes between *vrs5* and Bowman, we compared the transcriptomes in two different ways, namely at each developmental stage specifically (VA, TA, TM, and LP/SP), and throughout development using a generalized linear model (GLM) taking all four stages into account (**Table S1**). When comparing differentially expressed transcripts (DETs) at each developmental stage, most DETs (1286) were found at TM, whereas at VA the least DETs (598) were found (**Figure 1C**). Comparing the overlap in DETs in the different stages revealed that 133 transcripts were different between *vrs5* and Bowman in all developmental stages (**Figure 1D**). Of the total amount of DETs found, the majority (~75%) was downregulated in *vrs5* compared to Bowman, indicating that VRS5 mainly acts as a transcriptional activator (**Figure 1**).

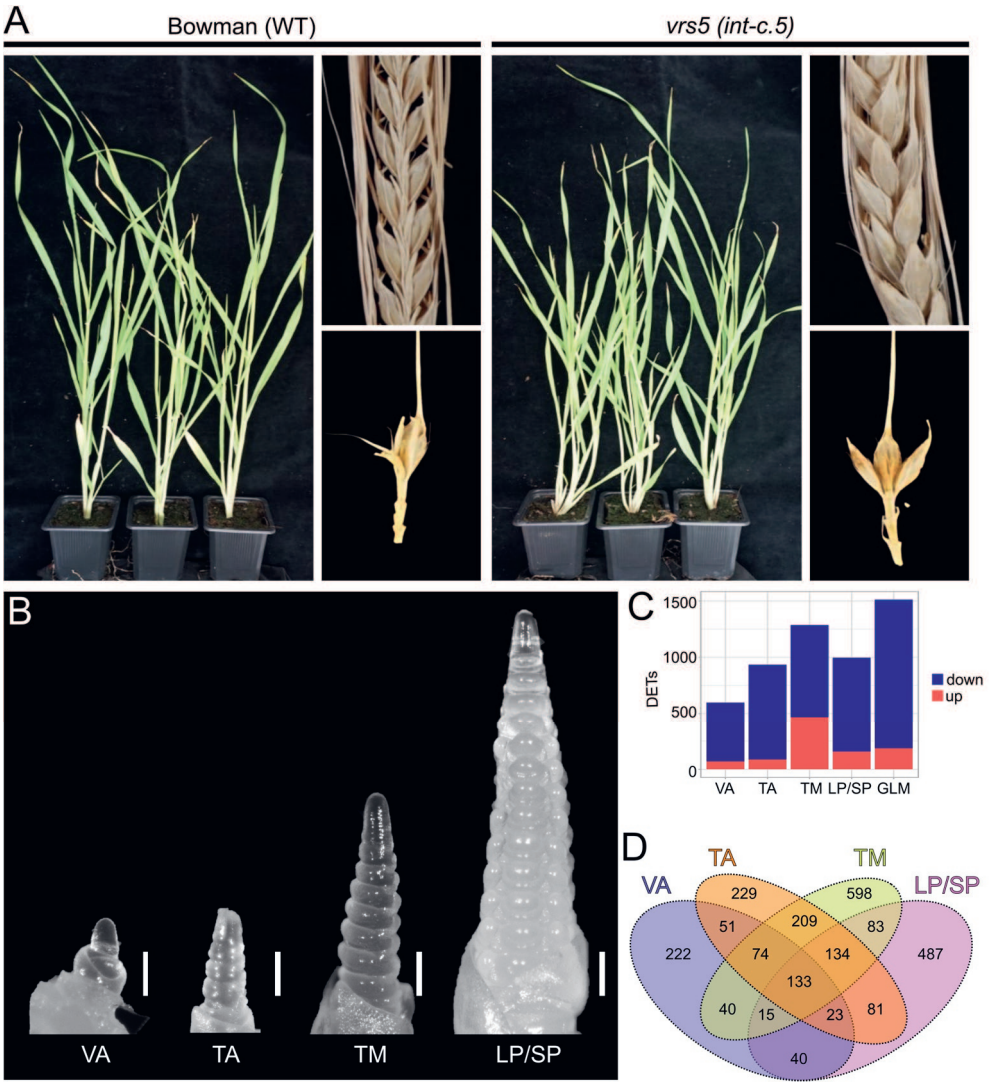


Figure 1: VRS5 regulates both tiller number and lateral spikelet development in barley. A) Four-week-old plants, dried spike and spikelet triplet of Wild type (WT) (Bowman) and *vrs5* (*int-c.5*) respectively. The lateral spikelets of WT have not developed, whereas the lateral spikelets of *vrs5* have developed into grains. B) Binocular images of developing inflorescence meristems representing the four stages used for transcriptome data, namely: vegetative apex (VA), transition apex (TA), triple mound (TM), and lemma and stamen primordia (LP/SP).Images were digitally extracted for comparison. The white bar represents a length of 200 µm. C) Bar graph showing number of differentially expressed transcripts (DETs) per developmental stage (VA, TA, TM, and LP/SP) and throughout development using a general linear model (GLM). The direction of differential expression in *vrs5* compared to Bowman is shown in blue (down) and red (up). For each developmental stage, three biological replicates were used. D) Venn-diagram showing overlap of DETs at different developmental stages (VA, TA, TM, and LP/SP).

Transcriptional profiling of genes differentially regulated in *vrs5*

To gain a deeper understanding of differential gene expression between the wild type and *vrs5* mutant over development, a co-expression clustering was performed using 2,872 DETs that were differentially regulated in one or more stages, or independent of development. This yielded 39 clusters, which were subdivided into three main groups based on their expression pattern (**Figure 2A, Figure S3, Table S2**): Group 1 represents genes that are highly expressed at VA and show a downward expression trend towards LP/SP stage; Group 2 represents genes that are lowly expressed at VA, and show an upward expression trend towards LP/SP stage; Group 3 represents genes that have a similar expression over the developmental stages (**Figure 2A**). Group 1 has clearly the most DETs, from which the majority, are in group 1A (1,776, ~62%), which consists of DETs that go down in expression over time and have lower expression in *vrs5* (**Figure 2A**).

To gain insight in the downstream processes VRS5 regulates during development, GO-term enrichment was performed on the expression groups. Genes that are highly expressed during VA (Group 1), and differentially regulated in *vrs5* when compared to wild-type lines are significantly enriched for GO-terms related to protein phosphorylation and phytohormone response and signaling (**Figure 2B**). DETs in group 1, annotated with these GO terms include several Jasmonate ZIM-domain containing proteins (JAZ), involved in jasmonic acid (JA) signaling: *JAZ11* (*HORVU.MOREX.r3.2HG0163880), TIFY10C (HORVU.MOREX.r3.5HG0480600), JAZ2 (HORVU.MOREX.r3.4HG0405240)*, and *JAZ6* (*HORVU.MOREX.r3.2HG0125430*), which are all downregulated in *vrs5* (**Figure 2C, Figure S4)**. Genes involved in abscisic acid (ABA) biosynthesis and signaling are also enriched in group 1, like *NCED1 (HORVU.MOREX.r3.5HG0508150)* a 9-cis-epoxycarotenoid dioxygenase (NCED) involved in ABA biosynthesis and *PYL5 (HORVU.MOREX.r3.4HG0383820),* an ABA receptor. Orthologs of these genes are also differentially expressed in maize *tb1* mutants compared to WT (Dong et al., 2019), suggesting a conserved regulation by the transcription factor proteins encoded by the orthologous genes *ZmTB1* and *VRS5*. Next to GO-terms involved in phytohormone signaling, GO-terms involved in stress response are highly enriched early in development.

Genes in group 2 are highly expressed at LP/SP stage when compared to VA and TA stages. GO-overrepresentation analysis of DETs between Bowman and *vrs5* lines showed that in this group genes that are involved in “regulation of meristem development”, “plant organ development”, and “cell differentiation” are

overrepresented (**Figure 2B**). This may reflect the subsequent development of lateral florets in *vrs5* in contrast to their repression in WT. In line with this, we also identified floral homeotic genes amongst the upregulated genes including *MADS4 (HORVU.MOREX.r3.1HG0065060)*, homologous to *Arabidopsis PISTILLATA*; and all identified E-class MIKCc MADS box genes in barley: *MADS1 (HORVU.MOREX.r3.4HG0396400)*, *MADS5 (HORVU.MOREX.r3.7HG0654930), MADS34 (HORVU.MOREX.r3.5HG0511250), MADS7 (HORVU.MOREX.r3.7HG0684020),* and *MADS8 (HORVU.MOREX.r3.5HG0494190)* **(Figure 2C, Figure S4)** (Kuijer et al., 2021). Also other MIKCc MADS box genes were differentially expressed in *vrs5*, including *AGL6 (HORVU.MOREX.r3.6HG0604360)*, orthologous to rice *MADS6,* and wheat *AGL6*, which is also upregulated in *vrs5* **(Figure 2C)** (Kuijer et al., 2021). In barley and wheat, *agl6* mutants are infertile due to defective pistils. Moreover, *TaAGL6* was shown to act upstream of several floral homeotic genes (Kong et al., 2022; Shen et al., 2024).

Our results show that VRS5 during early, tiller developmental stages, is targeting amongst others, phytohormone and stress signaling associated genes. In contrast, during inflorescence development mainly genes involved in meristem development and floral organ identity are differentially regulated in the absence of VRS5. Together, our results suggest that VRS5 regulates different genes and processes depending on the specific developmental stage.

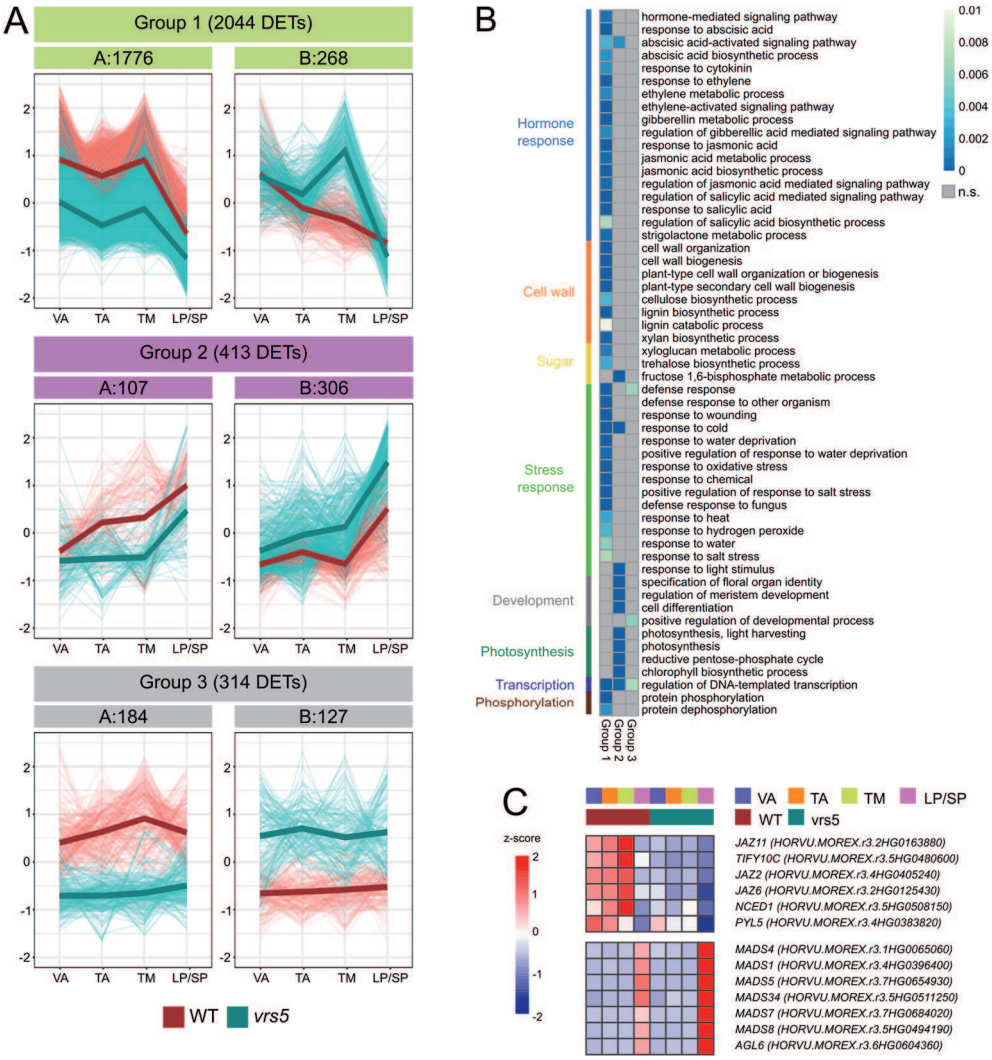


Figure 2: Transcriptional profiling of VRS5 shows changes in gene expression during development A) Line graphs of z-scores of differentially expressed transcripts (DETs) in three main co-expression cluster groups: group 1 showing a downward expression trend, group 2 showing an upward expression trend, and group 3 showing no differential expression throughout development. Lines are colored red for Wild type (WT) and cyan for vrs5. Each plot has the developmental stages used for RNA-seq on the x-axis: vegetative apex (VA), transition apex (TA), triple mound (TM), and lemma and stamen primordia (LP/SP). For each developmental stage, three biological replicates were used. The groups are divided in A (lower expression in vrs5 compared to WT), and B (higher expression in vrs5 compared to WT). B) Enriched GO-terms for Biological Processes per cluster group where the more blue means a lower p-value. A grey color means that the GO-term is not enriched in that cluster group ($p > 0.01$) or the number of DETs belonging to that GO-term are lower than three. C) Heatmap of z-scores of expression of a selection of DETs at each developmental stage: vegetative apex (VA), transition apex (TA), triple mound (TM), and lemma and stamen primordia (LP/SP), for Wild type (WT) and vrs5.

Genome wide identification of the *bona fide* VRS5 targets

The transcriptome profiling showed that there are differences in the differentially regulated genes between early, tillering, versus later inflorescence developmental stages. As a transcription factor, VRS5 is expected to regulate the expression of downstream target genes by directly binding to the (distal) promoter region of these genes. As key regulator, VRS5 may only bind to a limited number of downstream genes to trigger a wider transcriptional response. Alternatively, VRS5 may directly activate the majority of the genes identified as DET. To gain more insight into which genomic regions are bound by VRS5, and which of these are within a promoter region of a gene, we performed a DNA-affinity purification followed by genome wide sequencing (DAP-Seq) (Bartlett et al., 2017). To construct our DAP-Seq libraries, we used DNA isolated from barley developing inflorescences (Waddington stage ~4) . VRS5 fused to a FLAG-tag was used as bait, while GFP, which is expected not to bind DNA, fused to a FLAG-tag was used as negative control. Regions in the genome enriched for VRS5-binding compared to GFP are called peaks and considered genomic VRS5 binding sites. Only the peaks with an adjusted p-value smaller than 1^{-10} were kept, which resulted in 99,567 peaks **(Table S3).** The sequences of all the peaks were analyzed for de-novo enriched motifs. The most frequently abundant motif was GGGNCCCAC, found in 72% of the peaks **(Figure 3A).** This motif was distributed closely around the peak summit **(Figure 3B),** indicating the GGGNCCCAC motif is the primary DNA motif bound by VRS5. This motif resembles a consensus class II TCP-binding motif (GGGNCCAC), and the consensus binding motifs found for homologous TCP transcription factors in *Arabidopsis* and maize (Dong et al., 2019; Gonzalez-Grandio et al., 2017; Kosugi & Ohashi, 2002; van Es et al., 2024). This supports the association of identified peaks as likely genomic VRS5 binding sites.

To assign peaks to putative target genes, we selected a region of 15kb up and downstream of all predicted barley open reading frames. Within these genomic regions, we found 21% of all identified VRS5-DAP-seq peaks. The other peaks were located outside this region and classified therefore as “Distal intergenic”. Only a few binding sites, 0.1% of the total number of peaks, were identified in intronic regions (**Table S4**). To further understand where the peaks are located in the upstream and downstream region of the gene, we generated a frequency plot of all peaks that were found in genes that are expressed in at least one of the VA, TA, TM, or LP/SP stages. Results showed that peaks in expressed genes were mostly found to bind the up-and downstream region (15 kb) of the gene body which includes the promoter and terminator, rather than the gene body

itself (**Figure 3C**). By combining the VRS5 binding peaks with the DETs found in our expression analysis between *vrs5* and WT, we identified putative direct downstream targets of VRS5 (*bona fide* VRS5 targets). We identified DAP peaks corresponding to all three co-expression groups (**Figure 3D**) with: Group 1 representing genes highly expressed at the vegetative apex (VA) and downregulated at late reproductive stages, and enriched for ABA and JA hormone pathways; Group 2, representing genes highly expressed during inflorescence development and low expressed during the early developmental stages, genes in this group include key regulators of inflorescence and floral organ development, such as MIKC-type MADS-box genes and the barley *lgm1* candidate**;** and group 3, which mainly contains genes over represented in development and defense responses (**Figure 2B**). To evaluate if these are equally distributed over the three expression groups identified in the co-expression clustering, we compared the percentage of genes that were differentially regulated in the transcriptional profiling, and of which the upstream and/or downstream region was bound by VRS5 within the DAP-Seq experiment. Results showed that in all three expression groups, the percentage of DETs with a VRS5-DAP-Seq peak was similar (~20-25%). This suggests that VRS5 is directly regulating transcription of its targets throughout the developmental stages tested. Next, we extended our data set that comprises 675 *bona fide* targets through reanalysis of publicly available transcriptome data. These set include differentially regulated genes of *vrs5* (*int-c.5*) versus wild type of the stamen primordia (SP) and awn primordia (AP) stages (van Esse et al., 2017) and the tiller buds only (H. Wang et al., 2022). Inclusion of these additional stage resulted in 754 *bona fide* targets (**Table S5-S7**). Taken together, our analysis results in the identification of *bona fide* VRS5 targets.

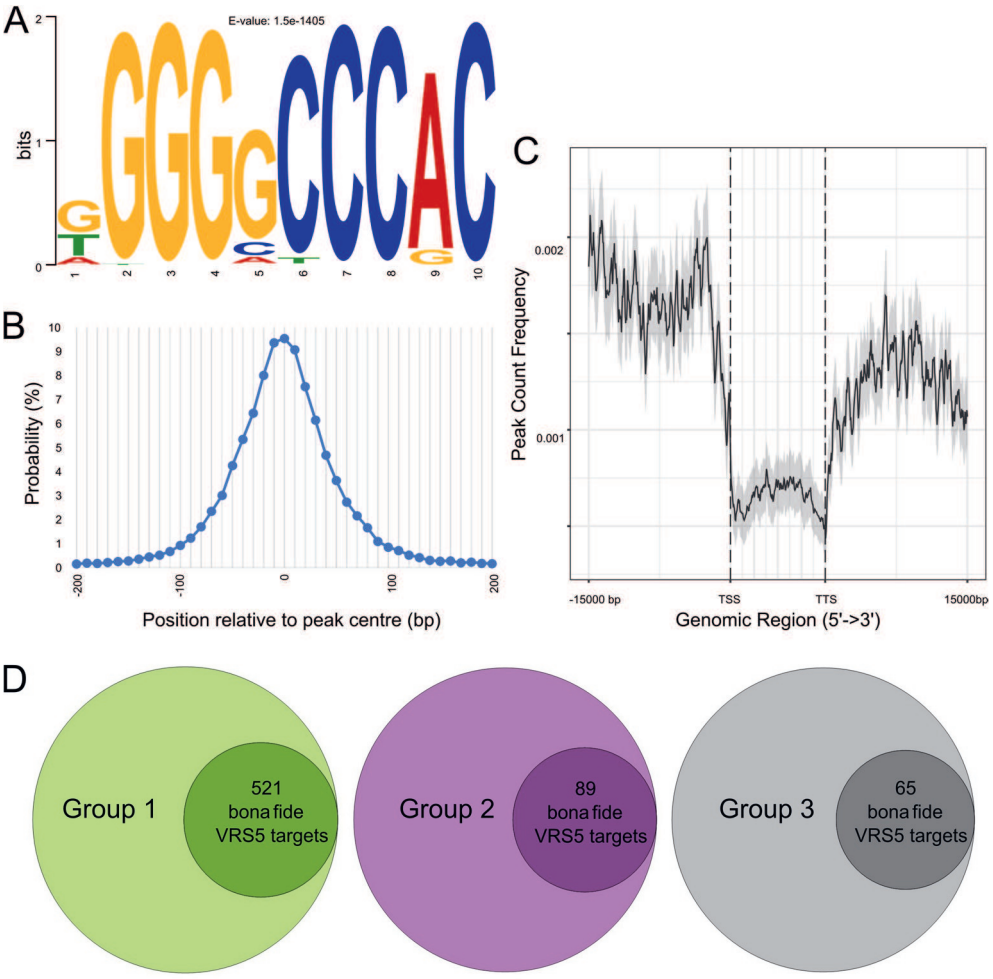


Figure 3: DAP-Seq of VRS5 on barley genomic DNA library. A) Enriched sequence logo in the VRS5 bound DAP-seq peaks, identified using STREME. B) The position of the motif shown in A relative to the center of the VRS5 DAP-seq peak as a probability percentage of bins of 10 bp. C) Frequency distribution plot of the VRS5 peaks 15kb upstream of the TSS and 15 kb downstream of TTS along expressed genes in the developmental stages sampled. D) Differentially regulated transcripts (DETs) per group that have a VRS5 binding peak within 15kb of their open reading frame in the DAP-Seq experiment. n= 6 DAP-Seq libraries for VRS5 with n=6 controls.

VRS5 controls genes involved in inflorescence development

To further explore the role of VRS5 in regulating genes involved in inflorescence development, we focus on the *bona fide* VRS5 targets identified in group 2, which comprises DETs that are low at VA and TA and high at the LP/SP stages. We identified several known genes in inflorescence and flower development. For example, a C2H2 zinc finger (*HORVU.MOREX.r3.2HG0170820*), which is identified as candidate for the long glume mutant (*lgm1)* in barley (Z. Zhang et al., 2024) was significantly upregulated in *vrs5* when compared to wild type and amongst the *bona fide* targets. Its ortholog in wheat is causing awn suppression (DeWitt et al., 2020; D. Huang et al., 2020). Other targets known in inflorescence and flower development include several MIKC-type MADS-box genes, which have a conserved role in the specification of floral organ identity (Kuijer et al., 2021). Amongst these are orthologs of floral organ development genes such as: *MADS4* (*HORVU.MOREX.r3.1HG0065060)*, *MADS1* (*HORVU.MOREX.r3.4HG0396400), AGL6 (HORVU.MOREX.r3.6HG0604360)*, and *SOC1-like* (*HORVU.MOREX.r3.1HG0054220*), that also contained a DAP-Seq peak and were differentially upregulated in *vrs5* mutants when compared to wild type lines in the RNA-Seq (**Figure 2C, Table S3**).

CENTRORADIALIS (HvCEN; HORVU.MOREX.r3.2HG0166090), is a gene involved in the regulation of meristem development, and downregulated in *vrs5* throughout development compared to Bowman (**Figure 4B, Figure S4**). Next to that, a VRS5 DAP-peak was found ~7 kb upstream of the coding sequence of *CENTRORADIALIS*. HvCEN acts as a floral repressor and mutants show early flowering, shorter spikes and less tillers at maturity (Bi et al., 2019; Comadran et al., 2012). To confirm the DAP-Seq results, we performed an EMSA using probes of DNA sequences extracted from the DAP-peak that contained the VRS5 binding site GGGNCCCAC. We used the DAP-peaks identified within upstream regions of *HvCEN, MADS4*, and *SOC1-like*. The peak upstream of *HvCEN* contained two putative VRS5 binding sites, while in the peaks upstream of *MADS4* and *SOC1-like* , one was found. Our results showed that VRS5 can indeed bind to the core VRS5 binding motif GGGNCCCAC in these peaks (**Figure 4C**). To further confirm the binding of VRS5 to the core motif GGGNCCCAC and its role in regulating target gene expression, we performed a dual-luciferase transactivation assay. Regions identified in the DAP peaks upstream of *HvCEN*, *MADS4*, and *SOC1-like* were cloned upstream of the luciferase reporter gene. Transactivation was then tested in *Nicotiana benthamiana* using VRS5 as the effector and Renilla luciferase as an internal control (**Figure 4D**).

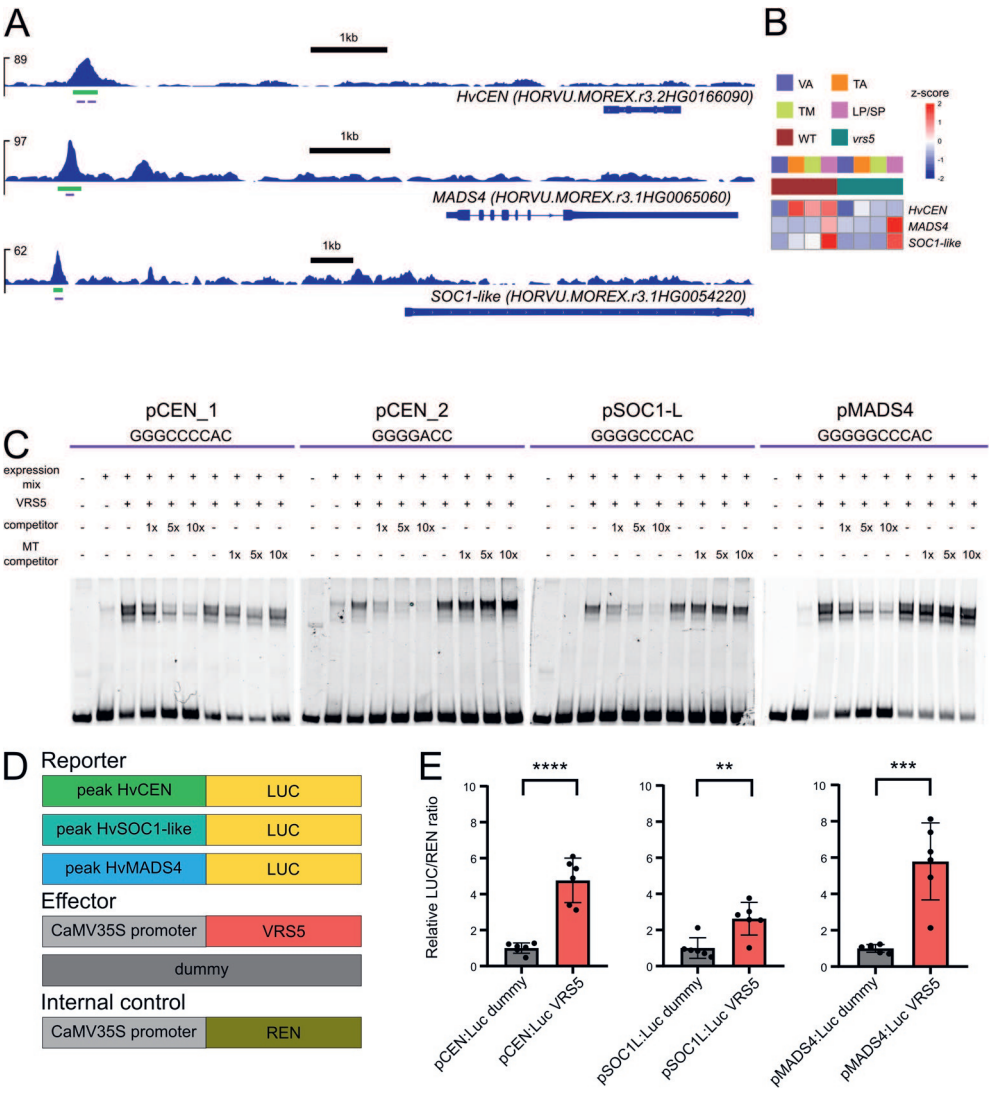

A
1kb
89
HvCEN (HORVU.MOREX.r3.2HG0166090)
97
MADS4 (HORVU.MOREX.r3.1HG0065060)
62
SOC1-like (HORVU.MOREX.r3.1HG0054220)
B
VA
TA
TM
LP/SP
WT
vrs5
z-score
HvCEN
MADS4
SOC1-like
C
pCEN_1
GGGCCCCAC
pCEN_2
GGGGACC
pSOC1-L
GGGGCCCAC
pMADS4
GGGGGCCCAC
expression mix
VRS5
competitor
MT competitor
1x 5x 10x
D
Reporter
peak HvCEN
LUC
peak HvSOC1-like
LUC
peak HvMADS4
LUC
Effector
CaMV35S promoter
VRS5
dummy
Internal control
CaMV35S promoter
REN
E
Relative LUC/REN ratio
****
**
***
pCEN:Luc dummy
pCEN:Luc VRS5
pSOC1L:Luc dummy
pSOC1L:Luc VRS5
pMADS4:Luc dummy
pMADS4:Luc VRS5

Figure 4: VRS5 binds to regions upstream of genes involved in inflorescence development. A) VRS5 DAP-seq peaks identified upstream of *MADS4*, *SOC1-like* and *HvCEN*. The green bars represent the peak significant compared to the control. The purple bars mark the VRS5 binding sites within the peaks. B) Heatmap of z-scores of expression of a selection of DETs at each developmental stage: vegetative apex (VA), transition apex (TA), triple mound (TM), and lemma and stamen primordia (LP/SP), for Wild type (WT) and *vrs5*. C) Confirmation of the VRS5 binding to DAP-Seq peaks using EMSAs on the VRS5 binding sites identified upstream of *HvCEN* (pCEN), *MADS4* (pMADS4), and *SOC1-like* (pSOC1-L). The peak upstream of *HvCEN* contained two putative VRS5 binding sites within the DAP peak, which are indicated as pCEN_1 and pCEN_2. Each probe is ~80 bp long and the sequence of the TCP binding site is indicated. For each probe the first lane contains only labeled DNA probe, the second lane contains labeled DNA probe and expression mix without VRS5 plasmid, and the other lanes contain labeled DNA probe and expression mix with VRS5 plasmid. Unlabeled competitor or unlabeled shuffled competitor (MT competitor) is added to indicated lanes in 1x, 5x, and 10x concentrations compared to labeled probe. D) Schematic overview of the different reporter and effector combinations used. For the reporter constructs, the VRS5 DAP-peak was cloned before the CDS of Luciferase. E) Data shows relative LUCIFERASE (LUC)/RENILLA (REN) ratio in a dual-luciferase assay in *Nicotiana benthamiana* leaves. The mean LUC/REN ratios are relative to the mean LUC/REN ratio of the dummy for each reporter. The red bar shows the mean LUC/REN ratio when VRS5 is used as effector. Black dots indicate individual measurements (n=6). Error bars indicate standard deviation. Asterisks designate significant differences of the mean (Student's t-test, **: $p<0.01$, ***: $p<0.001$, and ****: $p<0.0001$).

Co-expression of VRS5 significantly increased luciferase expression for all three reporters when compared to the control (**Figure 4E**). Our data thus confirms that VRS5 is able to bind to the selected upstream regions, and regulate the expression of the downstream target, in this case luciferase. While our RNA-seq data showed that *MADS4* expression is increased in the absence of VRS5, suggesting that VRS5 reduces *MADS4* expression, the transactivation assay showed an increase in *MADS4* expression when VRS5 was present (**Figure 4A-E**). This suggests that the actual direction of regulation *in vivo* may be influenced by the presence of additional cofactors that are not present in the transactivation assay.

Taken together, our data shows that VRS5 binds to a core GGGNCCCA motif present upstream of genes involved in inflorescence development to regulate their expression.

DAP-Seq and RNA-Seq reveal a conserved mode of action of VRS5

In the dicot model plant *Arabidopsis* BRC1, a homolog of *VRS5*, directly binds to the promoter of HD-Zip genes HB21, HB40, and HB53 to regulate their expression (Gonzalez-Grandio et al., 2017; van Es et al., 2024). The regulation of HD-Zip genes is conserved in maize, where ZmTB1 directly binds to the promoter of *GRASSY TILLERS* (*ZmGT1*). Given the conserved role of TB1 and BRC1 in regulation of HD-ZIP transcription factors, we first explored if amongst our *bona fide* targets HD-ZIP TF were present. Interestingly, the row-type related gene *VRS1* (*HORVU.MOREX.r3.2HG0184740*) was amongst the *bona fide* downstream targets of VRS5, showing a decreased expression at AP in *vrs5* compared to WT (**Figure 5A, Table S7**). *VRS1* encodes a HD-ZIP protein that is closely related to *ZmGT1* and the *Arabidopsis* HD-Zip genes. VRS1 is well known for its role in lateral spikelet development in barley. Plants that do not have functional VRS1 exhibit a six-rowed spike architecture (Komatsuda et al., 2007; Liller et al., 2015; Zwirek et al., 2019). Our targeted mutagenesis using CRISPR corroborated the crucial role of *VRS1* in inhibiting the outgrowth of lateral florets (**Figure 5B-C**). The VRS5 binding peak in our DAP-seq experiment was found around 7kb upstream of the *VRS1* translational start site. Sequence analysis of the region of this DAP-peak showed that there are three putative VRS5 binding sites within the center of this peak (**Figure 5D**). To verify if VRS5 was indeed capable of binding to the core VRS5 binding motifs found in this region, we performed an EMSA targeting all three putative VRS5 binding sites separately. This assay revealed that VRS5 was capable of binding to all three putative binding sites (**Figure 5E**). Next to that, a dual-luciferase transactivation assay was done to show that VRS5 cannot only bind to this peak, but also use it to regulate Luciferase expression (**Figure 5F**). Together, this provides evidence that VRS5 can directly bind upstream of *VRS1* to regulate *VRS1* expression.

Aside from *VRS1*, our transcriptional profiling combined with GO annotation showed that genes which are highly expressed at VA and low at the LP/SP stages (Group 1) are overrepresented for ABA and JA related genes. Previously, it was demonstrated in maize that ABA and JA related genes are among the putative downstream targets of ZmTB1 in tiller development (Dong et al., 2019). To further explore which *bona fide* VRS5 targets are conserved in maize, we used ZmTB1 targeted ABA and JA related genes and identified their orthologous genes in barley. All of the identified barley orthologs were downregulated in *vrs5* compared to WT and most were grouped in cluster group 1A, based on their expression pattern (**Table S8**). This suggests that these genes are mostly import early in development, when the tillers are formed. We found that indeed ZmTB1

and VRS5 share overlapping *bona fide* ABA and JA-related targets: AP2/B3 transcription factor *RELATED TO ABI3/VP 2 (RAV2) (HORVU.MOREX.r3.3HG0281730)*; several lipoxygenases, including *TASSELSEED1* (*HORVU.MOREX.r3.2HG0171680)*; and *JAZs* (**Table S8, Figure S4**)**.** This shows that the regulation of ABA and JA related genes is a conserved function between barley VRS5 and the maize ortholog TB1.

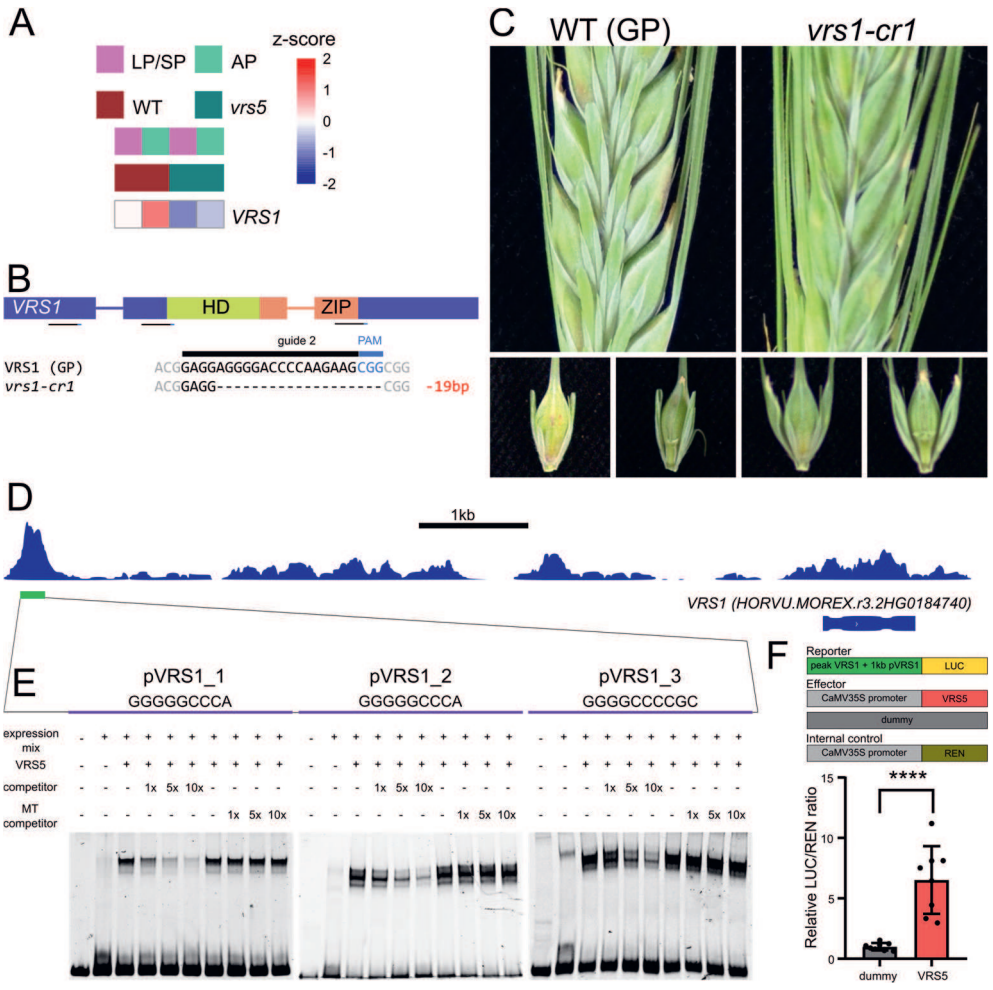

A
LP/SP
AP
WT
vrs5
VRS1
z-score
2
1
0
-1
-2
B
VRS1
HD
ZIP
guide 2
PAM
VRS1 (GP) ACGGAGGAGGGGACCCCAAGAAGCGGCGG
vrs1-cr1 ACGGAGG----------CGG -19bp
C
WT (GP)
vrs1-cr1
D
1kb
VRS1 (HORVU.MOREX.r3.2HG0184740)
E
pVRS1_1
GGGGGCCCA
pVRS1_2
GGGGGCCCA
pVRS1_3
GGGGCCCCGC
expression mix
VRS5
competitor
MT competitor
1x 5x 10x
F
Reporter
peak VRS1 + 1kb pVRS1
LUC
Effector
CaMV35S promoter
VRS5
dummy
Internal control
CaMV35S promoter
REN
****
Relative LUC/REN ratio
15
10
5
0
dummy
VRS5

Figure 5: VRS5 binds to the promoter of VULGARE ROWTYPE SIX 1 (VRS1) to regulate its expression. A) Heatmap of z-scores of expression of VRS1 at developmental stages: lemma and stamen primordia (LP/SP), and awn primorida (AP) for Wild type (WT) and *vrs5*. Data is reanalyzed from GSE102191 (van Esse et al., 2017). B) Gene editing of *VRS1* with targeted mutagenesis (CRISPR). C) Phenotype of gene edited *vrs1* mutant in the genetic background of GOLDEN PROMISE (GP) compared to the GP parental line. VRS1 lines have a six-rowed spike architecture. D) VRS5 binding region identified with DAP-Seq upstream of *VRS1*. There are three putative VRS5 binding sites within this peak. E) EMSA confirms the DAP-Seq data that demonstrated binding of VRS5 to the three VRS5 binding sites upstream of *VRS1* (pVRS1_1, pVRS1_2, and pVRS1_3). Each probe is ~80 bp long and the sequence of the TCP binding site is indicated. For each probe the first lane contains only labeled DNA probe, the second lane contains labeled DNA probe and expression mix without VRS5 plasmid, and the other lanes contain labeled DNA probe and expression mix with VRS5 plasmid. Unlabeled competitor or unlabeled shuffled competitor (MT competitor) is added to indicated lanes in 1x, 5x, and 10x concentrations compared to labeled probe. F) Dual-Luciferase transient transactivation assay. Data shows relative LUC/REN ratio in a dual-luciferase assay in Nicotiana benthamiana leaves using the DAP-peak identified upstream of VRS1 + 1kb promoter of VRS1 in front of Luciferase. The mean LUC/REN ratios are relative to the mean LUC/REN ratio of the dummy. The red bar shows the mean LUC/REN ratio when VRS5 is used as effector. Black dots indicate individual measurements (n=8). Error bars indicate standard deviation. Asterisks designate significant differences of the mean (Student's t-test, ****: $p<0.0001$).

Discussion

VRS5 is an important domestication gene in barley that plays a crucial role in tillering and row-type determination (Liller et al., 2015; Ramsay et al., 2011; Zwirek et al., 2019). Using a combination of transcriptomics and localizing genome-wide binding sites of VRS5, we identified its putative direct downstream targets. Different from ChIP-sequencing, which is a more *in vivo* method to find transcription factor binding sites (TFBS) and where inaccessible DNA cannot be bound, DAP-sequencing is a method where naked DNA is used, so chromatin context is not kept (Bartlett et al., 2017; Hajheidari & Huang, 2022). Nevertheless, despite the lack of chromatin context in DAP-seq, the overlap between DAP-seq and ChIP-seq peaks is generally high (O'Malley et al., 2016). Of the DAP peaks found for VRS5, a significant part was found distal intergenic. A recent study performed DAP-sequencing of a large number of transcription factors in *Triticum urartu,* that has a genome size comparable to barley. They found for the majority of transcription factors that more than 50% of the DAP-seq peaks were located more than 10kb from the gene body (Y. Zhang et al., 2021). Similarly, in strawberry DAP-Seq of a TCP transcriptional regulator revealed also presence of the majority of peaks in the distal intergenic region (X. Chen et al., 2024). Together, this indicates that for DAP-sequencing on a large genome such as barley, a large portion of distal intergenic peaks can be expected. As an *in vitro* technique, DAP-sequencing might yield binding sites that would never be accessible under *in vivo* circumstances. In part, this could result in a higher number of distal intergenic DAP-peaks (Maher et al., 2018). To what extend distal intergenic DAP-peaks in general, and for VRS5 in this study, represent biological relevant long distal regulatory elements still needs to be elucidated. In barley, the most accessible chromatin regions (ACRs) are found between 10 and 100 kb from the nearest gene (Lu et al., 2019). Recent studies using STARR-Seq indicate that about ~37% of the enhancers had potential target genes at a distance of 10kb, suggesting that only a minority of the genes in barley is regulated by adjacent enhancers (Zhou et al., 2024). In our study, we focused on DAP-peaks found within 15 kb of their nearest gene whilst a significant portion of the DAP-Seq peaks was found in distal-intergenic regions. Given the observation that in barley, enhancers may lie up to 100 kb (Zhou et al., 2024) from a target gene, biological relevance of other DAP-peaks beyond our window cannot be excluded. Knowing the ACRs in tissues where VRS5 is expressed and under different environmental circumstances could give a better understanding and biological relevance to these other peaks. Taken together, to truly place distal-intergenic peaks into a

biological context, a more in-depth study of the 3-D genome makeup at high resolution is imperative.

Nevertheless, in our analysis we identified >700 *bona fide* VRS5 targets and reveals an overlap in ABA and JA-related targets in maize and barley (**Figure 6)**. This suggests that the network of tiller development via ABA and JA signaling is partially conserved between barley and maize. In the model plant *Arabidopsis,* ABA related genes are directly targeted by the class II TCP transcription factor BRC1 to regulate axillary branching (Gonzalez-Grandio et al., 2017; van Es et al., 2024). This implies that the regulation of ABA signaling by BRC1/TB1 proteins is evolutionarily ancient and precede the divergence of monocotyledonous and dicotyledonous plants (van Es et al., 2024). Interestingly, some of these genes found as *bona fide* VRS5 target may have a role in inflorescence development, from which the most known gene is *VRS1* (**Figure 6**). Intriguingly, VRS1 and VRS5 alleles have been co-selected for increased lateral grain size in six-rowed cultivars (Ramsay 2011), and *vrs5 vrs1* double mutants have an additive effect when compared to the respective single mutants (Zwirek et al., 2019). In addition, *vrs5* mutants have an intermediate phenotype, whereas *vrs1* lines have a complete six-rowed phenotype (Liller et al., 2015; Zwirek et al., 2019). Combined, this suggest that there are other activators of *VRS1* that may act redundant, or in parallel to VRS5.

Aside from VRS1, our analysis also revealed other genes involved in inflorescence development amongst the *bona fide* VRS5 targets. For example, we identified a ortholog of *TASSELSEED1* as *bona fide* target of VRS5. In maize, *TASSELSEED1* is a lipoxygenase involved in JA biosynthesis and known for its important role in sex-determination of maize florets by repressing carpel development (Acosta et al., 2009). Furthermore, in our data we observed an upregulation of genes involved in flowering and floral organ identity, such as MIKC-type MADS-box genes, in *vrs5* compared to WT. MIKC-type MADS-box genes, which include the ABCDE-genes that are known for regulating floral homeotic patterning, are mostly upregulated during inflorescence development in barley (Digel et al., 2015; Kuijer et al., 2021; H. Liu et al., 2020). Our observation that floral homeotic genes are upregulated in *vrs5* when compared to Bowman may reflect an increased expression of these genes in lateral spikelet primordia in *vrs5*. However, the presence of a VRS5 DAP-peak within the promoter region of some of these MIKC-type MADS-box genes suggests a more direct effect of VRS5 on the regulation of these floral homeotic genes. Intriguingly, *HvMADS1*, which in barley regulates lemma and awn development and prevents inflorescence branching under high ambient temperatures (G. Li et al., 2021; Y. Zhang, Shen, Li, et al.,

2024) is among the *bona fide* VRS5 targets. Moreover, an ortholog of AGL6 was identified as *bona fide* VRS5 target that is significantly upregulated in the *vrs5* mutant when compared to WT. In barley, *agl6* mutants are infertile due to defective pistils and homeotic conversions from two stamens into lemma-like structures in the central spikelets. In the lateral spikelets the underdeveloped stamens showed a homeotic conversion to bract-like structures in the *agl6* mutant (Shen et al., 2024). In wheat, *agl6* mutants are also infertile and TaAGL6 acts upstream of several other floral homeotic genes (Kong et al., 2022). These results suggest that VRS5 may also inhibit lateral spikelet development in two-rowed cultivars by directly reducing the expression of these genes that are involved in floral organ development (**Figure 6)**. In agreement with this hypothesis, row-type genes prevent the development of carpels in the two-rowed spike architecture (Zwirek et al., 2019), while loss of function mutants of *vrs5* and other row-type genes have an increased lateral floret fertility. While *ZmTASSELSEED1* was found as target of ZmTB1, orthologs of the other genes involved in floral development targeted by VRS5 were not found as target of ZmTB1 or AtBRC1. This implies a more specific group of targets for barley VRS5 in lateral spikelet development, which is a barley specific function of VRS5 compared to its orthologs, although differences due to sampling between our experiment and previous data sets generated on ZmTB1 and AtBRC1 (Dong et al., 2019; van Es et al., 2024) cannot be excluded. So next to a more conserved set of VRS5 targets in tillering a more barley specific set of targets is found in regulating lateral spikelet development.

Aside from the floral homeotic genes, *HvCEN* is also identified amongst the *bona fide* targets VRS5. HvCEN acts antagonistically to FLOWERING LOCUS-T (FT) in regulating floral transition (Bi et al., 2019; Colleoni et al., 2024). In wheat and *Arabidopsis*, TaTB-D1 and AtBRC1 respectively, are shown to interact with the FT1 ortholog of their species (Dixon et al., 2020; Niwa et al., 2013). To what extent binding of VRS5 to the *HvCEN* promoter impacts on floral transition, flowering or meristem development remains to be elucidated (**Figure 6**). However, our results do suggest a role of VRS5 in the direct regulation of *PEBP* genes through binding to the promoter to activate the expression aside from the previously described regulation through protein-protein interaction.

In conclusion, with this study, we showed that barley VRS5 binds a class II TCP DNA motif GGGNCCCAC and acts mainly as a transcriptional activator. *Bona fide* VRS5 target genes include genes involved in ABA-signaling, which seems to be a conserved role for TB1-like proteins in both monocots and dicots to regulate tillering or axillary branching. We also revealed a role for VRS5 in regulation of

floral homeotic and meristem identity genes. Our study exemplifies that it is essential to not only identify the molecular networks in model plants like *Arabidopsis*, but also in key crops such as barley to reveal conservation, but more important to identify divergence explaining the species-specific architecture. The study presented here offers a solid and crucial starting point for mutant analyses of a selection of *bona fide* targets to gain a deeper understanding of the VRS5 network and to enlighten its mode of action in shaping barley development.

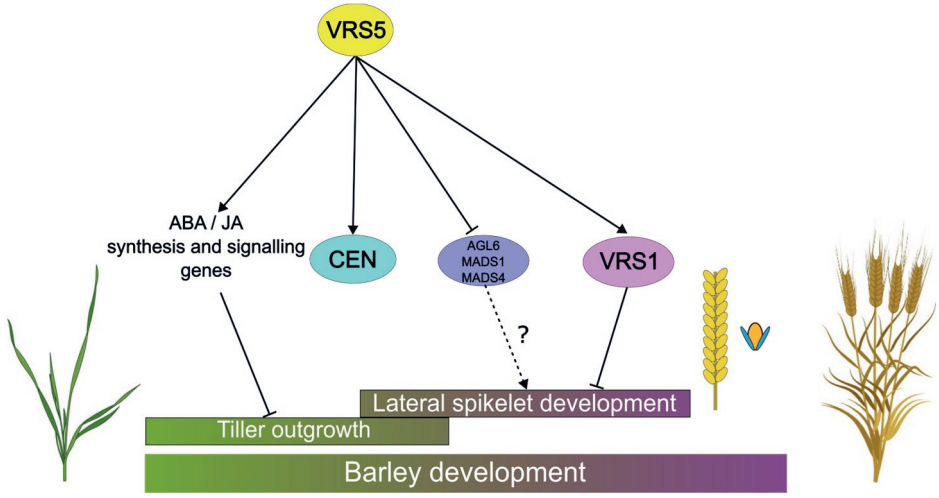


Figure 6: VRS5 network over development
VRS5 inhibits tiller outgrowth through regulating ABA/JA synthesis and signalling genes early in development. Later in development, VRS5 inhibits lateral spikelet development directly via *VRS1*. VRS5 also inhibits expression of *AGL6*, *MADS1*, and *MADS4* directly, which might play a role in lateral spikelet development. Additionally, VRS5 induces the expression of *HvCEN*. On the right a barley spike is shown next to a barley triple floret, where the central spikelet is shown in yellow and the two lateral spikelets in blue.

Materials & Methods

Phenotypic analysis

Seeds of Bowman and *int-c.5* (GSHO 2003) were stratified on wet tissue paper in the dark at 4°C for three days, before sowing them in 1.3L pots. Plants were grown in the greenhouse under 16h light 21°C, 8h dark 18°C conditions. Tiller number was counted per plant at 7, 10, and 14 days after emergence (DAE). The same procedure, and growth conditions were used for Golden Promise, and *vrs1* mutants in this background. Pictures of the spikes were taken after flowering when the seeds were filling.

RNA isolation and RNA-Sequencing

Seeds of cv. Bowman and *int-c.5* were sown in 84-well trays. A stratification treatment by exposing the seeds at 4°C in the dark for three days was provided to enhance equal germination. After stratification, plants were transferred to soil in a growth chamber under long day (LD) conditions (16h light/ 8h dark) at 20°C. Developmental stages of the meristems were scored using the Waddington scale (WADDINGTON et al., 1983) by dissecting three plants of each genotype on the day of sampling. Shoot apical meristems were sampled over time at four different stages: W0, vegetative apex (VA); W1, transition apex (TA); W2.25, triple mound (TM); and W3-3.5, lemma and stamen primordia (LP/SP). Samples were taken in the afternoon (6 hours before the end of the LD period). Leaves surrounding the apex were removed manually, before cutting the apex. Apexes were immediately frozen in liquid nitrogen and stored at -80°C before RNA isolation. Three biological replicates were taken for each developmental stage, each consisting of 10-20 apexes. Frozen tissue was disrupted using the Tissuelyser LT (Qiagen). RNA extraction was performed on disrupted tissues using columns from the GeneJET plasmid miniprep kit (Thermo Fischer Scientific), as described previously (Yaffe et al., 2012). Extracted RNA was treated with DNase I (Qiagen) and RiboLock (Fermentas). Extracted RNA samples that were used for RNA-Seq were sent to Novogene Europe (Cambridge Science Park, United Kingdom), where mRNA was purified from total RNA using poly-T oligo-attached magnetic beads. After fragmentation, the first strand cDNA was synthesized using random hexamer primers, followed by the second strand cDNA synthesis. Samples were sequenced using the Illumina platform with a sequencing depth of 20 million reads per sample using 150 bp paired-end reads.

Differential gene expression analysis

Raw paired RNA-seq reads were cleaned using Trimmomatic 0.39 (Bolger et al., 2014) with parameters: ILLUMINACLIP:adapters.fa:2:30:10 LEADING:3 TRAILING:3 SLIDINGWINDOW:4:15 MINLEN:36. The file adapters.fa contains nucleotide sequences of Illumina adapters used for library construction. From the trimmed reads, transcripts were quantified with the MorexV3 transcriptome as reference (Mascher et al., 2021) using salmon (Patro et al., 2017) and the softclip parameter (**Table S9**). Differentially expressed genes were identified using the R package DESeq2 (Love et al., 2014) per developmental stage (VA, TA, TM, and LP/SP), and over development by adding developmental stage to the model (GLM). Identified differentially expressed genes were considered significant when the false discovery rate (FDR) < 0.05 and the absolute log2 fold change (LFC) was more than 0.58. Data from the later developmental stages, namely the stamen primordia stage (SP), and the awn primordia stage (AP), when the carpels are formed and the first phenotypical differences between Bowman and *int-c.5* in spike development emerge, are extracted from Gene Expression Omnibus (GEO) expression data set GSE102191 (van Esse et al., 2017). The data from these stages were re-analyzed against the Morex V3 genome in the same way as the newly generated RNA-Seq samples from the VA, TA, TM and LP/SP developmental stages (**Table S5**). Data from the tiller buds specifically of *int-c.5* and Bowman were extracted from microarrays performed before (H. Wang et al., 2022). The differentially expressed genes between *int-c.5* and Bowman tiller buds under control conditions were reannotated to MorexV3 by blasting the sequences of the harvEST:Barley ID against MorexV3 (**Table S6**).

qPCR

RNA from the above described samples was used to make first strand cDNA from 1 µg RNA per sample using iScript cDNA Synthesis Kit (Bio-Rad). qPCR was performed using iQ SYBR Green Supermix (Bio-Rad). Relative expression compared to *HvActin* is calculated (Gines et al., 2018). Primers used are described in **Table S10**.

Gene names, Gene Ontology (GO) term annotation, enrichment and cluster analysis

Unless previously characterized, gene names are based on the orthologous genes in rice according to ensemble plants release 60 (https://plants.ensembl.org/index.html). Naming of MIKCc MADS box genes is in accordance with Kuijer et al., 2021. Using Pannzer2 (Törönen et al., 2018), the coding sequences of MorexV3 reference genome (Mascher et al., 2021) were

annotated and assigned GO-terms (accessed 21-06-2023). Genes that were significant differentially expressed in at least one developmental stage and/or independent of developmental stage were clustered based on their expression pattern per genotype using the degPatterns function from the R package DEGreport. In total, 2,869 transcripts show differential expression with |Log2FoldChange| > 0.58 and FDR < 0.05 in at least one of the developmental stages or independent of developmental time in the GLM. Clusters were grouped manually based on their global trend over time in six cluster groups. GO-term enrichment of the differentially expressed genes was done for each cluster group using the R package topGO using the "classic" algorithm as parameter followed by the Fisher's Exact Test , taking into account only those GO-terms that have at least 10 annotated genes in the designated term.

DNA affinity purification and sequencing (DAP-seq)

DNA libraries for DAP-Seq were made as previously described (Bartlett et al., 2017). For each replicate, genomic DNA was extracted from 100 mg developing inflorescences of barley cv. Morex, four weeks after sowing in 84-well trays (Waddington stage ~W4) using the DNeasy Plant Mini kit (Qiagen). The DNA was fragmented with ten sonication steps of ten seconds using the Sonicator 150 (MSE) and allowing 45 seconds of rest on ice between each step. The fragmented DNA was end-repaired using the End-It kit (Lucigen) and A-tailed using Klenow fragment (3'-5' exo-; NEB). The truncated Illumina Y-adapter was ligated to the DNA using T4 DNA ligase (Promega).

The CDS of VRS5 (cv. Bowman) without the stop codon was cloned, via Golden Gate cloning, together with a C-terminal 3xFLAGtag (MoClo toolbox; pICSL50007) (Engler et al., 2014) behind the SP6 promoter into the pSPUTK expression vector (Stratagene) that was made Golden Gate compatible as described (Kerstens et al., 2024). Similarly, eGFP was cloned from pICH41531. The FLAG-tagged VRS5 and GFP were expressed *in vitro* using 2 µg plasmid and TnT® SP6 High-Yield Wheat Germ Protein Expression System (Promega). Expressed FLAG-tagged proteins were bound with prepared DNA libraries for 2 hours at RT followed by immobilization by anti-FLAG magnetic beads (SIGMA). The mix was washed, and eventually DNA was eluted by competition with 3xFLAG peptide (APExBIO). Eluted DNA was amplified by PCR with primers completing the Illumina sequencing adapter of which one primer was indexed (**Table S10**). Amplified products were run on a 1.5% agarose gel, and DNA between 200 and 600 bp was cut out and purified using GeneJET Gel Extraction Kit (Thermo Scientific). Six replicates (**Figure S5**) were sequenced using the

HiSeq X-ten platform with a sequencing depth of 50 million reads per sample using 150 bp paired-end reads (BGI Europe).

DAP-seq analysis

Raw paired DAP-seq reads were cleaned using Trimmomatic 0.39 (Bolger et al., 2014) using parameters ILLUMINACLIP:adapters.fa:2:30:10 LEADING:3 TRAILING:3 SLIDINGWINDOW:4:15 MINLEN:36 , where adapters.fa is a file containing nucleotide sequences of the used adapters (**Table S10**). Paired reads were mapped to the Barley MorexV3 reference genome (Mascher et al., 2021) using BWA-MEM v0.7.17 (Li, 2013, preprint; Li and Durbin, 2010). Peak calling was done using MACS2 v2.2.7.1 (Y. Zhang et al., 2008), using the callpeak function, where the VRS5 samples were compared to the GFP control samples. The genome size parameter was set to 5.4e9, corresponding to the barley genome size. The "KEEP-DUP" parameter was set to "auto", meaning that the MACS2 algorithm calculates the number of reads that are allowed to be identical, leading to a maximum of two identical reads. Genomic regions that had a high number of reads in the control samples (GFP-FLAG) were identified using the "greenscreen" method (Klasfeld et al., 2022). Called peaks overlapping with a "greenscreen" region were filtered out using bedtools intersect function (Quinlan & Hall, 2010). Peaks with a $q < 10^{-10}$ were kept and considered true peaks. The DNA sequences of the true peaks were used for de novo motif discovery using STREME from MEME-suite v5.4.1 (Bailey, 2021; Bailey et al., 2015). The bdg files from MACS2 output were converted to tdf files for visualization using the Integrative Genomics Viewer v.2.11.9 (Robinson et al., 2011).

Overlap with ZmTB1 targets

To check if previously identified ZmTB1 targets (Dong et al., 2019) are also targeted by VRS5, we used Orthofinder (Emms & Kelly, 2019) to infer the barley orthologs of the ZmTB1 targets. As input the following proteomes are downloaded from Phytozome: *Arabidopsis thaliana* TAIR10 (Lamesch et al., 2012), *Brachypodium distachyon* v3 (Vogel et al., 2010), *Hordeum vulgare* (barley) MorexV3 (Mascher et al., 2021), *Lolium perenne* MPB_Lper_Kyuss_1697 (Frei et al., 2021), *Triticum aestivum* (wheat) IWGSC (ENA: GCA_900519105.1), *Oryza sativa* (rice) IRGSP 1.0 (Ouyang et al., 2007), and *Zea mays* (maize) AGPv3.31 (NCBI: GCF_000005005.1), which was used as reference by Dong et al., 2019.

Electrophoretic Mobility Shift assay (EMSA)

EMSA was performed as described previously (Smaczniak et al., 2012). Briefly, DNA probes of around 50 bp are designed from genomic regions and corresponding primers were synthesized (Biolegio). Synthesized primers were

annealed and obtained probes were cloned into pGEM-T. Subsequently, the probes were labeled using CY5.5 labeled primers using PCR based amplification. The VRS5 CDS was cloned into pDONR201 (Gateway), and subsequently, into a gateway compatible pSPUTK expression vector (Stratagene), which uses a SP6 promoter to induce expression (Jiang et al., 2022). The VRS5 protein was prepared *in vitro* using TNT SP6 Wheat germ protein expression system (Promega). Using the VRS5 protein, a EMSA binding reaction was performed for 45 minutes on ice using a binding reaction mixture (1.2 mM EDTA (pH 8.0), 0.25 mg/ml BSA, 7.2 mM HEPES (pH 7.3), 0.7 mM DTT, 60 µg/ml salmon sperm DNA, 1.3 mM spermidine, 2.5% CHAPS, 8% glycerol, 6.6 nmol/ml single-labelled dsDNA, and 2 µl of in vitro-synthesized proteins). When an unlabelled competitor probe was used, 6.6 nmol/ml (1x), 33 nmol/ml (5x), or 66 nmol/ml (10x) was added to the binding reaction mixture. The mixture was then loaded on a 5% polyacrylamide gel. The gel was run in 1× TBE buffer at 75 V for about 90 min. Labelled DNA shifts were visualized using a LiCor Odyssey imaging system at 700 nm.

Dual-luciferase transactivation assay

To test transactivation of luciferase by VRS5 constructs were created using Golden Gate cloning (Engler et al., 2014). Synthesized DNA fragments containing identified DAP-peaks were synthesized and cloned in front of an minimal 35S promoter followed by Luciferase CDS terminated by a NOS terminator, using an in-house vector (available at Addgene: #231035), to form the expression vector. Next to that the CDS of VRS5 was cloned into pL0-CDS (pICH41308) and subsequently into pL1-F2 (pICH47742) behind a 2xCaMV 35S promoter (pICH51288) and terminated by a NOS terminator (pICH41421) to form the effector vector. A third pL1 construct was used to normalize luciferase activity. This control vector contains the Renilla Luciferase coding sequence, made Golden Gate compatible from pGreenII-0800 (Hellens et al., 2005), and a 2xCaMV 35S promoter and NOS terminator. For all combinations, the three L1 vectors were assembled in a pL2 (pAGM4723). As negative controls the effector plasmid was replaced by a pL1-F2 dummy (pICH54022). The assembled L2 constructs were transformed into *A. tumefaciens* strain AGL1 pSOUP. Transformed cells were grown overnight at 28°C in LB. This culture was used to inoculate YEB containing 200µM Acetosyrengone and 10mM MES. This culture was grown overnight at 28°C to an OD_{600} of ~1. These cell cultures were spun down and resuspended in 15mL MMA containing 200µM Acetosyrengone and left at 28°C for 2-3 hours. For transfection, the abaxial side of leaves of 4-5 week old (non-flowering) *Nicotiana benthamiana* plants were infiltrated with the *A. tum*

cell culture with an OD ~ 1, using a needleless syringe. At least five different plants were infected with the same construct and were treated as biological replicates. The plants were grown for 2 days in a growth chamber. Samples of infiltrated leaf parts were taken and snap-frozen in liquid nitrogen. For luciferase measurement of the samples, the Dual-Luciferase Reporter Assay kit (Promega) was used. Measurements were done using a GlowMax Navigator Microplate Luminometer. For each sample the ratio of Firefly/Renilla Lucifarase was calculated relative to the mean ratio of each expression vector combination without VRS5 TF. Statistical difference was tested using Student's t-tests, for each expression vector.

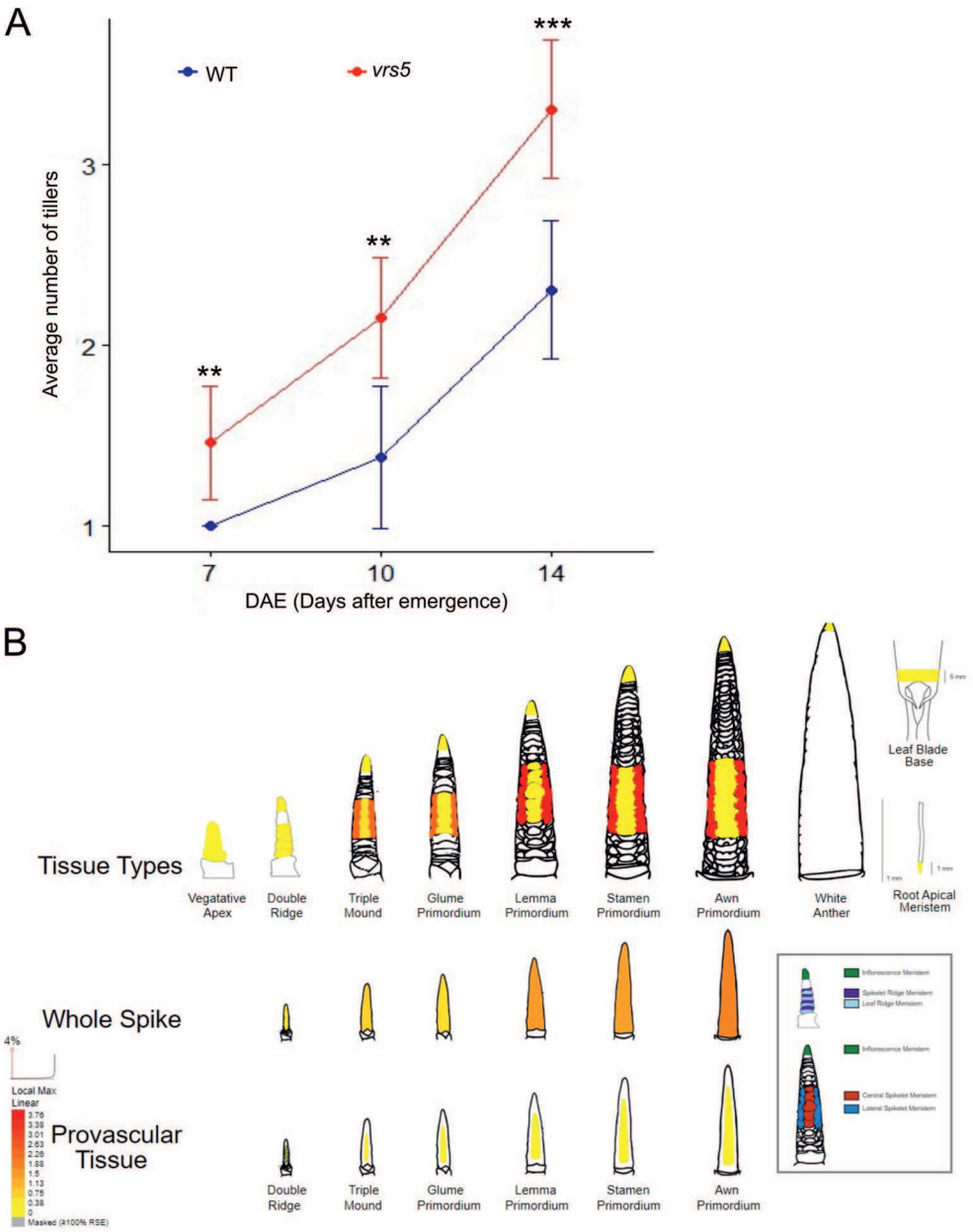
CRISPR-Cas9 mutagenesis

For CRISPR-Cas9 targeted mutagenesis of *VRS1*, three guides were designed, targeting different regions of the coding sequence. (guide 1: 5'-ACGTGGACACGACTTTCTTC-3', guide 2: 5'-GAGGAGGGGACCCCAAGAAG-3', and guide 3: 5'-GGAGGTGCGGCGCCTCAGGT-3'). Final vectors were created using both our in-house CRISPR vector system (available at Addgene: #231030 - #231033) and already available modular cloning toolkits (Engler et al., 2014; Lawrenson et al., 2015). Guides were synthesized as complementary oligos (**Table S10**) and cloned in an optimized Cas9 scaffold (Dang et al., 2015; Parry et al., 2016) (scaffold sequence, where NNNNNNNNNNNNNNNNNNNN corresponds to the guide: 5'GNNNNNNNNNNNNNNNNNNNNGTTTCAGAGCTATGCTGGAAACAGCATAG CAAGTTGAAATAAGGCTAGTCCGTTATCAACTTGAAAAAGTGGCACCGAGTC GGTGCTTTTTTTCTAGACCCAGCTTTCTTGTACAAAGTTGGCATTACGCTAGA GACCACGAAGTG-3'). The level 1 backbone vector with the modified scaffold has been designed so that the digestion-ligation of the double-stranded guide using the Type IIS restriction enzyme BsmBI removes the mRFP1 expression cassette (Engler et al., 2014). This allows for a pink-white screening of the recombined level 1 vectors. The final level 2 vector used for plant transformation contains the intron-optimized hygromycin resistance cassette (pICSL11059), the Cas9 expression cassette (pICSL11056), and the three single guide RNAs targeting *VRS1* coding sequence under the control of the TaU6 promoter. The sequence-verified construct was introduced in the hypervirulent *Agrobacterium tumefaciens* strain *AGL1 pSOUP*, and used for *Agrobacterium*-mediated transformation of barley cv. *Golden Promise* immature embryos (Hensel et al., 2009). T_0 plants were genotyped for CRISPR cuts using the Phire Plant Direct PCR Kit (Thermo Fisher Scientific) using primers described in **Table S10**. Amplified fragments were sequenced directly.

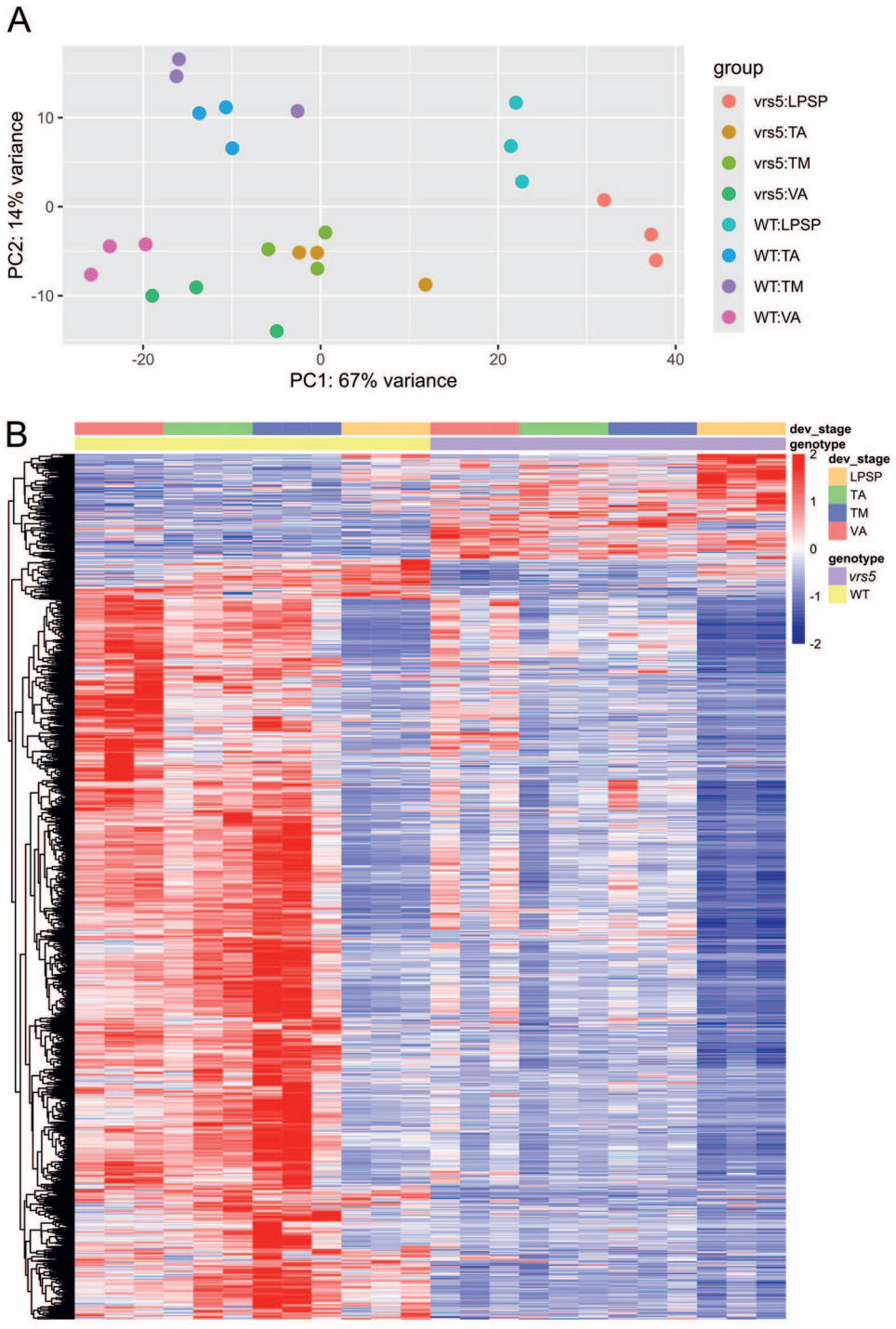
Data availability

The data generated in this publication have been deposited in NCBI's Gene Expression Omnibus (Barrett et al., 2013; R. Edgar et al., 2002) and are accessible through GEO Series accession number GSE272367 and GSE272368.

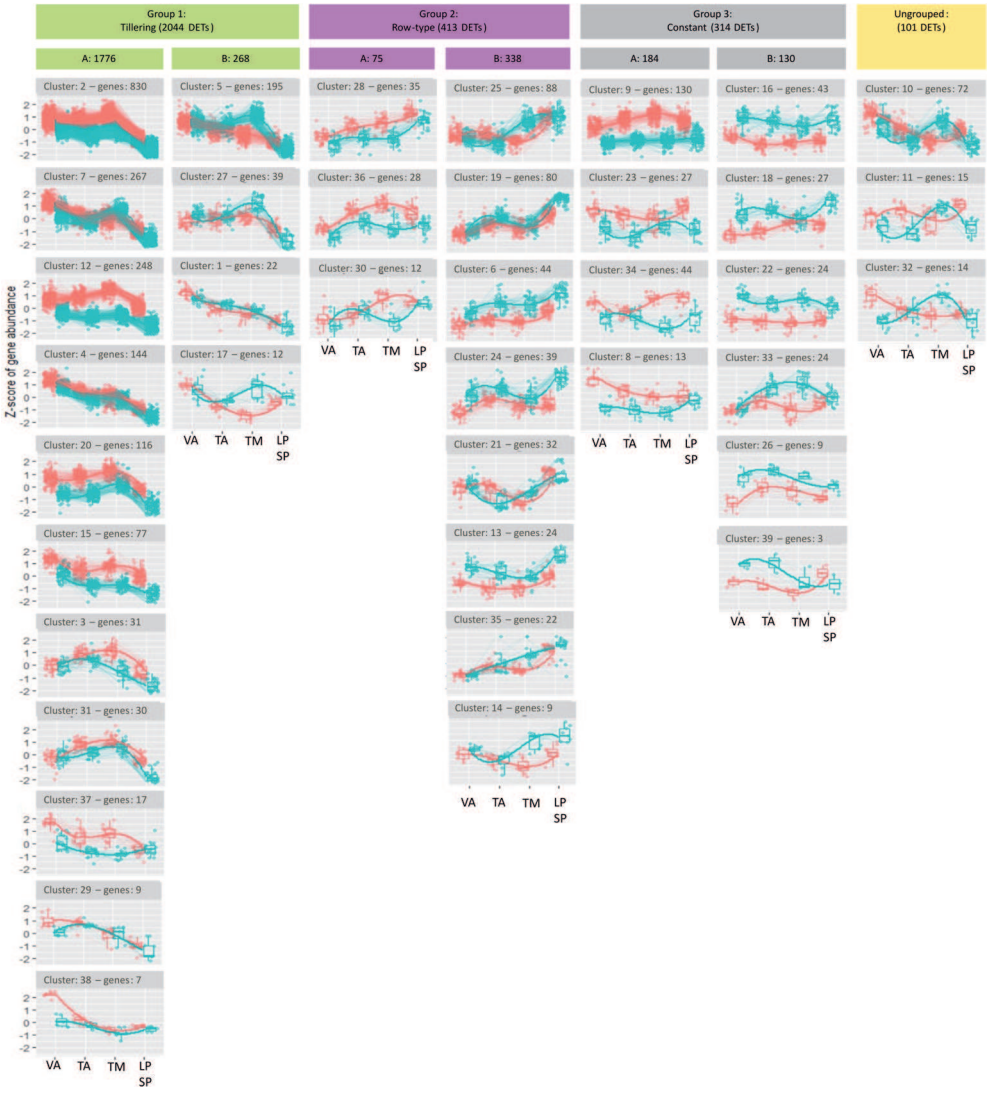
Supplementary Figures



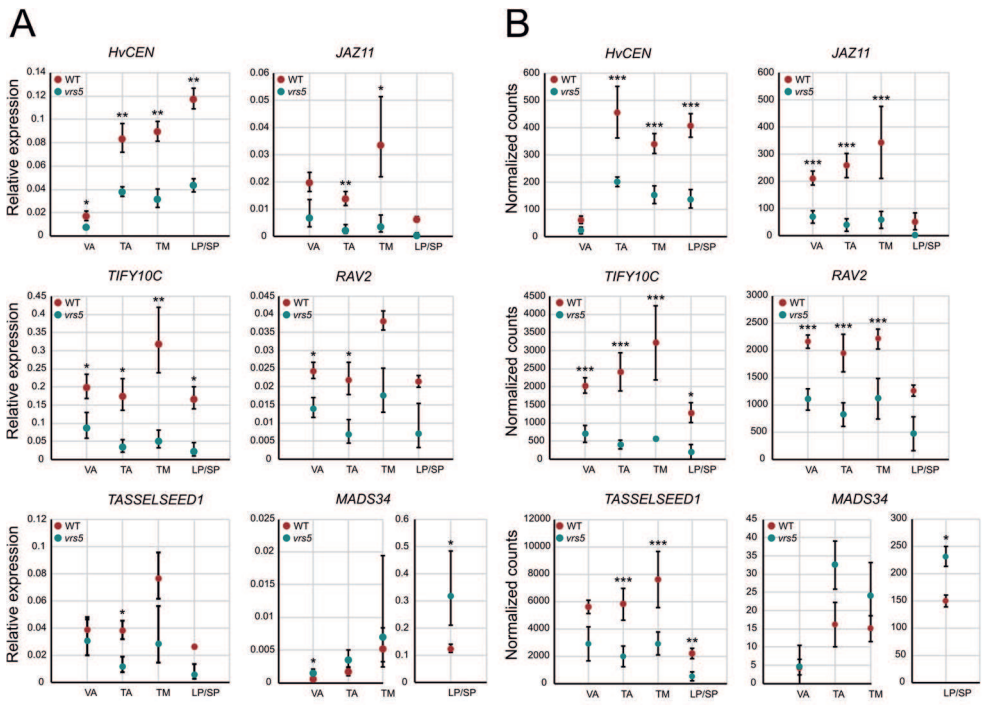
Supplementary Figure S1: VRS5 influences tillering and row-type. A) Line graph of mean number of tillers per plant over time with *int-c.5* shown in red and Bowman in blue. n=13 for each genotype. Differences at each timepoint are calculated using student's t-test; asterisks indicate significance (*: $p < 0.05$, **: $p < 0.01$, ***: $p < 0.001$). Error bars indicate standard error of the mean. B) expression pattern of VRS5 (*HORVU.MOREX.r3.4HG0336690*) retrieved from the ePlant expression atlas that uses the Thiel et al., 2021 dataset. Red indicates high expression, whereas yellow indicates low expression.


A
PC2: 14% variance
10
0
-10
-20
0
20
40
PC1: 67% variance
group
vrs5:LPSP
vrs5:TA
vrs5:TM
vrs5:VA
WT:LPSP
WT:TA
WT:TM
WT:VA
B
dev_stage
genotype
2
1
0
-1
-2
dev_stage
LPSP
TA
TM
VA
genotype
vrs5
WT

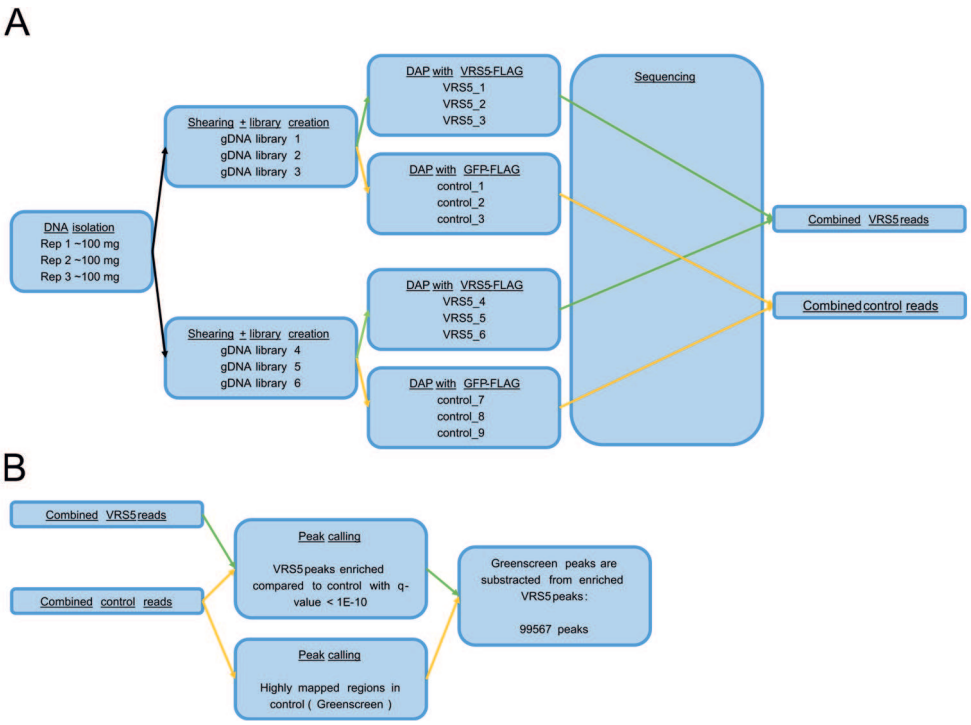
Supplementary Figure S2: RNA-seq quality control A) Principal component analysis of the TPM values of RNA-seq samples. Dots indicated with the same color represents replicates of the same sample group. B) Clustered heatmap of z-scores per sample of expression levels of differentially expressed transcripts (DETs) between WT (Bowman) and *vrs5* (*int-c.5*) over developmental stages tested, namely: vegetative apex (VA), transition apex (TA), triple mound (TM), and lemma and stamen primordia (LP/SP). For each developmental stage and genotype combination three biological replicates are used. The columns represent the different samples, grouped by genotype and developmental stage. Each row represents a DET.



Supplementary Figure S3: Grouping of co-expression clusters. Co-expression clusters of differentially expressed genes between *vrs5* and WT over development using R package degPatterns, grouped in three main groups: 1) downward expression throughout development; 2) upward expression throughout development; 3) static expression throughout development; and lastly ungrouped clusters that do not follow either of the trends. The groups are sub-divided in A (lower expression in *vrs5* compared to WT), and B (higher expression in *vrs5* compared to WT). Each cluster shows the z-score of expression of the genes within the cluster, colored by genotype (red: WT (Bowman), cyan: *vrs5* (*int-c.5*)) over developmental stages tested, namely: vegetative apex (VA), transition apex (TA), triple mound (TM), and lemma and stamen primordia (LP/SP). The boxes indicate median +/- quartile, the whiskers indicate minimum and maximum values excluding outliers. For each developmental stage and genotype combination three biological replicates are used.



Supplementary Figure S4: q-PCR confirmation of RNA-seq data for a selection of targets A) Relative expression of *HvCEN, JAZ11, TIFY10C, RAV2, TASSELSEED1*, and *MADS34* compared to *Actin* using qRT-PCR and B) Normalized expression of *HvCEN, JAZ11, TIFY10C, RAV2, TASSELSEED1*, and *MADS34* in our RNA-seq dataset at each developmental stage tested: vegetative apex (VA), transition apex (TA), triple mound (TM), and lemma and stamen primordia (LP/SP) in WT (red) and *vrs5* (cyan). The error bars indicate standard deviation. For each developmental stage and genotype combination three biological replicates are used. Significance in A is tested using a Student's t-test at each developmental stage and indicated using asterisks (*: p< 0.05, **: p< 0.01, ***: p<0.001). Significance in B is tested using DESEQ2 and indicated using asterisks (*: FDR< 0.05, **: FDR< 0.01, ***: FDR<0.001).



Supplementary Figure S5: Set-up DAP-Seq experiment VRS5. A) generation of DAP-Seq libraries that are sequenced. B) Bioinformatic analysis scheme for the DAP-Seq libraries.

Supplementary Tables

Supplementary Tables can be accessed at the online version of the published chapter at: https://doi-org.ezproxy.library.wur.nl/10.1093/plphys/kiaf309

Supplementary Table S1: DESEQ2 results for each gene

Supplementary Table S2: division of differentially expressed genes over expression cluster groups.

Supplementary Table S3: DAP-sequencing peaks of VRS5 and their location and annotation in the genome

Supplementary Table S4: Distribution of annotation of DAP-sequencing peaks of VRS5 in the genome

Supplementary Table S5: DESEQ2 results of the reanalysis of GSE102191

Supplementary Table S6: Reannotation of Microarray of barley tiller buds of *int-c.5* vs. WT published by Wang et al., 2022

Supplementary Table S7: list of bona fide VRS5 targets

Supplementary Table S8: list of ZmTB1 targets involved in Jasmonate (JA) and abscisic acid (ABA) synthesis and signaling and their corresponding barley orthologs

Supplementary Table S9: TPM values for each gene for each sample

Supplementary Table S10: Primers used in this study



Chapter

3

A novel VRS5 variant untangles pleiotropic effects on barley tillering and row-type

Ton Winkelmolen
Pierangela Colleoni
Marijke Hartog
Richard G. H. Immink
G. Wilma van Esse

Manuscript in preparation

Abstract

The transcription factor TEOSINTE BRANCHED1 (TB1) and its orthologs have been central to crop domestication due to their roles in suppressing axillary branching. Our analysis of conserved TB1 domains showed that in *Poaceae* (Grasses), which include rice, maize and barley, there is an alternative transcriptional start sites (aTSS) in *TB1.* To understand the impact of the aTSS on plant development, we used barley (*Hordeum vulgare*), a key crop and model plant within the *Poaceae*. In barley, the *TB1* ortholog ***V****ulgare* ***R****ow-type* ***S****ix 5 (VRS5)* regulates tiller and spike development. The identified aTSS results into two distinct VRS5 isoforms, VRS5α and VRS5β. Through targeted mutagenesis, we show that expression of only VRS5β enables untangling of pleotropic effects of VRS5 on tillering and lateral spikelet development, with VRS5α being essential for repressing tillering, but not for lateral spikelet repression. Furthermore, we show that VRS5 regulates lateral spikelet development together with HvTB2 through forming a protein-protein interaction. Intriguingly, VRS5α and VRS5β differ functionally from each other through different DNA binding in complex with HvTB2. Our findings show that the generation of *VRS5* transcript isoforms adds an additional, not yet recognized regulatory layer, allowing fine-tuning of plant and spike architecture in barley.

Introduction

Modification of plant architectural traits have been a central strategy in crop improvement since the earliest stages of domestication, when humans started to select enhanced performance and resilience in a particular growth habit (X. Huang et al., 2021). A classic example is the suppression of spike brittleness to prevent natural dispersal of seeds, a trait that was targeted in major cereals such as rice, wheat and barley (Konishi et al., 2006; Pourkheirandish et al., 2015; Simons et al., 2006). Shoot architecture has played a similarly central role, as underscored by the success of the green revolution with semidwarf rice (Oryza sativa) and wheat (Triticum aestivum) cultivars carrying reduced-height alleles such as *semi-dwarf1 (sd1)*, which conferred lodging resistance and improved harvest index under high-input conditions (Khush, 2001; Spielmeyer et al., 2002). Similarly, the domestication of maize (*Zea mays*) from its wild ancestor teosinte (*Z. mays ssp. parviglumis*) required discarding highly branched phenotypes in favor of a single dominant stem bearing a terminal tassel and paired lateral ears, a transformation largely orchestrated by the increased expression of *TEOSINTE BRANCHED1* (**TB1**) gene (L. Liu et al., 2019). The pursuit of higher crop productivity through optimization of plant architecture stands as both a promising frontier and an enduring challenge (van Esse, 2022). Yield is a complex trait, governed by not a single attribute but by an interplay between interdependent components such as grain number and size, branching patterns, and inflorescence architecture. Changing one of these yield components often influences others, making it hard to optimize yield through changing a single trait. The correlations that underlie tradeoffs have been well described in cereals. For example, enhancing grain number often reduces grain size due to limitations in resource allocation (Peltonen-Sainio et al., 2007; Slafer et al., 1996). While resource distribution plays a role in yield-related trade-offs, it is not the sole factor; genetic regulation, hormonal signaling, and developmental timing also contribute to these complex interdependencies. Recent studies suggest that overlapping developmental windows for grain number and grain size determination also contribute to this trade-off (Vicentin et al., 2024; Xie & Sparkes, 2021). Moreover, genetic analyses have revealed that many loci influencing grain number and grain weight co-localize and exert inverse effects, indicating a strong genetic basis for this trade-off (Sukumaran et al., 2018; Xie & Sparkes, 2021). Similarly, genes that influence both shoot and inflorescence architecture often act across multiple developmental axes, which makes the genetic decoupling of these traits inherently difficult (Liller et al., 2015). *TB1* was targeted during the domestication of several cereal crops for its role in tiller development (Clark et al., 2004; Igartua et al., 2020; Ramsay et al., 2011; Takeda

et al., 2003). Beyond tillering, *TB1* also affects inflorescence determinacy, plant height, and root architecture, underscoring its pleiotropic impact on plant form (Dixon et al., 2018, 2020; Gaudin et al., 2014; Hubbard et al., 2002). Similar multifunctionality has been observed across cereals: in barley, its homolog **VRS5/INT-C** regulates tillering and spikelet fertility (Liller et al., 2015; Ramsay et al., 2011); in wheat, elevated *TB1* dosage alters growth rate, spikelet number, and shoot morphology (Dixon et al., 2018, 2020). Despite these insights, no study has successfully decoupled *TB1*'s effects on vegetative and reproductive traits, highlighting a regulatory constraint conserved across cereal species.

We performed a detailed phylogenetic analysis of *TB1* orthologs in monocots and identified a conserved alternative transcriptional start site present in only the *Poaceae*. Using barley, a cereal plant model, we show that this alternative transcriptional start site gives rise to a second *TB1* isoform. With targeted mutagenesis, we generated lines that only harbor one isoform, causing an untangling of pleiotropic *vrs5* phenotypes on tillering and inflorescence development in barley. We also show that the protein isoforms bind differentially at different VRS5 target gene loci. Taken together, our results provide unique insights into the core role of alternative *TB1* transcriptional start sites in orchestrating plant architecture and development, representing core domestication-related traits in cereals.

Results

TB1 structure and phylogeny

To gain more insights into the overall protein structure of TB1 orthologues, we first performed a detailed analysis of TB1 in monocots. TB1, as well as dicot BRANCED1 (BRC1), belong to the CYC/TB1 subgroup of the class II TCP transcription factors (TFs) in plants (Martín-Trillo & Cubas, 2010). The TCP TFs are characterized by a conserved TCP domain with a non-canonical basic-helix-loop-helix (bHLH) structure, which facilitates DNA binding. Phylogenetic analysis of TB1 and BRC1 across monocots and dicots shows that the evolutionary divergence between TB1 and BRC1 occurred after the monocot-dicot split (**Figure S1A, Table S1, Table S2**). Next to a conserved TCP-domain (**Figure S1B)**, the CYC/TB1 TCPs also have a conserved R-domain (**Figure S1C**). Further analysis of the monocot-specific branch (**Figure S2**) shows two clades; the TB1 clade and a sister clade (**Figure S1A**), corroborating previous reports (Bai et al., 2012; de Souza Moraes et al., 2022). The TB1 clade contains ZmTB1, OsTB1, VULGARE ROW-TYPE SIX 5 (VRS5, HvTB1), and the *Triticeae*-specific duplication proteins, including HvTB1-like. The grass-specific sister clade includes BRANCHED ANGLE DEFECTIVE 1 (ZmBAD1), TILLER INCLINED GROWHT 1 (ZmTIG1), and TEOSINTE BRANCHED 2 (HvTB2). Protein alignment of the monocot-specific branch shows that this last clade has lost several amino acids in the R-domain, while the TB1 clade still has an R-domain, like the CYC/TB1 proteins in the dicots (**Figure S2A**). To understand more about the conserved domains of TB1 specifically, we generated alignments of TB1 and most closely related clades. Previously, a phylogenetic study in TB1 orthologs in grasses revealed another conserved domain in the N-terminal part of the protein, rich in serine and proline residues, named the SP-domain (Lukens & Doebley, 2001). In our alignment, we also find this domain, but only in the subclade containing VRS5, ZmTB1, and OsTB1 (**Figure S2B**). Intriguingly, we also observed a conserved methionine in this clade, further downstream (**Figure 1A**). Although proteins can contain multiple methionines, we hypothesized that such a highly conserved methionine may point towards the presence of an alternative translational initiation site (aTIS) within TB1. Translational initiation, which marks the beginning of protein synthesis, can happen on a different methionine on the same mRNA, but alternatively can also be forced by a different mRNA isoform from the same locus as a consequence of an alternative transcriptional start site (aTSS). To understand *TB1* on a transcriptional level, we reanalyzed published long-read sequencing of pooled barley RNA (Coulter et al., 2022) and maize (B. Wang et al., 2016). Intriguingly, there are two distinct *VRS5* RNA transcripts present in barley (**Figure 1B**), and of TB1 in maize (**Figure S3**), suggesting that a different

mRNA is formed through an aTSS. The shorter transcript, *VRS5β*, starts after the annotated translational start present in the long *VRS5α* isoform (**Figure 1B**). To gain more insights into these transcripts, we focused on barley VRS5. We performed a qPCR with two sets of primers, one set only amplifying *VRS5α*, while the other set can amplify both. Three developmental stages at which *VRS5* is expressed were tested: double ridge (DR), lemma and stamen primordia (LP/SP), and awn primordia (AP). Significant differences between the total transcript (*VRS5α* and *VRS5β*) and *VRS5α* were observed at the DR and AP stage, with the highest *VRS5β/VRS5α* ratio in the AP stage (**Figure 1C**), highlighting the presence of both the *VRS5α* and *VRS5β* isoforms and their differential regulation. Our data point to the presence of two transcript isoforms, the long *VRS5α* and short *VRS5β* transcripts, formed through aTSS, and both present at different levels in subsequent developmental stages.

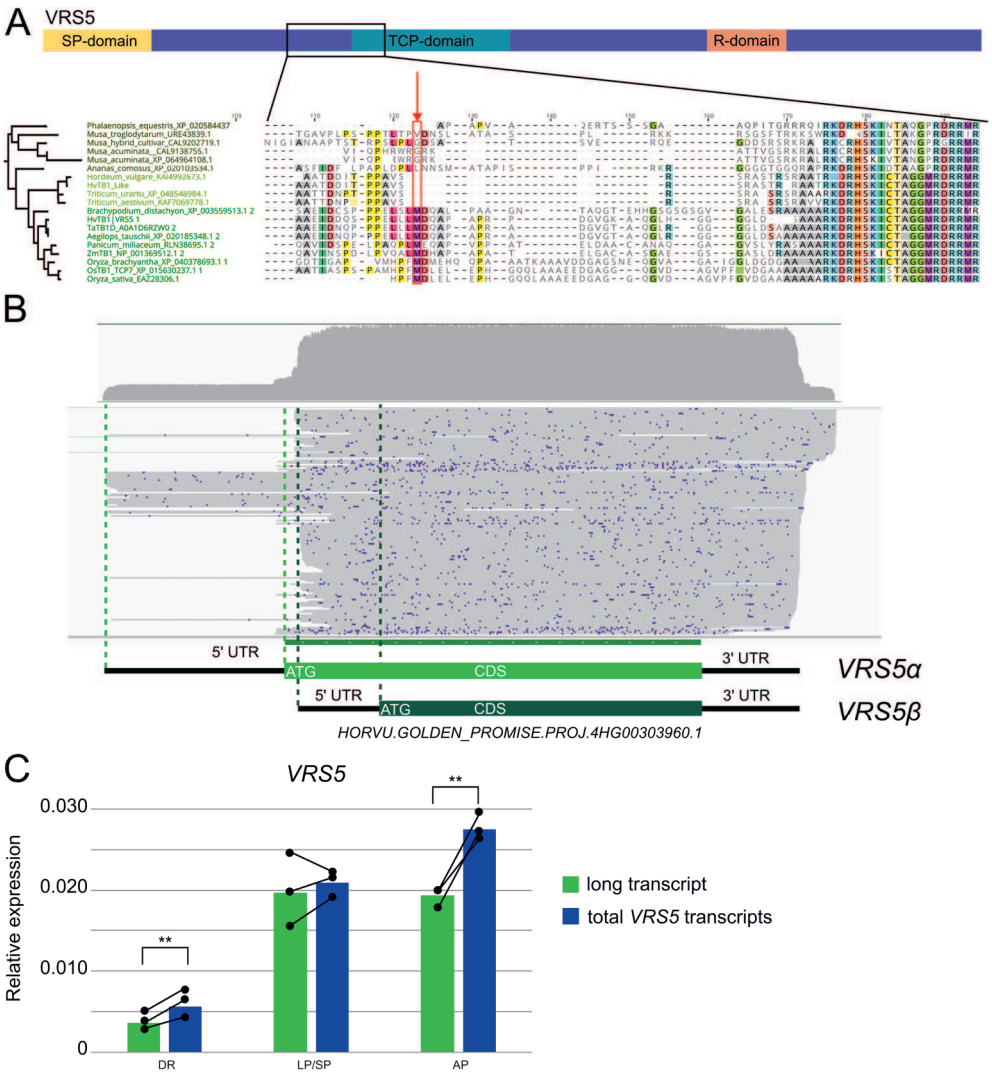


Figure 1. Conserved domains in TB1, and closely related orthologues. A) Protein alignment of TB1 and closely related TCPs from various species showing the conserved methionine specifically in the TB1 sub-clade. B) Alignment of long-read RNA sequencing reads of pooled barley RNA of cv. Barke (Coulter et al., 2022) mapped against *VRS5* in Golden Promise (Jayakodi et al., 2024). The dashed lines represent the location of the transcriptional start site (TSS) and start codon (ATG) of *VRS5α* and *VRS5β* respectively, showing a schematic overview of the two *VRS5* isoforms and their corresponding coding sequences (CDS) for VRS5α and VRS5β. C) qPCR of *VRS5* isoforms in cv. Golden Promise relative to *HvActin* at different developmental stages: double ridge (DR), Lemma and stamen primordia (LP/SP), and awn primordia (AP). Primers for *VRS5α* are designed on the 5'UTR of *VRS5α* to only amplify the long *VRS5α* transcript. Primers that amplify both VRS5 transcripts are designed on the CDS that is shared between both transcripts. Statistical difference between *VRS5α* and total *VRS5* transcripts is calculated using a paired t-test with asterisks indicating significance (*: $p<0.05$, **: $p<0.01$). n = 3 biological replicates.

Control of tillering and row-type through different VRS5 isoforms

The shorter transcript, *VRS5β*, starts after the annotated translational start present in the long *VRS5α* isoform, meaning that translation of VRS5 cannot occur from this transcript (**Figure 1B**). Using the hypothesis that the conserved methionine in VRS5 (**Figure 1A**) can indeed be used as an alternative translational initiation site, the shorter transcript can form a protein VRS5β (**Figure 1B**). The longer transcript would be able to translate VRS5 protein, hereafter named VRS5α, but potentially VRS5β as well (**Figure 1C**). Predictive modeling using AlphaFold predicted that both the VRS5α and VRS5β would give rise to a DNA-binding protein, with main difference being the absence of the SP domain in the VRS5β-isoform, while the DNA-binding TCP domain is unaltered (**Figure S4**). To understand the function of the VRS5 isoforms in barley, we performed gene editing to generate lines that can only form the short isoform VRS5β. This resulted in two independent lines, *vrs5α-1* and *vrs5α-2*, that have deletions in the coding sequence of VRS5α, causing a frameshift, while the CDS of VRS5β remains unchanged (**Figure 2A, Figure S5A**). For comparison in an isogenic background, we also included a full knockout of both isoforms, *vrs5,* which has an 857bp deletion (**Figure 2A, Figure S5A**). The *vrs5* mutant showed a significantly increased tiller number compared to WT and an intermediate row-type phenotype (**Figure 2B,C,D**), corroborating previous reports (Liller et al., 2015; Ramsay et al., 2011; Zwirek et al., 2019). Also, a difference in plant height and flag leaf emergence was observed between *vrs5* and WT (**Figure S6A,B,C**), as reported previously (Zwirek et al., 2019). Intriguingly, *vrs5α-1* and *vrs5α-2*, which can only translate the short VRS5β protein, showed a significantly increased tiller number compared to WT (**Figure 2B**), but a two-rowed spike like WT (**Figure 2C,D**). This suggests that VRS5β can regulate lateral spikelet development, but not tiller development. Moreover, although *vrs5α* mutant spikes are two-rowed, the spikes are shorter and the central spikelets are smaller compared to WT (**Figure S7, Figure S8**). Expression of only the VRS5β isoform thus results in an uncoupling of the tillering and row-type phenotypes of *vrs5*, as well as an uncoupling of the row-type phenotype with other spike architectural traits, such as spike length and central spikelet size.

Taken together, our results show that there are two isoforms of VRS5, from which the long isoform VRS5α is essential to regulate tiller development while having only the short isoform VRS5β is enough to regulate lateral spikelet development.

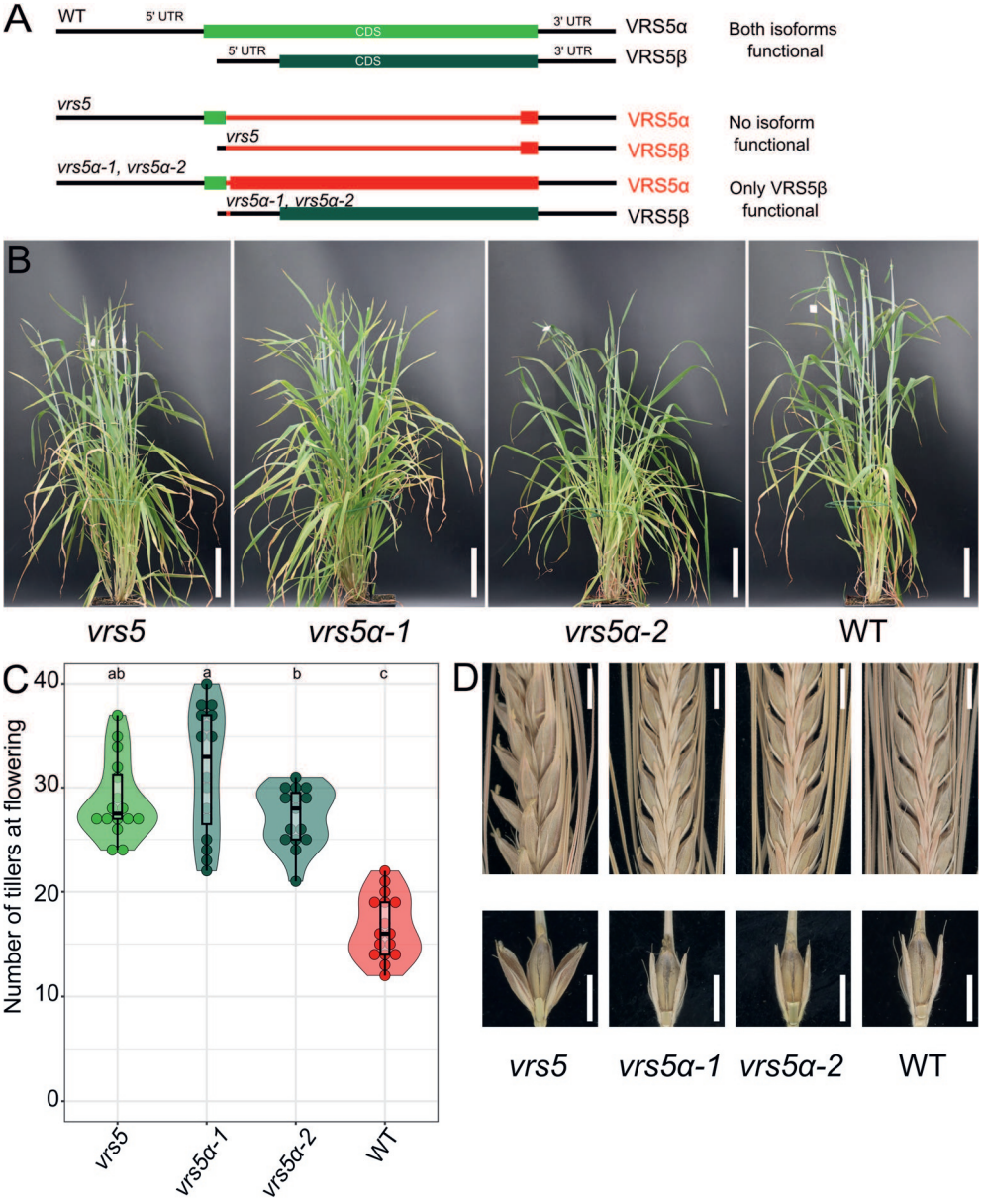


Figure 2. CRISPR mutagenesis of *VRS5* results in untangling pleiotropic effects on tillering and row-type. A) schematic protein overview of both VRS5α and VRS5β and the created mutants. B) Plant pictures of *vrs5α* lines compared to the full knockout *vrs5* and WT (cv. Golden Promise). Pictures were taken at flowering. The white bars represent a length of 10 cm. C) Number of tillers at flowering of *vrs5α* and *vrs5* lines in comparison to WT (cv. Golden Promise). Significant differences are calculated using a one-way ANOVA followed by Tukey's HSD. Different letters indicate significant differences between the lines ($p<0.05$). $n \geq 12$ biological replicates. D) Spike phenotype of *vrs5α* lines compared to the full knockout *vrs5* and WT (cv. Golden Promise). Lower images show triple spikelets, showing developed lateral spikelets for *vrs5* only. The white bars represent a length of 0.5 cm.

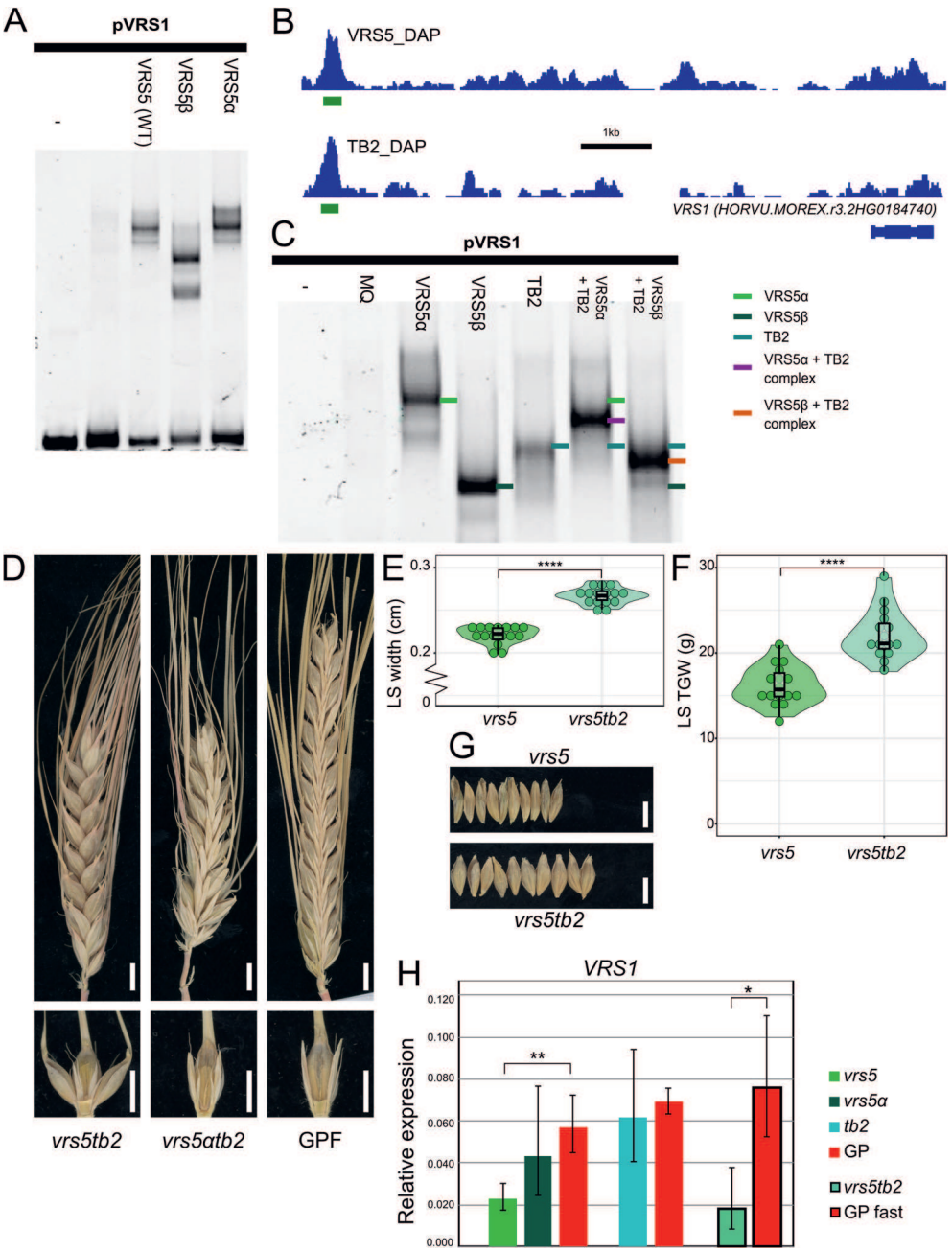

A
pVRS1
-
VRS5 (WT)
VRS5β
VRS5α
B
VRS5_DAP
TB2_DAP
1kb
VRS1 (HORVU.MOREX.r3.2HG0184740)
C
pVRS1
-
MQ
VRS5α
VRS5β
TB2
VRS5α + TB2
VRS5β + TB2
VRS5α
VRS5β
TB2
VRS5α + TB2 complex
VRS5β + TB2 complex
D
vrs5tb2
vrs5αtb2
GPF
E
LS width (cm)
0.3
0.2
0
****
vrs5
vrs5tb2
F
LS TGW (g)
30
20
10
0
****
vrs5
vrs5tb2
G
vrs5
vrs5tb2
H
VRS1
Relative expression
0.120
0.100
0.080
0.060
0.040
0.020
0.000
**
*
vrs5
vrs5α
tb2
GP
vrs5tb2
GP fast

Figure 3. HvTB2 has an additive effect to VRS5 on the regulation of row type. A) EMSA of VRS5 isoforms binding to a labeled DNA probe containing the VRS5 binding site in the promoter of *VRS1*. B) DAP-Seq trace file of *VRS1* promoter showing DAP-peaks for both VRS5 and TB2; C) EMSA of VRS5 isoforms and TB2 binding to a labeled DNA probe containing the TCP binding site in the DAP peak of VRS5 and TB2 in the promoter of *VRS1* (pVRS1). The colored bars represent the (expected) heights of the protein complexes. D) Spike images of *vrs5tb2, vrs5αtb2*, and WT (cv. Golden Promise Fast (GPF)). Lower images show triple spikelets, showing developed lateral spikelets for *vrs5tb2* only. The white bars represent a length of 0.5 cm. Plots showing E) average lateral spikelet (LS) width and F) lateral spikelet (LS) thousand grain weight (TGW) of *vrs5* and *vrs5tb2*. Significant difference is calculated using a One-way ANOVA, with asterisks indicating significance (****: $p<0.0001$). $n \geq 15$ biological replicates. G) Representation of lateral spikelet width showing 10 lateral spikelets of *vrs5* and *vrs5tb2*. White bars indicate a length of 0.5 cm. H) qPCR showing relative expression of *VRS1* compared to *HvActin* in developing inflorescences at lemma and stamen primordium (LP/SP) stage in *vrs5, vrs5α, tb2,* cv. Golden Promise (GP), *vrs5tb2* and cv. Golden promise fast (GPF). Error bars indicate standard deviation. n = 3 biological replicates. Asterisks indicate statistical significance calculated using a student's t-test between the mutants and their corresponding WT (* : $p<0.05$, ** : $p<0.01$).

VRS5 regulates row-type through interaction with HvTB2

Phenotypically, the *vrs5* mutants showed a six rowed-intermediate spike architecture, while *vrs5α-1* and *vrs5α-2* do not have a row-type phenotype (**Figure 2D**). We therefore hypothesized that both isoforms are still capable of binding and activating *VULGARE ROW-TYPE SIX1 (VRS1).* This gene is directly downstream of VRS5 in the regulation of lateral spikelet development (Winkelmolen et al., 2025)(**Chapter 2**). To test this hypothesis, we performed an Electro Mobility Shift Assay (EMSA) on the *VRS1* promoter fragment containing the VRS5 binding site. Both VRS5α and VRS5β can bind to the VRS5 binding site present in the promoter of *VRS1* (**Figure 3A**). Previously it was show that another class II TCP transcription factor, HvTB2 (also referred to as COMPOSITUM 1) can form a protein–protein interaction with VRS5 (de Souza Moraes et al., 2022). Moreover, our DNA Affinity Purification Sequencing (DAP-seq) of VRS5 and TB2 showed that both VRS5 and TB2 bind to the same region within the VRS1 promoter (**Figure 3B**). We therefore hypothesized that VRS5 and TB2 may together bind in a protein complex to the *VRS1* promoter. To test this hypothesis, we performed an EMSA to evaluate the interaction of the VRS5α/TB2 and VRS5β/TB2 protein complexes with the *VRS1* promoter. These confirmed that both VRS5 isoforms, TB2, as well as the VRS5α/TB2 and VRS5β/TB2 complexes can bind to the *VRS1* promoter fragment (**Figure 3C, Figure S9A,C**). This also suggests that VRS5 and TB2 may act together in the regulation of row-type through *VRS1*. To test this hypothesis, we generated *vrs5tb2* double mutants. The *vrs5tb2* double mutants have fully fertile awned lateral spikelets that develop into grains (**Figure 3D**). These lateral spikelets of *vrs5tb2* are wider and heavier

compared to *vrs5* lateral spikelets (**Figure 3E-3G**), showing an additive effect on lateral spikelet development compared to the *vrs5* single mutant (**Figure 3D**). In line with this, the *VRS1* expression was significantly downregulated in the *vrs5* and *vrs5tb2* mutants at the lemma and stamen primodium (LP/SP) stage, while *VRS1* expression in *vrs5α* was not reduced (**Figure 3H**). Moreover, *vrs5αtb2*, which can still express *VRS5β*, showed no six-rowed spike architecture, but a spike resembling *tb2,* with indeterminate spikelets at the basal part of the spike, and further two-rowed (**Figure 3D**)(de Souza Moraes et al., 2022; Poursarebani et al., 2020; Y. Shang et al., 2020). Together, our data suggest that VRS5 and TB2 act additively in the regulation of row-type through *VRS1* and that VRS5β on its own is sufficient to activate VRS1.

VRS5 isoforms show altered binding to the *HvGT1* promoter

In the regulation of row-type, both VRS5 isoforms bind to the VRS1 promoter together with TB2. This is in line with the two-rowed spike architecture of the *vrs5α-1* and *vrs5α-2* lines, in which only the short VRS5β isoform can be formed. However, the presence of a tillering phenotype in these lines **(Figure 2C)** suggests that the long *VRS5α* is essential for regulation of tiller bud outgrowth. Previously, it was shown that in maize and Arabidopsis, TCP transcriptional regulators regulate bud outgrowth through homeobox transcription factors closely related to VRS1; GRASSY TILLERS (ZmGT1) in maize, directly downstream of ZmTB1 (Dong et al., 2019; Whipple et al., 2011), and HOMEBOX PROTEINS (HB21, HB40, and HB53) in *Arabidopsis,* directly downstream of BRANCHED1 (BRC1) (Gonzalez-Grandio et al., 2017). To measure expression of *HvGT1* in barley *vrs5* and *tb2* lines, we performed q-PCR on crown tissue of the mutant lines at the double ridge stage. We show that *HvGT1* expression is significantly downregulated in *vrs5* and *tb2,* as well as in *vrs5tb2* (**Figure 4A**). We therefore postulated that the role of *HvGT1* in axillary bud outgrowth and its upstream regulation may be conserved across species. In barley, *HvGRASSY TILLERS* (*HORVU.MOREX.r3.4HG0399240*) has been described in relation to tip degeneration, and mutants in this gene produced more rachis nodes (Shanmugaraj et al., 2023). We generated two independent mutants of *HvGT1*, *gt1-1* and *gt1-2*. These lines showed indeed an increased number of rachis nodes, corroborating previous reports (**Figure S10**)(Shanmugaraj et al., 2023). As postulated, both *gt1-1* and *gt1-2* showed an increased number of tillers compared to WT (**Figure 4B**), similar to *vrs5* (**Figure 4B**), indicating its importance in the regulation of tiller bud outgrowth. Although *HvGT1* is downregulated in *vrs5*, no direct binding of VRS5 to the *HvGT1* locus was observed in our DAP-Seq experiment (**Figure 4C**). In contrast, the DAP-Seq of HvTB2 showed a peak ~ 1kb

upstream of *HvGT1* (**Figure 4C**). To confirm binding of HvTB2 to this region, an EMSA was performed using the TCP binding site in the TB2 binding peak as a probe. HvTB2 was able to bind to the *HvGT1* promoter fragment, while both VRS5 isoforms were not, corroborating both DAP-seq experiments (**Figure 4D**). We also tested the binding of the VRS5/HvTB2 protein complex. VRS5*α* was only able to bind to the *HvGT1* promoter together with HvTB2. This suggests that VRS5 requires the presence of HvTB2 to bind to the *HvGT1* promoter (**Figure 4D, Figure S9B,D**). Intriguingly, VRS5β was unable to bind to the *HvGT1* promoter, even in the presence of HvTB2 (**Figure 4D, Figure S9B,D**). This shows that the long VRS5α isoform is required for binding of the VRS5/TB2 complex to the *HvGT1* promoter, suggesting that VRS5α is essential to regulate tillering via *HvGT1*. This corresponds to our observation that both *vrs5α* and *hvtb2* showed a significant increased tillering (**Figure 2B,C, Figure 4B**). In line with this, also the *vrs5tb2* and *vrs5αtb2* showed an increased number of tillers at flowering compared to WT (**Figure 4E**). Taken together, VRS5 binding to the *HvGT1* promoter depends on the isoform and the presence of TB2. This points towards a mechanism, where the different isoforms have distinct DNA binding properties, depending on the protein complex.

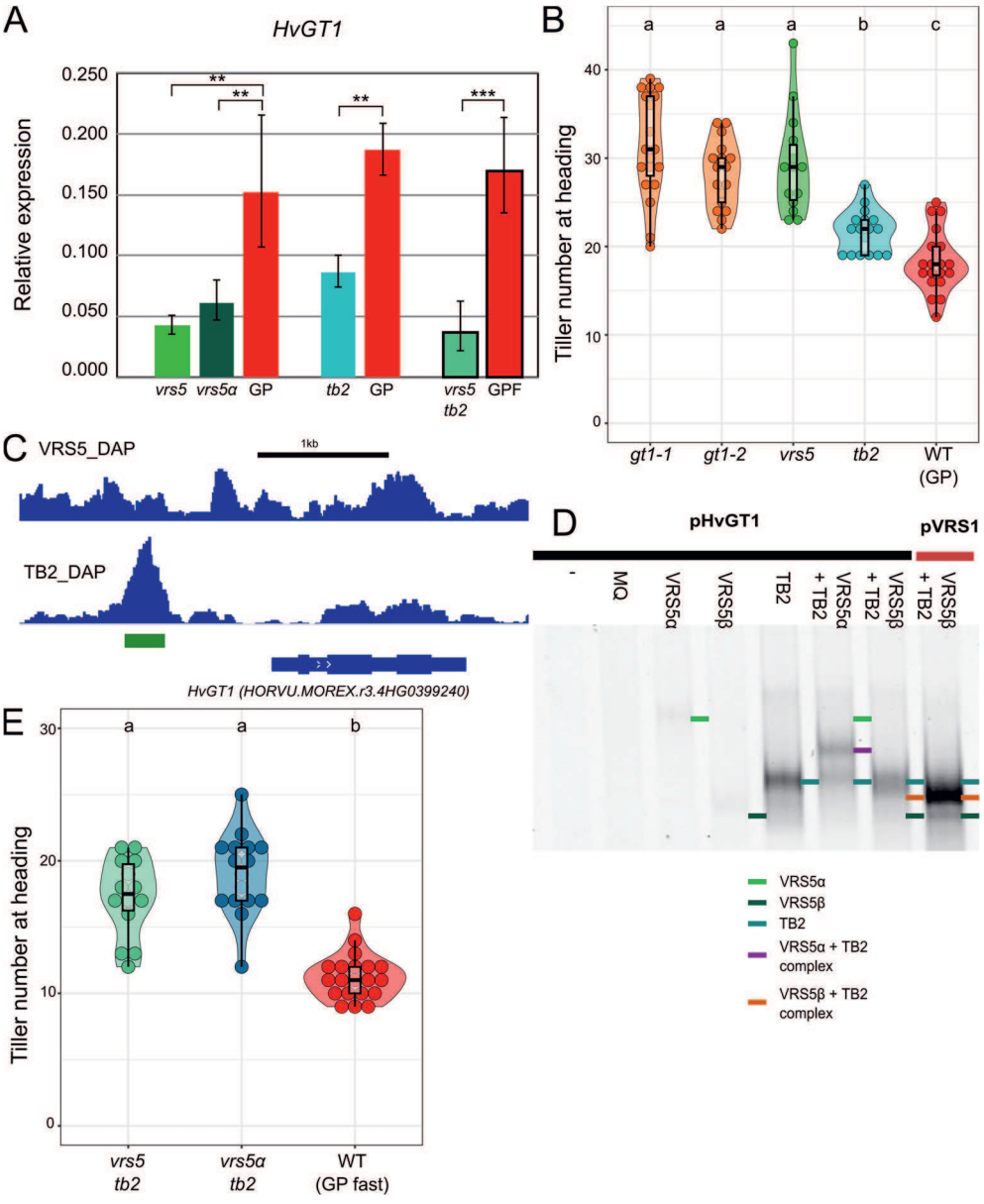

A
HvGT1
Relative expression
0.250
0.200
0.150
0.100
0.050
0.000
**
**
**
***
vrs5
vrs5α
GP
tb2
GP
vrs5 tb2
GPF
B
Tiller number at heading
a
a
a
b
c
40
30
20
10
0
gt1-1
gt1-2
vrs5
tb2
WT (GP)
C
VRS5_DAP
1kb
TB2_DAP
HvGT1 (HORVU.MOREX.r3.4HG0399240)
D
pHvGT1
pVRS1
-
MQ
VRS5α
VRS5β
TB2
VRS5α + TB2
VRS5β + TB2
VRS5α + TB2 + VRS5β + TB2
VRS5α
VRS5β
TB2
VRS5α + TB2 complex
VRS5β + TB2 complex
E
Tiller number at heading
a
a
b
30
20
10
0
vrs5 tb2
vrs5α tb2
WT (GP fast)

Figure 4: The long VRS5*α* isoform is required for tiller development. A) qPCR showing relative expression of *HvGT1* compared to *Actin* in crown tissue at double ridge stage in *vrs5, vrs5α, tb2,* cv. Golden Promise (GP), *vrs5tb2,* and cv. Golden promise fast (GPF). *vrs5, vrs5α,* and GP are grown together, while *tb2* and another GP are grown at a different time. Therefore, both corresponding GPs are shown. Error bars indicate standard deviation. n = 3 biological replicates. Asterisks indicate statistical significance calculated using a student's t-test between the mutants and their corresponding WT (** : p<0.01, *** : p<0.001). B) Tiller number of *vrs5, tb2, gt1-1, gt1-2*, and WT (cv. GP) at flowering. Different letters indicate significant differences ($p < 0.05$) between the lines, calculated using Kruskal-Wallis test followed by Dunn's to adjust for multiple testing. $n \geq 14$ biological replicates. C) DAP-Seq trace file of *HvGT1* promoter. Bar below the trace file shows significant enrichment compared to control, only for TB2, but not VRS5. D) EMSA of VRS5 isoforms and TB2 binding to a labeled DNA probe containing the TCP binding site in the DAP peak of TB2 in the promoter of *HvGT1* (*pHvGT1*). The colored bars represent the (expected) heights of the protein complexes. To show that the VRS5α/TB2 complex was formed, binding of that complex to an infrared-labeled DNA probe containing the TCP binding site in the DAP peak of VRS5 and TB2 in the promoter of *VRS1* (*pVRS1*) was shown in the last lane. E) Tiller number of *vrs5tb2, vrs5αtb2*, and WT (cv. GPF) at flowering. Significance is calculated using One-way ANOVA followed by Tukey's HSD. Different letters indicate significant difference between the lines ($p < 0.05$). $n \geq 14$ biological replicates.

Discussion

The central dogma of molecular biology describes the flow of genetic information from DNA to mRNA to protein, traditionally supporting the one gene one protein model. While the one gene–one enzyme hypothesis (1941) by Beadle and Tatum was revolutionary, molecular biology has since shown that genes are far more versatile than originally thought. Beginning in the 70's, with the discovery of alternative splicing (AS), followed by the characterization of alternative transcriptional start sites (aTSS) and translational initiation sites (aTIS), it became evident that this linear model was overly simplistic (Berget et al., 1977; de Klerk & 't Hoen, 2015; Gilbert, 1978; Pelletier & Sonenberg, 1988; Sarnow, 1989). Mechanisms such as AS and aTSS, allow for the generation of multiple transcript isoforms from a single gene, representing nature's strategy to maximize functional output from limited genomic space. Instead of encoding one protein per gene, eukaryotic cells employ these regulatory layers to tailor protein diversity.

In barley, the generation of protein isoforms, for example, has been described in response to drought (Collin et al., 2025). Similarly, the barley pan-transcriptome shows the presence of alternative transcript variants, generated through AS and aTSS (W. Guo et al., 2025). The usage of aTSS has been described in plants as a potential mechanism to generate distinct protein isoforms, and the presence of aTSS is reported in transcriptome or specific TSS identification studies (Alfonso-Gonzalez & Hilgers, 2024; Mejía-Guerra et al., 2015; Ozcan & Monroe, 2023; Pavlu et al., 2024; Thieffry et al., 2022; Ushijima et al., 2017). Moreover, the natural variation in TSS have been described in cereals, highlighting the presence of plasticity in promoter regions (Mejía-Guerra et al., 2015; Ozcan & Monroe, 2023). However, despite accumulating evidence for functional transcript diversity, the phenotypic consequences of selectively disturbing individual transcript isoforms remain largely unexplored. Here we show that the main domestication related gene *TB1* has an evolutionary conserved aTSS in the *Poaceae*. Using barley, a monocot model, we show that there are two distinct transcripts, the long *VRS5α* and short *VRS5β* isoforms, of which the shorter one is formed through aTSS. While the absence of both isoforms results in plants that have both a tillering and row-type phenotype, the *vrs5α* lines only have a tillering phenotype while the spike is two-rowed, similar to wild type lines that have a fully functional VRS5. Disrupting formation of the longer VRS5α isoform, resulting in *vrs5α* mutants that only harbor the VRS5β isoform, thus leads to a decoupling of the tillering and row type phenotype, indicating that trait decoupling is possible and potentially modulated by transcriptional start site variation. Although the row-type was decoupled from tillering, our *vrs5α* lines still showed shorter spikes and smaller

central grains despite being two-rowed. Previously, this was thought to be source-sink related due to the development of lateral spikelets acting as additional sinks (Liller et al., 2015; Sakuma et al., 2017; Thirulogachandar et al., 2021). Our results, however, imply a direct genetic role for *VRS5* in regulating central grain size and spike length, next to row-type.

Recently, we showed that VRS5 binds directly to the *VRS1* promoter to regulate its expression (Winkelmolen et al., 2025). *VRS1* is a well-known gene in barley, which is the most downstream target in the VRS network that suppresses the development of lateral florets (Komatsuda et al., 2007). Mutations in *vrs1* result in a complete six-rowed spike architecture, while a full *vrs5* knockout has an intermediate six-rowed phenotype, suggesting that VRS5 is not the only regulator of VRS1 expression. Our data suggest that the TCP transcription factor TB2, which was previously shown to interact with VRS5, binds to the promoter of VRS1 together with VRS5. Mutations in *HvTB2* disrupt spike determinacy in barley, leading to ectopic branching and indeterminate growth, with phenotype severity modulated by genetic background (de Souza Moraes et al., 2022; Poursarebani et al., 2020; Y. Shang et al., 2020). Here we show that the VRS1 expression is downregulated in both *vrs5* and *vrs5tb2* double mutants. The latter have a six-rowed spike architecture and a disrupted spikelet identity. This spike phenotype is similar to *vrs4* (Koppolu et al., 2013; Zwirek et al., 2019). VRS4 was shown to be upstream of *VRS5* and *VRS1* in the regulation of lateral spikelet development (van Esse et al., 2017), and *TB2* in regulating the spikelet determinacy (de Souza Moraes et al., 2022; Poursarebani et al., 2020). Our results show that TB2 and VRS5 both contribute to row-type regulation, but TB2 additionally controls spikelet determinacy, suggesting partial functional redundancy as well as distinct developmental roles. While in the regulation of row-type, both VRS5 isoforms bind to the *VRS1* promoter in the presence and absence of TB2, the interaction with *HvGT1* in the regulation of tillering differs between the VRS5 isoforms. Binding of TB1 to the *HvGT1* promoter was previously shown in a maize *in vivo* ChIP-Seq experiment (Dong et al., 2019). Like in maize, HvGT1 in barley is involved in the regulation of tillering, yet the role of VRS5 in the regulation of *HvGT1* was thus far unclear. While our DAP-Seq experiment showed no binding of VRS5 to the barley *HvGT1* promoter, the *HvGT1* expression in the *vrs5* mutants was significantly reduced. Intriguingly, VRS5α can only bind the promoter of *HvGT1* in complex with TB2, whereas VRS5β cannot. This suggests that the observed tillering phenotype in *vrs5α* may be attributed to distinct interactions of the isoforms. To what extent this mechanism expands genome-wide remains to be elucidated. Our findings challenge the prevailing view that architectural traits in cereals are constrained by pleiotropy at key developmental regulators such as *TB1*. Demonstrating that vegetative and

reproductive traits can be uncoupled reveals unexpected modularity in cereal development. This insight opens new avenues for precision breeding, enabling the design of ideotypes that combine optimized shoot architecture with enhanced reproductive output. More broadly, it suggests that even deeply conserved gene networks, such as for TB1 in *Poaceae*, may retain functional plasticity, offering a new perspective on how developmental constraint can be overcome and how regulatory modules evolve in plant systems.

Materials & Methods

CRISPR mediated mutagenesis

CRISPR-Cas9 mediated mutagenesis of *VRS5,* and *HvGT1* was performed using the previously described in-house CRISPR vector system (Winkelmolen et al., 2025). For each target, three guides were designed (**Table S3**) and cloned into an optimized Cas9 scaffold under control of the TaU6 promoter (Dang et al., 2015; Parry et al., 2016), available at addgene: ID:231030 - 231033. The final level 2 vector used for *in-planta* transformation contained the intron-optimized hygromycin resistance cassette (pICSL11059), the Cas9 expression cassette (pICSL11056), and three guide RNAs specific for the targeted gene. The construct was cloned in the hypervirulent *Agrobacterium tumefaciens* strain *AGL1 pSOUP,* and used for *Agrobacterium*-mediated transformation of barley cv. Golden Promise immature embryos (Hinchliffe & Harwood, 2019). T_0 plants were genotyped for CRISPR mutations using the Phire Plant Direct PCR Kit (Thermo Fisher Scientific) using primers described in **Table S3**. Amplified fragments were sequenced directly. For the generation of double mutants, the codon-optimized Cas9 containing 13 introns and two nuclear localization signals (pAGM47523) was used (Grützner et al., 2021) in combination with four guide RNAs; two targeting *VRS5*, and two targeting *TB2* (**Table S3**).

Phenotyping

For the phenotyping of the *vrs5* mutants, seeds of *vrs5, vrs5α-1, vrs5α-2* **(Figure S5A)**, and Golden Promise (WT) were sown in square 1.3L pots containing soil. To phenotype the *hvgt1* mutants, seeds of *gt1-1, gt1-2, vrs5, tb2-1* **(Figure S5A, S10A)**, and Golden Promise (WT) were sown in square 1.3L pots containing soil. For phenotyping of the *vrs5tb2* mutants, seeds of two primary transformants and Golden Promise Fast (WT) were sown in 84-well trays containing soil. To equalize germination, the pots or trays were kept at 4°C in the dark for 5 days, before putting them in the greenhouse. Plants were grown in the greenhouse (16h light 21°C, 8h dark 18°C). The plants in the trays were genotyped for *VRS5, TB2, and* Cas9 as described above. After genotyping, a selection of plants that are either *vrs5tb2* or *vrs5αtb2* were repotted in square 1.3L pots containing soil. Also, WT plants were repotted in the same way. *Vrs5tb2* and *vrs5αtb2* are a mix of plants that still contain the *Cas9* gene and plants that no longer contain the *Cas9* gene. For each round of phenotyping, tiller number per plant was recorded twice a week until flowering. After harvest, three spikes of each plant, including the main spike, were measured for spike length and number of rachis nodes. After that, the individual seeds per spike were scanned using an Epson V850 Pro scanner. Using ImageJ, the seed dimensions were analyzed and averaged per spike per

plant. The total number of seeds of three spikes of a plant was weighed to impute thousand grain weight (TGW).

Electrophoretic mobility shift assay (EMSA)
EMSA was performed as described (**Chapter 2**) (Winkelmolen et al., 2025). DNA probes of 50bp were designed from genomic DNA and synthesized (Biolegio). Probes were cloned into pGEM-T. The probes were labeled by PCR amplification using CY5.5-labeled primers. VRS5α CDS was synthesized by changing the ATG codon in VRS5 coding for a methionine into GCG, making it code for an alanine, making sure no VRS5β can be formed (**Table S3**). VRS5β CDS was cloned into pDONR201 using primers amplifying from the start codon of VRS5β to the stop codon (**Table S3**). TB2 CDS was cloned into pDONR201 using primers described (**Table S3**). CDSs in pDONR201 were cloned into an expression vector under the SP6 promoter (Jiang et al., 2022). VRS5, VRS5α, VRS5β, and TB2 proteins were prepared using TNT SP6 Wheat germ protein expression system (Promega). Combination of proteins were prepared by adding identical amount of each representative plasmid to the expression system. The EMSA binding reaction was performed for 45 minutes on ice using a binding reaction mixture (1.2 mM EDTA (pH 8.0), 0.25 mg/ml BSA, 7.2 mM HEPES (pH 7.3), 0.7 mM DTT, 60 µg/ml salmon sperm DNA, 1.3 mM spermidine, 2.5% CHAPS, 8% glycerol, 6.6 nmol/ml single-labelled dsDNA, and 2 µl of in vitro-synthesized proteins. The mixture was loaded on a 5% polyacrylamide gel and run in 1x TBE buffer for 180 minutes at 75V. The gels were scanned using a LiCor Odyssey Imaging system at 700nm. To visualize the free probes, the gels were also scanned after running for 90 minutes, after which the running of the gels was continued.

Phylogenetic analysis of TB1 clade
Protein sequences of *TEOSINTE BRANCHED1* (TB1) from maize (*Zea mays*), wheat (*Triticum aestivum*), and barley (*Hordeum vulgare*), as well as TEOSINTE BRANCHED2 (TB2) from barley and BRANCH ANGLE DEFECTIVE1 (BAD1) from maize, were used as input for the blast search in NCBI against 48 plant species spanning monocots. Gene ID of the input sequences, as well as the target plant species, can be found in **Table S1** and **Table S2**. As input for the blastp we used VRS5(HvTB1), ZmTB1, TaTB1-D, AtBRC1, and SiBRC1. Using these sequences against the NCBI ClusteredNR database (clustered at 90% identity) enables fast and representative similarity searches while minimizing redundancy. The blast searches were performed using standard settings which are: Expected threshold, word size 5, matrix BLOSUM65, Gap Cost, Existence 11, extension 1, and conditional compositional score matrix adjustments. All blast hits were filtered to match records with: percent identity between 60 and 95%, expect value 1e-6; query coverage between 15 and 100. The barley gene TB1-like was

added manually, as this gene is not present in the Morex V3 genome. Subsequently, all partial sequences and duplicates were removed, retaining in total 105 proteins, from both monocots and dicots, which were aligned using MUSCLE (R. C. Edgar, 2004). A maximum likelihood phylogenetic tree was constructed using RAxML (Stamatakis, 2014), as described previously (de Souza Moraes et al., 2022). As outgroup, the blastp hit from *Amborella_trichopoda* (ERN05207) was used. An Auto MRE model was used to assess convergence during bootstrapping, which was met after 400 bootstraps.

Long-read RNA-sequencing alignment

Previously published long-read RNA-sequencing data were used that contain RNA transcripts of a pool of barley tissues (Coulter et al., 2022). This dataset was realigned against the cv. Golden Promise reference genome from the barley pangenome (Jayakodi et al., 2024). Previously published long-read RNA-sequencing of maize containing RNA transcripts of the maize tassel and ears was used as well (B. Wang et al., 2016). The reads were realigned against the NAM 5.0 B73 maize reference genome (Hufford et al., 2021). Raw reads were aligned using Minimap2 (H. Li, 2018). For visualization of transcripts, IGV was used (Thorvaldsdóttir et al., 2013).

DAP-sequencing TB2

DAP-sequencing of TB2 was performed and the raw data were analyzed as described before for VRS5 (**Chapter 2**) (Winkelmolen et al., 2025). The coding sequence of TB2 from cv. Bowman was cloned into the pSPUTK vector, where a 3xFLAG tag (pICSL50007) was fused C-terminally. As a negative control, 3xFLAG fused to GFP was used. For both TB2 and the negative control, three replicates were performed and sequenced.

RNA isolation and quantitative PCR

Seeds of *vrs5, vrs5α-1, tb2,* and WT (cv. Golden Promise), and *vrs5tb2* and WT (cv. Golden Promise fast) were sown in soil in 84-well trays. The trays were kept at 4°C in the dark for three days to enhance equal germination. After that, the plants were transferred to a growth chamber under long day conditions (16h light/8h dark) at 20°C. To score the developmental stages, three plants of each genotype were dissected under a stereomicroscope using the Waddington scale (WADDINGTON et al., 1983). Developing inflorescences were sampled at different stages: double ridge (DR), lemma and stamen primordia (LP/SP), and awn primordia (AP). Samples were immediately frozen in liquid nitrogen and stored at -80°C until RNA isolation. *vrs5, vrs5α*, and their corresponding GP control were grown together in one experiment, while *tb2* and its GP control were grown separately in a different experiment. Therefore, both GP controls are

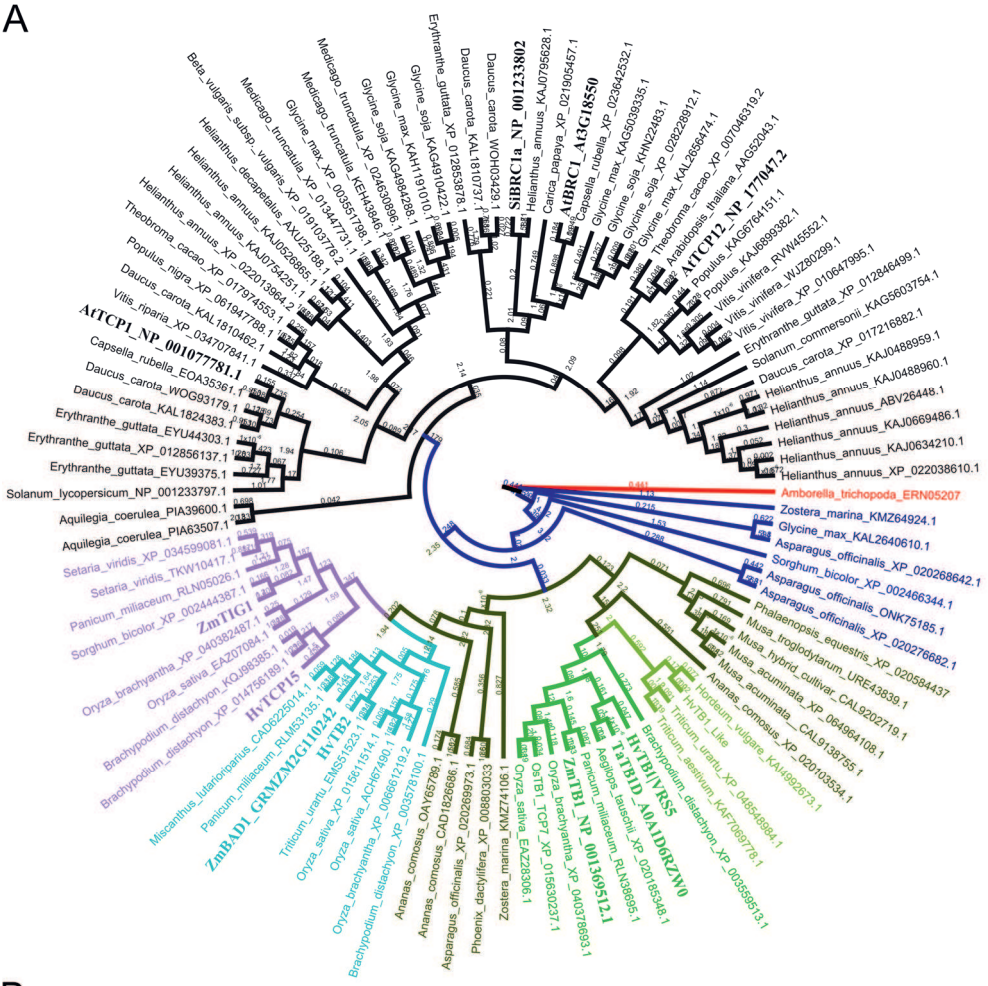
shown, and statistical comparisons were made relative to the GP control used in each respective experiment. For each developmental stage and each genotype, three biological replicates were taken, consisting of ~10 developing inflorescences. RNA extraction and quantitative PCR was performed as described (**Chapter 2**)(Winkelmolen et al., 2025). The primers used for quantitative PCR are described in **Table S3**.

AlphaFold protein modeling

To get the 3D prediction of the TCP dimers, we used AlphaFold3 (Abramson et al., 2024), accessed on: 03 June 2025. To include the crystallographic structures presented in (Y. Zhang et al., 2023) as models onto which to predict the TCPs protein structure, we set the closest possible date for the retrieval of PDB models (03 February 2025). The predictions were visualized using ChimeraX v1.9 (Meng et al., 2023). The best predictions were selected based on pLDDT and PAE values. The figures for the paper were obtained using ChimeraX v1.9.

Supplemental Figures

A



B



C



Figure S1: Phylogenetic analysis of TB1 and BRC1 in monocots and dicots. A) Phylogenetic analysis of TB1/BRC1. TB1 (green) and BRC1 (blue) homologs based on blastp of Maize, Barley, and wheat TB1 (ZmTB1, HvVRS5 (HvTB1), TaTB1D) as well as Arabidopsis and Tomato BRANCHED1 (AtBRC1, SlBRC1). This shows that divergence of the TB1 clade occurred after the monocot/dicot split. Amborella (red) was used as an outgroup. In black, dicot sequences clustering with BRC1, AtTCP1 and AtTCP12. Purple: sequences clustering with ZmTIG1 and HvTCP15, Cyan: sequences clustering with ZmBAD1 and HvTB2, Green: Sequences clustering with VRS5, HvTB1, and OsTB1. Light green: *Triticeae*-specific duplication containing HvTB1-like. Brown: Other monocot TCPs diverged after the monocot dicot split. Dark blue, dicot and monocot TCPs that are not in the BRC1 or TB1 clades. Convergence was met after 400 bootstraps, based on a AutoMRE model. The tree was generated using RaXML and visualized in Geneious prime. B) Protein sequence consensus motif of the TCP-domain of all TCPs in the tree. C) Protein consensus motif of the R-domain of all TCPs in the tree.

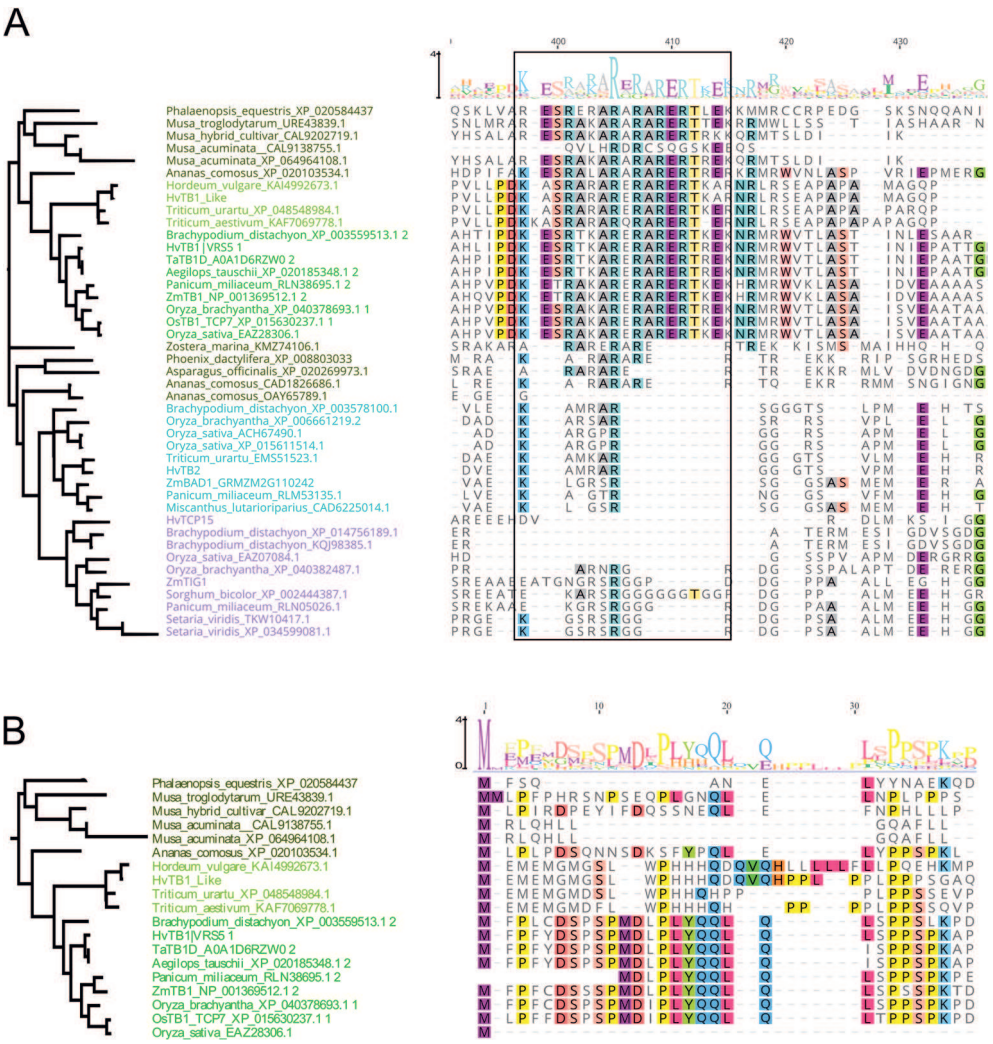


Figure S2: Conservation of the R-domain and SP-domain in monocot CYC/TB1 TCPs A) protein alignment of the R-domain of the grass-specific clade of CYC/TB1 TCPs. B) Protein alignment of the SP-domain, only present in the sub-clade containing VRS5, ZmTB1 and OsTB1.

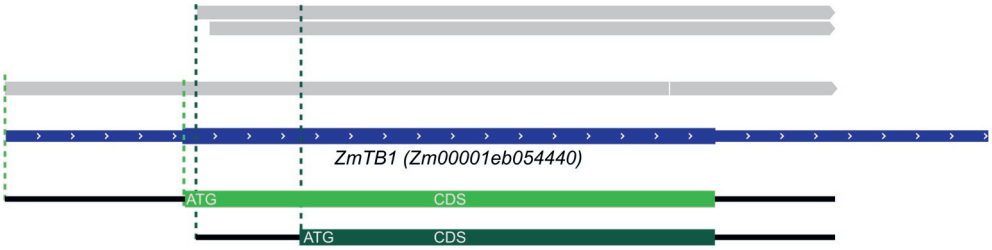


Figure S3: Long read sequencing of maize shows two TB1 isoforms. Long read RNA sequencing data of maize B73 (B. Wang et al., 2016) was re-analyzed and mapped against ZmTB1 from maize NAM5.0 (Hufford et al., 2021). The dashed green lines represent the location of the start codon and transcriptional start site (TSS) of ZmTB1α and ZmTB1β respectively, showing a schematic overview of the two *TB1* isoforms and their corresponding coding sequences (CDS).

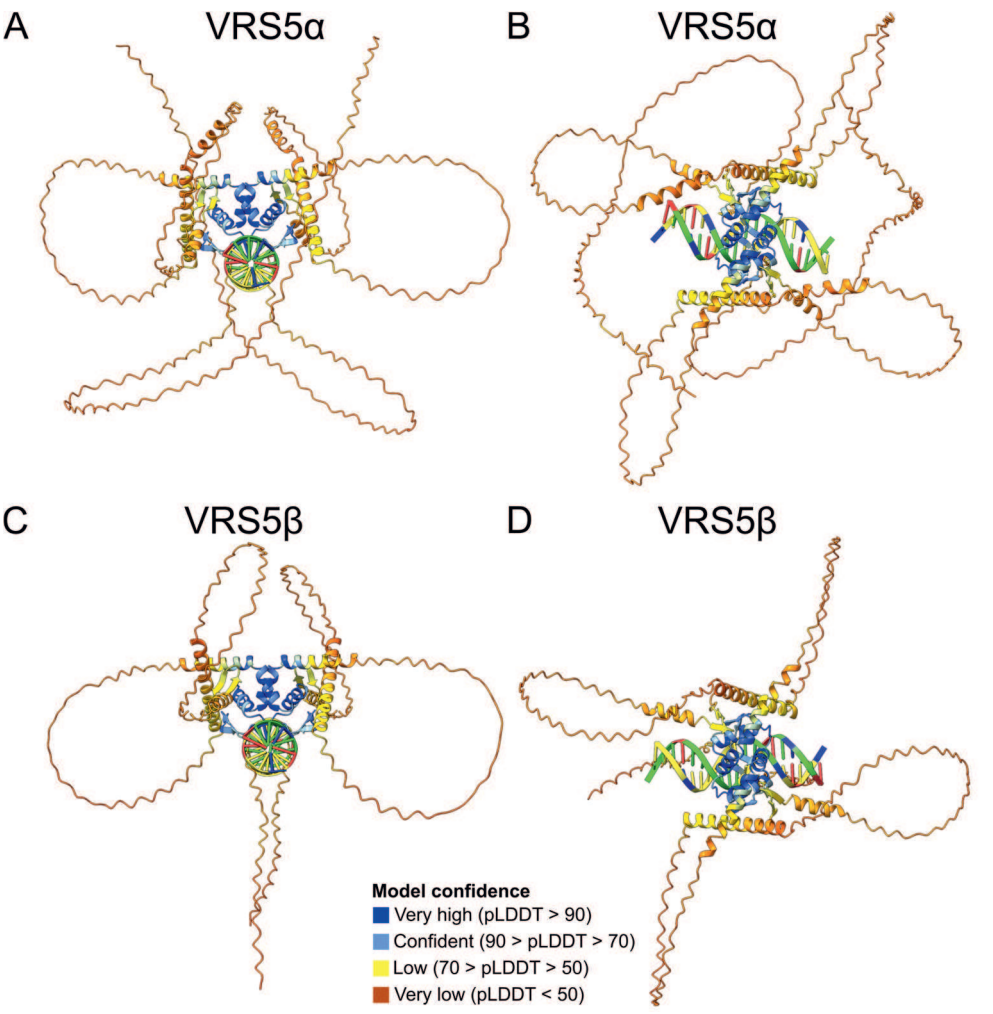


Figure S4: Alphafold-based predictions of the 3D structure of VRS5 isoforms. A+B) VRS5α heterodimer binding to DNA from the A) front and B) top and C+D) VRS5β heterodimer binding to DNA from the C) front and D) top. Color of the protein structure is based on the model confidence (pLDDT), showing that in both cases the TCP domain, forming several alpha helices coupled by small loops and binding the DNA is predicted confidently. Other parts of the proteins are predicted with low confidence.

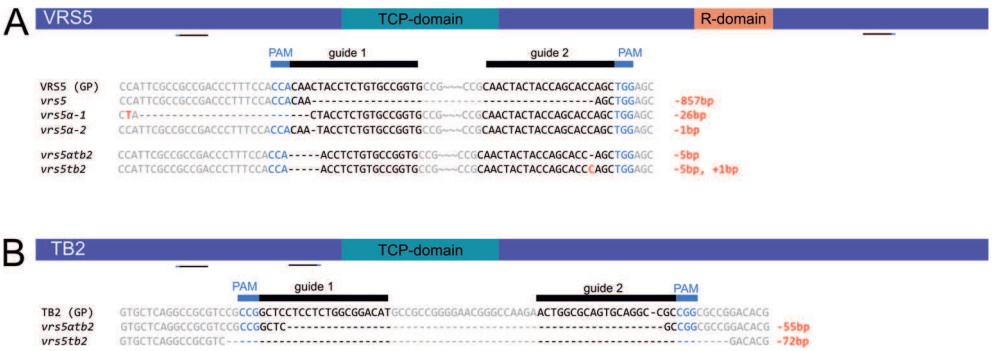


Figure S5: Mutations of created CRISPR mutants of A) *VRS5* and B) *TB2*

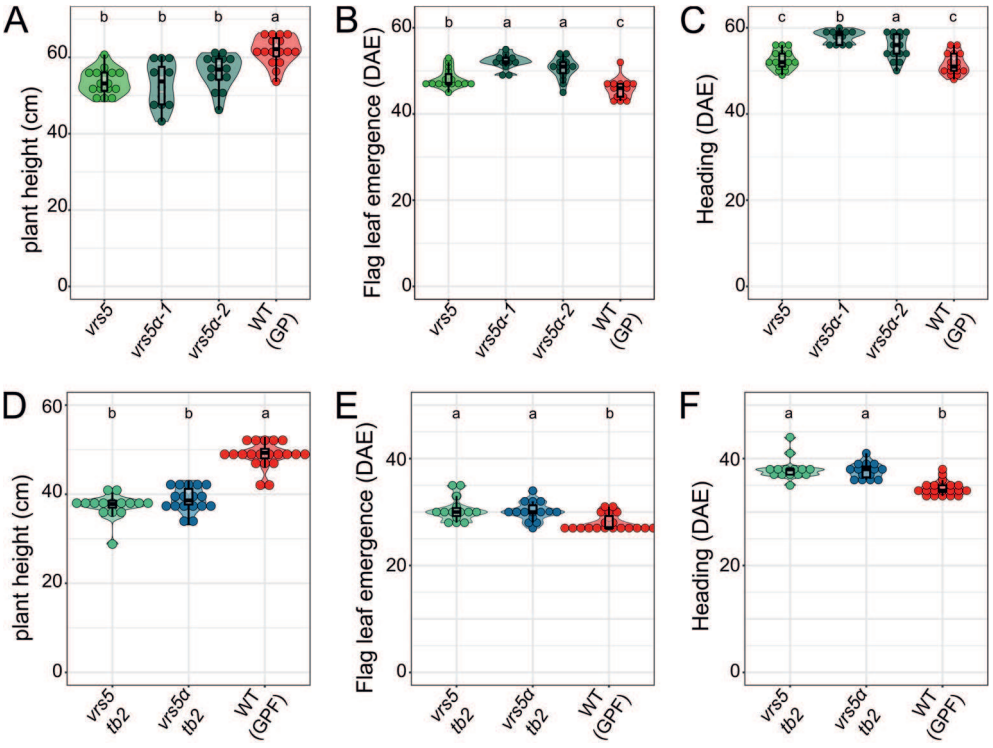


Figure S6: Plant height and flowering time of *vrs5* and *vrs5tb2* double mutants. Plots of A) plant height, B) days to flag leaf emergence, and C) days to heading of *vrs5, vrs5α-1, vrs5α-2,* and WT (cv. Golden promise). Plots of D) plant height, E) days to flag leaf emergence, and F) days to heading of *vrs5tb2, vrs5αtb2,* and WT (cv. Golden Promise Fast). Different letters indicate significant ($p < 0.05$) differences between the lines calculated using one-way ANOVA followed by Tukey's HSD (A) or Kruskal-Wallis test followed by Dunn's to adjust for multiple testing (B,C,D,E,F). $n \geq 12$ biological replicates.

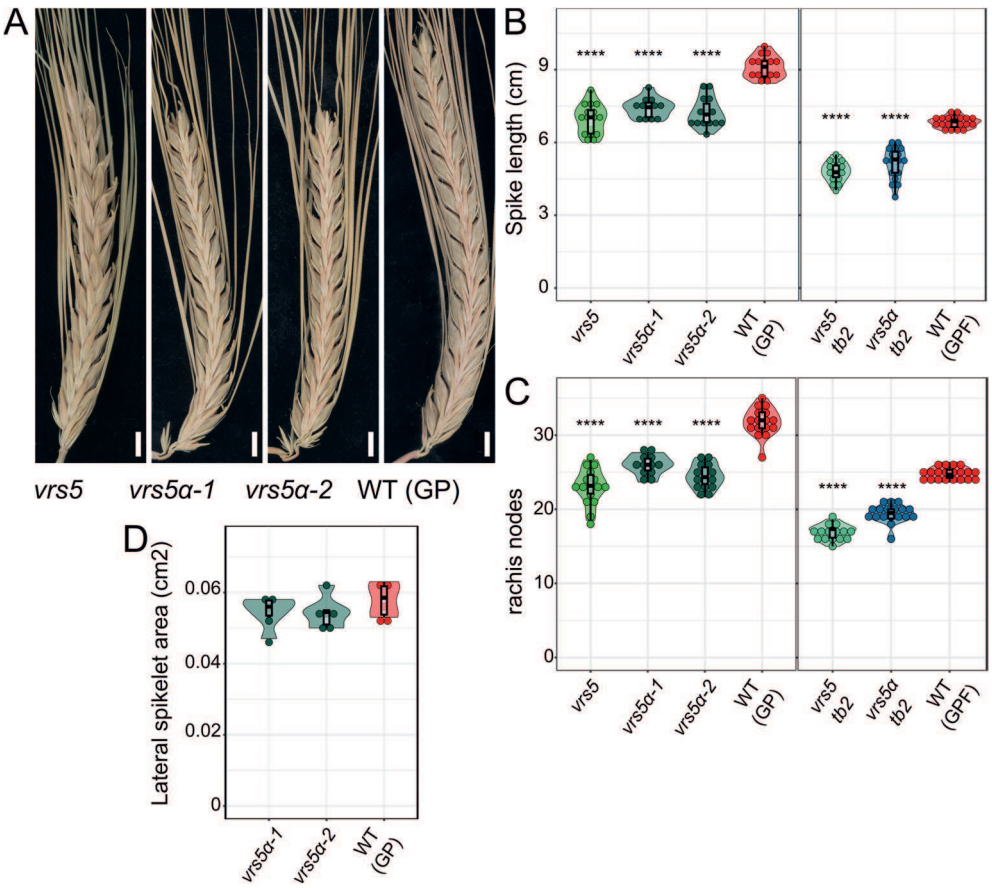


Figure S7: Detailed spike phenotype of vrs5 isoform mutants A) Spike images of vrs5, vrs5α-1, vrs5α-2, and wildtype (cv. Golden Promise). Plot of B) spike length and C) number of rachis nodes of vrs5, vrs5α-1, vrs5α-2, and wildtype (cv. Golden Promise); and vrs5tb2, vrs5αtb2, and wildtype (cv. Golden Promise fast). n ≥ 12 biological replicates. D) Plot of average lateral spikelet area of ten non-developed sterile lateral spikelets of six plants of the two-rowed lines vrs5α-1, vrs5α-2, and wildtype (cv. Golden Promise). n = 6 biological replicates. Asterisks indicate statistical differences between the mutant lines and their respective wild type. (****: $p < 0.0001$), calculated using Kruskal-Wallis test followed by Dunn's to adjust for multiple testing.

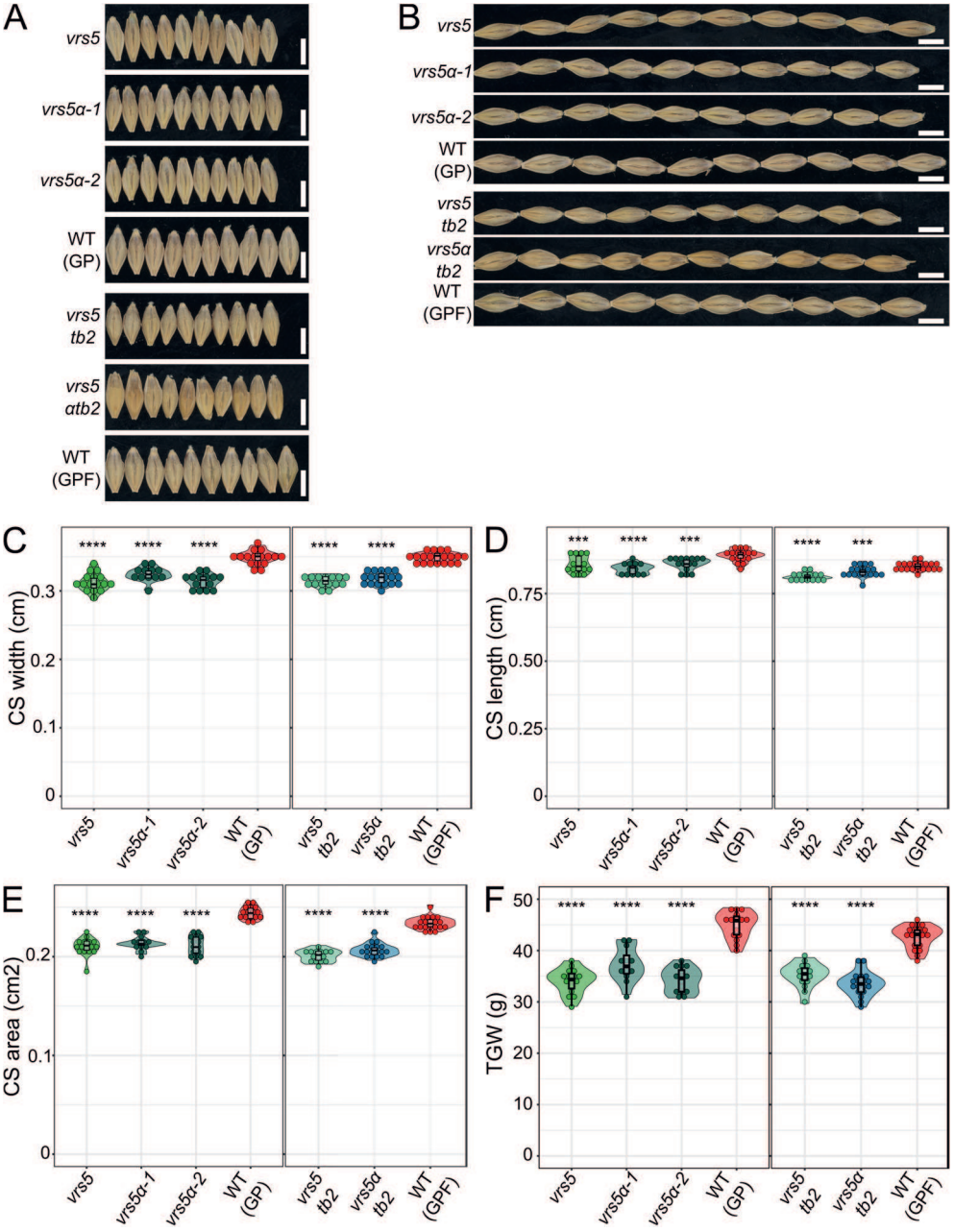

A
vrs5
vrs5α-1
vrs5α-2
WT (GP)
vrs5 tb2
vrs5 αtb2
WT (GPF)
B
vrs5
vrs5α-1
vrs5α-2
WT (GP)
vrs5 tb2
vrs5α tb2
WT (GPF)
C
CS width (cm)
D
CS length (cm)
E
CS area (cm2)
F
TGW (g)

Figure S8: Detailed central spikelet phenotype of *vrs5* isoform mutants A+B) Pictures of ten central spikelets of *vrs5, vrs5α-1, vrs5α-2,* and wildtype (cv. Golden Promise); and *vrs5tb2, vrs5αtb2,* and wildtype (cv. Golden Promise fast). Plots of central spikelet (CS) C) width, (D) length, (E) Area, and (F) thousand grain weight (TGW) of *vrs5, vrs5α-1, vrs5α-2,* and wildtype (cv. Golden Promise); and *vrs5tb2, vrs5αtb2,* and wildtype (cv. Golden Promise fast). Asterisks indicate statistical differences between the mutant lines and their respective wild type. (***: $p < 0.001$, ****: $p < 0.0001$), calculated using D) Kruskal-Wallis test followed by Dunn's to adjust for multiple testing, or C,E,F) One-way ANOVA followed by Tukey's HSD to adjust for multiple testing. $n \geq 12$ biological replicates.

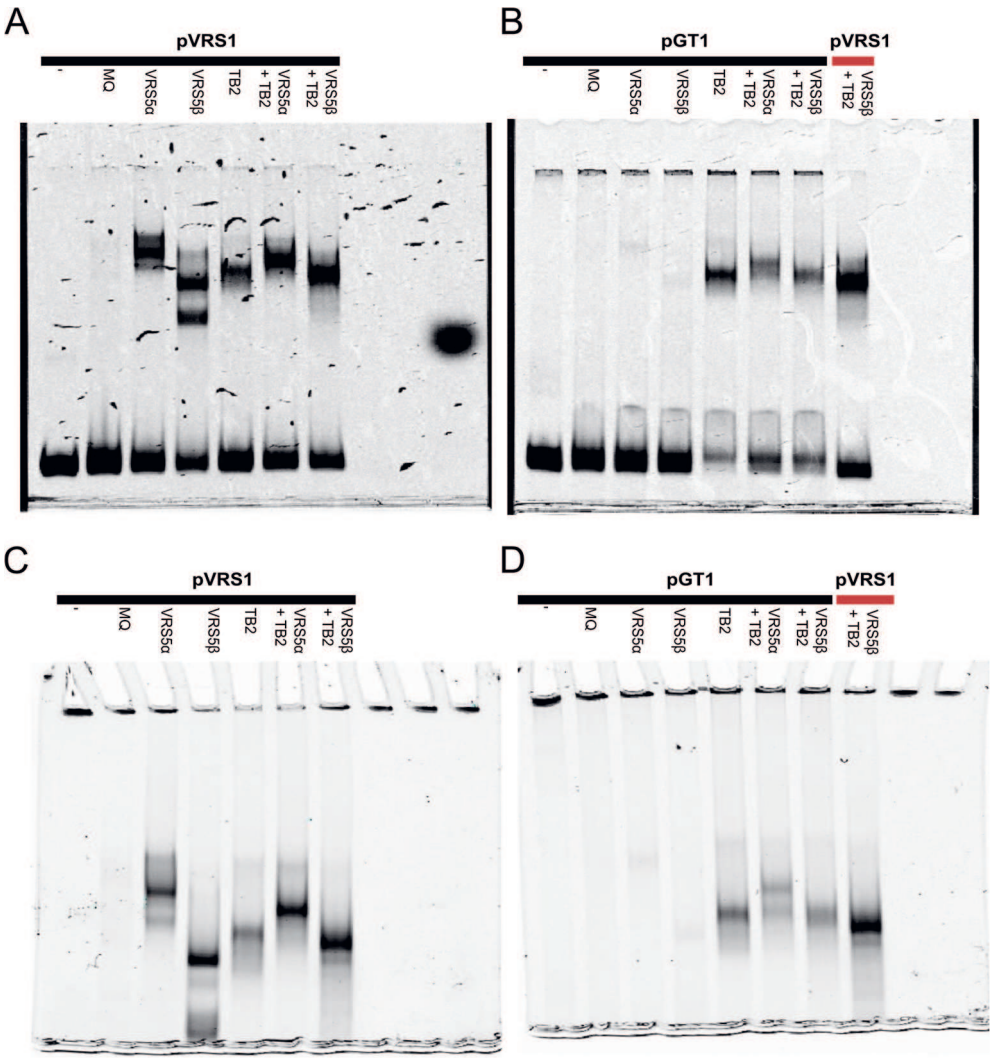


Figure S9: Full EMSA gels. Full EMSA gels of VRS5 isoforms and TB2 binding to an infrared-labeled DNA probe in the A+C) *VRS1* promoter or B+D) *GT1* promoter after running for A+B) 1.5h and C+D) 3h.

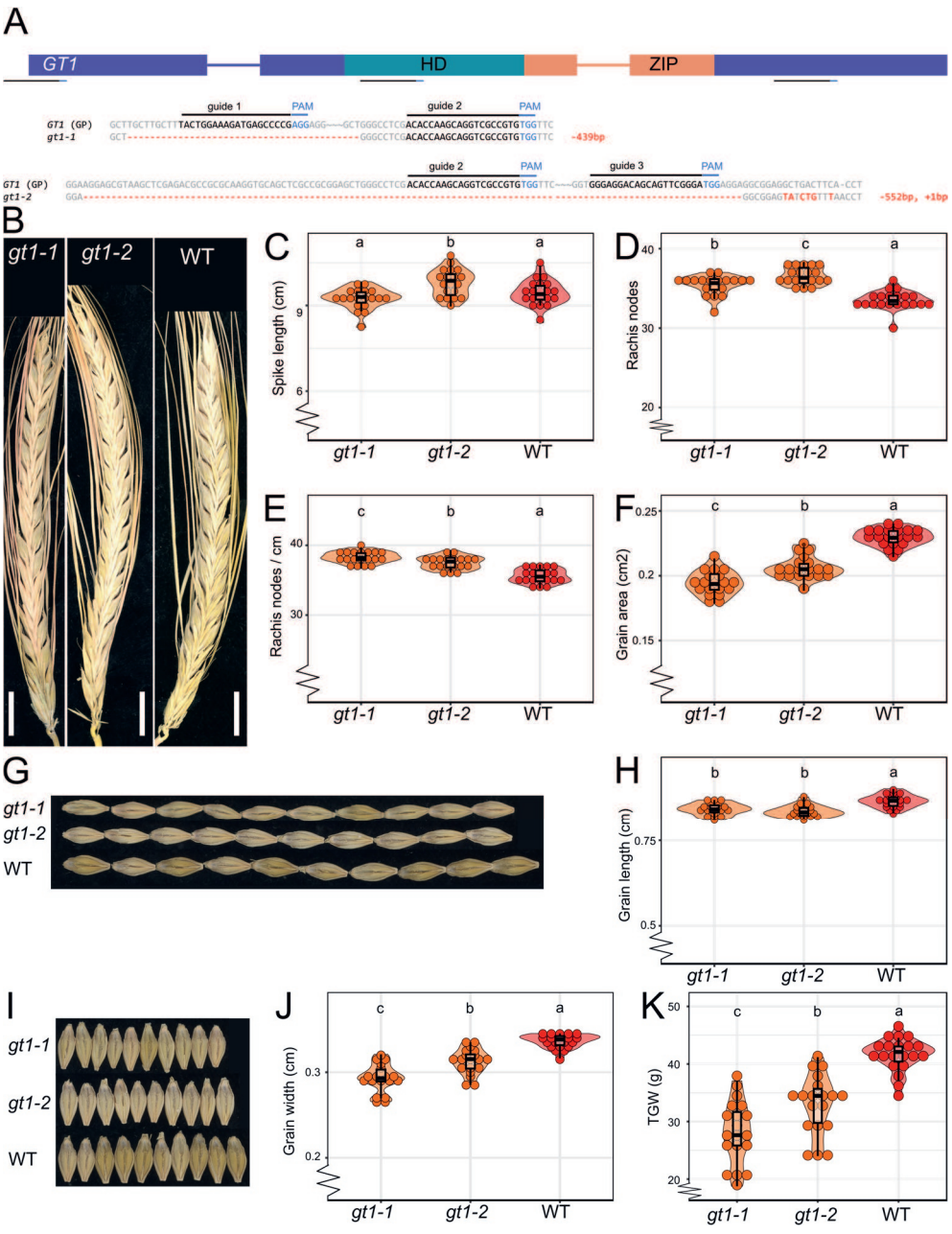

A
GT1
HD
ZIP
guide 1
PAM
guide 2
PAM
GT1 (GP)
gt1-1
-439bp
guide 2
PAM
guide 3
PAM
GT1 (GP)
gt1-2
-552bp, +1bp
B
gt1-1
gt1-2
WT
C
Spike length (cm)
D
Rachis nodes
E
Rachis nodes / cm
F
Grain area (cm2)
G
gt1-1
gt1-2
WT
H
Grain length (cm)
I
gt1-1
gt1-2
WT
J
Grain width (cm)
K
TGW (g)

Figure S10: Spike phenotype of *HvGT1* mutants A) overview of created CRISPR mutants of *HvGT1*. B) representative spikes of *gt1-1, gt1-2, and* WT (cv. Golden Promise). Plots of C) spike length, D) number of rachis nodes, E) rachis nodes density, and F) grain area of *gt1-1, gt1-2, and* WT (cv. Golden Promise). G) Pictures of ten grains of *gt1-1, gt1-2, and* WT (cv. Golden Promise) as representation of grain length. H) plot of grain length of *gt1-1, gt1-2, and* WT (cv. Golden Promise). I) Pictures of ten grains of *gt1-1, gt1-2, and* WT (cv. Golden Promise) as representation of grain width. Plots of J) grain width and K) thousand grain weight (TGW) of *gt1-1, gt1-2, and* WT (cv. Golden Promise). Different letters indicate significant ($p < 0.05$) differences between the lines calculated using one-way ANOVA followed by Tukey's HSD (C, E, F, H) or Kruskal-Wallis test followed by Dunn's to adjust for multiple testing. $n \geq 19$ biological replicates.

Supplementary Tables

All supplementary tables are available on: https://doi.org/10.5281/zenodo.17157733 or can be send by the authors upon request

Table S1: Species used for blastp of TB1 (*Zea mays*), VRS5 (*Hordeum vulgare*), TB-D1 (*Triticum aestivum*), BRC1 (*Arabidopsis thaliana*), and BRC1 (*Solanum lycopersicum*)

Table S2: Protein IDs and sequences from NCBI used in phylogenetic analysis

Table S3: oligonucleotides used in this study



Chapter

4

SOC1-like acts downstream of VRS1 and VRS5 in lateral spikelet development

Ton Winkelmolen
Pierangela Colleoni
Marijke Hartog
Richard G. H. Immink
G. Wilma van Esse

Manuscript in preparation

Abstract

VRS1 is an HD-ZIP transcription factor and key regulator of row-type in barley. Knockout mutations of *VRS1* lead to six-rowed barley spikes, where the lateral spikelets are fertile and develop into seeds. A different *VRS1* allele, *Vrs1.t*, leads to an opposite phenotype, namely the extreme suppression of the lateral spikelets, known as the *deficiens* phenotype. In this study, we identified the genome wide binding sites of barley VRS1 and identified its consensus binding sequence. In combination with RNA-seq of barley having the *Vrs1.t* allele in comparison to WT, we identified potential direct VRS1 targets. One of these targets is *SOC1-like,* which was previously also found as direct target of VRS5. Here we show that a frame shift mutation in *SOC1-like* was highly selected for in six-rowed barley. Knock-outs of *SOC1-like* in barley showed smaller lateral spikelets compared to the two-rowed WT, a phenotype similar to *deficiens*. All together, we showed that *SOC1-like* is a new important player for lateral spikelet development downstream of VRS1 and VRS5.

Introduction

Spike architecture in temperate cereals is an essential yield component that was targeted during domestication. In barley (*Hordeum vulgare* subsp. *vulgare*), one of the most profound features that governs differences in spike architecture is the development of the triple floret meristem. Elite barley cultivars exist in two groups: either six-rowed or two-rowed. In six-rowed varieties, each floret within the triple floret meristem develops into a grain, while in the two-rowed varieties, only the central spikelet is fully fertile and develops into a grain. So far, five different loci, collectively called the *VRS* genes, are involved in controlling the row-type phenotype, namely *VULGARE ROW-TYPE SIX 1* (*VRS1), VRS2, VRS3, VRS4* and *VRS5*. Remarkably, all VRS loci, except *VRS3*, code for transcription factors (TF): *VRS1* encodes a HD-ZIP TF, which is functionally conserved in wheat; *VRS2* encodes a SHORT INTERNODES (SHI) transcriptional regulator; *VRS4*, encodes a LATERAL ORGAN BOUNDARY TF and is homologues to maize *RAMOSA2* (*RA2*); and *VRS5*, which is an ortholog of *TEOSINTE BRANCHED 1* (*TB1*), encodes a class II TCP TF (Komatsuda et al., 2007; Koppolu et al., 2013; Ramsay et al., 2011; van Esse et al., 2017; Youssef, Eggert, et al., 2017). The VRS network suppresses the development of the lateral spikelets. VRS1 is the most downstream component, where reduced expression, or loss of function, of *VRS1* results in the development of lateral spikelets. Within the VRS network, only *VRS1* and *VRS5* harbor naturally occurring allelic variation that affects spike row-type in cultivated barley populations (Komatsuda et al., 2007; Ramsay et al., 2011; Youssef, Mascher, et al., 2017). For example, six-rowed varieties carry distinct *VRS1* haplotypes not typically found in wild barley (*H. spontaneum*), indicating that *VRS1* was targeted during domestication for its role in spike development (Komatsuda et al., 2007). Six-rowed barley varieties arise through independent loss-of-function mutations (e.g. *Vrs1.a*) that restore lateral spikelet fertility and diversify spike morphology (**Figure 1**)(Komatsuda et al., 2007). While the ancestral *Vrs1.b* allele maintains the canonical two-rowed phenotype found in traditional landraces, several derived alleles have reshaped row-type diversity and influenced breeding trajectories. Among these is the *deficiens* phenotype, characterized by an extreme suppression of the lateral florets resulting in enlarged central grains (**Figure 1**)(Sakuma et al., 2017). The *deficiens* phenotype is caused by the *Vrs1.t* alleles, which consist of two independent non-synonymous SNPs in a serine-rich motif in *VRS1.* The different SNPs cause a change of different serines into a different amino acid. *Vrs1.t* alleles have become dominant in modern two-rowed European cultivars (Sakuma et al., 2017). The architecture of the spike is thus, for a large part, governed by allelic variation at the *VRS1* locus (**Figure 1**).

Despite the importance of the *VRS1* gene in the regulation of lateral floret outgrowth, there is limited knowledge on the molecular mode of action of VRS1. VRS1 belongs to the HD-ZIP transcriptional regulators, which bind to the DNA to regulate expression of their downstream targets, but little is known about the protein-DNA interactions of VRS1. In this study, we performed a DNA affinity purification followed by sequencing (DAP-seq) to determine the core binding motif of VRS1. Using this, we also extracted genes that are potential downstream targets of VRS1. To gain a better understanding of the suppression of the lateral florets, as observed in the *deficiens* lines, we compared the potential VRS1 target loci to a list of differentially expressed genes in the *deficiens* line (*Vrs1.t2*). One of the genes that was identified as a potential VRS1 target and differentially regulated was *SOC1-like*. We show that CRISPR mutants in *SOC1*-like have a decreased lateral spikelet size, similar to *deficiens.* Next to that, mutations in this locus were co-selected in six-rowed barley varieties. Together, this work provides new insights into the targets of VRS1, a core regulator of spike development, and identified SOC1-like as the most downstream regulator acting in this regulatory network.

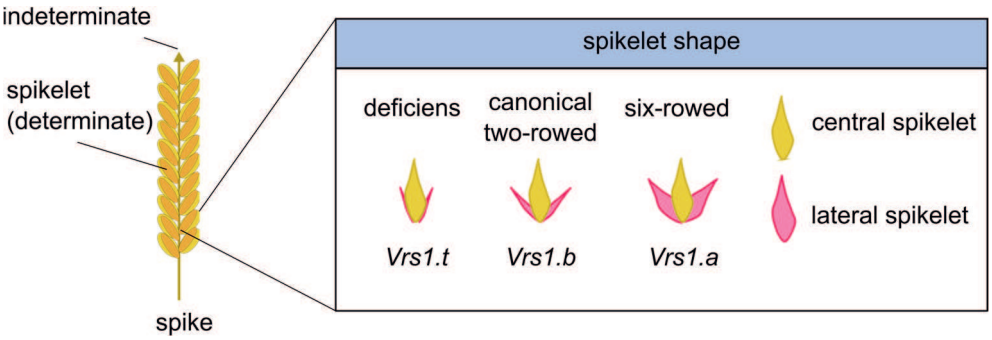


Figure 1: Spike phenotypes of *vrs1* alleles. The barley spike is indeterminate, while the spikelets are determinate. The spikelets have a triple floret meristem, where the outgrowth of the lateral florets is mostly determinant for the spike architecture. The *VRS1* alleles influence the outgrowth of these lateral florets and grains. Allelic variation within *VRS1* was selected for in spikelet architecture with: *Vrs1.t*, giving rise to *the deficiens* two-rowed phenotype, characterized by an extreme suppression of the lateral florets and an enlarged central floret; *Vrs1.b*, correlating with the canonical two-rowed varieties with moderate development but of the lateral florets, but infertile; *Vrs1.a*, with fully developed and fertile lateral florets.

Results

VRS1 binds to a core ATNATTG motif

VRS1 (*HORVU.MOREX.r3.2HG0184740*) is a homeobox transcriptional regulator, which binds to the DNA to regulate the expression of downstream genes. However, the core binding motif of VRS1, which determines its DNA binding specificity, has not yet been characterized. To identify the core binding motif of VRS1 and potential direct VRS1 target loci, we performed DNA affinity purification followed by sequencing (DAP-seq)(Bartlett et al., 2017). DAP-Seq libraries were generated using DNA from barley apical meristems, as described previously (Winkelmolen et al., 2025); **Chapter 2**). FLAG-tagged VRS1 (*Vrs1.b*) served as bait, while FLAG-tagged GFP, lacking specific DNA-binding activity, was used as a negative control. Genomic regions significantly enriched in VRS1 over GFP were defined as binding peaks. Applying an adjusted p-value threshold (<1e–5) yielded 13945 peaks (**Table S1**). Motif discovery analysis was performed on all identified peak sequences to uncover short overrepresented DNA-sequences. The most enriched motif found was AATWATTGK, present in 49.2% of the peaks (**Figure 2A**) and was tightly centered around the peak summits (**Figure 2B**), suggesting it represents the DNA sequence recognized by VRS1. Other identified, enriched motifs contained a shorter but overlapping ATNATTG motif (**Figure 2C**). This closely mirrors the pseudo-palindromic sequence CAAT(G/C)ATTG, which was previously identified as core binding motif of HD-ZIP transcription factors in the model plant *Arabidopsis* (Sessa et al., 1993). To understand which sequences are present in the half of the peaks that do not contain the most enriched motif, we performed again motif discovery analysis on the peaks not containing this motif. This analysis revealed that these peaks contain a core ATYATYG motif (**Figure S1A)**, which is slightly less specific. Of all the peaks identified, ~30% were found within 15kb of a gene (**Figure 2D, Table S1**). To identify if there are differences in the enriched DNA motifs found in the peaks within 15kb and the peaks that are distal intergenic, we did motif enrichment for both sets of peaks separately. No clear difference was found in the most enriched motif in the distal intergenic peaks and peaks within 15kb of a gene (**Figure S1B**). Taken together, we identified the ATNATTG motif as the core consensus binding sequence that is recognized by VRS1.

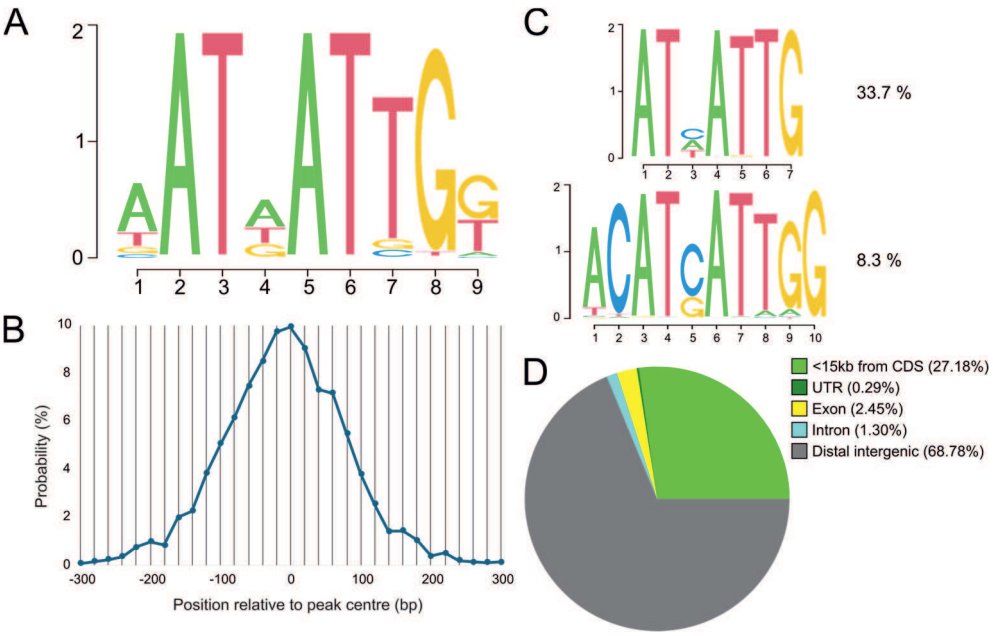


Figure 2: VRS1 binds to a core ATNATTG motif. A) Most enriched sequence logo in the VRS1-bound DAP-seq peaks, identified using STREME. B) The position of the motif shown in A relative to the center of the VRS1 DAP-seq peak as a probability percentage of bins of 20 bp. C) Second and third most enriched sequence logo in the VRS1 bound DAP-seq peaks, identified using STREME. D) Genomic distribution of all the VRS1 DAP-seq peaks.

VRS1 target genes are involved in chromatin and heterodimerization

Our DAP-Seq analysis revealed the core binding motif and genomic regions that are bound by VRS1. To identify potential direct target genes, we compared the list of loci with upstream or downstream VRS1-bound regions (**Table S1**), with a list of differentially expressed genes in the *deficiens Vrs1.t2* mutant, generated based on reanalysis of publicly available RNA-seq data (Sakuma et al., 2017)(**Table S2**). The exact SNP in the *Vrs1.t2* allele causes a change from a serine into a glycine in a serine-rich region in the C-terminal part of the VRS1 protein. The stretch of serines are hypothesized to be phosphorylated resulting in a more stable and longer-active VRS1 protein, and therefore, extreme suppression of lateral spikelets (Sakuma et al., 2017). Based on this hypothesis, we assume that Vrs1.t2 is an overactive protein, that upon binding results in enhanced regulation of its targets, which either can mean a higher or lower expression of the targets compared to WT. Note that the genes differentially regulated in *deficiens* are, either directly or indirectly regulated by VRS1. We reanalyzed the RNA-seq data (Sakuma et al., 2017) using the MorexV3 reference

transcriptome (Mascher et al., 2021). In total, 1255 differentially expressed genes with an FDR < 0.05 and a |LFC| < 0.58 were found (**Table S2**). Of these, 823 were upregulated in *deficiens*, while 432 were downregulated compared to WT. In the upregulated genes most enriched GO-terms are "structural constituent of chromatin" and "protein heterodimerization activity" (**Figure S2A**). In the downregulated genes, the most enriched GO-terms are "sequence-specific DNA binding" and "microtubule binding" (**Figure S2B**). These results corroborate previous findings (Sakuma et al., 2017).

Of the genes that are differentially regulated in *deficiens*, 64 also have a VRS1 DAP-peak within 15 kb of their gene body (**Table S3**), and are considered potential VRS1 targets. Of these genes 18 were downregulated in *deficiens*, while the remaining 46 were upregulated in *deficiens*. Of the total 64 potential VRS1 targets, the most enriched GO-terms are "structural constituent of chromatin" and "protein heterodimerization activity" (**Figure S2C**), which are similar to the downregulated genes in *deficiens*.

SOC1-like is regulated by VRS1 and VRS5 and one of its haplotypes is strongly selected for in six-rowed barley

VRS1 is a direct target of the TCP TF VRS5 in barley (Winkelmolen et al., 2025). In analogy, in Arabidopsis it has been found that the three closely related HD-ZIP genes *HB21, HB40*, and *HB53* are direct targets of the TCP TF BRC1, and together these TFs regulate genes inhibiting axillary branching (Gonzalez-Grandio et al., 2017). Given this similarity, we hypothesized that identifying genes co-targeted by VRS1 and VRS5 could reveal relevant and conserved targets for controlling lateral spikelet suppression.

We therefore compared the 64 VRS1 targets, which are differentially regulated in *deficiens* (*Vrs1.t2*) with the *bona fide* targets of VRS5. In total, there were seven genes that are targeted by VRS1 and differentially regulated in *deficiens*, and also amongst the *bona fide* VRS5 targets (**Table S4**). Interestingly, one of the seven genes is *SOC1-like (HORVU.MOREX.r3.1HG0054220,* also referred to as *HvMADS56),* in which variation was previously correlated with lateral spikelet development (Sayed et al., 2021). *SOC1-like* is downregulated in *deficiens* and has a VRS1 binding peak in its first intron (**Figure 3A**). To better understand how SOC1-like is related to other SOC1 and SOC1-like proteins, a phylogenetic analysis was done on both monocot and dicot proteins similar to barley SOC1-like. The analysis showed that the duplication resulting in barley *SOC1* and *SOC1-like* emerged after the monocot-dicot split (**Figure S3**). More specifically, there is

a grass-specific duplication resulting in *SOC1* and *SOC1-like*. Barley SOC1 clustered together with OsMADS50, of which an RNAi mutant causes late flowering (Lee et al., 2004). Barley SOC1-like clustered with OsMADS56, corroborating previous reports (Kuijer et al., 2021). *SOC1-like* is expressed during inflorescence development mainly in the lateral spikelets (**Figure S4**), pointing towards a more specific role for SOC1-like in these organs. To assess if variation in *SOC1-like* was co-selected during domestication, we reanalyzed existing exome data of 389 two-rowed and six-rowed barley cultivars and landraces (Bustos-Korts et al., 2019). There were three variants found at the *SOC1-like* locus in this dataset with an allele frequency higher than 0.05 (**Figure 3B**). The first variant is a synonymous A/C SNP, not resulting in a change in amino acid in the protein. The second variant is an intronic SNP, which has no effect on the protein, but might have implications on gene expression, as the first intron in MADS-box TFs is important for their expression (Fu et al., 2005; Hussain et al., 2019; Jeon et al., 2008; Schauer et al., 2008, 2009). This intronic SNP is outside the VRS1 binding peak observed in the first *SOC1-like* intron (**Figure 3A**). The third variant is a 1bp deletion, that would result in a frameshift, causing an early stop codon (**Figure 3D**). Next, we investigated the distribution of the haplotypes among the two-rowed and six-rowed barley lines. Interestingly, the six-rowed barleys in this dataset have almost exclusively haplotype 1 (Hap1), which contains the 1bp deletion causing an early stop codon (**Figure 3C**). Structural analysis using AlphaFold of this protein variant, reveals that the MADS-domain, I-domain and the first alpha-helix of the K-box are structurally predicted to be still intact (**Figure S5**). The MADS-domain binds to the DNA, while the I and K-domain are important for dimerization (Käppel et al., 2023; Lai et al., 2019). Presence of these domains might suggest that both proteins translated by Hap1 and Hap2 are (partly) functional. Previously, it was shown that six-rowed barleys contain strong selection for *Vrs1.a* and *Vrs5.a* (also referred to as *Int-c.a*) (Komatsuda et al., 2007; Ramsay et al., 2011). Our results show that in six-rowed barleys Hap1 of *SOC1-like* is co-selected together with *Vrs1.a* and *Vrs5.a*. Genetically these loci are all on different chromosomes, so co-selection because of linkage would be unlikely. This suggests that Hap1 of *SOC1-like* has a crucial beneficial effect in six-rowed barley.

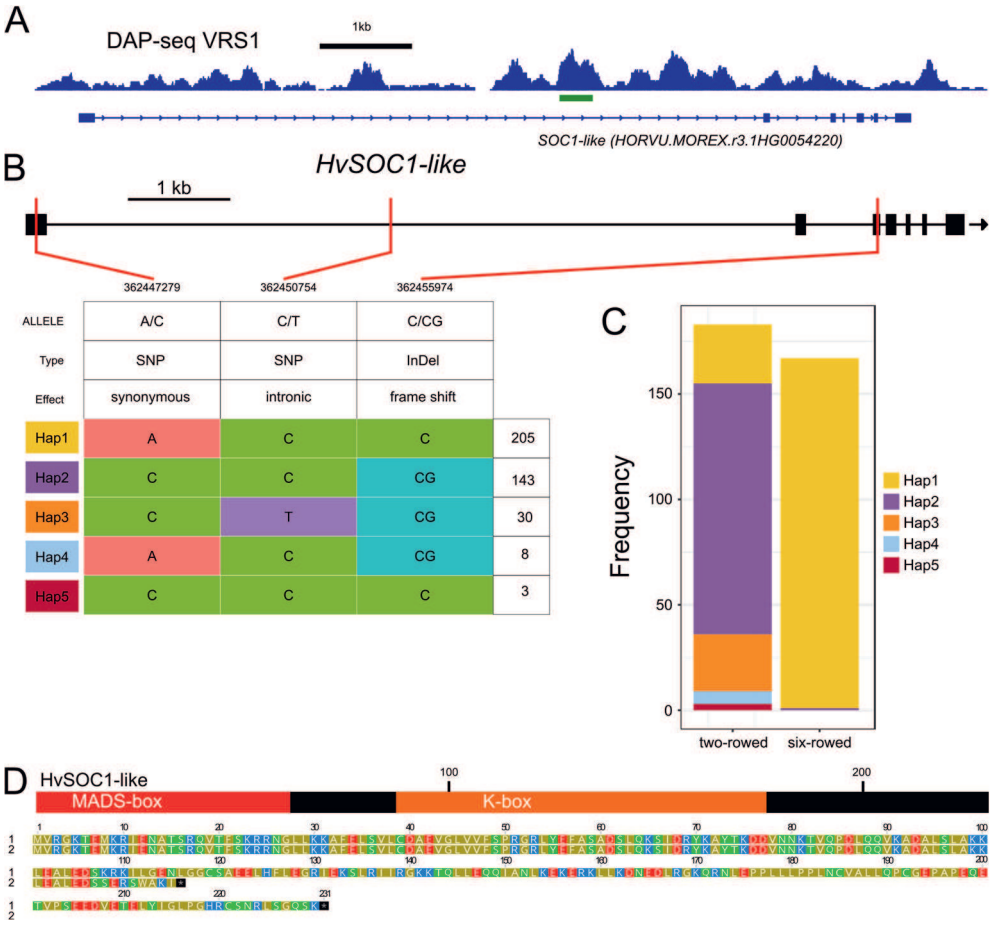


Figure 3: Haplotype analysis of *HvSOC1-like*. A) DAP-seq of VRS1 at the *SOC1-like* locus. The green bar indicates a peak significantly enriched compared to WT. Beneath the *SOC1-like* gene is represented, with blue boxes indicating exons and lines with arrows indicating introns. B) Schematic overview of the *HvSOC1-like* gene with observed variants. The boxes indicate exons, while the horizontal lines indicate introns. The red vertical lines indicate the locations of the variants. C) distribution of haplotypes shown in A over two-rowed and six-rowed barley variants. D) schematic overview of the SOC1-like protein domains identified by Prosite and protein alignment of the protein sequence of SOC1-like of 1) cv. Golden Promise containing haplotype 1 (Hap1) and 2) cv. Morex containing haplotype 2 (Hap2), showing the termination of the SOC1-like protein in the K-box in the protein sequence of cv. Morex.

SOC1-like regulates suppression of the lateral florets

Being a potential direct target of VRS1 and VRS5, having expression in the lateral spikelets, and the existence of strong selection for a specific mutation in *SOC1-like* in six-rowed barleys, all point to an important role for this gene in lateral spikelet development. To test this hypothesis, we generated CRISPR mutants targeting *SOC1-like.* To understand the phenotype of the *soc1-like* mutants, we grew two independent lines, *soc1-like_1* and *soc1-like_2,* which are homozygous or biallelic mutants of *SOC1-like* (**Figure S6A**), together with the wild type line Golden Promise Fast. Interestingly, lateral spikelet area is significantly reduced in both *soc1-like* lines (**Figure 4A-C**). While the average lateral spikelet area in WT is 0.043 ± 0.004 cm^2, the lateral spikelets in the *soc1-like_1* and *soc-like_2* were respectively 0.026 ± 0.002 cm^2 and 0.027 ± 0.004 cm^2. The observed reduction in lateral spikelet area is caused by a reduction in both length and width (**Figure 4A-E)**. Such suppression of the lateral spikelets was also observed in *deficiens* (Sakuma et al., 2017). In *deficiens*, the size of the central spikelets is increased compared to WT. We therefore also measured the central spikelet size in the *soc1-like* mutants. We observed a minor, but significant increase in central spikelet size, in *soc1-like_2* in both width and length, while this phenotype was not observed in *soc1-like_1* (**Figure S6E,F,G**). No difference in thousand grain weight (TGW) between *soc1-like* lines and WT was observed (**Figure S6H**). In *vrs1* and *vrs5* mutants, the spikes are shorter compared to WT (Liller et al., 2015; Zwirek et al., 2019). The *soc1-like* mutants did not have a significant difference in spike length and number of rachis nodes when compared to the wild type lines (**Figure S6B,C**). However, the density, the number of rachis nodes per cm of spike, was significantly decreased in both *soc1-like* lines (**Figure S6D**). Constitutive high expression of the rice ortholog of *SOC1-like*, Os*MADS56*, resulted in delayed flowering (Ryu et al., 2009), and therefore, we also phenotyped the flowering time. Concerning this trait, our knock-out mutants did not show a difference compared to WT (**Figure S6I)**.

Taken together, we identified *SOC1-like* as a de novo target of both VRS1 and VRS5, and as regulator of lateral spikelet development.

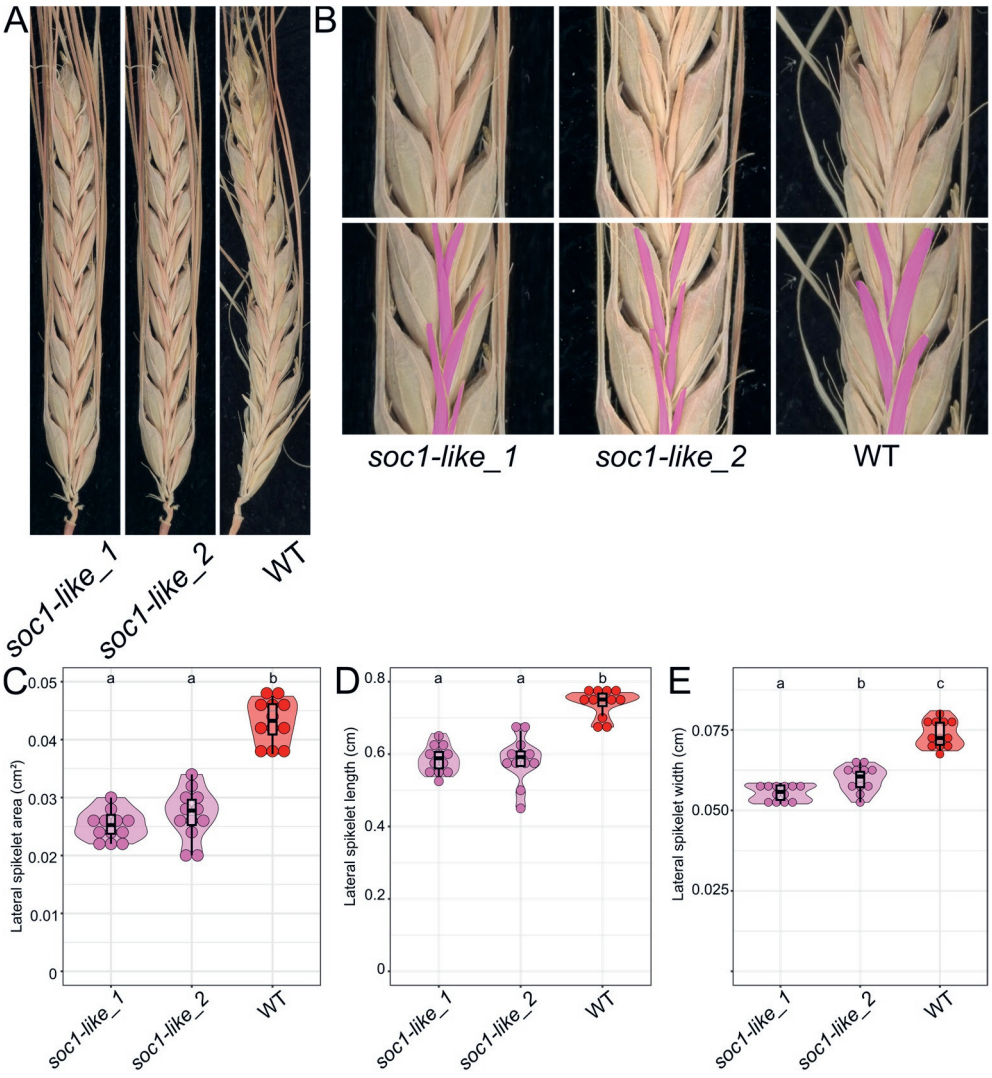


Figure 4: *soc1-like* mutant lines show decreased lateral spikelet size. A) spikes of *soc1-like_1, soc1-like_2,* and WT (cv. Golden Promise Fast). B) Zoomed-in image of *soc1-like_1, soc1-like_2,* and WT (cv. Golden Promise Fast) spikes, where in the bottom panel the lateral spikelets are colored pink for better visualization. C) Lateral spikelet area, D) lateral spikelet length, and E) lateral spikelet width of *soc1-like* lines and WT (cv. Golden Promise Fast). The colored dots indicate the average per plant, with n = 12 plants for each. Different letters indicate significant ($p < 0.05$) differences between the lines, calculated using ANOVA followed by TukeyHSD (D+F), or Kruskal-Wallis followed by Dunn's (E).

Discussion

Row-type is a major architectural trait in barley. A major player in this is VRS1, which represses lateral spikelet development when active. When VRS1 is non-functional, the lateral spikelets do develop and form grains. Despite its importance in the regulation of row-type, the molecular mode of action of VRS1 is largely unknown. As an HD-ZIP class I TF, VRS1 can bind DNA and regulate downstream targets. Here, we showed using DAP-seq that VRS1 binds to the core consensus motif ATNATTG. This is similar, but shorter than the pseudo-palindromic repeat CAATNATTG previously described as an HD-ZIP binding motif in *Arabidopsis,* based on random-sequence DNA (Sessa et al., 1993). More recently, using DAP-seq, the preferred binding motif of several *Arabidopsis* HD-ZIP class I TFs was found to be AATNATTN (W. Chen et al., 2025). This shows that HD-ZIP class I TFs bind similar but not identical DNA sequences.

Opposite to the six-rowed phenotype of the *Vrs1.a* alleles, a different set of *VRS1* alleles, *Vrs1.t*, is responsible for the *deficiens* phenotype, where there is extreme suppression of the lateral spikelets (Sakuma et al., 2017). The *deficiens* mutants are all affected in a serine-rich region in the C-terminal part of the VRS1 protein, which is supposed to result in hypophosphorylated VRS1 proteins. However, the actual hypophosphorylation of Vrs1.t and its assumed effect on VRS1 protein stability have never been proven. We assumed that Vrs1.t2 is overactive on the native targets, but we cannot exclude that this VRS1 variant binds other targets, or is incorporated into different protein complexes compared to the functional Vrs1.b variant. In this respect, a comparison of the DAP-seq of VRS1 with an RNA-seq of a *vrs1* knockout would be better to identify *bona fide* direct VRS1 targets. Nevertheless, we believe that the analysis of the *deficiens Vrs1.t2* RNA-seq resulted in biological relevant information, as among the overlap with the VRS1 DAPseq data was *SOC1-like.* Previously, resequencing of several MADS-box TFs in *deficiens* and *semi-deficiens* barley lines revealed the presence of mutations in *SOC1-like*, also referred to as *HvMADS56* (Sayed et al., 2021). In our analysis of *soc1-like* mutant lines, we did observe a reduction in lateral spikelet size compared to WT, confirming that *SOC1-like* is important for lateral spikelet development. This phenotype is in line with the observation that *SOC1-like* is downregulated in the *Vrs1.t2 deficiens* mutant. Hence, this extreme suppression can be useful for two-rowed barley lines. Surprisingly and counterintuitively, we found that almost all six-rowed barleys have a frameshift mutation of *SOC1-like,* resulting in an early stop-codon in the region coding for the K-box. This truncated protein, when formed, still contains the DNA binding MADS domain and the first alpha helix of the K-box important for MADS domain protein dimerization (Lai et

al., 2019). This suggests that this specific SOC1-like variant is still functional or even represents a gain-of-function isoform. At first glance, the fact that this exact mutation is also present in some *deficiens* and *semi-deficiens* lines (Sayed et al., 2021) seems to contradict this reasoning. However, in the *deficiens* mutants, there is a strong downregulation at the transcriptional level of the *SOC1-like* gene. Alternatively, the truncated *SOC1-like* allele is non-functional, and a knock-out of *HvSOC1-like* behaves differently in a six-rowed background compared to a two-rowed background. Combining the *soc1-like* null mutant alleles with *vrs1* and/or *vrs5* might be a good starting point to shed light on this.

Together, we found that VRS1 binds an ATNATTG motif and directly targets *HvSOC1-like*. *HvSOC1-like* is important for lateral spikelet development, as a knock-out results in extreme suppression of lateral spikelets in a two-rowed background. Haplotype analysis showed that a specific mutation in *HvSOC1-like* is co-selected in six-rowed barleys, suggesting that this variant has an agriculturally desirable effect in six-rowed barley backgrounds.

Materials & Methods

DAP-seq

DAP-sequencing of VRS1 was performed and the raw data were analyzed as described before for VRS5 (**Chapter 2**) (Winkelmolen et al., 2025). The coding sequence of VRS1 from cv. Bowman (Vrs1.b) was cloned into the pSPUTK vector, where a 3xFLAG tag (pICSL50007) was fused C-terminally. As a negative control, 3xFLAG fused to GFP was used. For both VRS1 and the negative control, three replicates were performed and sequenced.

RNA-seq analysis

Raw published RNA-seq reads of *deficiens* and WT (cv. Foma) with accession number DRA005563 were downloaded from the DDBJ sequence read archive (Sakuma et al., 2017). Raw reads were trimmed using Trimmomatic 0.39 (Bolger et al., 2014). Transcripts were quantified with the MorexV3 transcriptome as reference (Mascher et al., 2021) using salmon v1.8.0 (Patro et al., 2017) using standard settings. Differential gene expression between *deficiens* and WT was calculated using the R package DESeq2 (Love et al., 2014). Genes were considered differentially expressed when the false discovery rate (FDR) < 0.05 and the absolute log2 fold change was more than 0.58.

Phylogenetic analysis of SOC1-like

Phylogenetic analysis of SOC1-like was done as described (**Chapter 3**). Protein sequence of HvSOC1-like was used in the blast search. Gene ID of the input sequences, as well as the target plant species, can be found in **Table S5** and **Table S6**. In total, 100 protein sequences, from both monocots and dicots, were aligned using MUSCLE (R. C. Edgar, 2004). A maximum likelihood tree was constructed using RAxML, using 100 bootstraps (Stamatakis, 2014).

Identification of variants and haplotype analysis

Sequenced exome data and metadata were retrieved from the Plant Genomics and Phenomics Research Data Repository with reference number 10.5447/IPK/2019/5 (Bustos-Korts et al., 2019). Raw reads were trimmed using Trimmomatic 0.39 (Bolger et al., 2014) using the adapters described in **Table S4**. All paired reads were aligned to the barley MorexV3 reference genome (Mascher et al., 2021) using bwa (H. Li, 2013). For the variant calling GATK pipeline was used (McKenna et al., 2010). Because the GATK toolkit can only handle chromosomes smaller than 500MB, each chromosome is split in two at the centromere. After variant calling per sample using GATK function

HaplotypeCaller, the files were combined using the GATK function GenomicsDBImport. For each split chromosome, so 14 in total, the genotypes are combined into one vcf using the GATK function GenotypeGVCFs. From this file, the variants in the *SOC1-like* gene +- 5000bp with an allele frequency higher than 0.05 were selected, resulting in three variants. These variants were further analyzed in R using the package geneHapR (R. Zhang et al., 2023).

AlphaFold protein modeling

To get the 3D prediction of the SOC1-like haplotypes, we used AlphaFold3 (Abramson et al., 2024), accessed on: 15 September 2025. The protein sequences used are from Golden Promise, representing Hap1; and Morex, representing Hap2. The protein sequences were retrieved from the panBARLEX web portal (Jayakodi et al., 2024). The predictions were visualized using ChimeraX v1.9 (Meng et al., 2023). The best predictions were selected based on pLDDT and PAE values.

CRISPR mediated mutagenesis of *HvSOC1-like*

CRISPR-Cas9-mediated mutagenesis of *HvSOC1-like* was performed using the previously described in-house CRISPR vector system (Winkelmolen et al., 2025). Three guides were designed (**Table S4**) and cloned into an optimized Cas9 scaffold under control of the TaU6 promoter (Dang et al., 2015; Parry et al., 2016), available at addgene: ID:231030 - 231033. As Cas9 enzyme, the codon-optimized Cas9 containing 13 introns and two nuclear localization signals (pAGM47523) (Grützner et al., 2021) under control of the maize *Ubiquitin* promoter was used. The final level 2 vector used for *in-planta* transformation contained the intron-optimized hygromycin resistance cassette (pICSL11059), the Cas9 expression cassette as described above, and three guide RNAs specific for *HvSOC1-like*. The construct was cloned into the hypervirulent *Agrobacterium tumefaciens* strain *AGL1 pSOUP,* and used for *Agrobacterium*-mediated transformation of barley cv. Golden Promise fast immature embryos (Hinchliffe & Harwood, 2019). T_0 plants were genotyped for CRISPR mutations using the Phire Plant Direct PCR Kit (Thermo Fisher Scientific) and the primers described in **Table S4**. Amplified fragments were sequenced directly.

Phenotyping

To phenotype the *soc1-like* mutants, seeds of *soc1-like_1, soc1-like_2,* and cv. Golden Promise fast (WT)(Gol et al., 2021) were sown in square 0.5L pots containing soil. To equalize germination, the pots were kept at 4°C in the dark for 4 days, before putting them in a growth chamber, where the plants were grown to maturity (16h light 21°C, 8 h dark 20°C). Flowering time was scored.

Plants were harvested 12 weeks after emergence. Spike length and number of rachis nodes were measured for two spikes per plant, including the main spike. Of these spikes, the individual seeds, from the central spikelets and the undeveloped lateral spikelets were scanned using an Epson V850 Pro scanner. Using ImageJ, grain and lateral spikelet dimensions were analyzed and averaged per spike per plant. The total number of seeds of both spikes of a plant was weighed to impute thousand grain weight (TGW).

Supplementary Figures

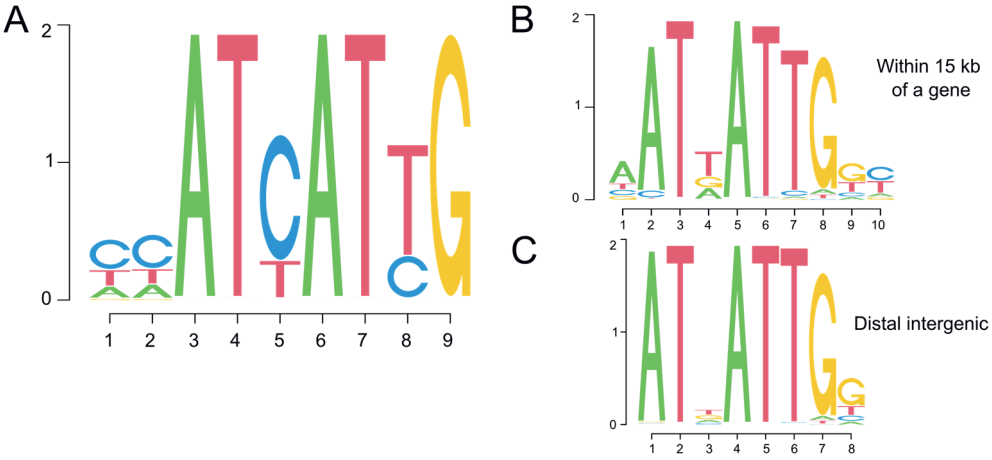


Figure S1: Enriched sequence motifs. A) Most enriched motif in all the VRS1 peaks that do not contain the most enriched motif presented in Figure 2A. B) Most enriched motif in all the VRS1 peaks within 15 kb of gene. C) Most enriched motif in all the distal intergenic VRS1 peaks.

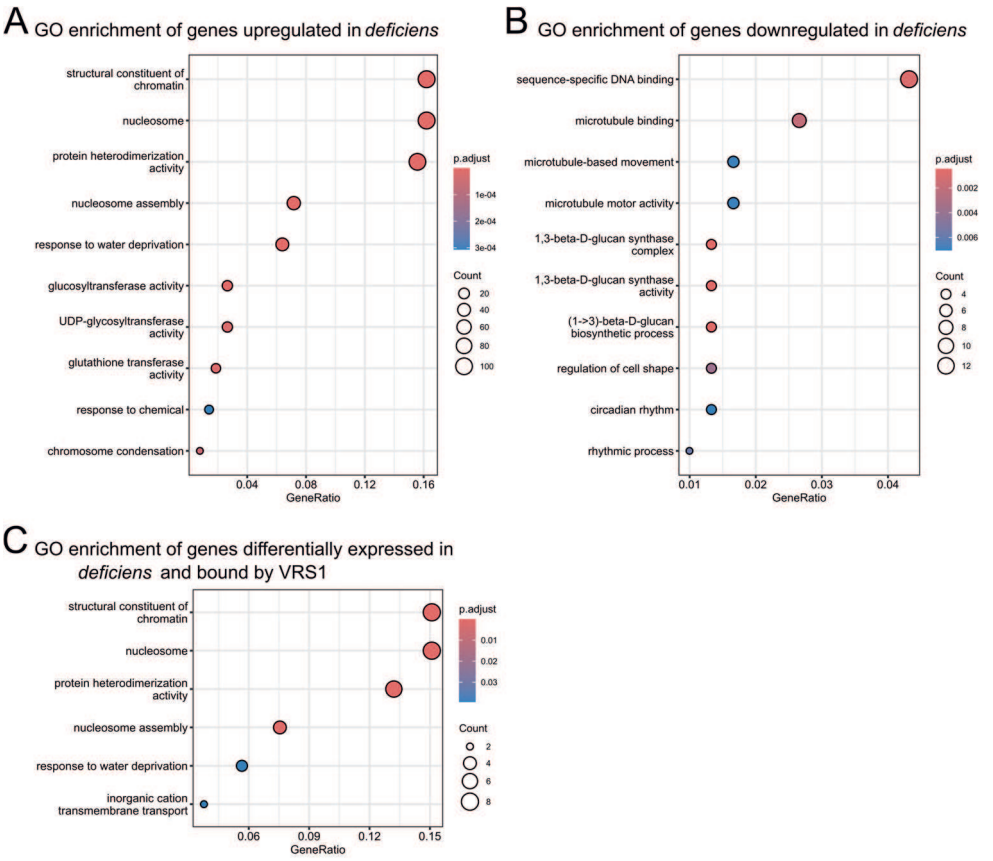


Figure S2: Enriched GO terms in A) genes upregulated in deficiens compared to WT, B) genes downregulated in deficiens compared to WT, and C) genes differentially expressed in deficiens compared to WT and having a DAP-seq peak of VRS1 within 15 kb of the gene body.

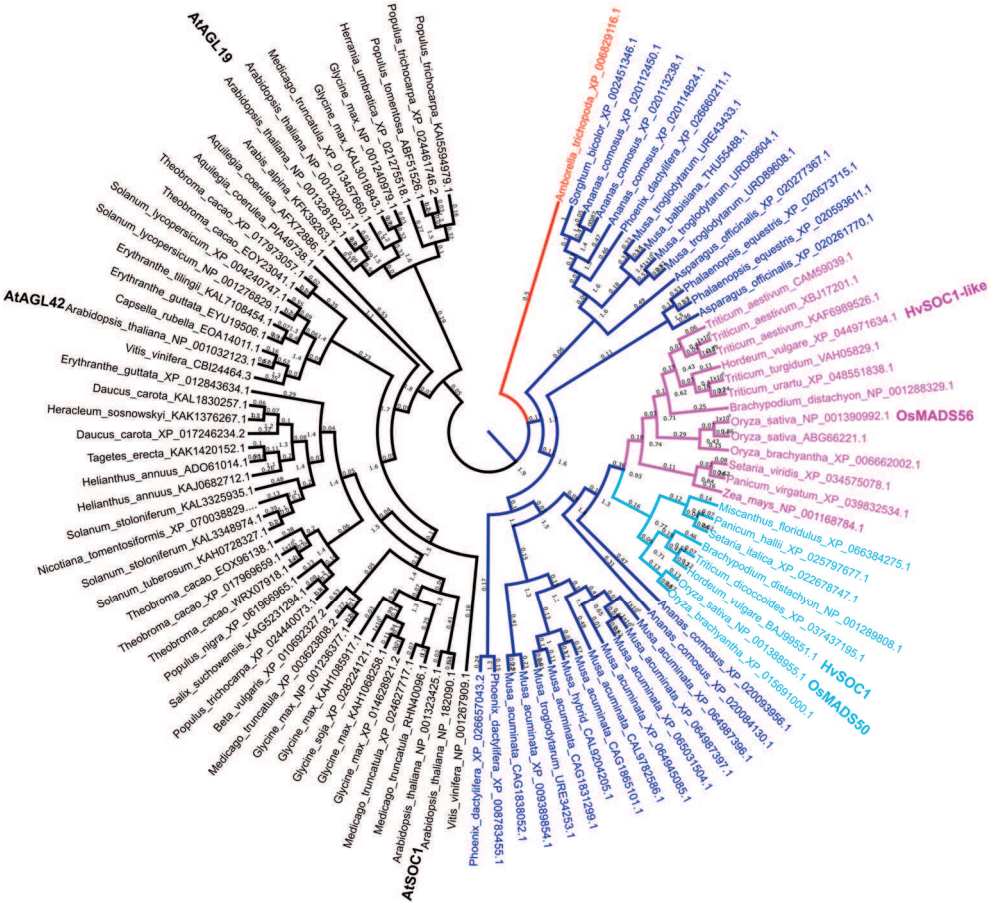


Figure S3: Phylogenetic tree of SOC1 and SOC1-like proteins in monocots and dicots. Analysis based on protein sequences similar to barley SOC1 and SOC1-like using blastp. The tree was generated using RaXML and visualized in Geneious prime.

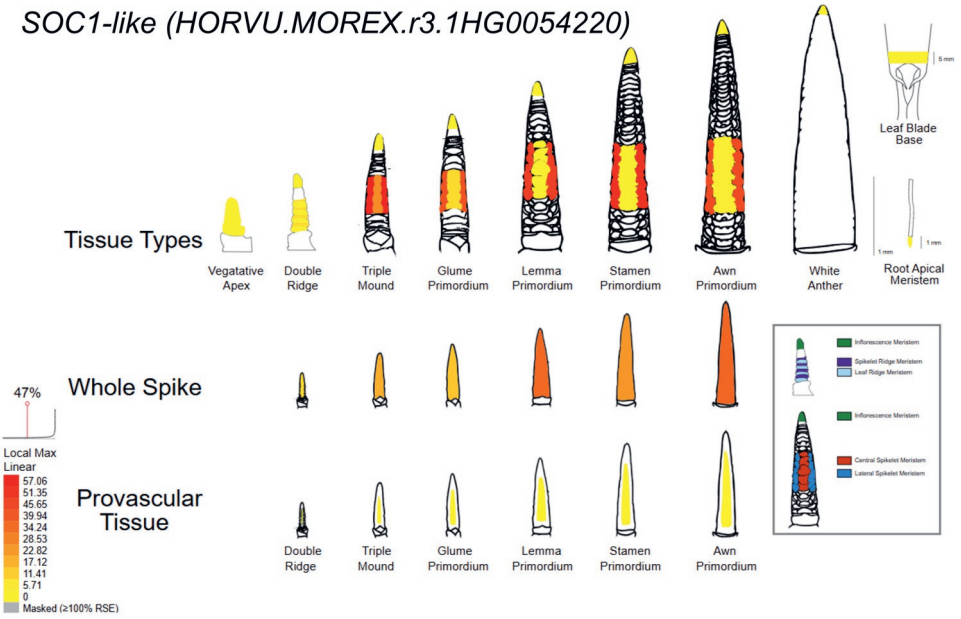


Figure S4: Expression of *SOC1-like* in the developing inflorescence retrieved from the ePlant expression atlas that uses the Thiel et al., 2021 dataset. Red indicates high expression, whereas yellow indicates low expression.

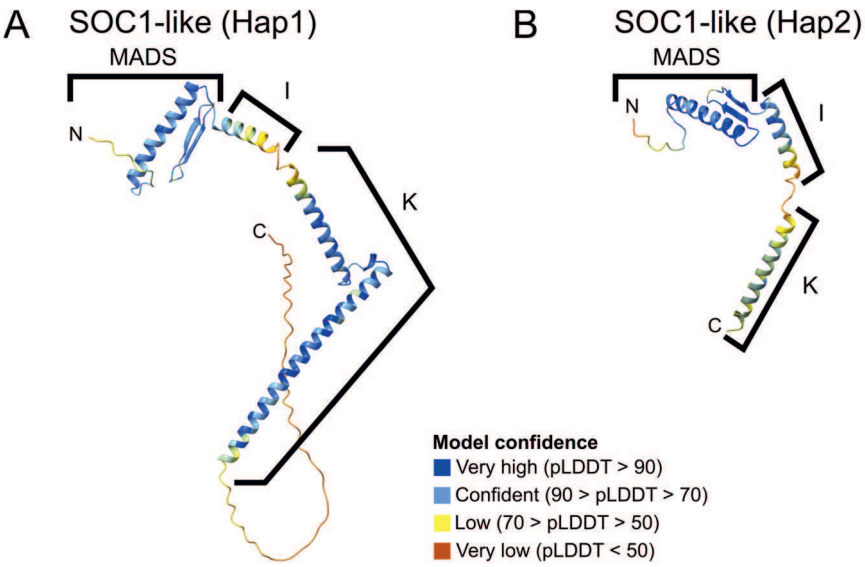


Figure S5: Alphafold-based predictions of the 3D structure of SOC1-like proteins translated by the different haplotypes. A) SOC1-like from cv. Golden Promise representing Hap1. The protein contains the MADS-domain, consisting of an alpha helix and a two-stranded beta sheet; The I-domain, consisting of one alpha helix; and the K-box, consisting of one shorter and one longer alpha helix. B) SOC1-like from cv. Morex representing Hap2. The protein contains the MADS-domain, consisting of an alpha helix and a two-stranded beta sheet; The I-domain, consisting of one alpha helix; and the shorter alpha helix from the K-box. Structural domains are indicated as described (Käppel et al., 2023).

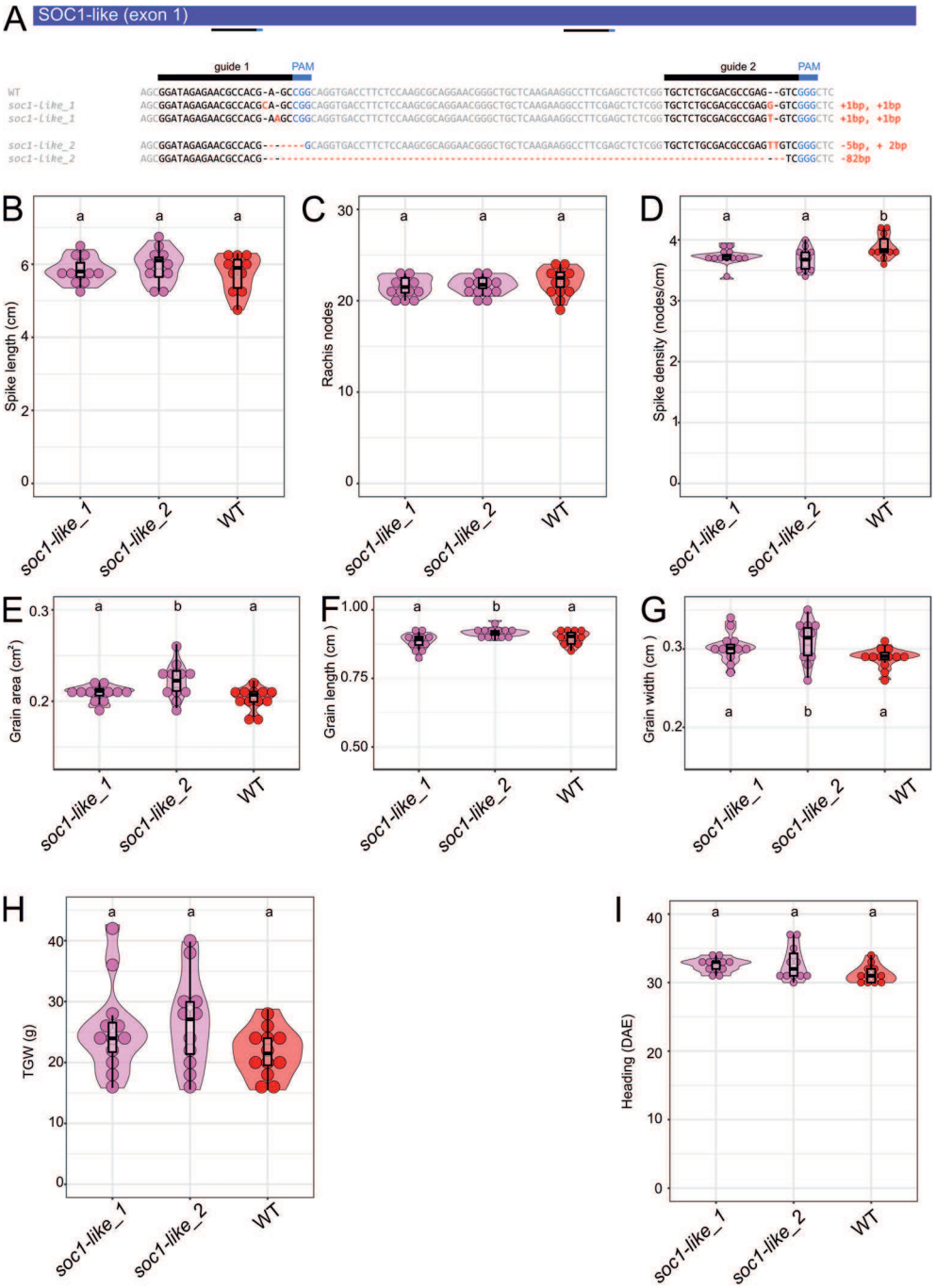

A
SOC1-like (exon 1)
guide 1
PAM
guide 2
PAM
WT
soc1-like_1
soc1-like_1
soc1-like_2
soc1-like_2
+1bp, +1bp
+1bp, +1bp
-5bp, + 2bp
-82bp
B
Spike length (cm)
C
Rachis nodes
D
Spike density (nodes/cm)
E
Grain area (cm²)
F
Grain length (cm)
G
Grain width (cm)
H
TGW (g)
I
Heading (DAE)
soc1-like_1
soc1-like_2
WT

Figure S6: Detailed spike measurements *soc1-likes.* A) schematic overview of the mutations in lines *soc1-like_1* and *soc1-like_2* in the first exon of *HvSOC1-like*. Plants in each line are either homozygous for one of the two mutations shown or biallelic. Plots of B) spike length, C) rachis nodes, D) spike density, E) grain area of the central spikelets, F) grain length of the central spikelets, G) grain width of the central spikelets, H) thousand grain weight (TGW) of the central spikelets, and I) days until heading in days after emergence (DAE) of *soc1-like_1, soc1-like_2* and WT (cv. Golden Promise Fast). Different letters indicate significant ($p < 0.05$) differences between the lines, calculated using ANOVA followed by TukeyHSD (B,C,E,F,G,H), or Kruskal-Wallis followed by Dunn's (D+I).

Supplementary Tables

All supplementary tables are available on https://doi.org/10.5281/zenodo.17157733 or can be send by the authors upon request

Table S1: DAP-sequencing peaks of VRS1 and their location and annotation in the genome (MorexV3)

Table S2: DESEQ2 results of the reanalysis of DRA005563 (Sakuma et al., 2017)

Table S3: list of genes that have a VRS1 DAP-peak within 15 kb and are differentially expressed in *deficiens*

Table S4: Oligonucleotides used in this study

Table S5: Species used in the blastp of SOC1-like (*Hordeum vulgare*)

Table S6: Protein IDs and sequences from NCBI used in phylogenetic analysis

Table S7: Genes that are both bound and regulated by VRS5 and VRS1



Chapter

5

An extension of the Golden Gate toolkit for CRISPR-Cas9 mutagenesis in barley: improved cloning efficiency, sgRNA design, and editing efficiency

Ton Winkelmolen
Marijke Hartog
Richard G. H. Immink
G. Wilma van Esse

Manuscript in preparation

Abstract

Background

CRISPR-Cas-based genome editing has become a routine and powerful tool in plant biology, mainly for the generation of knock-outs. Numerous strategies for optimal guide RNA expression, efficient vector delivery, and multiplexing have been described in literature, providing a strong conceptual framework for effective genome editing. However, translating these strategies into practice often remains challenging, as used vector systems are either multistep assembly workflows, or lack compatibility with the target species. As a result, even well-documented approaches are not always easily deployable. Our aim was to extend the current toolbox for gene editing in cereals combing latest advances in a single cloning system.

Results

Here we present a streamlined CRISPR-Cas9 based vector system optimized for rapid cloning of sgRNA compatible with the Golden Gate cloning system. Following reported improvements, we equipped the sgRNA scaffold used with an extension and nucleotide change. Combined with an effective guide design and a codon and intron optimized Cas9 variant, this reduces cloning time and resources, especially when targeting multiple genes in a single constructs. We found that by combining these advances in gene editing, we created a fast and reliable way to generate constructs for gene knockouts in cereals.

Conclusion

This updated toolkit offers a practical improvement to current CRISPR cloning systems for the cereal research community. It is particularly suited to users seeking a cloning system for generating multiple gene knockouts in cereals. We demonstrated the effectiveness of this tool in the monocot model barley. We also provide a comprehensive overview of the state-of the art, and a easy and reliable protocol for cloning. While we did not test the system in wheat, the vector components and design are fully compatible with wheat transformation systems and can therefore be a useful resource for future translation to wheat.

Introduction

CRISPR (Clustered Regularly Interspaced Short Palindromic Repeats) has rapidly transitioned from a breakthrough technology to a routine method for generating targeted mutations in plant molecular biology. CRISPR technology enables targeted mutagenesis by directing site-specific double-stranded DNA breaks (DSBs) within the genome. These breaks are typically repaired through error-prone pathways like non homologous end joining (NHEJ), often resulting in insertions or deletions that disrupt gene function (Garneau et al., 2010; Ran et al., 2013). The high precision and relative simplicity of CRISPR has presented a leap forward from the earlier, untargeted mutagenesis techniques such as those based on chemical agents like ethyl methanesulfonate (EMS) (Greene et al., 2003; Shirasawa et al., 2016). Target specificity is achieved through a single-guide RNA (sgRNA), which forms a complex with the Cas nuclease and directs it to a complementary DNA sequence within the genome (Garneau et al., 2010; Gasiunas et al., 2012; Jinek et al., 2012).

Despite the routine use of CRISPR-Cas in plant research, generating reliable gene knock-outs still presents several technical hurdles that can limit editing efficiency, especially when applied in crops. Off-targets is one of the challenges in knock-out strategies. While the system in principle offers high targeting specificity, imperfect base pairing between the sgRNA and genomic DNA, especially at the distal end from the protospacer adjacent motif (PAM), can still lead to unintended cleavage events. The extent to which Cas9 tolerates mismatches varies, but even single mismatches outside the seed region can result in off-target double-stranded breaks, particularly in complex plant genomes with high levels of redundancy and repeats. Several computational tools have been designed in the past years, such as CRISPOR (Concordet & Haeussler, 2018) and Cas-Designer (Park et al., 2015), which allow identification of off targets, also for cereal crops like wheat and barley. These tools are also effective in improving the overall guide RNA structure by evaluating factors such as GC content and mismatch sensitivity at potential off-target sites. By optimizing these parameters, such tools not only help reduce unintended edits but also enhance on-target cutting efficiency (Doench et al., 2014; Hsu et al., 2013; Reynolds et al., 2004). In addition, genome-specific scoring systems and integrated reference annotations enable more accurate predictions of guide activity, ultimately contributing to more reliable and efficient gene editing outcomes in cereals. Improving the efficiency of CRISPR-Cas9 mutagenesis in plants has increasingly focused on optimizing the structure and stability of the guide RNA, particularly the scaffold region (Hassan et al., 2021; P. Yuan et al.,

2024). A harpin extension and single nucleotide flip, originally described in mammalian systems (B. Chen et al., 2013; Dang et al., 2015), introduce a short extension and a structural flip in the sgRNA scaffold that enhances Cas9-guide complex stability. These modifications have been shown to significantly increase editing frequencies in transient assays and stably transformed plants (Castel et al., 2019)**.** While these modifications may offer an increased stability, the promoter driving expression of the guide is also important. In barley and wheat the *TaU6* promoter has been well described, and is highly effective (Lawrenson et al., 2015; Shan et al., 2013). Another crucial factor influencing genome editing efficiency is the Cas enzyme itself, and significant progress has been made in optimizing its performance specifically for plant systems (Castel et al., 2019). Native Cas enzymes, such as SpCas9, were originally derived from bacterial systems and are not inherently tailored to the expression and processing machinery of plant cells. To address this, plant-optimized variants of Cas9, incorporating elements such as codon optimization, nuclear localization signals, and importantly, intron insertions, are now widely adopted within model plants such as *Arabidopsis* and tobacco (Grützner et al., 2021). These intron-optimized versions of Cas9 have been shown to outperform the original enzyme, in several plant species by enhancing expression levels and improving overall editing efficiency (Grützner et al., 2021). Such advancements underscore the importance of adapting genome editing tools to the specific plant species in order to maximize their efficiency in the target crop.

To integrate these improvements into currently available user-friendly platforms, we developed an extension on the current modular Golden Gate-based toolkit for Cas9-mediated mutagenesis in barley (Lawrenson & Harwood, 2019). Golden Gate cloning has been widely adopted in plant genome editing due to its compatibility with modular toolkits (e.g., MoClo, GreenGate, GoldenBraid) (Engler et al., 2014; Lampropoulos et al., 2013). In the context of CRISPR-Cas9, it enables fast and flexible assembly of sgRNA expression cassettes, multiplexed guide arrays, and binary vectors for Agrobacterium-mediated transformation (**Figure 1**). Numerous studies have outlined individual strategies to improve editing outcomes in plants through refined guide RNA structure, promoter selection, and codon optimization of nucleases (Castel et al., 2019; B. Chen et al., 2013; Dang et al., 2015; Grützner et al., 2021), yet these insights have often remained scattered or incompatible with monocots. Our work bridges this gap and provides an efficient cloning of sgRNAs, designed with compatibility to the Golden Gate system and scalability in mind. It incorporates up-to-date knowledge on guide design, scaffold optimization, Cas9 codon and intron optimization, and regulatory

elements suited for monocots. In doing so, the toolkit extension facilitates reliable guide assembly and highly improved editing efficiency. We also provide a protocol for guide design and a comprehensive overview of the available plasmids, offering a solid foundation for efficient generation of targeted knockouts in barley.

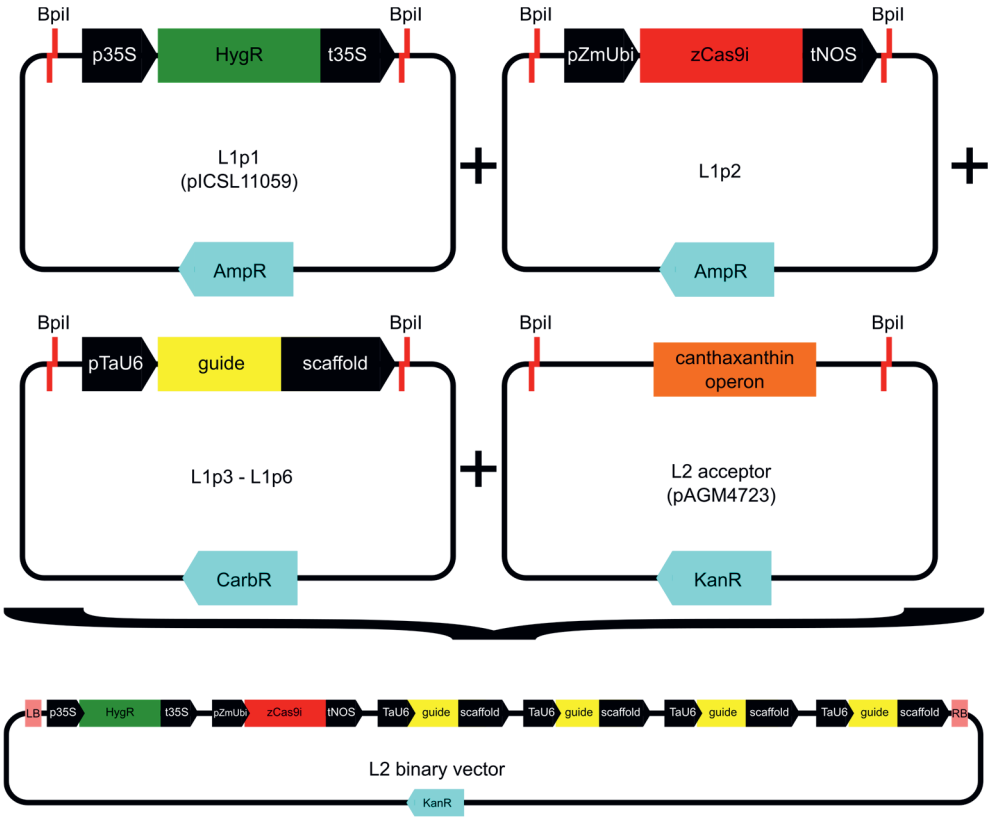


Figure 1: General strategy of the Golden Gate based cloning system for CRISPR knockouts. Using Type II restriction enzymes (e.g. BsaI or BpiI) that cut outside their recognition sites, unique overhangs are generated. This allows seamless and directional ligation of parts in a one-pot reaction with high efficiency. Each Level 1 (L1) vector is designed to accept parts destined for specific positions (L1pX) within the final Level 2 (L2) binary vector, facilitating ordered assembly. In most CRISPR based strategies the Level 1 position 1 (L1p1) contains the plant resistance cassette, in barley this is usually hygromycin. We use pICH47732, which contains the Hygromycin resistance gene (HygR) behind the CaMV35S promoter (p35S) and terminated by the CaMV3S terminator (t35S) (Lawrenson et al., 2015); L1p2 contains the zCas9i enzyme, which is codon optimized for plants, has 13 introns and two nuclear localization signals (Grützner et al., 2021). Expression is driven by the maize *Ubiquitin* promoter (pZmUbi) and terminated by the NOS terminator; L1p3-L1p6 contain the sgRNAs driven by the wheat U6 promoter (pTaU6) and a termination sequence in the designed scaffold. The level 2 acceptor (pAGM4723), contains the canthaxanthin operon, which is removed when other parts are successfully inserted, allowing for orange/white screening (Weber et al., 2011).

Results

Generating a Golden Gate compatible sgRNA scaffold for Cas9

In the natural CRISPR system Cas9 interacts with two separate sgRNAs: the CRISPR RNA (crRNA) and the transactivating CRISPR RNA (tracrRNA), while for gene editing a fusion of these two sgRNAs is used (Deltcheva et al., 2011; Hsu et al., 2014; Jinek et al., 2012). The stability of the sgRNA has been proposed as one of the limiting factors in CRISPR mediated gene editing (Jinek et al., 2013). Chen et al, designed an optimized sgRNA (B. Chen et al., 2013). This optimized sgRNA includes an hairpin extension, and a T-A switch, to prevent a sequence of four thymines right after the guide sequence. These could potentially reduce transcription efficiency as a continuous sequence of thymines is a pause signal for RNA polymerase III (Nielsen et al., 2013). This improved sgRNA design also improved gene editing efficiency in combination with Cas9 in Arabidopsis (Castel et al., 2019). Similarly, in wheat the efficiency of the gene editing is improved when extending the duplex length and mutating the fourth thymine of the continuous sequence (Ni et al., 2023). Dang et al, later found that a T-C switch resulted in an even higher gene editing efficiency in human cell lines (Dang et al., 2015). To gain insights into the scaffolds used in the current Golden Gate barley toolkit (Lawrenson & Harwood, 2019), we aligned the scaffold sequences from the current toolbox, to the one presented by Dang et al. (Dang et al., 2015). The scaffold in the currently used barley protocol has a sgRNA structure with a shortened duplex when compared to the optimized scaffold, as well as four continuous thymines right after the guide sequence (**Figure 2A**). We therefore designed a new Golden Gate compatible level 1, using the improved sgRNA. The current protocols for barley and wheat transformation use the TaU6 promoter (pTaU6) to drive the expression of the sgRNA, which we did not change (Gasparis et al., 2018; Lawrenson & Harwood, 2019; Smedley et al., 2021). For easy cloning, we placed the pTaU6 in Level 0 with a RFP module before the optimized scaffold flanked by BsmBI sites (**Figure 2B).** This allows a one-directional cloning of the protospacer in front of the scaffold sequence into several level 1 positions (**Figure 2B-D**). When cut with BsmBI, overhangs are created directly after the TaU6 promoter, and before the scaffold. For the protospacer to be incorporated in that place, the opposite overhangs are added to the protospacer (**Figure 2C**). Selection of the successful L1 is based on pink/white screening, where white colonies carry the protospacer. The resulting level 1 constructs (L1p3-L1p6) can directly be used to clone the level 2 binary vector (**Figure 1**). Our modified L1 acceptors provide a new sgRNA scaffold configuration compatible with Golden Gate assembly, specifically optimized for

barley, enabling seamless and efficient direct cloning of guide expression cassettes.

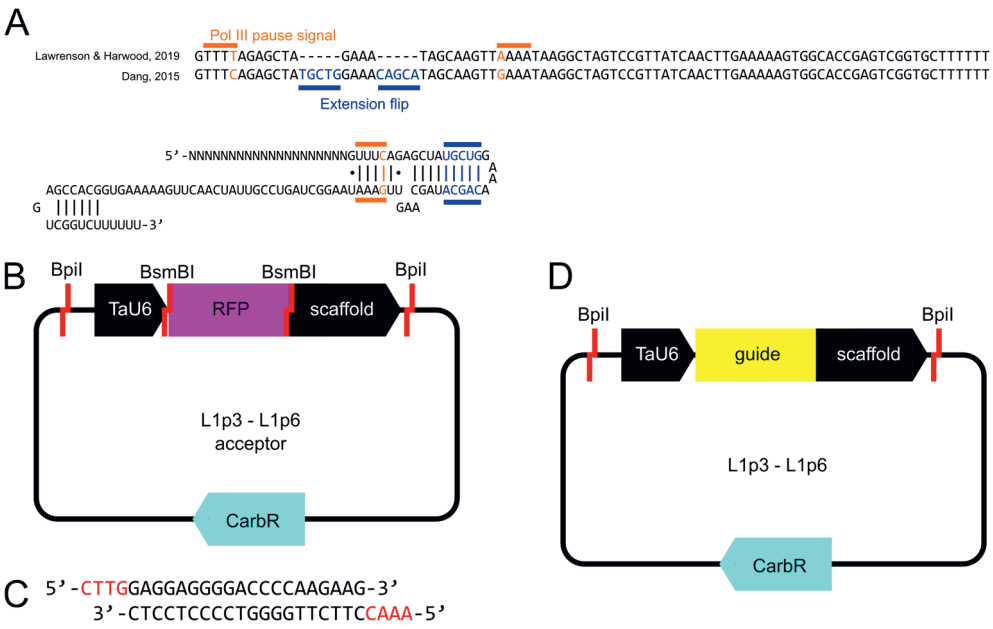


Figure 2. Extended scaffold design for CRISPR mutagenesis. A) Design of new scaffold with extension-flip and removal of the 4x thymine as described (Dang et al., 2015) compared to the previously used scaffold in barley (Lawrenson & Harwood, 2019). Below is the changed single stranded RNA structure shown with the 20xN representing the specific protospacer B) Design of level 1 golden gate vector, ready to use for guide assembly, and overhangs in the matching primer pairs. The guide can be cloned using BsmBI between the TaU6 promoter and the scaffold. For selection the acceptor plasmid contains the RFP module, which is removed when the protospacer is incorporated, allowing for pink/white screening C) Explanation how to order 20nt primers to ligate in the level 1 guide acceptor. D) eventual L1 vector containing the guide (sgRNA) correctly positioned in the scaffold. Generated L1p3 – L1p6 acceptors are now publicly available via Addgene (231030-231035).

Designing Guide RNAs (sgRNAs) for barley

Efficient CRISPR/Cas genome editing in barley (*Hordeum vulgare*) relies heavily on the precise design of single-guide RNAs (sgRNAs). Each sgRNA contains a 20-nucleotide protospacer sequence complementary to the genomic target, positioned directly upstream of a PAM motif, typically NGG for SpCas9 (Jinek et al., 2012; Sapranauskas et al., 2011). The large and repetitive genome of cereals like barley demands careful off-target analysis during guide design. We initially used CRISPR-Local (J. Sun et al., 2019), a tool ideal for non-model species or cultivars not yet supported in mainstream platforms as it enables usage through command line options, incorporating a specific user defined reference genome. More recently, the reference genome for the transformation-friendly cultivar Golden Promise has been assembled (Schreiber et al., 2020) and was included in online sgRNA design tools such as CRISPOR (Concordet & Haeussler, 2018). This makes it straightforward to design guides with enhanced on-target accuracy and off targets analysis tailored to this variety.

When designing the guides one needs to take into account the promoter that is used to express the sgRNA, in barley these are typically U3 or U6 promoters, which impose a requirement that the protospacer begins with respectively an A or G. In our design, we deployed TaU6, so the protospacer needs to start with a G (Belhaj et al., 2013). The sgRNA is composed of two main parts: a 20-nucleotide protospacer that directs the Cas enzyme to the DNA target, and a scaffold region that physically binds to the Cas protein (e.g., Cas9). For the system to function properly, the sgRNA must adopt a specific secondary structure that allows stable interaction with the Cas nuclease and proper positioning of the protospacer for DNA recognition (Ma et al., 2015; Nishimasu et al., 2014). An efficient sgRNA should have three stem-loops folded (Liang et al., 2016)(**Figure 3A-B**). Moreover, no more than 12 bp of the protospacer are acceptable to pair with the rest of the sgRNA (**Figure 3C**), of which a maximum of 7 bp can pair consecutively (Liang et al., 2016). Additionally, the protospacer should not have more than 6 internal base pair folding (**Figure 3D**). To assess proper folding one can use structure prediction tools such as RNAfold (Schuster, 2014) or UNAfold (Markham & Zuker, 2008). Some of the sgRNA design platforms (e.g. CRISPOR) integrate modelling based on effectivity of sgRNA screens (Doench et al., 2014). For choosing the protospacers specific for our targets, we used CRISPOR to find all potential protospacers for that target, and selected the ones with zero off-targets, even with up to three mismatches. To check how the protospacer folds into the scaffold, the folding is assessed using RNAfold.

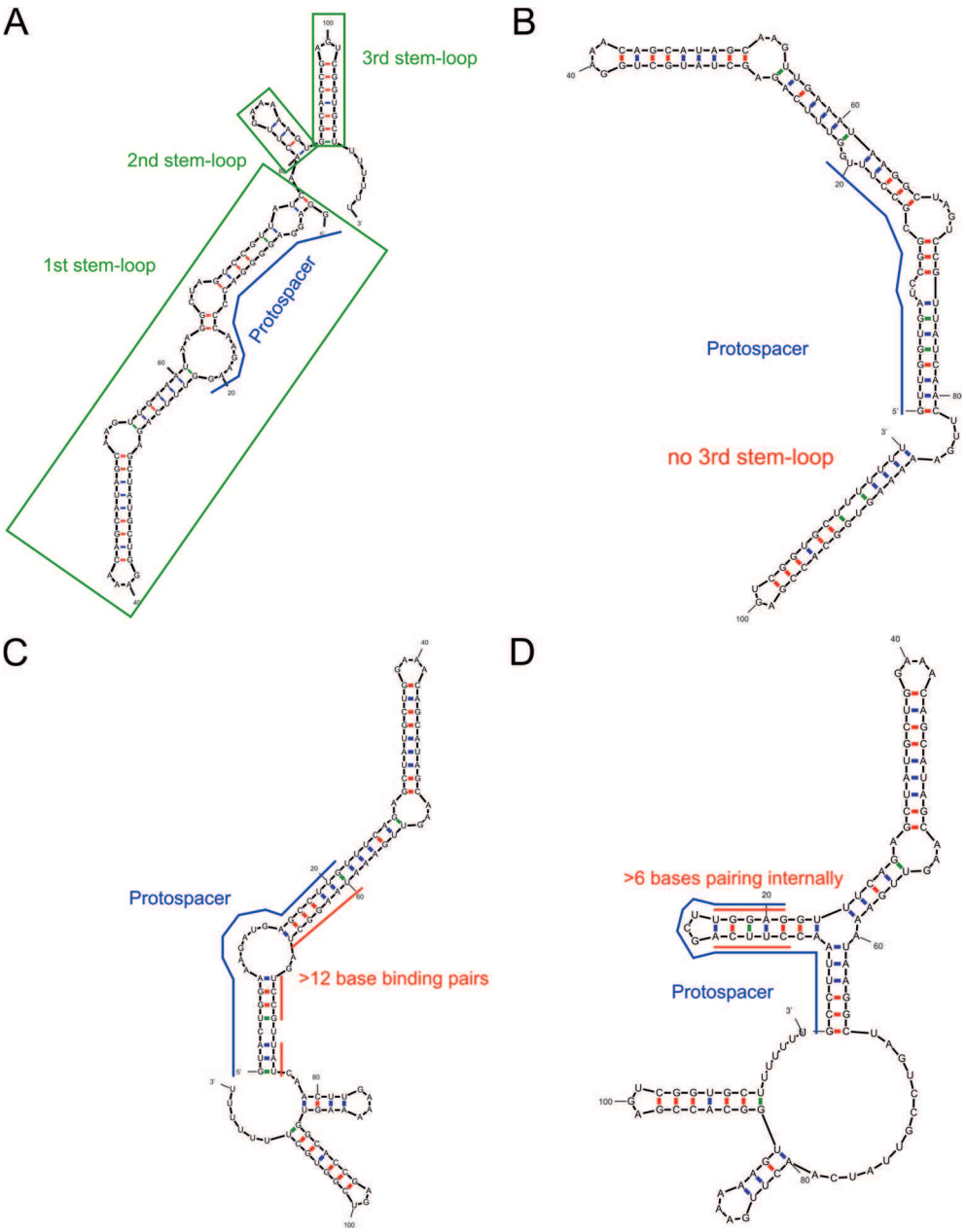


Figure 3: sgRNA folding is important for efficient genome editing. A) example of a sgRNA folding into three stem-loops. B) example of a sgRNA not folding into three stem-loops. C) example of a sgRNA having more than 12 base binding pairs between the protospacer and the scaffold, likely decreasing editing efficiency. D) example of a sgRNA having more than 6 bases of the protospacer pairing within the protospacer, likely decreasing editing efficiency.

Combining the optimized sgRNA scaffold with zCas9i significantly improves genome editing efficiency in Barley

Next to optimizing the sgRNA scaffold and design, we also changed the Cas9 cassette. In early gene editing toolkits for barley, the standard *Streptococcus pyogenes* Cas9 (spCas9) coding sequence together with a shorter, conventional sgRNA scaffold was used (Lawrenson et al., 2015). Previously, it was shown that a plant codon-optimized form of Cas9 with 13 introns and two nuclear localization signals (zCas9i), strongly improved editing efficiency in plants (Grützner et al., 2021). We created a Cas9 cassette using this zCas9i and put it under expression of the maize Ubiquitin promoter (pZmUbi). The pZmUbi is known for its strong and constitutive expression in monocots including barley (Christensen & Quail, 1996; Feike et al., 2019; Schultheiss et al., 2005). Subsequently, we tested our combined modifications of new scaffold design and zCas9i against the barley system described by Lawrenson et al. 2015. Using the spCas9 and short scaffolds, gene editing efficiencies were between 0-5 %. (**Table 1**). When using a improved sgRNA design and scaffold, we obtained editing efficiencies ranging from 5 – 45 % in barley, depending on the target (**Table 1**). After implementing also the ZmUbi:zCas9i, editing efficiencies improved even more, ranging from 53 – 100 %. Especially the amount of primary transformants that were already homozygous or biallelic highly increased, even when two instead of three sgRNAs were used (**Table 1**). With efficiencies this high, the system enabled multiplexing to target multiple genes. Using both our improved sgRNA design and ZmUbi:zCas9i, we successfully targeted multiple genes efficiently using a single construct (**Table 2**). Of the primary transformants ~30% were even homozygous or biallelic mutants for both targets (**Table 2**). This system enables efficient generation of double mutants with high frequency, demonstrating robustness and multiplex editing capability.

Taken together, our data demonstrate that simultaneous optimization of the sgRNA scaffold and Cas9 coding sequence both can enhance the genome editing capacity in barley. This integrated approach provides a powerful toolkit for rapid and reliable gene functional studies in this important cereal crop.

Table 1: editing efficiencies of barley transformants using several methods

Target	Improved sgRNA design	ZmUbi:zCas9i	# guides used	# transformants (Cas9 positive)	# plants with at least one edit	# Plants with homozygous or biallelic mutations
VRS5	No	No	2	52	0 (0 %)	0
TCP15	No	No	2	48	0 (0 %)	0
TB1-like	No	No	3	62	0 (0 %)	0
TB2	No	No	3	38	2 (5%)	0
VRS1	**Yes**	No	3	40	6 (15%)	0
VRS5	**Yes**	No	3	61	3 (5%)	0
TCP15	**Yes**	No	3	35	5 (14%)	0
GT1	**Yes**	No	3	74	33 (45%)	1 (1%)
TB1-like	**Yes**	No	3	18	8 (44%)	0
SOC1-like	**Yes**	**Yes**	3	6	6 (100%)	4 (80%)
VRS5	**Yes**	**Yes**	2	103	81 (79%)	47 (48%)
TB2	**Yes**	**Yes**	2	36	25 (69%)	18 (50%)
TCP15	**Yes**	**Yes**	2	17	14 (82%)	8 (47%)
VRS1	**Yes**	**Yes**	2	30	22 (73%)	12 (40%)
TB1-like	**Yes**	**Yes**	2	18	10 (53%)	10 (53%)

Table 2: editing efficiencies of barley transformations targeting two genes

Targets	# guides used per target	# transformants (Cas9 positive)	# plants with at least one edit in both targets	# plants with homozygous or biallelic mutations in both targets
VRS5 + TB2	2	36	24 (67 %)	14 (39%)
VRS5 + TCP15	2	22	14 (63 %)	7 (32%)
VRS5 + TB1-like	2	18	12 (67%)	5 (28%)
VRS5 + VRS1	2	30	20 (67%)	10 (33%)
VRS5 + VRS4	2	2	2 (100%)	2 (100%)

Discussion

In this study, we report a rapid and effective upgrade of an existing CRISPR-Cas toolkit for barley and wheat, achieved through rational guide RNA architecture improvements and usage of intron-optimized *Zea mays* Cas9 (zCas9i). This Cas9 enzyme contains 13 synthetic introns and two nuclear localization signals. This version has consistently outperformed human- or Arabidopsis-codon optimized Cas9 variants in experiments in other plant species, such as *Arabidopsis thaliana, Nicotiana benthamiana*, and *Catharanthus roseus*, with reported editing efficiencies exceeding 95% (Grützner et al., 2021). our work uniquely combines the zCas9i coding sequence with a strong, constitutive maize *UBIQUITIN* promoter (ZmUbi), a promoter with documented high expression in barley (Christensen & Quail, 1996). Recently, Lawrenson et. Al. (2024) independently identified the same codon-optimized, intron-rich Cas9, under the ZmUbi as highly effective in barley and wheat (Lawrenson et al., 2024). Similar to our strategy, they used a Golden Gate based cloning system. Our work extents this toolkit with a improved sgRNA design, which was based on a previously reported designs with improved folding and stability (Castel et al., 2019; B. Chen et al., 2013; Dang et al., 2015). The combined strategy, incorporating improved Cas9 and scaffold designs, resulted in a genome editing efficiency well above 50%, with the percentage of plants having homozygous or biallelic edits not lower than 40% of all the transformants.

Reaching such high editing efficiencies allows for multiplexing for multiple targets in one construct. Logical next steps of employing this system would also be the generation of more precise and directed single nucleotide changes with the use of base-editing (Komor et al., 2016; X. Li et al., 2018; Nishida et al., 2016). With another method, prime editing, exact mutations as desired can be made (Anzalone et al., 2019; P. J. Chen et al., 2021). Such a method has been described in wheat recently (Ni et al., 2023). Although these methods might need different sgRNA scaffolds and Cas enzymes tailored for the specific method, knowledge on efficient RNA folding and codon usage in plants is valuable to successfully implement these methods. Next to NHEJ, Homologous recombination (HR), is another DNA repair mechanism, where a donor sequence is inserted using overlapping flanks (Filippo et al., 2008). Although successfully performed in plants including barley, HR is thus far very inefficient (Mengiste & Paszkowski, 1999; Paszkowski et al., 1988; Terada et al., 2002; Watanabe et al., 2016). In conclusion, here an efficient genome editing toolbox is described for barley. With the combinations of improvements we made to the current system, also HR

efficiencies might be improved, opening increasing possibilities to the molecular toolbox in barley.

Materials & Methods

Guide design

For the selection of guides targeting our desired sequences, CRISPOR is used (Concordet & Haeussler, 2018). As input the desired target sequence is given, while as PAM NGG is used, since we use Cas9. All available guides are in the barley cv. Golden Promise for the target sequence are shown, and can be sorted by on-target score and off-target score. Only guides are considered that have 0 off-targets even with 3 mismatches. The guide, including the scaffold up until the termination signal (TTTTTT), is used to predict RNA folding using UNAfold (Markham & Zuker, 2008). The sgRNA should have three stem-loops. Moreover, no more than 12 bp of the protospacer are acceptable to pair with the rest of the sgRNA, of which a maximum of 7 bp can pair consecutively. Additionally, the protospacer should not have more than 6 internal base pair folding (Liang et al., 2016) (**Figure 3**). The selected 20 bp guides are then ordered as two single stranded oligos including 5'- overhangs for cloning into the L1 scaffolds: CTTG is added at the 5' end of the forward guide; for the reverse guide AAAC is added to the 5' end (**Figure 2C**).

sgRNA cloning

The ordered oligos (**Table S1, Table S2**) are mixed and hybridized by adding 5 µL of each probe (100 µM) into 40 µL of MQ followed by incubation at 98°C for 5 minutes. The hybridized guides are diluted 150x and cloned into the L1 vector, which contains the optimized scaffold and the TaU6 promoter (**Figure 2**), available at addgene: #231030 - #231033. Assembly is performed in a total volume of 20µL, containing 100-200 ng acceptor plasmid, 1µL 150x diluted hybridized guides, 10U BsmBI (Thermo Scientific), 1x buffer Tango (Thermo Scientific), 30U T4 DNA ligase (Thermo Scientific), 1mM ATP. The mixture is then placed in a thermocycler using the following protocol: 3x (10 min, 40°C; 10 min 16°C); 10 min 50°C; 20 min 80°C. The resulting assemblies are directly transformed in electrocompetent *E. coli* cells and grown overnight at 37°C on plates. White colonies, do not have the RFP module anymore, and should be selected. These are then grown overnight in liquid culture at 37°C. The plasmids are isolated and checked for the correct insert by sequencing.

Binary vector cloning and Agrobacterium mediated transformation

For cloning of the binary Level 2 vector, the following Level 1 vectors are used: L1p1, plant resistance cassette containing the hygromycin resistance gene under control of the CaMV35S promoter (pICH47732); L1p2, zCas9i cassette containing the zCas9i with two nuclear localization signals (Grützner et al., 2021),

under control of the ZmUbi promoter; L1p3-L1p6, sgRNAs as described above (**Figure 1**). To make sure the inserts assemble together to the level 2 acceptor again, an end-linker is used. When using six level 1 parts, this is pICH41822. If less sgRNAs are used, the corresponding end-linker should be used (Engler et al., 2014). These level 1 vectors and end-linker are cloned into level 2 acceptor pAGM4723. This acceptor contains the canthaxanhin operon giving an orange color when expressed. Successful assembly should remove the canthaxanhin operon, allowing for orange/white screening. Assembly is performed in a total volume of 20 µL, containing 100-200 ng acceptor plasmid, all other L1 plasmids in a 2:1 molar ratio of insert:acceptor, 1.5 uL T4 Ligase buffer (Thermo Scientific), 1.5 µL bovine serum albumin (Thermo Scientific), 15U T4DNA Ligase, (Thermo Scientific), 5U BpiI (Thermo Scientific). The mixture is then placed in a thermocycler using the following protocol: 20s 37°C; 26x (3 min 37°C; 4 min 16°C); 5 min 50°C; 5 min 80°C.

Resulting assemblies are directly transformed into electrocompetent *E. coli* cells and grown overnight at 37°C on plates. White colonies should be selected and grown overnight in liquid culture at 37°C. The plasmids are isolated and digestion is performed using PvuII. Plasmids following the expected digestion pattern are then checked for the correct inserts by sequencing. Correct plasmids are then transformed into hypervirulent electrocompetent *A. tumefaciens* cells (AGL1 pSOUP) and grown for three days at 28°C. For Agrobacterium mediated transformation of barley the previously described protocol is used (Hinchliffe & Harwood, 2019).

Supplementary Tables

Table S1: ordered guide sequences to be cloned in L1 scaffold sequences without optimized sgRNA design

Target			Sequence
VRS5	guide 1	Forward	GGCAAGCTGCAGCTGCTGGTAAAG
		Reverse	AAACCTTTACCAGCAGCTGCAGCT
	guide 2	Forward	GGCATTTCCACCACAACTACCTCT
		Reverse	AAACAGAGGTAGTTGTGGTGGAAA
TCP15	guide 1	Forward	GGCAAGCCGGGGGGCGCCCTCGCC
		Reverse	AAACGGCGAGGGCGCCCCCCGGCT
	guide 2	Forward	GGCAAGCAAGATCCGCACGGCGCA
		Reverse	AAACTGCGCCGTGCGGATCTTGCT
TB1-like	guide 1	Forward	GGCAAAGGCATCTTGTGCTCCCGA
		Reverse	AAACTCGGGAGCACAAGATGCCTT
	guide 2	Forward	GGCAAGCAAGATATGCACGGCGGG
		Reverse	AAACCCCGCCGTGCATATCTTGCT
	guide 3	Forward	GGCAAGAAGCGGCGGGCCACGTCC
		Reverse	AAACGGACGTGGCCCGCCGCTTCT
TB2	guide 1	Forward	GGCAAGGCGCCATGGAGAAGCTGC
		Reverse	AAACGCAGCTTCTCCATGGCGCCT
	guide 2	Forward	GGCAATGTCCGCCAGAGGAGGAGC
		Reverse	AAACGCTCCTCCTCTGGCGGACAT
	guide 3	Forward	GGCAACTGGCGCAGTGCAGGCCGC
		Reverse	AAACGCGGCCTGCACTGCGCCAGT

Table S2: ordered guide sequences to be cloned in L1 scaffold with optimized sgRNA design

Target	Primer		Sequence	used for creation double mutants
VRS1	guide 1	Forward	CTTGACGTGGACACGACTTTCTTC	Yes
		Reverse	AAACGAAGAAAGTCGTGTCCACGT	
	guide 2	Forward	CTTGGAGGAGGGGACCCCAAGAAG	Yes
		Reverse	AAACCTTCTTGGGGTCCCCTCCTC	
	guide 3	Forward	CTTGGGAGGTGCGGCGCCTCAGGT	
		Reverse	AAACACCTGAGGCGCCGCACCTCC	
VRS5	guide 1	Forward	CTTGAGAACTTGCGGGCGACGTCG	
		Reverse	AAACCGACGTCGCCCGCAAGTTCT	
	guide 2	Forward	CTTGCACCGGCACAGAGGTAGTTG	Yes
		Reverse	AAACCAACTACCTCTGTGCCGGTG	
	guide 3	Forward	CTTGCAACTACTACCAGCACCAGC	Yes
		Reverse	AAACGCTGGTGCTGGTAGTAGTTG	
TCP15	guide 1	Forward	CTTGCTCGCCGAAAGACGACGACG	Yes
		Reverse	AAACCGTCGTCGTCTTTCGGCGAG	
	guide 2	Forward	CTTGGCTTGACTGGTTCATGTCGG	
		Reverse	AAACCCGACATGAACCAGTCAAGC	
	guide 3	Forward	CTTGGGACCTCCTCGGCTTCGACA	Yes
		Reverse	AAACTGTCGAAGCCGAGGAGGTCC	
GT1	guide 1	Forward	CTTGTACTGGAAAGATGAGCCCCG	
		Reverse	AAACCGGGGCTCATCTTTCCAGTA	
	guide 2	Forward	CTTGACACCAAGCAGGTCGCCGTG	
		Reverse	AAACCACGGCGACCTGCTTGGTGT	
	guide 3	Forward	CTTGGGGAGGACAGCAGTTCGGGA	
		Reverse	AAACTCCCGAACTGCTGTCCTCCC	
TB1-like	guide 1	Forward	CTTGTATGCACGGCGGGAGGGATG	
		Reverse	AAACCATCCCTCCCGCCGTGCATA	
	guide 2	Forward	CTTGCGGACATGGATGCGGCCAGG	Yes
		Reverse	AAACCCTGGCCGCATCCATGTCCG	
	guide 3	Forward	CTTGCCTTAACCTTGGGCTTGGAG	Yes
		Reverse	AAACCTCCAAGCCCAAGGTTAAGG	
SOC1-like	guide 1	Forward	CTTGGGATAGAGAACGCCACGAGC	
		Reverse	AAACGCTCGTGGCGTTCTCTATCC	
	guide 2	Forward	CTTGCAAGAAGGCCTTCGAGCTAT	
		Reverse	AAACATAGCTCGAAGGCCTTCTTG	
	guide 3	Forward	CTTGTGCTCTGCGACGCCGAGGTC	
		Reverse	AAACGACCTCGGCGTCGCAGAGCA	
TB2	guide 1	Forward	CTTGAGGCGCCATGGAGAAGCTGC	
		Reverse	AAACGCAGCTTCTCCATGGCGCCT	
	guide 2	Forward	CTTGATGTCCGCCAGAGGAGGAGC	Yes
		Reverse	AAACGCTCCTCCTCTGGCGGACAT	
	guide 3	Forward	CTTGACTGGCGCAGTGCAGGCCGC	Yes
		Reverse	AAACGCGGCCTGCACTGCGCCAGT	



Chapter

6

General Discussion

Plant architecture is a highly dynamic trait that is influenced by the environment. Depending on environmental cues, developmental and architectural choices are made. These choices are tightly regulated by several key transcription factors. Perhaps one of the most famous transcriptional regulators that orchestrate plant architectural traits is TEOSINTE BRANCED 1, which was key to maize domestication (J. Doebley et al., 1995, 1997). *TB1* in monocots and it's closely related genes in dicots such as *BRANCED1 (BRC1)* are well known for their conserved roles in regulation of axillary bud outgrowth (J. Doebley et al., 1995; Gao et al., 2016; González-Grandío et al., 2013; Kebrom et al., 2006; Martín-Trillo et al., 2011; Ramsay et al., 2011; Takeda et al., 2003). Besides its conserved role in regulating axillary bud outgrowth, *TB1* ortholog *VRS5* in barley, also regulates lateral spikelet development, controlling row-type in the spike. Both of these processes are important yield related traits in barley, and their genetic connection makes it difficult to manipulate these traits independently.

This thesis started with the main objective to gain molecular insights in how VRS5 regulates tillering and lateral spikelet development. As a transcription factor, VRS5 can directly bind to DNA and regulate the expression of downstream targets. Even though the same DNA is present in every cell, actual binding of TFs to targets depends on the chromatin context, DNA methylation, and the availability of potential cofactors. This means that the VRS5 targets might differ between tissues and development. Understanding what these targets are can help to better understand how VRS5 exactly functions and regulates these different processes. In **Chapter 2**, we identified these direct targets in barley by combining two techniques. Using DNA-affinity purification followed by sequencing (DAP-seq), we identified the genome-wide binding sites of VRS5 independent of chromatin context and cofactors. Next to that, we compared gene expression in *vrs5* mutants to wild-type at four developmental stages using RNA sequencing, where the tissue and developmental context are taken into account. By combining the genes that are differentially expressed in *vrs5* and the loci where VRS5 binds, we obtained a set of *bona fide* VRS5 targets that are thus bound by and regulated by VRS5. By investigating four different developmental stages by RNA sequencing, we could identify which of these targets mostly play a role early in development, and presumably in tillering, and which of the targets mostly play a role later in development, when the inflorescence is developing.

Next, we looked in more detail at VRS5 as a protein in **Chapter 3**. We found that in barley, two different protein isoforms of VRS5 can be formed, VRS5α and VRS5β, originating from two different *VRS5* transcripts. We showed that these isoforms function differently by CRISPR mutagenesis, mutating only one of the protein isoforms. While complete knock-out lines of *vrs5* have both an increased number of tillers and a six-rowed to intermediate spike phenotype, the *vrs5α* mutants only show increased tillering, but a two-rowed spike. Previously, it was found that VRS5 can form heterodimers *in-vitro* with other CYC/TB1 TCPs, including TB2 (de Souza Moraes et al., 2022). In **Chapter 3**, we looked into more detail of this interaction and found that VRS5 and TB2 can also bind DNA together. Differences in binding between the VRS5 isoforms in complex with TB2 to one of the targets, are likely the cause of the observed phenotypical differences between the *vrs5* mutants and the *vrs5α* mutants.

In this chapter, I will further highlight these obtained results and integrate them into a broader perspective.

VRS5 has a conserved function in apical dominance

During plant development, multiple growth axes are created besides the main one. In the leaf axils, axillary meristems and eventually axillary buds are formed. Differences in the actual outgrowth of these buds cause a lot of architectural variation both between and within species. This process is tightly regulated and depends on external as well as internal cues. One of the integrators of these signals across various plant species is *BRC1/TB1* (M. Wang et al., 2019). *BRC1* and *TB1* and their orthologs in multiple species were shown to inhibit axillary bud outgrowth (Aguilar-Martínez et al., 2007; Finlayson, 2007; Kebrom et al., 2006; Martín-Trillo et al., 2011; Ramsay et al., 2011; A. J. Studer & Doebley, 2012; Takeda et al., 2003), revealing their highly conserved function. In response to different environmental cues, plants inhibit or increase their axillary bud outgrowth. Under shading conditions, for example, plants invest more energy in their main shoot and inhibit their axillary branches, which is one of the architectural changes occurring under the so-called shade avoidance response (Casal et al., 1986; Kasperbauer, 1971; Kebrom et al., 2010). *BRC1/TB1* expression is increased under shade, and consequently, axillary bud outgrowth is repressed (González-Grandío et al., 2013; Kebrom et al., 2010; H. Wang et al., 2022). The direct downstream targets of BRC1 and TB1 in regulating axillary branching have been identified in Arabidopsis and maize (Dong et al., 2019; Gonzalez-Grandio et al., 2017; van Es

et al., 2024). These studies found that BRC1/TB1 increase Abscisic acid (ABA) synthesis and response. In **Chapter 2**, we identified the *bona fide* direct targets of VRS5 in barley. We also found that in tillering, genes supposed to be involved in abscisic acid synthesis and response are directly regulated by VRS5, showing that not only the function of BRC1/TB1 is conserved, but also the downstream acting mechanisms and pathways themselves.

DAP-seq can provide novel insights in complex specificity of VRS5 DNA binding

Direct targets in this pathway are HD-ZIP transcription factors HB21, HB40, HB53 in *Arabidopsis* (Gonzalez-Grandio et al., 2017; van Es et al., 2024) and GRASSY TILLERS1 (GT1) in maize (Dong et al., 2019; Whipple et al., 2011). The ortholog in barley of *GT1, HvGT1,* was not in our *bona fide* target list of VRS5, but was downregulated in *vrs5* compared to WT. In **Chapter 3**, we showed that VRS5 cannot bind to the promoter of *HvGT1* as a homodimer, but only in a complex with TB2. This suggests that both VRS5 and TB2 are needed to regulate *HvGT1*. This corroborates the increased tillering in *hvgt1, vrs5,* and *tb2* mutants, as shown in **Chapter *3.*** For DAP-seq, we used only VRS5, and hence, only targets that can be bound by monomers or multimers of VRS5 could be identified (Bartlett et al., 2017; Winkelmolen et al., 2025). The previously mentioned studies in *Arabidopsis* and maize used ChIP-seq to identify genome-wide binding sites, which is an *in vivo* method that takes all loci bound by BRC1/TB1, even if these TCP proteins are in a complex with other proteins or transcription factors (Dong et al., 2019; Gonzalez-Grandio et al., 2017; van Es et al., 2024). This suggests that previous ChIP-seq studies provide a mix of targets from TB1/BRC1 complexes, while our DAP-seq provides VRS5-only targets. This shows that, depending on if VRS5 binds as a homodimer or in a complex, the DNA-binding specificity changes. This gives opportunities to investigate what these changes are and which targets are bound specifically in complex. A DAP-seq can come in handy here, as specific protein complexes can be used as prey, while using the individual proteins/homodimers as control (M. Li et al., 2023). Given the observed conservation of BRC1/TB1/VRS5 targets in tillering, these insights might be useful in the field of plant branching and genetic control of apical dominance.

Previously, it was shown that VRS5 can also form heterodimers with the CYC/TB1 TCP TFs, TCP15, and TB1-like (de Souza Moraes et al., 2022). The function of these two TCP TFs in barley has not been characterized yet, but several

orthologs of *TCP15* in other grasses have architectural functions. In rice, *TILLER INCLINED GROWTH 1 (TIG1)*, controls the angle at which tillers grow towards the main culm (W. Zhang et al., 2019). In sorghum, mutation of *MULTISEEDED1 (MSD1)* causes an increase in inflorescence size and spikelet fertility, greatly increasing the number of seeds per panicle (Jiao et al., 2018). This shows the functional diversity, and would suggest that also in barley, these uncharacterized CYC/TB1 TCPs might have an architectural function. Whether VRS5 also binds DNA together with TB1-like and TCP15 *in planta*, is still to be investigated. VRS5 binding in complex with other TCP TFs can alter the DNA binding specificity, as we have shown for VRS5 and TB2. Understanding for which targets a heterodimerization partner is needed can be of importance in modulating certain traits, increasing opportunities to untangle pleiotropic effects.

The VRS5-VRS1 hub has a grass-specific function in inflorescence development

Besides regulating axillary bud outgrowth, *VRS5* orthologs in some other grasses also have a phenotype in the inflorescence. In wheat, for example, overexpression of *TB-D1* shows an increased amount of paired spikelets (Dixon et al., 2018). In maize, *tb1* mutants show masculinized lateral inflorescences (ears), which are normally only female in WT (J. Doebley et al., 1995; Hubbard et al., 2002). In barley, besides tillering, *VRS5* regulates lateral spikelet development (Liller et al., 2015; Ramsay et al., 2011; Zwirek et al., 2019). This shows the pleiotropy of such an important domestication gene in grasses. Knowing VRS5 targets during inflorescence development thus yields potential targets for trait development, not only in barley but also in other grasses. Thus far known, *VRS1,* is the most downstream player in regulating lateral spikelet development, with VRS5 genetically upstream (van Esse et al., 2017). In **Chapter 2**, we showed that VRS5 directly binds to the promoter of *VRS1* to regulate its expression. Knock-out mutants of *VRS1* have a six-rowed spike, with fully developed lateral spikelets (**Chapter 4**)(Komatsuda et al., 2007). Even though the presence and development of lateral spikelets are specific to the barley spike, orthologs of *VRS1* in other grasses also play an important role in spike architecture and development. In wheat, individual spikelets are indeterminate and can thus produce multiple florets, and consequently, grains per spikelet. The *VRS1* ortholog in wheat, *TaGNI1,* regulates the fertility of the florets (Sakuma et al., 2019). Reduced function of the homeolog *TaGNI-A1* increases the floret fertility and therefore yield (Sakuma et al., 2019). In maize, there are two types of

inflorescences: the ears, which harbor only female florets, and the tassel, which harbors only male florets. That means that normally the carpel is repressed in the tassel, while the stamens develop normally. The maize ortholog of *VRS1, ZmHB13,* acts together with closely related *GT1* to repress the carpel in maize tassels (Y. Yuan et al., 2025). In two-rowed barley, the lateral spikelets do form stamen primordia, but no carpel primordia. In contrast, in *vrs1* and *vrs5* single mutants, carpel primordia do form in the lateral spikelets (Zwirek et al., 2019). That means that even though grass inflorescence architecture is very diverse, there seems to be a conserved function for *VRS1/ZmHB13* in carpel repression, although in maize, *GT1* is needed for that as well. As described in **Chapter 3,** barley *HvGT1* represses tillering downstream of VRS5 and TB2, but also regulates tip degeneration in the barley spike (Shanmugaraj et al., 2023).

Although *VRS1* is the most downstream gene in the described VRS pathway, *vrs1vrs5* double mutants show an increased lateral spikelet development compared to *vrs1* single mutants, indicating that lateral spikelet development does not solely depend on *VRS1* (Zwirek et al., 2019). With our dataset of *bona fide* VRS5 targets defined in **Chapter 2**, we have a starting point to identify other genes important for lateral spikelet development, independent of *VRS1.* Some of these direct downstream targets of VRS5 during inflorescence development are members of the MIKCc MADS-box transcription factor family, such as *AGL6, MADS1,* and *MADS4*. These MADS-box transcription factors are part of the ABC-model of floral development, which specifies the identity of floral organs during flower development (Coen & Meyerowitz, 1991; Rijpkema et al., 2010). This model is also conserved in barley, and expression patterns of these ABC-model genes correspond largely to the original model based on *Arabidopsis* and *Antirrhinum* (G. Chen et al., 2023; Demesa-Arevalo et al., 2025; Kuijer et al., 2021). In barley, *mads1* mutants have smaller awns and lemmas, leading to a reduction in seed size (Y. Zhang, Shen, Li, et al., 2024). Next to that, *MADS1* is needed for keeping an unbranched spike under high ambient temperature (G. Li et al., 2021). Mutants of *AGL6* cause homeotic conversion of all floral organs to lemma-like structures, except for the ovule (M. Sun et al., 2024). For *MADS4,* mutants cause a homeotic conversion of stamens into ovules (M. Sun et al., 2024). These genes are needed for normal floret development, and it seems that VRS5 directly targets them specifically in the lateral spikelets to repress flower development.

Besides row-type, VRS5 regulates also spike length and central spikelet size in the barley inflorescence (Liller et al., 2015; Zwirek et al., 2019). In **Chapter 3**, we also observed a reduction in spike length and central spikelet size in both our *vrs5* and *vrs5α* isoform mutants, showing that the long VRS5α isoform is essential for regulating spike length and central spikelet size. In **Chapter 2,** we identified *HvCEN* as one of the *bona fide* targets of VRS5. *Hvcen* mutants show early flowering, less tillering, but also a strong reduction in spike length (Bi et al., 2019). Furthermore, mutants of *HvCEN* orthologs in other species cause a reduction in inflorescence size (Kaneko-Suzuki et al., 2018; Shannon & Meeks-Wagner, 1991; Wen et al., 2019), as these genes are responsible for inflorescence meristem maintenance (Cerise et al., 2023). This suggests that *HvCEN* regulates spike length by keeping the inflorescence meristem in an indeterminate state. In *vrs5* mutants, *HvCEN* expression is reduced throughout development. This coincides with the observed spike length reduction in *vrs5* mutants, suggesting that VRS5 regulates spike length by directly regulating *HvCEN* expression. As both *vrs5* and *vrs5α* mutants showed a reduced spike length, this would imply that VRS5α regulates *HvCEN* expression, while VRS5β cannot.

A novel layer of regulation for TB1 proteins

Throughout biology, there are several ways to generate different mRNA transcripts from the same locus, increasing the potential functional spectrum of a single gene. The most common examples are alternative splicing (AS) and alternative transcription start site (aTSS) usage. During splicing, usually introns are removed from the pre-mRNA, while the exons are retained. With AS, exon skipping, intron retention, or alternative 5'- or 3'-splice sites result in different mRNA transcripts from the same locus, which could potentially be translated into different protein isoforms. This mechanism has been reviewed extensively, mainly focusing on animal systems (Kelemen et al., 2013; Marasco & Kornblihtt, 2023; Y. Wang et al., 2015). Also in plants, including crop species, there are plenty of examples of alternative splicing with biological relevance, as reviewed (Tognacca et al., 2023). For example, in wheat, TaGS3 regulates seed size. While constitutive high expression of the most abundant isoform leads to a strong reduction in grain size (Ren et al., 2021; W. Zhang et al., 2020), constitutively high expression of an exon-skipped isoform leads to an increase in grain size, caused by altered dimerization capacities of the encoded protein (Ren et al., 2021). In rice, AS of *REGULATOR OF LEAF INCLINATION1 (RLI1)* is changed by phosphate starvation (M. Guo et al., 2022). Constitutive overexpression of one isoform leads to a higher

leaf angle, while overexpression of the other isoform does not (M. Guo et al., 2022). In this case, the functional difference between the isoforms was shown to be a more specific DNA binding of one isoform compared to the other (M. Guo et al., 2022).

While AS needs a gene containing multiple exons, this necessity is not needed for aTSS. With aTSS, transcription starts at a different site, upstream or downstream of the conventional TSS. This mechanism was mainly reviewed in mammalian systems (Davuluri et al., 2008), but genome-wide TSS studies in plants showed that this mechanism is also widespread in plants (Kurihara et al., 2018; Mejía-Guerra et al., 2015; Pavlu et al., 2024; Thieffry et al., 2022; Ushijima et al., 2017). aTSS can have important functional implications. In pear, for example, different transcripts of *PbELF3*, a regulator of the circadian clock, lead to differences in the number of flower buds produced (P. Wang et al., 2023). The existence of these transcripts was also shown in *Arabidopsis* and therefore, functionally conserved (P. Wang et al., 2023).

Alternatively, other functional implications of aTSS are mostly found to be related to subcellular localization. Both in maize and *Arabidopsis*, several genes have isoforms formed by aTSS that lost a signal peptide, normally used to localize the protein in the nucleus or plastids (Mejía-Guerra et al., 2015; Ushijima et al., 2017). Even though different protein isoforms for countless loci exist, functional characterization in plants is scarce. If at all, constitutive overexpression is used for phenotyping, which mostly does not represent normal *in planta* function, as expression is both ectopically and massively increased.

Looking specifically to genes described in this thesis, different protein isoforms were also observed in *BRC1* orthologs caused by AS. In tomato, two orthologs of *BRC1* exist, *SlBRC1a* and *SlBRC1b* (Martín-Trillo et al., 2011). For *SlBRC1a*, two protein isoforms were described, of which the shorter one lost a C-terminal part by an early stop codon caused by intron retention (Martín-Trillo et al., 2011). The existence of these isoforms of the BRC1a proteins seems to be conserved in the *Solanum* clade. In potato BRC1a controls lateral branching, both of the shoot and underground (Nicolas et al., 2015). Similar to tomato, potato BRC1a can form two isoforms, that are functionally different. Although both isoforms have a predicted nuclear localization signal (NLS), the shorter isoform is not localizing in the nucleus and reduces the transcriptional activity of the longer isoform (Nicolas et al., 2015).

For monocot *TB1* orthologs, to the best of our knowledge, different isoforms have not been described yet. However, in **Chapter 3**, we identified two different *VRS5* transcripts, formed by aTSS. Translation of these transcripts results in the longer canonical VRS5α and the shorter VRS5β isoforms, which misses an N-terminal part. By mutating VRS5α, while keeping VRS5β intact, we were able to untangle traits regulated by VRS5. The *vrs5α* mutants showed an increase in tillering, like *vrs5* knock-outs, but had a two-rowed spike, as opposed to an *intermedium* spike in *vrs5* knock-outs. That means we not only showed the presence of different isoforms, but we also showed the phenotypical implications when one of them is absent. Both isoforms were able to bind DNA in an *in vitro* assay, including binding the promoter of *VRS1*, which is needed to activate *VRS1* expression, causing the two-rowed spike. As mentioned above, VRS5 can also form heterodimers with TB2. We showed that, in complex with TB2, VRS5α is able to bind the promoter of *HvGT1*, while VRS5β is not. This showed that VRS5α is essential to bind *HvGT1* together with TB2 in order to regulate tillering. These differences in DNA binding of both isoforms in complex, raises the question what more targets are differentially bound by the isoforms in complex with TB2 and potentially other CYC/TB1 TCPs. Answering this could explain further the observed differences in phenotype, but also help predict what functional differences the isoforms of *VRS5* orthologs have and their phenotypical implications.

A question that remains unanswered is how the alternative transcription is regulated. We showed that both transcripts are present at awn primordium stage, when the repression of lateral spikelets normally begins (Zwirek et al., 2019) and at the double ridge stage, when there are no spikelet primordia formed yet. This raises the question if there are certain tissues, developmental timepoints, or circumstances where only one of the isoforms is present or this ratio is different.

For example, changes in DNA methylation can influence the expression of different transcripts form the same gene (Pumplin et al., 2016). aTSS usage can be triggered by blue light (Kurihara et al., 2018) or phytochromes (Ushijima et al., 2017). Expression of *VRS5* and *BRC1* orthologs is increased under shade via phytochrome B (PhyB) (Gonzalez-Grandio et al., 2017; Kebrom et al., 2006; H. Wang et al., 2022). However, if also the aTSS usage in VRS5 is triggered by PhyB remains unclear. A more thorough analysis of VRS5 isoform expression is needed. Investigating if the VRS5 isoform ratio can be changed under certain circumstances, like shading, or in certain cell types will insight if and how aTSS

usage of VRS5 is regulated. Next to that, investigating how the VRS5 promoter changed during evolution, specifically before and after the occurrence of the conserved aTSS, gives an idea which regions in the promoter are more conserved and potentially are important for regulation.

Concluding remarks and outlook

In this thesis, I have shown several potential ways to untangle yield-related traits in barley, specifically via VRS5 (**Figure 1**). By knowing the direct targets of VRS5 in regulating either tillering or lateral spikelet development, some new potential targets were found that might tweak one of these traits, without having an effect on the other (**Figure 1A-B**). In **Chapter 4**, we followed up on one of these targets, namely *SOC1-like,* regulating lateral spikelet development. Another strategy could be to specifically mutate the VRS5 binding site of one of these targets to potentially remove the VRS5 specific regulation (**Figure 1C**). This way the targets function in other processes might be retained, while the regulation on either lateral spikelet development or tillering is removed or reduced. Knowing the direct targets for VRS5 can not only be beneficial in barley, as we showed that there is some overlap in targets and processes targeted by VRS5, TB1, and BRC1, especially in regulating axillary bud outgrowth. This conservation implies that these processes and targets can be shared in many more species.

Next to that, we showed that VRS5 can bind DNA in complex with TB2 (**Figure 1D**). For some targets this complex formation is even necessary to bind DNA, like for binding to the promoter of *HvGT1*. This broadens the list of potential VRS5 targets that might be used for trait development. Knowing the targets that can only be bound in a complex (**Figure 1E**) might help predict phenotypic responses when either one of the complex partners is removed.

Next to that, the identification of two distinct VRS5 isoforms, showed the ability to untangle row-type from tillering in barley (**Figure 1F**). Further investigation of functional differences of these isoforms can help to further untangle VRS5 related yield traits, not only in barley but also other grasses, as the aTSS usage seems to be conserved in grasses. Next to that, the differences in DNA binding in complex of both isoforms raises the question what more targets are differentially bound by the isoforms in complex with TB2 and potentially other CYC/TB1 TCPs (**Figure 1G**). Therefore, this thesis is an important step towards a

better understanding how protein isoforms can be exploited to untangle yield related traits in cereals.

To conclude, this thesis is a nice example of the ability to do fundamental research directly on a crop. With tools available as a complete reference pangenome, natural variation in combination with phenotyping data, and an efficient transformation protocol (**Chapter 5**), the way is open to successfully perform fundamental research that can more easily be applied in the development of stable, climate-change-proof cereals.

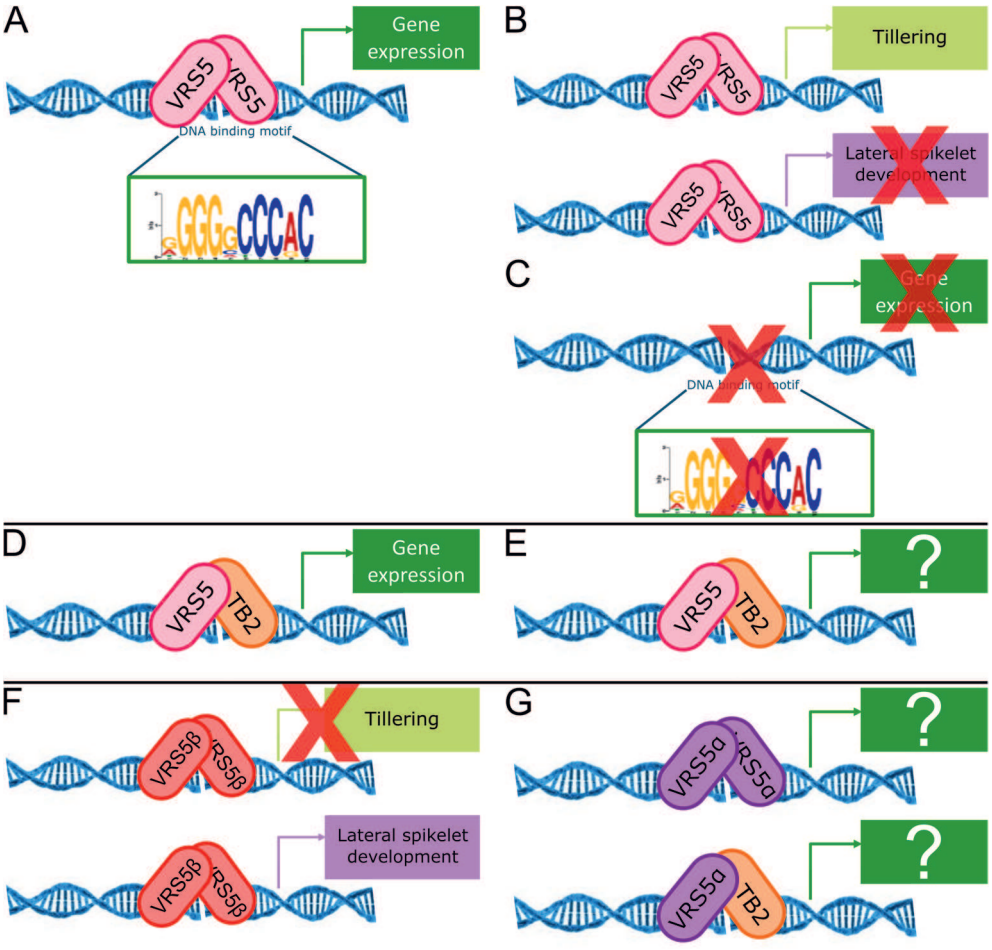


Figure 1: Graphical summary and outlook of strategies to untangle pleiotropy via VRS5. A) In Chapter 2, we showed the *bona fide* VRS5 targets for regulating tillering and lateral spikelet development. This gives opportunities to B) mutate targets specific for one of these processes or C) mutate the VRS5 binding sites for VRS5 targets to inhibit VRS5 specific regulation. In Chapter 3, we showed that VRS5 can bind DNA together with TB2. For binding to the *HvGT1* promoter, VRS5 needs TB2 to be able to bind. E) investigating which targets are bound by the VRS5-TB2 complex instead of VRS5 only, will give additional targets that may be involved in the pleiotropy of VRS5. F) In Chapter 3, we showed that a shorter protein isoform of VRS5, VRS5β, can regulate lateral spikelet development, but not tillering, showing that pleiotropy of VRS5 on lateral spikelet development and tillering can be untangled. G) Better understanding of the differences in DNA binding and targets of VRS5α and VRS5β, both as homodimer and in complex with TB2 can be used to predict how exactly pleiotropy of VRS5 can be untangled using different protein isoforms.



Reference list

R

Abramson, J., Adler, J., Dunger, J., Evans, R., Green, T., Pritzel, A., Ronneberger, O., Willmore, L., Ballard, A. J., Bambrick, J., Bodenstein, S. W., Evans, D. A., Hung, C.-C., O'Neill, M., Reiman, D., Tunyasuvunakool, K., Wu, Z., Žemgulytė, A., Arvaniti, E., ... Jumper, J. M. (2024). Accurate structure prediction of biomolecular interactions with AlphaFold 3. *Nature*, *630*(8016), 493–500. https://doi.org/10.1038/s41586-024-07487-w

Acosta, I. F., Laparra, H., Romero, S. P., Schmelz, E., Hamberg, M., Mottinger, J. P., Moreno, M. A., & Dellaporta, S. L. (2009). Tasselseed1 Is a Lipoxygenase Affecting Jasmonic Acid Signaling in Sex Determination of Maize. *Science*, *323*(5911), 262–265.

Aguilar-Martínez, J. A., Poza-Carrión, C., & Cubas, P. (2007). Arabidopsis BRANCHED1 Acts as an Integrator of Branching Signals within Axillary Buds. *The Plant Cell*, *19*(2), 458–472. https://doi.org/10.1105/tpc.106.048934

Agusti, J., & Greb, T. (2013). Going with the wind – Adaptive dynamics of plant secondary meristems. *Mechanisms of Development*, *130*(1), 34–44. https://doi.org/10.1016/j.mod.2012.05.011

Alfonso-Gonzalez, C., & Hilgers, V. (2024). (Alternative) transcription start sites as regulators of RNA processing. *Trends in Cell Biology*, *34*(12), 1018–1028. https://doi.org/10.1016/j.tcb.2024.02.010

Alqudah, A. M., Koppolu, R., Wolde, G. M., Graner, A., & Schnurbusch, T. (2016). The Genetic Architecture of Barley Plant Stature. *Frontiers in Genetics*, *7*. https://doi.org/10.3389/fgene.2016.00117

Anzalone, A. V., Randolph, P. B., Davis, J. R., Sousa, A. A., Koblan, L. W., Levy, J. M., Chen, P. J., Wilson, C., Newby, G. A., Raguram, A., & Liu, D. R. (2019). Search-and-replace genome editing without double-strand breaks or donor DNA. *Nature*, *576*(7785), 149–157. https://doi.org/10.1038/s41586-019-1711-4

Arite, T., Umehara, M., Ishikawa, S., Hanada, A., Maekawa, M., Yamaguchi, S., & Kyozuka, J. (2009). D14, a Strigolactone-Insensitive Mutant of Rice, Shows an Accelerated Outgrowth of Tillers. *Plant and Cell Physiology*, *50*(8), 1416–1424. https://doi.org/10.1093/pcp/pcp091

Babb, S., & Muehlbauer, G. (2003). Genetic and morphological characterization of the barley uniculm2 (cul2) mutant. *Theoretical and Applied Genetics*, *106*(5), 846–857. https://doi.org/10.1007/s00122-002-1104-0

Bai, F., Reinheimer, R., Durantini, D., Kellogg, E. A., & Schmidt, R. J. (2012). TCP transcription factor, BRANCH ANGLE DEFECTIVE 1 (BAD1), is required for normal tassel branch angle formation in maize. *Proceedings of the National Academy of Sciences of the United States of America*, *109*(30), 12225–12230. https://doi.org/10.1073/pnas.1202439109

Bailey, T. L. (2021). STREME: accurate and versatile sequence motif discovery. *Bioinformatics*, *37*(18), 2834–2840. https://doi.org/10.1093/bioinformatics/btab203

Bailey, T. L., Johnson, J., Grant, C. E., & Noble, W. S. (2015). The MEME Suite. *Nucleic Acids Research*, *43*(W1), W39–W49. https://doi.org/10.1093/nar/gkv416

Bakht, J., Shafi, M., Zubair, M., Aman, M., & Shah, Z. (2000). *EFFECT OF FOLIAR VS SOIL APPLICATION OF NITROGEN ON YIELD AND YIELD COMPONENTS OF WHEAT VARIETIES*.

Barrett, T., Wilhite, S. E., Ledoux, P., Evangelista, C., Kim, I. F., Tomashevsky, M., Marshall, K. A., Phillippy, K. H., Sherman, P. M., Holko, M., Yefanov, A., Lee, H., Zhang, N., Robertson, C. L., Serova, N., Davis, S., & Soboleva, A. (2013). NCBI GEO: Archive for functional genomics data sets—update. *Nucleic Acids Research*, *41*(D1), D991–D995. https://doi.org/10.1093/nar/gks1193

Bartlett, A., O'Malley, R. C., Huang, S. S. C., Galli, M., Nery, J. R., Gallavotti, A., & Ecker, J. R. (2017). Mapping genome-wide transcription-factor binding sites using DAP-seq. *Nature Protocols*, *12*(8), 1659–1672. https://doi.org/10.1038/nprot.2017.055

Belhaj, K., Chaparro-Garcia, A., Kamoun, S., & Nekrasov, V. (2013). Plant genome editing made easy: Targeted mutagenesis in model and crop plants using the CRISPR/Cas system. *Plant Methods*, *9*(1), 39. https://doi.org/10.1186/1746-4811-9-39

Berget, S. M., Moore, C., & Sharp, P. A. (1977). Spliced segments at the 5′ terminus of adenovirus 2 late mRNA*. *Proceedings of the National Academy of Sciences*, *74*(8), 3171–3175. https://doi.org/10.1073/pnas.74.8.3171

Beveridge, C. A., Rameau, C., & Wijerathna-Yapa, A. (2023). Lessons from a century of apical dominance research. *Journal of Experimental Botany*, *74*(14), 3903–3922. https://doi.org/10.1093/jxb/erad137

Bi, X., Esse, W. V., Mulki, M. A., Kirschner, G., Zhong, J., Simon, R., & Korff, M. V. (2019). Centroradialis interacts with flowering locus t-like genes to control floret development and grain number. *Plant Physiology*, *180*(2), 1013–1030. https://doi.org/10.1104/pp.18.01454

Bolger, A. M., Lohse, M., & Usadel, B. (2014). Trimmomatic: A flexible trimmer for Illumina sequence data. *Bioinformatics*, *30*(15), 2114–2120. https://doi.org/10.1093/bioinformatics/btu170

Bull, H., Casao, M. C., Zwirek, M., Flavell, A. J., Thomas, W. T. B., Guo, W., Zhang, R., Rapazote-Flores, P., Kyriakidis, S., Russell, J., Druka, A., McKim, S. M., & Waugh, R. (2017). Barley SIX-ROWED SPIKE3 encodes a putative Jumonji C-type H3K9me2/me3 demethylase that represses lateral spikelet fertility. *Nature Communications*, *8*(1), 936. https://doi.org/10.1038/s41467-017-00940-7

Bustos-Korts, D., Dawson, I. K., Russell, J., Tondelli, A., Guerra, D., Ferrandi, C., Strozzi, F., Nicolazzi, E. L., Molnar-Lang, M., Ozkan, H., Megyeri, M., Miko, P., Çakır, E., Yakışır, E., Trabanco, N., Delbono, S., Kyriakidis, S., Booth, A., Cammarano, D., … van Eeuwijk, F. A. (2019). Exome sequences and multi-environment field trials elucidate the genetic basis of adaptation in barley. *Plant Journal*, *99*(6), 1172–1191. https://doi.org/10.1111/tpj.14414

Cao, D., Chabikwa, T., Barbier, F., Dun, E. A., Fichtner, F., Dong, L., Kerr, S. C., & Beveridge, C. A. (2023). Auxin-independent effects of apical dominance induce changes in phytohormones correlated with bud outgrowth. *Plant Physiology*, *192*(2), 1420–1434. https://doi.org/10.1093/plphys/kiad034

Casal, J. J., Sanchez, R. A., & Deregibus, V. A. (1986). The effect of plant density on tillering: The involvement of R/FR ratio and the proportion of radiation intercepted per plant. *Environmental and Experimental Botany*, *26*(4), 365–371. https://doi.org/10.1016/0098-8472(86)90024-9

Castel, B., Tomlinson, L., Locci, F., Yang, Y., & Jones, J. D. G. (2019). Optimization of T-DNA architecture for Cas9-mediated mutagenesis in Arabidopsis. *PLoS ONE*, *14*(1), e0204778. https://doi.org/10.1371/journal.pone.0204778

Cerise, M., Falavigna, V. S., Rodríguez-Maroto, G., Signol, A., Severing, E., Gao, H., van Driel, A., Vincent, C., Wilkens, S., Iacobini, F., Formosa-Jordan, P., Pajoro, A., & Coupland, G. (2023). Two modes of gene regulation by TFL1 mediate its dual function in flowering time and shoot determinacy of Arabidopsis. *Development*, dev.202089. https://doi.org/10.1242/dev.202089

Chaturvedi, G. S., Aggarwal, P. K., Singh, A. K., Joshi, M. G., & Sinha, S. K. (1981). Effect of irrigation on tillering in wheat, triticale and barley in a water-limited environment. *Irrigation Science*, *2*(4), 225–235. https://doi.org/10.1007/BF00258376

Chen, B., Gilbert, L. A., Cimini, B. A., Schnitzbauer, J., Zhang, W., Li, G.-W., Park, J., Blackburn, E. H., Weissman, J. S., Qi, L. S., & Huang, B. (2013). Dynamic Imaging of Genomic Loci in Living Human Cells by an Optimized CRISPR/Cas System. *Cell*, *155*(7), 1479–1491. https://doi.org/10.1016/j.cell.2013.12.001

Chen, G., Mishina, K., Wang, Q., Zhu, H., Tagiri, A., Kikuchi, S., Sassa, H., Oono, Y., & Komatsuda, T. (2023). Organ-enriched gene expression during floral morphogenesis in wild barley. *The Plant Journal*, *116*(3), 887–902. https://doi.org/10.1111/tpj.16416

Chen, L., Zhao, Y., Xu, S., Zhang, Z., Xu, Y., Zhang, J., & Chong, K. (2018). OsMADS57 together with OsTB1 coordinates transcription of its target OsWRKY94 and D14 to switch its organogenesis to defense for cold adaptation in rice. *New Phytologist*, *218*(1), 219–231. https://doi.org/10.1111/nph.14977

Chen, P. J., Hussmann, J. A., Yan, J., Knipping, F., Ravisankar, P., Chen, P.-F., Chen, C., Nelson, J. W., Newby, G. A., Sahin, M., Osborn, M. J., Weissman, J. S., Adamson, B., & Liu, D. R. (2021). Enhanced prime editing systems by manipulating cellular determinants of editing outcomes. *Cell*, *184*(22), 5635-5652.e29. https://doi.org/10.1016/j.cell.2021.09.018

Chen, W., Yan, W., Jiang, K., & Huang, H. (2025). Molecular insights into DNA recognition by HD-Zip transcription factors. *Plant Physiology*, *198*(3), kiaf292. https://doi.org/10.1093/plphys/kiaf292

Chen, X., Gao, J., & Shen, Y. (2024). Abscisic acid controls sugar accumulation essential to strawberry fruit ripening via the FaRIPK1-FaTCP7-FaSTP13/FaSPT module. *The Plant Journal*, *n/a*(n/a). https://doi.org/10.1111/tpj.16862

Chomicki, G., Coiro, M., & Renner, S. S. (2017). Evolution and ecology of plant architecture: Integrating insights from the fossil record, extant morphology, developmental genetics and phylogenies. *Annals of Botany*, *120*(6), 855–891. https://doi.org/10.1093/aob/mcx113

Christensen, A. H., & Quail, P. H. (1996). Ubiquitin promoter-based vectors for high-level expression of selectable and/or screenable marker genes in monocotyledonous plants. *Transgenic Research*, *5*(3), 213–218. https://doi.org/10.1007/BF01969712

Chuck, G., Meeley, R., & Hake, S. (2008). Floral meristem initiation and meristem cell fate are regulated by the maize AP2 genes ids1 and sid1. *Development*, *135*(18), 3013–3019. https://doi.org/10.1242/dev.024273

Chuck, G., Muszynski, M., Kellogg, E., Hake, S., & Schmidt, R. J. (2002). The Control of Spikelet Meristem Identity by the branched silkless1 Gene in Maize. *Science*, *298*(5596), 1238–1241. https://doi.org/10.1126/science.1076920

Clark, R. M., Linton, E., Messing, J., & Doebley, J. F. (2004). Pattern of diversity in the genomic region near the maize domestication gene tb1. *Proceedings of the National Academy of Sciences*, *101*(3), 700–707. https://doi.org/10.1073/pnas.2237049100

Coen, E. S., & Meyerowitz, E. M. (1991). The war of the whorls: Genetic interactions controlling flower development. *Nature*, *353*(6339), 31–37. https://doi.org/10.1038/353031a0

Colleoni, P. E., van Es, S. W., Winkelmolen, T., Immink, R. G. H., & van Esse, G. W. (2024). Flowering time genes branching out. *Journal of Experimental Botany*, erae112. https://doi.org/10.1093/jxb/erae112

Collin, A., Matkowski, H., Sybilska, E., Biantari, A., Król, O., & Daszkowska-Golec, A. (2025). ABA-induced alternative splicing drives transcriptomic reprogramming for drought tolerance in barley. *BMC Plant Biology*, *25*(1), 445. https://doi.org/10.1186/s12870-025-06485-y

Comadran, J., Kilian, B., Russell, J., Ramsay, L., Stein, N., Ganal, M., Shaw, P., Bayer, M., Thomas, W., Marshall, D., Hedley, P., Tondelli, A., Pecchioni, N., Francia, E., Korzun, V., Walther, A., & Waugh, R. (2012). Natural variation in a homolog of Antirrhinum CENTRORADIALIS contributed to spring growth habit and environmental adaptation in cultivated barley. *Nature Genetics*, *44*(12), 1388–1391. https://doi.org/10.1038/ng.2447

Concordet, J.-P., & Haeussler, M. (2018). CRISPOR: Intuitive guide selection for CRISPR/Cas9 genome editing experiments and screens. *Nucleic Acids Research*, *46*(Web Server issue), W242–W245. https://doi.org/10.1093/nar/gky354

Coulter, M., Entizne, J. C., Guo, W., Bayer, M., Wonneberger, R., Milne, L., Schreiber, M., Haaning, A., Muehlbauer, G. J., McCallum, N., Fuller, J., Simpson, C., Stein, N., Brown, J. W. S., Waugh, R., & Zhang, R. (2022). BaRTv2: A highly resolved barley reference transcriptome for accurate transcript-specific RNA-seq quantification. *The Plant Journal*, *111*(4), 1183–1202. https://doi.org/10.1111/tpj.15871

Dabbert, T., Okagaki, R. J., Cho, S., Boddu, J., & Muehlbauer, G. J. (2009). The genetics of barley low-tillering mutants: Absent lower laterals (als). *Theoretical and Applied Genetics*, *118*(7), 1351–1360. https://doi.org/10.1007/s00122-009-0985-6

Dabbert, T., Okagaki, R. J., Cho, S., Heinen, S., Boddu, J., & Muehlbauer, G. J. (2010). The genetics of barley low-tillering mutants: Low number of tillers-1 (lnt1). *Theoretical and Applied Genetics*, *121*(4), 705–715. https://doi.org/10.1007/s00122-010-1342-5

Dang, Y., Jia, G., Choi, J., Ma, H., Anaya, E., Ye, C., Shankar, P., & Wu, H. (2015). Optimizing sgRNA structure to improve CRISPR-Cas9 knockout efficiency. *Genome Biology*, *16*(1), 1–10. https://doi.org/10.1186/s13059-015-0846-3

Danilevskaya, O. N., Meng, X., & Ananiev, E. V. (2010). Concerted Modification of Flowering Time and Inflorescence Architecture by Ectopic Expression of TFL1-Like Genes in Maize. *Plant Physiology*, *153*(1), 238–251. https://doi.org/10.1104/pp.110.154211

Davuluri, R. V., Suzuki, Y., Sugano, S., Plass, C., & Huang, T. H.-M. (2008). The functional consequences of alternative promoter use in mammalian genomes. *Trends in Genetics*, *24*(4), 167–177. https://doi.org/10.1016/j.tig.2008.01.008

de Klerk, E., & 't Hoen, P. A. C. (2015). Alternative mRNA transcription, processing, and translation: Insights from RNA sequencing. *Trends in Genetics*, *31*(3), 128–139. https://doi.org/10.1016/j.tig.2015.01.001

de Souza Moraes, T., van Es, S. W., Hernández-Pinzón, I., Kirschner, G. K., van der Wal, F., da Silveira, S. R., Busscher-Lange, J., Angenent, G. C., Moscou, M., Immink, R. G. H., & van Esse, G. W. (2022). The TCP transcription factor HvTB2 heterodimerizes with VRS5 and controls spike architecture in barley. *Plant Reproduction*, 2021.04.14.439785. https://doi.org/10.1007/s00497-022-00441-8

Deltcheva, E., Chylinski, K., Sharma, C. M., Gonzales, K., Chao, Y., Pirzada, Z. A., Eckert, M. R., Vogel, J., & Charpentier, E. (2011). CRISPR RNA maturation by trans-encoded small RNA and host factor RNase III. *Nature*, *471*(7340), 602–607. https://doi.org/10.1038/nature09886

Demesa-Arevalo, E., Dörpholz, H., Vardanega, I., Maika, J. E., Pineda-Valentino, I., Eggels, S., Lautwein, T., Köhrer, K., Schnurbusch, T., Korff, M. von, Usadel, B., & Simon, R. (2025). *Imputation integrates single-cell and spatial gene expression data to resolve transcriptional networks in barley shoot meristem development* (p. 2025.05.09.653223). bioRxiv. https://doi.org/10.1101/2025.05.09.653223

Derbyshire, P., & Byrne, M. E. (2013). *MORE SPIKELETS1*Is Required for Spikelet Fate in the Inflorescence of Brachypodium. *Plant Physiology*, *161*(3), 1291–1302. https://doi.org/10.1104/pp.112.212340

DeWitt, N., Guedira, M., Lauer, E., Sarinelli, M., Tyagi, P., Fu, D., Hao, Q., Murphy, J. P., Marshall, D., Akhunova, A., Jordan, K., Akhunov, E., & Brown-Guedira, G. (2020). Sequence-based mapping identifies a candidate transcription repressor underlying awn suppression at the B1 locus in wheat. *New Phytologist*, *225*(1), 326–339. https://doi.org/10.1111/nph.16152

Digel, B., Pankin, A., & von Korff, M. (2015). Global Transcriptome Profiling of Developing Leaf and Shoot Apices Reveals Distinct Genetic and Environmental Control of Floral Transition and Inflorescence Development in Barley. *The Plant Cell*, *27*(9), 2318–2334. https://doi.org/10.1105/TPC.15.00203

Dixon, L. E., Greenwood, J. R., Bencivenga, S., Zhang, P., Cockram, J., Mellers, G., Ramm, K., Cavanagh, C., Swain, S. M., & Boden, S. A. (2018). TEOSINTE BRANCHED1 regulates inflorescence architecture and development in bread wheat (Triticum aestivum). *Plant Cell*, *30*(3), 563–581. https://doi.org/10.1105/tpc.17.00961

Dixon, L. E., Pasquariello, M., & Boden, S. A. (2020). TEOSINTE BRANCHED1 regulates height and stem internode length in bread wheat. *Journal of Experimental Botany*, *71*(16), 4742–4750. https://doi.org/10.1093/jxb/eraa252

Dixon, L. E., Van Esse, W., Hirsz, D., Willemsen, V., & McKim, S. M. (2022). Cereal Architecture and Its Manipulation. *Annual Plant Reviews Online*, *5*(1), 1–54. https://doi.org/10.1002/9781119312994.apr0648

Doebley, J. (2004). The Genetics of Maize Evolution. *Annual Review of Genetics*, *38*(Volume 38, 2004), 37–59. https://doi.org/10.1146/annurev.genet.38.072902.092425

Doebley, J. F., Gaut, B. S., & Smith, B. D. (2006). The Molecular Genetics of Crop Domestication. *Cell*, *127*(7), 1309–1321. https://doi.org/10.1016/j.cell.2006.12.006

Doebley, J., Stec, A., & Gustus, C. (1995). teosinte branched1 and the origin of maize: Evidence for epistasis and the evolution of dominance. *Genetics*, *141*(1), 333–346. https://doi.org/10.1093/genetics/141.1.333

Doebley, J., Stec, A., & Hubbard, L. (1997). The evolution of apical dominance in maize. *Nature*, *386*(6624), 485–488. https://doi.org/10.1038/386485a0

Doench, J. G., Hartenian, E., Graham, D. B., Tothova, Z., Hegde, M., Smith, I., Sullender, M., Ebert, B. L., Xavier, R. J., & Root, D. E. (2014). Rational design of highly active sgRNAs for CRISPR-Cas9–mediated gene inactivation. *Nature Biotechnology*, *32*(12), 1262–1267. https://doi.org/10.1038/nbt.3026

Dong, Z., Xiao, Y., Govindarajulu, R., Feil, R., Siddoway, M. L., Nielsen, T., Lunn, J. E., Hawkins, J., Whipple, C., & Chuck, G. (2019). The regulatory landscape of a core maize domestication module controlling bud dormancy and growth repression. *Nature Communications*, *10*(1), 1–15. https://doi.org/10.1038/s41467-019-11774-w

Edgar, R. C. (2004). MUSCLE: Multiple sequence alignment with high accuracy and high throughput. *Nucleic Acids Research*, *32*(5), 1792–1797. https://doi.org/10.1093/nar/gkh340

Edgar, R., Domrachev, M., & Lash, A. E. (2002). Gene Expression Omnibus: NCBI gene expression and hybridization array data repository. *Nucleic Acids Research*, *30*(1), 207–210. https://doi.org/10.1093/nar/30.1.207

Emms, D. M., & Kelly, S. (2019). OrthoFinder: Phylogenetic orthology inference for comparative genomics. *Genome Biology*, *20*(1), 238. https://doi.org/10.1186/s13059-019-1832-y

Engler, C., Youles, M., Gruetzner, R., Ehnert, T. M., Werner, S., Jones, J. D. G., Patron, N. J., & Marillonnet, S. (2014). A Golden Gate modular cloning toolbox for plants. *ACS Synthetic Biology*, *3*(11), 839–843. https://doi.org/10.1021/sb4001504

Faure, S., Turner, A. S., Gruszka, D., Christodoulou, V., Davis, S. J., Von Korff, M., & Laurie, D. A. (2012). Mutation at the circadian clock gene EARLY MATURITY 8 adapts domesticated barley (Hordeum vulgare) to short growing seasons. *Proceedings of the National Academy of Sciences of the United States of America*, *109*(21), 8328–8333. https://doi.org/10.1073/PNAS.1120496109/SUPPL_FILE/PNAS.201120496SI.PDF

Feike, D., Korolev, A. V., Soumpourou, E., Murakami, E., Reid, D., Breakspear, A., Rogers, C., Radutoiu, S., Stougaard, J., Harwood, W. A., Oldroyd, G. E. D., & Miller, J. B. (2019). Characterizing standard genetic parts and establishing common principles for engineering legume and cereal roots. *Plant Biotechnology Journal*, *17*(12), 2234–2245. https://doi.org/10.1111/pbi.13135

Fernández-Calleja, M., Casas, A. M., & Igartua, E. (2021). Major flowering time genes of barley: Allelic diversity, effects, and comparison with wheat. *Theoretical and Applied Genetics*, *134*(7), 1867–1897. https://doi.org/10.1007/s00122-021-03824-z

Filippo, J. S., Sung, P., & Klein, H. (2008). Mechanism of Eukaryotic Homologous Recombination. *Annual Review of Biochemistry*, *77*(Volume 77, 2008), 229–257. https://doi.org/10.1146/annurev.biochem.77.061306.125255

Finlayson, S. A. (2007). Arabidopsis TEOSINTE BRANCHED1-LIKE 1 Regulates Axillary Bud Outgrowth and is Homologous to Monocot TEOSINTE BRANCHED1. *Plant and Cell Physiology*, *48*(5), 667–677. https://doi.org/10.1093/pcp/pcm044

Frei, D., Veekman, E., Grogg, D., Stoffel-Studer, I., Morishima, A., Shimizu-Inatsugi, R., Yates, S., Shimizu, K. K., Frey, J. E., Studer, B., & Copetti, D. (2021). Ultralong Oxford Nanopore Reads Enable the Development of a Reference-Grade Perennial Ryegrass Genome Assembly. *Genome Biology and Evolution*, *13*(8), evab159. https://doi.org/10.1093/gbe/evab159

Fu, D., Szűcs, P., Yan, L., Helguera, M., Skinner, J. S., von Zitzewitz, J., Hayes, P. M., & Dubcovsky, J. (2005). Large deletions within the first intron in VRN-1 are associated with spring growth habit in barley and wheat. *Molecular Genetics and Genomics*, *273*(1), 54–65. https://doi.org/10.1007/s00438-004-1095-4

Gao, Y. L., Song, Z. B., Li, W. Z., Jiao, F. C., Wang, R., Huang, C. J., Li, Y. P., & Wang, B. W. (2016). NtBRC1 suppresses axillary branching in tobacco after decapitation. *Genetics and Molecular Research: GMR*, *15*(4). https://doi.org/10.4238/gmr15049320

Garneau, J. E., Dupuis, M.-È., Villion, M., Romero, D. A., Barrangou, R., Boyaval, P., Fremaux, C., Horvath, P., Magadán, A. H., & Moineau, S. (2010). The CRISPR/Cas bacterial immune system cleaves bacteriophage and plasmid DNA. *Nature*, *468*(7320), 67–71. https://doi.org/10.1038/nature09523

Gasiunas, G., Barrangou, R., Horvath, P., & Siksnys, V. (2012). Cas9–crRNA ribonucleoprotein complex mediates specific DNA cleavage for adaptive immunity in bacteria. *Proceedings of the National Academy of Sciences*, *109*(39), E2579–E2586. https://doi.org/10.1073/pnas.1208507109

Gasparis, S., Kała, M., Przyborowski, M., Łyżnik, L. A., Orczyk, W., & Nadolska-Orczyk, A. (2018). A simple and efficient CRISPR/Cas9 platform for induction of single and multiple, heritable mutations in barley (Hordeum vulgare L.). *Plant Methods*, *14*, 111. https://doi.org/10.1186/s13007-018-0382-8

Gaudin, A. C., McClymont, S. A., Soliman, S. S., & Raizada, M. N. (2014). The effect of altered dosage of a mutant allele of Teosinte branched 1 (tb1-ref) on the root system of modern maize. *BMC Genetics*, *15*(1), Article 1. https://doi.org/10.1186/1471-2156-15-23

Gilbert, W. (1978). Why genes in pieces? *Nature*, *271*(5645), 501–501. https://doi.org/10.1038/271501a0

Gines, M., Baldwin, T., Rashid, A., Bregitzer, P., Maughan, P. J., Jellen, E. N., & Klos, K. E. (2018). Selection of Expression Reference Genes with Demonstrated Stability in Barley among a Diverse Set of Tissues and Cultivars. *Crop Science*, *58*(1), 332–341. https://doi.org/10.2135/CROPSCI2017.07.0443

Gol, L., Haraldsson, E. B., & Von Korff, M. (2021). Ppd-H1 integrates drought stress signals to control spike development and flowering time in barley. *Journal of Experimental Botany*, *72*(1), 122–136. https://doi.org/10.1093/jxb/eraa261

Gonzalez-Grandio, E., Pajoro, A., Franco-Zorrilla, J. M., Tarancon, C., Immink, R. G. H., & Cubas, P. (2017). Abscisic acid signaling is controlled by a BRANCHED1/HD-ZIP i cascade in Arabidopsis axillary buds. *Proceedings of the National Academy of Sciences of the United States of America*, *114*(2), E245–E254. https://doi.org/10.1073/pnas.1613199114

González-Grandío, E., Poza-Carrión, C., Sorzano, C. O. S., & Cubas, P. (2013). BRANCHED1 Promotes Axillary Bud Dormancy in Response to Shade in Arabidopsis. *The Plant Cell*, *25*(3), 834–850. https://doi.org/10.1105/tpc.112.108480

Greb, T., Clarenz, O., Schäfer, E., Müller, D., Herrero, R., Schmitz, G., & Theres, K. (2003). Molecular analysis of the LATERAL SUPPRESSOR gene in Arabidopsis reveals a conserved control mechanism for axillary meristem formation. *Genes & Development*, *17*(9), 1175–1187. https://doi.org/10.1101/gad.260703

Greene, E. A., Codomo, C. A., Taylor, N. E., Henikoff, J. G., Till, B. J., Reynolds, S. H., Enns, L. C., Burtner, C., Johnson, J. E., Odden, A. R., Comai, L., & Henikoff, S. (2003). Spectrum of Chemically Induced Mutations From a Large-Scale Reverse-Genetic Screen in Arabidopsis. *Genetics*, *164*(2), 731–740. https://doi.org/10.1093/genetics/164.2.731

Grützner, R., Martin, P., Horn, C., Mortensen, S., Cram, E. J., Lee-Parsons, C. W. T., Stuttmann, J., & Marillonnet, S. (2021). High-efficiency genome editing in plants mediated by a Cas9 gene containing multiple introns. *Plant Communications*, *2*(2), 100135. https://doi.org/10.1016/j.xplc.2020.100135

Guo, M., Zhang, Y., Jia, X., Wang, X., Zhang, Y., Liu, J., Yang, Q., Ruan, W., & Yi, K. (2022). Alternative splicing of REGULATOR OF LEAF INCLINATION 1 modulates phosphate starvation signaling and growth in plants. *The Plant Cell*, *34*(9), 3319–3338. https://doi.org/10.1093/plcell/koac161

Guo, S., Xu, Y., Liu, H., Mao, Z., Zhang, C., Ma, Y., Zhang, Q., Meng, Z., & Chong, K. (2013). The interaction between OsMADS57 and OsTB1 modulates rice tillering via DWARF14. *Nature Communications*, *4*(1), 1–12. https://doi.org/10.1038/ncomms2542

Guo, W., Schreiber, M., Marosi, V. B., Bagnaresi, P., Jørgensen, M. E., Braune, K. B., Chalmers, K., Chapman, B., Dang, V., Dockter, C., Fiebig, A., Fincher, G. B., Fricano, A., Fuller, J., Haaning, A., Haberer, G., Himmelbach, A., Jayakodi, M., Jia, Y., ... Waugh, R. (2025). A barley pan-transcriptome reveals layers of genotype-dependent transcriptional complexity. *Nature Genetics*, *57*(2), 441–450. https://doi.org/10.1038/s41588-024-02069-y

Hajheidari, M., & Huang, S. C. (2022). Elucidating the biology of transcription factor–DNA interaction for accurate identification of cis-regulatory elements. *Current Opinion in Plant Biology*, *68*, 102232. https://doi.org/10.1016/j.pbi.2022.102232

Hassan, M. M., Zhang, Y., Yuan, G., De, K., Chen, J.-G., Muchero, W., Tuskan, G. A., Qi, Y., & Yang, X. (2021). Construct design for CRISPR/Cas-based genome editing in plants. *Trends in Plant Science*, *26*(11), 1133–1152. https://doi.org/10.1016/j.tplants.2021.06.015

Hellens, R. P., Allan, A. C., Friel, E. N., Bolitho, K., Grafton, K., Templeton, M. D., Karunairetnam, S., Gleave, A. P., & Laing, W. A. (2005). Transient expression vectors for functional genomics, quantification of promoter activity and RNA silencing in plants. *Plant Methods*, *1*(1), 13. https://doi.org/10.1186/1746-4811-1-13

Hensel, G., Kastner, C., Oleszczuk, S., Riechen, J., & Kumlehn, J. (2009). *Agrobacterium*-Mediated Gene Transfer to Cereal Crop Plants: Current Protocols for Barley, Wheat, Triticale, and Maize. *International Journal of Plant Genomics*, *2009*, e835608. https://doi.org/10.1155/2009/835608

Hibara, K. I., Miya, M., Benvenuto, S. A., Hibara-Matsuo, N., Mimura, M., Yoshikawa, T., Suzuki, M., Kusaba, M., Taketa, S., & Itoh, J. I. (2021). Regulation of the plastochron by three many-noded dwarf genes in barley. *PLOS Genetics*, *17*(5), e1009292. https://doi.org/10.1371/JOURNAL.PGEN.1009292

Hinchliffe, A., & Harwood, W. A. (2019). Agrobacterium-mediated transformation of barley immature embryos. *Methods in Molecular Biology*, *1900*, 115–126. https://doi.org/10.1007/978-1-4939-8944-7_8/FIGURES/5

Holubová, K., Hensel, G., Vojta, P., Tarkowski, P., Bergougnoux, V., & Galuszka, P. (2018). Modification of Barley Plant Productivity Through Regulation of Cytokinin Content by Reverse-Genetics Approaches. *Frontiers in Plant Science*, *9*. https://doi.org/10.3389/fpls.2018.01676

Hsu, P. D., Lander, E. S., & Zhang, F. (2014). Development and Applications of CRISPR-Cas9 for Genome Engineering. *Cell*, *157*(6), 1262–1278. https://doi.org/10.1016/j.cell.2014.05.010

Hsu, P. D., Scott, D. A., Weinstein, J. A., Ran, F. A., Konermann, S., Agarwala, V., Li, Y., Fine, E. J., Wu, X., Shalem, O., Cradick, T. J., Marraffini, L. A., Bao, G., & Zhang, F. (2013). DNA targeting specificity of RNA-guided Cas9 nucleases. *Nature Biotechnology*, *31*(9), 827–832. https://doi.org/10.1038/nbt.2647

Hua, W., Tan, C., Xie, J., Zhu, J., Shang, Y., Yang, J., Zhang, X.-Q., Wu, X., Wang, J., & Li, C. (2020). Alternative splicing of a barley gene results in an excess-tillering and semi-dwarf mutant. *Theoretical and Applied Genetics*, *133*(1), 163–177. https://doi.org/10.1007/s00122-019-03448-4

Huang, D., Zheng, Q., Melchkart, T., Bekkaoui, Y., Konkin, D. J. F., Kagale, S., Martucci, M., You, F. M., Clarke, M., Adamski, N. M., Chinoy, C., Steed, A., McCartney, C. A., Cutler, A. J., Nicholson, P., & Feurtado, J. A. (2020). Dominant inhibition of awn development by a putative zinc-finger transcriptional repressor expressed at the B1 locus in wheat. *New Phytologist*, *225*(1), 340–355. https://doi.org/10.1111/nph.16154

Huang, X., Hilscher, J., Stoger, E., Christou, P., & Zhu, C. (2021). Modification of cereal plant architecture by genome editing to improve yields. *Plant Cell Reports*, *40*(6), 953–978. https://doi.org/10.1007/s00299-021-02668-7

Hubbard, L., McSteen, P., Doebley, J., & Hake, S. (2002). Expression patterns and mutant phenotype of teosinte branched1 correlate with growth suppression in maize and teosinte. *Genetics*, *162*(4), 1927–1935. https://doi.org/10.1093/genetics/162.4.1927

Hufford, M. B., Seetharam, A. S., Woodhouse, M. R., Chougule, K. M., Ou, S., Liu, J., Ricci, W. A., Guo, T., Olson, A., Qiu, Y., Della Coletta, R., Tittes, S., Hudson, A. I., Marand, A. P., Wei, S., Lu, Z., Wang, B., Tello-Ruiz, M. K., Piri, R. D., ... Dawe, R. K. (2021). De novo assembly, annotation, and comparative analysis of 26 diverse maize genomes. *Science*, *373*(6555), 655–662. https://doi.org/10.1126/science.abg5289

Hussain, T., Rehman, N., Inam, S., Ajmal, W., Afroz, A., Muhammad, A., Zafar, Y., Ali, G. M., & Khan, M. R. (2019). Homotypic Clusters of Transcription Factor Binding Sites in the First Large Intron of AGL24 MADS-Box Transcription Factor Are Recruited in the Enhancement of Floral Expression. *Plant Molecular Biology Reporter*, *37*(1), 24–40. https://doi.org/10.1007/s11105-019-01136-7

Hussien, A., Tavakol, E., Horner, D. S., Muñoz-Amatriaín, M., Muehlbauer, G. J., & Rossini, L. (2014). Genetics of Tillering in Rice and Barley. *The Plant Genome*, *7*(1), plantgenome2013.10.0032. https://doi.org/10.3835/PLANTGENOME2013.10.0032

Igartua, E., Contreras-Moreira, B., & Casas, A. M. (2020). TB1: From domestication gene to tool for many trades. *Journal of Experimental Botany*, *71*(16), 4621–4624. https://doi.org/10.1093/jxb/eraa308

Iltis, H. H. (1983). From Teosinte to Maize: The Catastrophic Sexual Transmutation. *Science*, *222*(4626), 886–894. https://doi.org/10.1126/science.222.4626.886

Jayakodi, M., Lu, Q., Pidon, H., Rabanus-Wallace, M. T., Bayer, M., Lux, T., Guo, Y., Jaegle, B., Badea, A., Bekele, W., Brar, G. S., Braune, K., Bunk, B., Chalmers, K. J., Chapman, B., Jørgensen, M. E., Feng, J.-W., Feser, M., Fiebig, A., ... Stein, N. (2024). Structural variation in the pangenome of wild and domesticated barley. *Nature*, 1–9. https://doi.org/10.1038/s41586-024-08187-1

Jeon, J.-S., Lee, S., & An, G. (2008). Intragenic Control of Expression of a Rice MADS Box Gene *OsMADS1*. *Molecules and Cells*, *26*(5), 474–480. https://doi.org/10.1016/S1016-8478(23)14025-8

Jiang, X., Lubini, G., Hernandes-Lopes, J., Rijnsburger, K., Veltkamp, V., de Maagd, R. A., Angenent, G. C., & Bemer, M. (2022). FRUITFULL-like genes regulate flowering time and inflorescence architecture in tomato. *The Plant Cell*, *34*(3), 1002–1019. https://doi.org/10.1093/plcell/koab298

Jiao, Y., Lee, Y. K., Gladman, N., Chopra, R., Christensen, S. A., Regulski, M., Burow, G., Hayes, C., Burke, J., Ware, D., & Xin, Z. (2018). MSD1 regulates pedicellate spikelet fertility in sorghum through the jasmonic acid pathway. *Nature Communications*, *9*(1). https://doi.org/10.1038/s41467-018-03238-4

Jin, J., Huang, W., Gao, J.-P., Yang, J., Shi, M., Zhu, M.-Z., Luo, D., & Lin, H.-X. (2008). Genetic control of rice plant architecture under domestication. *Nature Genetics*, *40*(11), 1365–1369. https://doi.org/10.1038/ng.247

Jinek, M., Chylinski, K., Fonfara, I., Hauer, M., Doudna, J. A., & Charpentier, E. (2012). A Programmable Dual-RNA–Guided DNA Endonuclease in Adaptive Bacterial Immunity. *Science*, *337*(6096), 816–821. https://doi.org/10.1126/science.1225829

Jinek, M., East, A., Cheng, A., Lin, S., Ma, E., & Doudna, J. (2013). RNA-programmed genome editing in human cells. *eLife*, *2*, e00471. https://doi.org/10.7554/eLife.00471

Joshi, S. (2023). Plant Adaptations to Extreme Environments: Survival Strategies for Plants in Harsh or Unique Habitats -A Review. *Advance Research in Sciences (ARS)*, *1*(2), 1–6. https://doi.org/10.54026/ARS/1010

Kaneko-Suzuki, M., Kurihara-Ishikawa, R., Okushita-Terakawa, C., Kojima, C., Nagano-Fujiwara, M., Ohki, I., Tsuji, H., Shimamoto, K., & Taoka, K. I. (2018). TFL1-Like Proteins in Rice Antagonize Rice FT-Like Protein in Inflorescence Development by Competition for Complex Formation with 14-3-3 and FD. *Plant and Cell Physiology*, *59*(3), 458–468. https://doi.org/10.1093/pcp/pcy021

Käppel, S., Rümpler, F., & Theißen, G. (2023). Cracking the Floral Quartet Code: How Do Multimers of MIKCC-Type MADS-Domain Transcription Factors Recognize Their Target Genes? *International Journal of Molecular Sciences*, *24*(9), 8253. https://doi.org/10.3390/ijms24098253

Karsai, I., Mészáros, K., Szűcs, P., Hayes, P. M., Láng, L., & Bedő, Z. (2006). The influence of photoperiod on the Vrn-H2 locus (4H) which is a major determinant of plant development and reproductive fitness traits in a facultative × winter barley (Hordeum vulgare L.) mapping population. *Plant Breeding*, *125*(5), 468–472. https://doi.org/10.1111/j.1439-0523.2006.01266.x

Kasperbauer, M. J. (1971). Spectral Distribution of Light in a Tobacco Canopy and Effects of End-of-Day Light Quality on Growth and Development 1. *Plant Physiology*, *47*(6), 775–778. https://doi.org/10.1104/pp.47.6.775

Kebrom, T. H., Brutnell, T. P., & Finlayson, S. A. (2010). Suppression of sorghum axillary bud outgrowth by shade, phyB and defoliation signalling pathways. *Plant, Cell and Environment*, *33*(1), 48–58. https://doi.org/10.1111/j.1365-3040.2009.02050.x

Kebrom, T. H., Burson, B. L., & Finlayson, S. A. (2006). Phytochrome B Represses Teosinte Branched1 Expression and Induces Sorghum Axillary Bud Outgrowth in Response to Light Signals. *Plant Physiology*, *140*(3), 1109–1117. https://doi.org/10.1104/pp.105.074856

Kelemen, O., Convertini, P., Zhang, Z., Wen, Y., Shen, M., Falaleeva, M., & Stamm, S. (2013). Function of alternative splicing. *Gene*, *514*(1), 1–30. https://doi.org/10.1016/j.gene.2012.07.083

Kelly, J. H., Gilmore, A. J., Situmorang, A., Porker, K. D., Marzec, M., Tucker, M. R., & Brewer, P. B. (2025). Strigolactones coordinate barley tillering and grain size. *Journal of Experimental Botany*, eraf229. https://doi.org/10.1093/jxb/eraf229

Kerstens, M., Galinha, C., Hofhuis, H., Nodine, M., Pardal, R., Scheres, B., & Willemsen, V. (2024). PLETHORA transcription factors promote early embryo development through induction of meristematic potential. *Development*, *151*(12), dev202527. https://doi.org/10.1242/dev.202527

Khush, G. S. (2001). Green revolution: The way forward. *Nature Reviews Genetics*, *2*(10), 815–822. https://doi.org/10.1038/35093585

Klasfeld, S., Roulé, T., & Wagner, D. (2022). Greenscreen: A simple method to remove artifactual signals and enrich for true peaks in genomic datasets including ChIP-seq data. *The Plant Cell*, *34*(12), 4795–4815. https://doi.org/10.1093/PLCELL/KOAC282

Komatsu, M., Chujo, A., Nagato, Y., Shimamoto, K., & Kyozuka, J. (2003). FRIZZY PANICLE is required to prevent the formation of axillary meristems and to establish floral meristem identity in rice spikelets. *Development*, *130*(16), 3841–3850. https://doi.org/10.1242/dev.00564

Komatsuda, T., Pourkheirandish, M., He, C., Azhaguvel, P., Kanamori, K., Perovic, D., Stein, N., Graner, A., Wicker, T., Tagiri, A., Lundqvist, U., Fujimura, T., Matsuoka, M., Matsumoto, T., & Yano, M. (2007). Six-rowed barley originated from a mutation in a homeodomain-leucine zipper I-class homeobox gene. *Proceedings of the National Academy of Sciences of the United States of America*, *104*(4), 1424–1429. https://doi.org/10.1073/pnas.0608580104

Komor, A. C., Kim, Y. B., Packer, M. S., Zuris, J. A., & Liu, D. R. (2016). Programmable editing of a target base in genomic DNA without double-stranded DNA cleavage. *Nature*, *533*(7603), 420–424. https://doi.org/10.1038/nature17946

Kong, X., Wang, F., Geng, S., Guan, J., Tao, S., Jia, M., Sun, G., Wang, Z., Wang, K., Ye, X., Ma, J., Liu, D., Wei, Y., Zheng, Y., Fu, X., Mao, L., Lan, X., & Li, A. (2022). The wheat AGL6-like MADS-box gene is a master regulator for floral organ identity and a target for spikelet meristem development manipulation. *Plant Biotechnology Journal*, *20*(1), 75–88. https://doi.org/10.1111/pbi.13696

Konishi, S., Izawa, T., Lin, S. Y., Ebana, K., Fukuta, Y., Sasaki, T., & Yano, M. (2006). An SNP Caused Loss of Seed Shattering During Rice Domestication. *Science*, *312*(5778), 1392–1396. https://doi.org/10.1126/science.1126410

Koppolu, R., Anwar, N., Sakuma, S., Tagiri, A., Lundqvist, U., Pourkheirandish, M., Rutten, T., Seiler, C., Himmelbach, A., Ariyadasa, R., Youssef, H. M., Stein, N., Sreenivasulu, N., Komatsuda, T., & Schnurbusch, T. (2013). *Six-rowed spike4* (*Vrs4*) controls spikelet determinacy and row-type in barley. *Proceedings of the National Academy of Sciences*, *110*(32), 13198–13203. https://doi.org/10.1073/pnas.1221950110

Koppolu, R., & Schnurbusch, T. (2019). Developmental pathways for shaping spike inflorescence architecture in barley and wheat. *Journal of Integrative Plant Biology*, *61*(3), 278–295. https://doi.org/10.1111/jipb.12771

Kosugi, S., & Ohashi, Y. (2002). DNA binding and dimerization specificity and potential targets for the TCP protein family. *Plant Journal*, *30*(3), 337–348. https://doi.org/10.1046/j.1365-313X.2002.01294.x

Kuijer, H. N. J., Shirley, N. J., Khor, S. F., Shi, J., Schwerdt, J., Zhang, D., Li, G., & Burton, R. A. (2021). Transcript Profiling of MIKCc MADS-Box Genes Reveals Conserved and Novel Roles in Barley Inflorescence Development. *Frontiers in Plant Science*, *12*, 1834. https://doi.org/10.3389/fpls.2021.705286

Kumar, V., Kim, S. H., Adnan, M. R., Heo, J., Jeong, J. H., Priatama, R. A., Lee, J. J., Kim, C. M., Je, B. I., Park, S. J., Xuan, Y. H., & Han, C. (2021). Tiller Outgrowth in Rice (Oryza sativa L.) is Controlled by OsGT1, Which Acts Downstream of FC1 in a PhyB-Independent Manner. *Journal of Plant Biology*, *64*(5), 417–430. https://doi.org/10.1007/s12374-021-09310-9

Kurihara, Y., Makita, Y., Kawashima, M., Fujita, T., Iwasaki, S., & Matsui, M. (2018). Transcripts from downstream alternative transcription start sites evade uORF-mediated inhibition of gene expression in Arabidopsis. *Proceedings of the National Academy of Sciences*, *115*(30), 7831–7836. https://doi.org/10.1073/pnas.1804971115

Lai, X., Daher, H., Galien, A., Hugouvieux, V., & Zubieta, C. (2019). Structural Basis for Plant MADS Transcription Factor Oligomerization. *Computational and Structural Biotechnology Journal*, *17*, 946–953. https://doi.org/10.1016/j.csbj.2019.06.014

Lamesch, P., Berardini, T. Z., Li, D., Swarbreck, D., Wilks, C., Sasidharan, R., Muller, R., Dreher, K., Alexander, D. L., Garcia-Hernandez, M., Karthikeyan, A. S., Lee, C. H., Nelson, W. D., Ploetz, L., Singh, S., Wensel, A., & Huala, E. (2012). The Arabidopsis Information Resource (TAIR): Improved gene annotation and new tools. *Nucleic Acids Research*, *40*(D1), D1202–D1210. https://doi.org/10.1093/nar/gkr1090

Lampropoulos, A., Sutikovic, Z., Wenzl, C., Maegele, I., Lohmann, J. U., & Forner, J. (2013). GreenGate – A Novel, Versatile, and Efficient Cloning System for Plant Transgenesis. *PLOS ONE*, *8*(12), e83043. https://doi.org/10.1371/journal.pone.0083043

Lawrenson, T., Clarke, M., Kirby, R., Forner, M., Steuernagel, B., Brown, J. K. M., & Harwood, W. (2024). An optimised CRISPR Cas9 and Cas12a mutagenesis toolkit for Barley and Wheat. *Plant Methods*, *20*(1), 123. https://doi.org/10.1186/s13007-024-01234-y

Lawrenson, T., & Harwood, W. A. (2019). Creating targeted gene knockouts in barley using CRISPR/Cas9. *Methods in Molecular Biology*, *1900*, 217–232. https://doi.org/10.1007/978-1-4939-8944-7_14

Lawrenson, T., Shorinola, O., Stacey, N., Li, C., Østergaard, L., Patron, N., Uauy, C., & Harwood, W. (2015). Induction of targeted, heritable mutations in barley and Brassica oleracea using RNA-guided Cas9 nuclease. *Genome Biology*, *16*(1), 258. https://doi.org/10.1186/s13059-015-0826-7

Lee, D.-Y., & An, G. (2012). Two AP2 family genes, SUPERNUMERARY BRACT (SNB) and OsINDETERMINATE SPIKELET 1 (OsIDS1), synergistically control inflorescence architecture and floral meristem establishment in rice. *The Plant Journal*, *69*(3), 445–461. https://doi.org/10.1111/j.1365-313X.2011.04804.x

Leopold, A. C. (1949). The Control of Tillering in Grasses by Auxin. *American Journal of Botany*, *36*(6), 437–440. https://doi.org/10.2307/2438077

Li, C., Lin, H., Chen, A., Lau, M., Jernstedt, J., & Dubcovsky, J. (2019). Wheat VRN1, FUL2 and FUL3 play critical and redundant roles in spikelet development and spike determinacy. *Development*, *146*(14), dev175398. https://doi.org/10.1242/dev.175398

Li, G., Kuijer, H. N. J., Yang, X., Liu, H., Shen, C., Shi, J., Betts, N., Tucker, M. R., Liang, W., Waugh, R., Burton, R. A., & Zhang, D. (2021). MADS1 maintains barley spike morphology at high ambient temperatures. *Nature Plants*, *7*(8), 1093–1107. https://doi.org/10.1038/s41477-021-00957-3

Li, H. (2013). *Aligning sequence reads, clone sequences and assembly contigs with BWA-MEM* (No. arXiv:1303.3997). arXiv. https://doi.org/10.48550/arXiv.1303.3997

Li, H. (2018). Minimap2: Pairwise alignment for nucleotide sequences. *Bioinformatics*, *34*(18), 3094–3100. https://doi.org/10.1093/bioinformatics/bty191

Li, H., & Durbin, R. (2010). Fast and accurate long-read alignment with Burrows–Wheeler transform. *Bioinformatics*, *26*(5), 589–595. https://doi.org/10.1093/BIOINFORMATICS/BTP698

Li, M., Yao, T., Lin, W., Hinckley, W. E., Galli, M., Muchero, W., Gallavotti, A., Chen, J.-G., & Huang, S. C. (2023). Double DAP-seq uncovered synergistic DNA binding of interacting bZIP transcription factors. *Nature Communications*, *14*(1), 2600. https://doi.org/10.1038/s41467-023-38096-2

Li, X., Qian, Q., Fu, Z., Wang, Y., Xiong, G., Zeng, D., Wang, X., Liu, X., Teng, S., Hiroshi, F., Yuan, M., Luo, D., Han, B., & Li, J. (2003). Control of tillering in rice. *Nature*, *422*(6932), 618–621. https://doi.org/10.1038/nature01518

Li, X., Wang, Y., Liu, Y., Yang, B., Wang, X., Wei, J., Lu, Z., Zhang, Y., Wu, J., Huang, X., Yang, L., & Chen, J. (2018). Base editing with a Cpf1–cytidine deaminase fusion. *Nature Biotechnology*, *36*(4), 324–327. https://doi.org/10.1038/nbt.4102

Liang, G., Zhang, H., Lou, D., & Yu, D. (2016). Selection of highly efficient sgRNAs for CRISPR/Cas9-based plant genome editing. *Scientific Reports*, *6*(1), 21451. https://doi.org/10.1038/srep21451

Liller, C. B., Neuhaus, R., Von Korff, M., Koornneef, M., & Van Esse, W. (2015). Mutations in barley row type genes have pleiotropic effects on shoot branching. *PLoS ONE*, *10*(10). https://doi.org/10.1371/journal.pone.0140246

Lin, Z., Li, X., Shannon, L. M., Yeh, C.-T., Wang, M. L., Bai, G., Peng, Z., Li, J., Trick, H. N., Clemente, T. E., Doebley, J., Schnable, P. S., Tuinstra, M. R., Tesso, T. T., White, F., & Yu, J. (2012). Parallel domestication of the Shattering1 genes in cereals. *Nature Genetics*, *44*(6), 720–724. https://doi.org/10.1038/ng.2281

Liu, H., Li, G., Yang, X., Kuijer, H. N. J., Liang, W., & Zhang, D. (2020). Transcriptome profiling reveals phase-specific gene expression in the developing barley inflorescence. *Crop Journal*, *8*(1), 71–86. https://doi.org/10.1016/j.cj.2019.04.005

Liu, L., Huang, J., He, L., Liu, N., Du, Y., Hou, R., Du, H., Qiu, F., & Zhang, Z. (2019). Dissecting the genetic architecture of important traits that enhance wild germplasm resource usage in modern maize breeding. *Molecular Breeding*, *39*(10), 1–11. https://doi.org/10.1007/s11032-019-1061-9

Liu, Y., Wang, Q., Ding, Y., Li, G., Xu, J., & Wang, S. (2011). Effects of external ABA, GA3 and NAA on the tiller bud outgrowth of rice is related to changes in endogenous hormones. *Plant Growth Regulation*, *65*(2), 247–254. https://doi.org/10.1007/s10725-011-9594-x

Love, M. I., Huber, W., & Anders, S. (2014). Moderated estimation of fold change and dispersion for RNA-seq data with DESeq2. *Genome Biology*, *15*(12), 550. https://doi.org/10.1186/s13059-014-0550-8

Lu, Z., Marand, A. P., Ricci, W. A., Ethridge, C. L., Zhang, X., & Schmitz, R. J. (2019). The prevalence, evolution and chromatin signatures of plant regulatory elements. *Nature Plants*, *5*(12), Article 12. https://doi.org/10.1038/s41477-019-0548-z

Lukens, L., & Doebley, J. (2001). Molecular evolution of the teosinte branched gene among maize and related grasses. *Molecular Biology and Evolution*, *18*(4), 627–638. https://doi.org/10.1093/oxfordjournals.molbev.a003843

Ma, X., Zhang, Q., Zhu, Q., Liu, W., Chen, Y., Qiu, R., Wang, B., Yang, Z., Li, H., Lin, Y., Xie, Y., Shen, R., Chen, S., Wang, Z., Chen, Y., Guo, J., Chen, L., Zhao, X., Dong, Z., & Liu, Y.-G. (2015). A Robust CRISPR/Cas9 System for Convenient, High-Efficiency Multiplex Genome Editing in Monocot and Dicot Plants. *Molecular Plant*, *8*(8), 1274–1284. https://doi.org/10.1016/j.molp.2015.04.007

Maher, K. A., Bajic, M., Kajala, K., Reynoso, M., Pauluzzi, G., West, D. A., Zumstein, K., Woodhouse, M., Bubb, K., Dorrity, M. W., Queitsch, C., Bailey-Serres, J., Sinha, N., Brady, S. M., & Deal, R. B. (2018). Profiling of accessible chromatin regions across multiple plant species and cell types reveals common gene regulatory principles and new control modules. *Plant Cell*, *30*(1), 15–36. https://doi.org/10.1105/tpc.17.00581

Marasco, L. E., & Kornblihtt, A. R. (2023). The physiology of alternative splicing. *Nature Reviews Molecular Cell Biology*, *24*(4), 242–254. https://doi.org/10.1038/s41580-022-00545-z

Markham, N. R., & Zuker, M. (2008). UNAFold. In J. M. Keith (Ed.), *Bioinformatics: Structure, Function and Applications* (pp. 3–31). Humana Press. https://doi.org/10.1007/978-1-60327-429-6_1

Martín-Trillo, M., & Cubas, P. (2010). TCP genes: A family snapshot ten years later. *Trends in Plant Science*, *15*(1), 31–39. https://doi.org/10.1016/j.tplants.2009.11.003

Martín-Trillo, M., Grandío, E. G., Serra, F., Marcel, F., Rodríguez-Buey, M. L., Schmitz, G., Theres, K., Bendahmane, A., Dopazo, H., & Cubas, P. (2011). Role of tomato BRANCHED1-like genes in the control of shoot branching. *The Plant Journal*, *67*(4), 701–714. https://doi.org/10.1111/j.1365-313X.2011.04629.x

Mascher, M., Jost, M., Kuon, J.-E., Himmelbach, A., Aßfalg, A., Beier, S., Scholz, U., Graner, A., & Stein, N. (2014). Mapping-by-sequencing accelerates forward genetics in barley. *Genome Biology*, *15*(6), R78. https://doi.org/10.1186/gb-2014-15-6-r78

Mascher, M., Wicker, T., Jenkins, J., Plott, C., Lux, T., Koh, C. S., Ens, J., Gundlach, H., Boston, L. B., Tulpová, Z., Holden, S., Hernández-Pinzón, I., Scholz, U., Mayer, K. F. X., Spannagl, M., Pozniak, C. J., Sharpe, A. G., Simková, H., Moscou, M. J., ... Stein, N. (2021). Long-read sequence assembly: A technical evaluation in barley. *The Plant Cell*, *33*(6), 1888–1906. https://doi.org/10.1093/PLCELL/KOAB077

Matsuoka, Y., Vigouroux, Y., Goodman, M. M., Sanchez G., J., Buckler, E., & Doebley, J. (2002). A single domestication for maize shown by multilocus microsatellite genotyping. *Proceedings of the National Academy of Sciences*, *99*(9), 6080–6084. https://doi.org/10.1073/pnas.052125199

McKenna, A., Hanna, M., Banks, E., Sivachenko, A., Cibulskis, K., Kernytsky, A., Garimella, K., Altshuler, D., Gabriel, S., Daly, M., & DePristo, M. A. (2010). The genome analysis toolkit: A MapReduce framework for analyzing next-generation DNA sequencing data. *Genome Research*, *20*(9), 1297–1303. https://doi.org/10.1101/gr.107524.110

Mejía-Guerra, M. K., Li, W., Galeano, N. F., Vidal, M., Gray, J., Doseff, A. I., & Grotewold, E. (2015). Core Promoter Plasticity Between Maize Tissues and Genotypes Contrasts with Predominance of Sharp Transcription Initiation Sites. *The Plant Cell*, *27*(12), 3309–3320. https://doi.org/10.1105/tpc.15.00630

Meng, E. C., Goddard, T. D., Pettersen, E. F., Couch, G. S., Pearson, Z. J., Morris, J. H., & Ferrin, T. E. (2023). UCSF ChimeraX: Tools for structure building and analysis. *Protein Science*, *32*(11), e4792. https://doi.org/10.1002/pro.4792

Mengiste, T., & Paszkowski, J. (1999). *Prospects for the Precise Engineering of Plant Genomes by Homologous Recombination*. *380*(7–8), 749–758. https://doi.org/10.1515/BC.1999.095

Meyer, R. S., & Purugganan, M. D. (2013). Evolution of crop species: Genetics of domestication and diversification. *Nature Reviews Genetics*, *14*(12), 840–852. https://doi.org/10.1038/nrg3605

Miralles, D. J., & Richards, R. A. (2000). Responses of Leaf and Tiller Emergence and Primordium Initiation in Wheat and Barley to Interchanged Photoperiod. *Annals of Botany*, *85*(5), 655–663.

Nahas, Z., Ticchiarelli, F., van Rongen, M., Dillon, J., & Leyser, O. (2024). The activation of Arabidopsis axillary buds involves a switch from slow to rapid committed outgrowth regulated by auxin and strigolactone. *New Phytologist*, *242*(3), 1084–1097. https://doi.org/10.1111/nph.19664

Nakagawa, M., Shimamoto, K., & Kyozuka, J. (2002). Overexpression of RCN1 and RCN2, rice TERMINAL FLOWER 1/CENTRORADIALIS homologs, confers delay of phase transition and altered panicle morphology in rice. *The Plant Journal*, *29*(6), 743–750. https://doi.org/10.1046/j.1365-313X.2002.01255.x

Ni, P., Zhao, Y., Zhou, X., Liu, Z., Huang, Z., Ni, Z., Sun, Q., & Zong, Y. (2023). Efficient and versatile multiplex prime editing in hexaploid wheat. *Genome Biology*, *24*, 156. https://doi.org/10.1186/s13059-023-02990-1

Nicolas, M., Rodríguez-Buey, M. L., Franco-Zorrilla, J. M., & Cubas, P. (2015). A Recently Evolved Alternative Splice Site in the *BRANCHED1a* Gene Controls Potato Plant Architecture. *Current Biology*, *25*(14), 1799–1809. https://doi.org/10.1016/j.cub.2015.05.053

Nielsen, S., Yuzenkova, Y., & Zenkin, N. (2013). Mechanism of Eukaryotic RNA Polymerase III Transcription Termination. *Science*, *340*(6140), 1577–1580. https://doi.org/10.1126/science.1237934

Nishida, K., Arazoe, T., Yachie, N., Banno, S., Kakimoto, M., Tabata, M., Mochizuki, M., Miyabe, A., Araki, M., Hara, K. Y., Shimatani, Z., & Kondo, A. (2016). Targeted nucleotide editing using hybrid prokaryotic and vertebrate adaptive immune systems. *Science*, *353*(6305), aaf8729. https://doi.org/10.1126/science.aaf8729

Nishimasu, H., Ran, F. A., Hsu, P. D., Konermann, S., Shehata, S. I., Dohmae, N., Ishitani, R., Zhang, F., & Nureki, O. (2014). Crystal Structure of Cas9 in Complex with Guide RNA and Target DNA. *Cell*, *156*(5), 935–949. https://doi.org/10.1016/j.cell.2014.02.001

Niwa, M., Daimon, Y., Kurotani, K. I., Higo, A., Pruneda-Paz, J. L., Breton, G., Mitsuda, N., Kay, S. A., Ohme-Takagi, M., Endo, M., & Araki, T. (2013). BRANCHED1 interacts with FLOWERING LOCUS T to repress the floral transition of the axillary meristems in Arabidopsis. *Plant Cell*, *25*(4), 1228–1242. https://doi.org/10.1105/tpc.112.109090

O'Malley, R. C., Huang, S. S. C., Song, L., Lewsey, M. G., Bartlett, A., Nery, J. R., Galli, M., Gallavotti, A., & Ecker, J. R. (2016). Cistrome and Epicistrome Features Shape the Regulatory DNA Landscape. *Cell*, *165*(5), 1280–1292. https://doi.org/10.1016/j.cell.2016.04.038

Ouyang, S., Zhu, W., Hamilton, J., Lin, H., Campbell, M., Childs, K., Thibaud-Nissen, F., Malek, R. L., Lee, Y., Zheng, L., Orvis, J., Haas, B., Wortman, J., & Buell, C. R. (2007). The TIGR Rice Genome Annotation Resource: Improvements and new features. *Nucleic Acids Research*, *35*(suppl_1), D883–D887. https://doi.org/10.1093/nar/gkl976

Ozcan, K. E., & Monroe, J. D. (2023). Maize β-amylase7 encodes 2 proteins using alternative transcriptional start sites: Nuclear BAM7 and plastidic BAM2. *Plant Physiology*, *192*(4), 2871–2882. https://doi.org/10.1093/plphys/kiad227

Park, J., Bae, S., & Kim, J.-S. (2015). Cas-Designer: A web-based tool for choice of CRISPR-Cas9 target sites. *Bioinformatics*, *31*(24), 4014–4016. https://doi.org/10.1093/bioinformatics/btv537

Parry, G., Patron, N., Bastow, R., & Matthewman, C. (2016). Meeting report: GARNet/OpenPlant CRISPR-Cas workshop. *Plant Methods*, *12*(1), 6. https://doi.org/10.1186/s13007-016-0104-z

Paszkowski, J., Baur, M., Bogucki, A., & Potrykus, I. (1988). Gene targeting in plants. *The EMBO Journal*, *7*(13), 4021–4026. https://doi.org/10.1002/j.1460-2075.1988.tb03295.x

Patro, R., Duggal, G., Love, M. I., Irizarry, R. A., & Kingsford, C. (2017). Salmon provides fast and bias-aware quantification of transcript expression. *Nature Methods*, *14*(4), Article 4. https://doi.org/10.1038/nmeth.4197

Pavlu, S., Nikumbh, S., Kovacik, M., An, T., Lenhard, B., Simkova, H., & Navratilova, P. (2024). Core promoterome of barley embryo. *Computational and Structural Biotechnology Journal*, *23*, 264–277. https://doi.org/10.1016/j.csbj.2023.12.003

Pelletier, J., & Sonenberg, N. (1988). Internal initiation of translation of eukaryotic mRNA directed by a sequence derived from poliovirus RNA. *Nature*, *334*(6180), 320–325. https://doi.org/10.1038/334320a0

Peltonen-Sainio, P., Kangas, A., Salo, Y., & Jauhiainen, L. (2007). Grain number dominates grain weight in temperate cereal yield determination: Evidence based on 30 years of multi-location trials. *Field Crops Research*, *100*(2), 179–188. https://doi.org/10.1016/j.fcr.2006.07.002

Pourkheirandish, M., Hensel, G., Kilian, B., Senthil, N., Chen, G., Sameri, M., Azhaguvel, P., Sakuma, S., Dhanagond, S., Sharma, R., Mascher, M., Himmelbach, A., Gottwald, S., Nair, S. K., Tagiri, A., Yukuhiro, F., Nagamura, Y., Kanamori, H., Matsumoto, T., … Komatsuda, T. (2015). Evolution of the Grain Dispersal System in Barley. *Cell*, *162*(3), 527–539. https://doi.org/10.1016/j.cell.2015.07.002

Poursarebani, N., Seidensticker, T., Koppolu, R., Trautewig, C., Gawroński, P., Bini, F., Govind, G., Rutten, T., Sakuma, S., Tagiri, A., Wolde, G. M., Youssef, H. M., Battal, A., Ciannamea, S., Fusca, T., Nussbaumer, T., Pozzi, C., Börner, A., Lundqvist, U., … Schnurbusch, T. (2015). The Genetic Basis of Composite Spike Form in Barley and 'Miracle-Wheat.' *Genetics*, *201*(1), 155–165. https://doi.org/10.1534/genetics.115.176628

Poursarebani, N., Trautewig, C., Melzer, M., Nussbaumer, T., Lundqvist, U., Rutten, T., Schmutzer, T., Brandt, R., Himmelbach, A., Altschmied, L., Koppolu, R., Youssef, H. M., Sibout, R., Dalmais, M., Bendahmane, A., Stein, N., Xin, Z., & Schnurbusch, T. (2020). COMPOSITUM 1 contributes to the architectural simplification of barley inflorescence via meristem identity signals. *Nature Communications*, *11*(1), 1–16. https://doi.org/10.1038/s41467-020-18890-y

Pumplin, N., Sarazin, A., Jullien, P. E., Bologna, N. G., Oberlin, S., & Voinnet, O. (2016). DNA Methylation Influences the Expression of DICER-LIKE4 Isoforms, Which Encode Proteins of Alternative Localization and Function. *The Plant Cell*, *28*(11), 2786–2804. https://doi.org/10.1105/tpc.16.00554

Qi, J., Qian, Q., Bu, Q., Li, S., Chen, Q., Sun, J., Liang, W., Zhou, Y., Chu, C., Li, X., Ren, F., Palme, K., Zhao, B., Chen, J., Chen, M., & Li, C. (2008). Mutation of the Rice Narrow leaf1 Gene, Which Encodes a Novel Protein, Affects Vein Patterning and Polar Auxin Transport. *Plant Physiology*, *147*(4), 1947–1959. https://doi.org/10.1104/pp.108.118778

Quinlan, A. R., & Hall, I. M. (2010). BEDTools: A flexible suite of utilities for comparing genomic features. *Bioinformatics*, *26*(6), 841–842. https://doi.org/10.1093/bioinformatics/btq033

Ramsay, L., Comadran, J., Druka, A., Marshall, D. F., Thomas, W. T. B., MacAulay, M., MacKenzie, K., Simpson, C., Fuller, J., Bonar, N., Hayes, P. M., Lundqvist, U., Franckowiak, J. D., Close, T. J., Muehlbauer, G. J., & Waugh, R. (2011). INTERMEDIUM-C, a modifier of lateral spikelet fertility in barley, is an ortholog of the maize domestication gene TEOSINTE BRANCHED 1. *Nature Genetics*, *43*(2), 169–172. https://doi.org/10.1038/ng.745

Ran, F. A., Hsu, P. D., Wright, J., Agarwala, V., Scott, D. A., & Zhang, F. (2013). Genome engineering using the CRISPR-Cas9 system. *Nature Protocols*, *8*(11), 2281–2308. https://doi.org/10.1038/nprot.2013.143

Ren, X., Zhi, L., Liu, L., Meng, D., Su, Q., Batool, A., Ji, J., Song, L., Zhang, N., Guo, L., Liu, X., Li, J., & Zhang, W. (2021). Alternative Splicing of TaGS3 Differentially Regulates Grain Weight and Size in Bread Wheat. *International Journal of Molecular Sciences*, *22*(21), 11692. https://doi.org/10.3390/ijms222111692

Reynolds, A., Leake, D., Boese, Q., Scaringe, S., Marshall, W. S., & Khvorova, A. (2004). Rational siRNA design for RNA interference. *Nature Biotechnology*, *22*(3), 326–330. https://doi.org/10.1038/nbt936

Riaz, A., Alqudah, A. M., Kanwal, F., Pillen, K., Ye, L., Dai, F., & Zhang, G. (2023). Advances in studies on the physiological and molecular regulation of barley tillering. *Journal of Integrative Agriculture*, *22*(1), 1–13. https://doi.org/10.1016/j.jia.2022.08.011

Rijpkema, A. S., Vandenbussche, M., Koes, R., Heijmans, K., & Gerats, T. (2010). Variations on a theme: Changes in the floral ABCs in angiosperms. *Seminars in Cell & Developmental Biology*, *21*(1), 100–107. https://doi.org/10.1016/j.semcdb.2009.11.002

Robinson, J. T., Thorvaldsdóttir, H., Winckler, W., Guttman, M., Lander, E. S., Getz, G., & Mesirov, J. P. (2011). Integrative genomics viewer. *Nature Biotechnology*, *29*(1), Article 1. https://doi.org/10.1038/nbt.1754

Ryu, C.-H., Lee, S., Cho, L.-H., Kim, S. L., Lee, Y.-S., Choi, S. C., Jeong, H. J., Yi, J., Park, S. J., Han, C.-D., & An, G. (2009). OsMADS50 and OsMADS56 function antagonistically in regulating long day (LD)-dependent flowering in rice. *Plant, Cell & Environment*, *32*(10), 1412–1427. https://doi.org/10.1111/j.1365-3040.2009.02008.x

Saisho, D., Ishii, M., Hori, K., & Sato, K. (2011). Natural Variation of Barley Vernalization Requirements: Implication of Quantitative Variation of Winter Growth Habit as an Adaptive Trait in East Asia. *Plant and Cell Physiology*, *52*(5), 775–784. https://doi.org/10.1093/pcp/pcr046

Sakuma, S., Golan, G., Guo, Z., Ogawa, T., Tagiri, A., Sugimoto, K., Bernhardt, N., Brassac, J., Mascher, M., Hensel, G., Ohnishi, S., Jinno, H., Yamashita, Y., Ayalon, I., Peleg, Z., Schnurbusch, T., & Komatsuda, T. (2019). Unleashing floret fertility in wheat through the mutation of a homeobox gene. *Proceedings of the National Academy of Sciences of the United States of America*, *116*(11), 5182–5187. https://doi.org/10.1073/pnas.1815465116

Sakuma, S., Lundqvist, U., Kakei, Y., Thirulogachandar, V., Suzuki, T., Hori, K., Wu, J., Tagiri, A., Rutten, T., Koppolu, R., Shimada, Y., Houston, K., Thomas, W. T. B., Waugh, R., Schnurbusch, T., & Komatsuda, T. (2017). Extreme Suppression of Lateral Floret Development by a Single Amino Acid Change in the VRS1 Transcription Factor. *Plant Physiology*, *175*(4), 1720–1731. https://doi.org/10.1104/pp.17.01149

Sapranauskas, R., Gasiunas, G., Fremaux, C., Barrangou, R., Horvath, P., & Siksnys, V. (2011). The Streptococcus thermophilus CRISPR/Cas system provides immunity in Escherichia coli. *Nucleic Acids Research*, *39*(21), 9275–9282. https://doi.org/10.1093/nar/gkr606

Sarnow, P. (1989). Translation of glucose-regulated protein 78/immunoglobulin heavy-chain binding protein mRNA is increased in poliovirus-infected cells at a time when cap-dependent translation of cellular mRNAs is inhibited. *Proceedings of the National Academy of Sciences*, *86*(15), 5795–5799. https://doi.org/10.1073/pnas.86.15.5795

Sayed, M. A., Allam, M., Heck, Q. K., Urbanavičiūtė, I., Rutten, T., Stuart, D., Zakhrabekova, S., Börner, A., Pillen, K., Hansson, M., & Youssef, H. M. (2021). Analyses of mads-box genes suggest hvmads56 to regulate lateral spikelet development in barley. *Plants*, *10*(12), 2825. https://doi.org/10.3390/plants10122825

Schauer, S. E., Baskar, R., Schlüter, P., Gheyselinck, J., Bolaños, A., Curtis, M. D., & Grossniklaus, U. (2008). Regulatory elements encoded in the first intron are necessary for proper expression of the MADS-box transcription factors AGL6 and AGL13 in *Arabidopsis thaliana*. *Developmental Biology*, *319*(2), 587. https://doi.org/10.1016/j.ydbio.2008.05.477

Schauer, S. E., Schlüter, P. M., Baskar, R., Gheyselinck, J., Bolaños, A., Curtis, M. D., & Grossniklaus, U. (2009). Intronic regulatory elements determine the divergent expression patterns of AGAMOUS-LIKE6 subfamily members in Arabidopsis. *The Plant Journal*, *59*(6), 987–1000. https://doi.org/10.1111/j.1365-313X.2009.03928.x

Schreiber, M., Mascher, M., Wright, J., Padmarasu, S., Himmelbach, A., Heavens, D., Milne, L., Clavijo, B. J., Stein, N., & Waugh, R. (2020). A Genome Assembly of the Barley 'Transformation Reference' Cultivar Golden Promise. *G3: Genes|Genomes|Genetics*, *10*(6), 1823–1827. https://doi.org/10.1534/g3.119.401010

Schultheiss, H., Hensel, G., Imani, J., Broeders, S., Sonnewald, U., Kogel, K.-H., Kumlehn, J., & Hückelhoven, R. (2005). Ectopic Expression of Constitutively Activated RACB in Barley Enhances Susceptibility to Powdery Mildew and Abiotic Stress. *Plant Physiology*, *139*(1), 353–362. https://doi.org/10.1104/pp.105.066613

Schumacher, K., Schmitt, T., Rossberg, M., Schmitz, G., & Theres, K. (1999). The Lateral suppressor (Ls) gene of tomato encodes a new member of the VHIID protein family. *Proceedings of the National Academy of Sciences*, *96*(1), 290–295. https://doi.org/10.1073/pnas.96.1.290

Schuster, P. (2014). *Fast folding and comparison of RNA secondary structures*. https://www.academia.edu/6873074/Fast_folding_and_comparison_of_RNA_secondary_structures

Sessa, G., Morelli, G., & Ruberti, I. (1993). The Athb-1 and -2 HD-Zip domains homodimerize forming complexes of different DNA binding specificities. *EMBO Journal*, *12*(9), 3507–3517. https://doi.org/10.1002/j.1460-2075.1993.tb06025.x

Shaaf, S., Bretani, G., Biswas, A., Fontana, I. M., & Rossini, L. (2019). Genetics of barley tiller and leaf development. *Journal of Integrative Plant Biology*, *61*(3), 226–256. https://doi.org/10.1111/jipb.12757

Shan, Q., Wang, Y., Li, J., Zhang, Y., Chen, K., Liang, Z., Zhang, K., Liu, J., Xi, J. J., Qiu, J.-L., & Gao, C. (2013). Targeted genome modification of crop plants using a CRISPR-Cas system. *Nature Biotechnology*, *31*(8), 686–688. https://doi.org/10.1038/nbt.2650

Shang, Q., Wang, Y., Tang, H., Sui, N., Zhang, X., & Wang, F. (2021). Genetic, hormonal, and environmental control of tillering in wheat. *The Crop Journal*, *9*(5), 986–991. https://doi.org/10.1016/j.cj.2021.03.002

Shang, Y., Yuan, L., Di, Z., Jia, Y., Zhang, Z., Li, S., Xing, L., Qi, Z., Wang, X., Zhu, J., Hua, W., Wu, X., Zhu, M., Li, G., & Li, C. (2020). A CYC/TB1-type TCP transcription factor controls spikelet meristem identity in barley. *Journal of Experimental Botany*, *71*(22), 7118–7131. https://doi.org/10.1093/jxb/eraa416

Shanmugaraj, N., Rajaraman, J., Kale, S., Kamal, R., Huang, Y., Thirulogachandar, V., Garibay-Hernández, A., Budhagatapalli, N., Tandron Moya, Y. A., Hajirezaei, M. R., Rutten, T., Hensel, G., Melzer, M., Kumlehn, J., von Wirén, N., Mock, H.-P., & Schnurbusch, T. (2023). Multilayered regulation of developmentally programmed pre-anthesis tip degeneration of the barley inflorescence. *The Plant Cell*. https://doi.org/10.1093/PLCELL/KOAD164

Shannon, S., & Meeks-Wagner, D. R. (1991). A Mutation in the Arabidopsis TFL1 Gene Affects Inflorescence Meristem Development. *The Plant Cell*, *3*(9), 877–892. https://doi.org/10.2307/3869152

SHARIF, R., & DALE, J. E. (1980). Growth-Regulating Substances and the Growth of Tiller Buds in Barley; Effects of Cytokinins. *Journal of Experimental Botany*, *31*(4), 921–930. https://doi.org/10.1093/jxb/31.4.921

Shen, C., Yang, X., Wang, D., Li, G., & Tucker, M. R. (2024). Functional retrogression of LOFSEPs in specifying floral organs in barley. *aBIOTECH*. https://doi.org/10.1007/s42994-024-00182-4

Shinohara, N., Taylor, C., & Leyser, O. (2013). Strigolactone Can Promote or Inhibit Shoot Branching by Triggering Rapid Depletion of the Auxin Efflux Protein PIN1 from the Plasma Membrane. *PLOS Biology*, *11*(1), e1001474. https://doi.org/10.1371/journal.pbio.1001474

Shirasawa, K., Hirakawa, H., Nunome, T., Tabata, S., & Isobe, S. (2016). Genome-wide survey of artificial mutations induced by ethyl methanesulfonate and gamma rays in tomato. *Plant Biotechnology Journal*, *14*(1), 51–60. https://doi.org/10.1111/pbi.12348

Simons, K. J., Fellers, J. P., Trick, H. N., Zhang, Z., Tai, Y.-S., Gill, B. S., & Faris, J. D. (2006). Molecular Characterization of the Major Wheat Domestication Gene Q. *Genetics*, *172*(1), 547–555. https://doi.org/10.1534/genetics.105.044727

Skinner, R. H., & Simmons, S. R. (1993). Modulation of leaf elongation, tiller appearance and tiller senescence in spring barley by far-red light. *Plant, Cell & Environment*, *16*(5), 555–562. https://doi.org/10.1111/j.1365-3040.1993.tb00903.x

Slafer, G. A., Calderini, D. F., & Miralles, D. J. (1996). Yield components and compensation in wheat: Opportunities for further increasing yield potential. *Increasing Yield Potential in Wheat: Breaking the Barriers*, 101–133.

Smaczniak, C., Immink, R. G. H., Muiño, J. M., Blanvillain, R., Busscher, M., Busscher-Lange, J., Dinh, Q. D. (Peter), Liu, S., Westphal, A. H., Boeren, S., Parcy, F., Xu, L., Carles, C. C., Angenent, G. C., & Kaufmann, K. (2012). Characterization of MADS-domain transcription factor complexes in Arabidopsis flower development. *Proceedings of the National Academy of Sciences*, *109*(5), 1560–1565. https://doi.org/10.1073/pnas.1112871109

Smedley, M. A., Hayta, S., Clarke, M., & Harwood, W. A. (2021). CRISPR-Cas9 Based Genome Editing in Wheat. *Current Protocols*, *1*(3), e65. https://doi.org/10.1002/cpz1.65

Spielmeyer, W., Ellis, M. H., & Chandler, P. M. (2002). Semidwarf (sd-1), "green revolution" rice, contains a defective gibberellin 20-oxidase gene. *Proceedings of the National Academy of Sciences*, *99*(13), 9043–9048. https://doi.org/10.1073/pnas.132266399

Stamatakis, A. (2014). RAxML version 8: A tool for phylogenetic analysis and post-analysis of large phylogenies. *Bioinformatics*, *30*(9), 1312–1313. https://doi.org/10.1093/bioinformatics/btu033

Studer, A. J., & Doebley, J. F. (2012). Evidence for a Natural Allelic Series at the Maize Domestication Locus teosinte branched1. *Genetics*, *191*(3), 951–958. https://doi.org/10.1534/genetics.112.138479

Studer, A., Zhao, Q., Ross-Ibarra, J., & Doebley, J. (2011). Identification of a functional transposon insertion in the maize domestication gene tb1. *Nature Genetics*, *43*(11), 1160–1163. https://doi.org/10.1038/ng.942

Sukumaran, S., Lopes, M., Dreisigacker, S., & Reynolds, M. (2018). Genetic analysis of multi-environmental spring wheat trials identifies genomic regions for locus-specific trade-offs for grain weight and grain number. *Theoretical and Applied Genetics*, *131*(4), 985–998. https://doi.org/10.1007/s00122-017-3037-7

Sun, J., Liu, H., Liu, J., Cheng, S., Peng, Y., Zhang, Q., Yan, J., Liu, H.-J., & Chen, L.-L. (2019). CRISPR-Local: A local single-guide RNA (sgRNA) design tool for non-reference plant genomes. *Bioinformatics*, *35*(14), 2501–2503. https://doi.org/10.1093/bioinformatics/bty970

Sun, M., Jiang, C., Gao, G., An, C., Wu, W., Kan, J., Zhang, J., Li, L., & Yang, P. (2024). A novel type of malformed floral organs mutant in barley was conferred by loss-of-function mutations of the MADS-box gene HvAGL6. *The Plant Journal*, *119*(6), 2609–2621. https://doi.org/10.1111/tpj.16936

Sussex, I. M., & Kerk, N. M. (2001). The evolution of plant architecture. *Current Opinion in Plant Biology*, *4*(1), 33–37. https://doi.org/10.1016/S1369-5266(00)00132-1

Takeda, T., Suwa, Y., Suzuki, M., Kitano, H., Ueguchi-Tanaka, M., Ashikari, M., Matsuoka, M., & Ueguchi, C. (2003). The OsTB1 gene negatively regulates lateral branching in rice. *The Plant Journal*, *33*(3), 513–520. https://doi.org/10.1046/J.1365-313X.2003.01648.X

Tavakol, E., Okagaki, R., Verderio, G., Shariati J., V., Hussien, A., Bilgic, H., Scanlon, M. J., Todt, N. R., Close, T. J., Druka, A., Waugh, R., Steuernagel, B., Ariyadasa, R., Himmelbach, A., Stein, N., Muehlbauer, G. J., & Rossini, L. (2015). The Barley Uniculme4 Gene Encodes a BLADE-ON-PETIOLE-Like Protein That Controls Tillering and Leaf Patterning. *Plant Physiology*, *168*(1), 164–174. https://doi.org/10.1104/pp.114.252882

Terada, R., Urawa, H., Inagaki, Y., Tsugane, K., & Iida, S. (2002). Efficient gene targeting by homologous recombination in rice. *Nature Biotechnology*, *20*(10), 1030–1034. https://doi.org/10.1038/nbt737

Thieffry, A., López-Márquez, D., Bornholdt, J., Malekroudi, M. G., Bressendorff, S., Barghetti, A., Sandelin, A., & Brodersen, P. (2022). PAMP-triggered genetic reprogramming involves widespread alternative transcription initiation and an immediate transcription factor wave. *The Plant Cell*, *34*(7), 2615–2637. https://doi.org/10.1093/plcell/koac108

Thiel, J., Koppolu, R., Trautewig, C., Hertig, C., Kale, S. M., Erbe, S., Mascher, M., Himmelbach, A., Rutten, T., Esteban, E., Pasha, A., Kumlehn, J., Provart, N. J., Vanderauwera, S., Frohberg, C., & Schnurbusch, T. (2021). Transcriptional landscapes of floral meristems in barley. *Science Advances*, *7*(18), 832–860. https://doi.org/10.1126/sciadv.abf0832

Thirulogachandar, V., Koppolu, R., & Schnurbusch, T. (2021). Strategies of grain number determination differentiate barley row types. *Journal of Experimental Botany*, *72*(22), 7754–7768. https://doi.org/10.1093/jxb/erab395

Thorvaldsdóttir, H., Robinson, J. T., & Mesirov, J. P. (2013). Integrative Genomics Viewer (IGV): High-performance genomics data visualization and exploration. *Briefings in Bioinformatics*, *14*(2), 178–192. https://doi.org/10.1093/bib/bbs017

Tognacca, R. S., Rodríguez, F. S., Aballay, F. E., Cartagena, C. M., Servi, L., & Petrillo, E. (2023). Alternative splicing in plants: Current knowledge and future directions for assessing the biological relevance of splice variants. *Journal of Experimental Botany*, *74*(7), 2251–2272. https://doi.org/10.1093/jxb/erac431

Törönen, P., Medlar, A., & Holm, L. (2018). PANNZER2: A rapid functional annotation web server. *Nucleic Acids Research*, *46*(W1), W84–W88. https://doi.org/10.1093/nar/gky350

Trevaskis, B., Bagnall, D. J., Ellis, M. H., Peacock, W. J., & Dennis, E. S. (2003). MADS box genes control vernalization-induced flowering in cereals. *Proceedings of the National Academy of Sciences*, *100*(22), 13099–13104. https://doi.org/10.1073/pnas.1635053100

Turner, A., Beales, J., Faure, S., Dunford, R. P., & Laurie, D. A. (2005). The Pseudo-Response Regulator Ppd-H1 Provides Adaptation to Photoperiod in Barley. *Science*, *310*(5750), 1031–1034. https://doi.org/10.1126/science.1117619

Ushijima, T., Hanada, K., Gotoh, E., Yamori, W., Kodama, Y., Tanaka, H., Kusano, M., Fukushima, A., Tokizawa, M., Yamamoto, Y. Y., Tada, Y., Suzuki, Y., & Matsushita, T. (2017). Light Controls Protein Localization through Phytochrome-Mediated Alternative Promoter Selection. *Cell*, *171*(6), 1316-1325.e12. https://doi.org/10.1016/j.cell.2017.10.018

van Es, S. W., Muñoz-Gasca, A., Romero-Campero, F. J., González-Grandío, E., de los Reyes, P., Tarancón, C., van Dijk, A. D. J., van Esse, W., Pascual-García, A., Angenent, G. C., Immink, R. G. H., & Cubas, P. (2024). A gene regulatory network critical for axillary bud dormancy directly controlled by Arabidopsis BRANCHED1. *New Phytologist*, *241*(3), 1193–1209. https://doi.org/10.1111/nph.19420

van Esse, G. W. (2022). The quest for optimal plant architecture. *Science*, *376*(6589), 133–134. https://doi.org/10.1126/science.abo7429

van Esse, G. W., Walla, A., Finke, A., Koornneef, M., Pecinka, A., & von Korff, M. (2017). Six-Rowed Spike3 (VRS3) Is a Histone Demethylase That Controls Lateral Spikelet Development in Barley. *Plant Physiology*, *174*(4), 2397–2408. https://doi.org/10.1104/pp.17.00108

van Heerwaarden, J., Doebley, J., Briggs, W. H., Glaubitz, J. C., Goodman, M. M., de Jesus Sanchez Gonzalez, J., & Ross-Ibarra, J. (2011). Genetic signals of origin, spread, and introgression in a large sample of maize landraces. *Proceedings of the National Academy of Sciences*, *108*(3), 1088–1092. https://doi.org/10.1073/pnas.1013011108

Vicentin, L., Canales, J., & Calderini, D. F. (2024). The trade-off between grain weight and grain number in wheat is explained by the overlapping of the key phases determining these major yield components. *Frontiers in Plant Science*, *15*. https://doi.org/10.3389/fpls.2024.1380429

Viola, I. L., Uberti Manassero, N. G., Ripoll, R., & Gonzalez, D. H. (2011). The Arabidopsis class I TCP transcription factor AtTCP11 is a developmental regulator with distinct DNA-binding properties due to the presence of a threonine residue at position 15 of the TCP domain. *Biochemical Journal*, *435*(1), 143–155. https://doi.org/10.1042/BJ20101019

Vogel, J. P., Garvin, D. F., Mockler, T. C., Schmutz, J., Rokhsar, D., Bevan, M. W., Barry, K., Lucas, S., Harmon-Smith, M., Lail, K., Tice, H., Schmutz (Leader), J., Grimwood, J., McKenzie, N., Bevan, M. W., Huo, N., Gu, Y. Q., Lazo, G. R., Anderson, O. D., … Manual annotation and gene family analysis. (2010). Genome sequencing and analysis of the model grass Brachypodium distachyon. *Nature*, *463*(7282), Article 7282. https://doi.org/10.1038/nature08747

WADDINGTON, S. R., CARTWRIGHT, P. M., & WALL, P. C. (1983). A Quantitative Scale of Spike Initial and Pistil Development in Barley and Wheat. *Annals of Botany*, *51*(1), 119–130. https://doi.org/10.1093/oxfordjournals.aob.a086434

Walla, A., Wilma van Esse, G., Kirschner, G. K., Guo, G., Brünje, A., Finkemeier, I., Simon, R., & von Korff, M. (2020). An Acyl-CoA N-Acyltransferase regulates meristem phase change and plant architecture in Barley. *Plant Physiology*, *183*(3), 1088–1109. https://doi.org/10.1104/pp.20.00087

Wang, B., Tseng, E., Regulski, M., Clark, T. A., Hon, T., Jiao, Y., Lu, Z., Olson, A., Stein, J. C., & Ware, D. (2016). Unveiling the complexity of the maize transcriptome by single-molecule long-read sequencing. *Nature Communications*, *7*(1), 11708. https://doi.org/10.1038/ncomms11708

Wang, C., Yang, X., & Li, G. (2021). Molecular Insights into Inflorescence Meristem Specification for Yield Potential in Cereal Crops. *International Journal of Molecular Sciences*, *22*(7), 3508. https://doi.org/10.3390/ijms22073508

Wang, H., Chen, W., Eggert, K., Charnikhova, T., Bouwmeester, H., Schweizer, P., Hajirezaei, M. R., Seiler, C., Sreenivasulu, N., von Wirén, N., & Kuhlmann, M. (2018). Abscisic acid influences tillering by modulation of strigolactones in barley. *Journal of Experimental Botany*, *69*(16), 3883–3898. https://doi.org/10.1093/jxb/ery200

Wang, H., Seiler, C., Sreenivasulu, N., Von Wirén, N., & Kuhlmann, M. (2022). INTERMEDIUM-C mediates the shade-induced bud growth arrest in barley. *Journal of Experimental Botany*, *73*(7), 1963–1977. https://doi.org/10.1093/jxb/erab542

Wang, M., Le Moigne, M.-A., Bertheloot, J., Crespel, L., Perez-Garcia, M.-D., Ogé, L., Demotes-Mainard, S., Hamama, L., Davière, J.-M., & Sakr, S. (2019). BRANCHED1: A Key Hub of Shoot Branching. *Frontiers in Plant Science*, *10*. https://www.frontiersin.org/articles/10.3389/fpls.2019.00076

Wang, P., Li, Y., Liu, Z., Li, X., Wang, Y., Liu, W., Li, X., Hu, J., Zhu, W., Wang, C., Li, S., Gu, T., Xu, D., Tang, C., Wang, Y., Li, C., Zhang, S., & Wu, J. (2023). Reciprocal regulation of flower induction by ELF3α and ELF3β generated via alternative promoter usage. *The Plant Cell*, *35*(6), 2095–2113. https://doi.org/10.1093/plcell/koad067

Wang, R.-L., Stec, A., Hey, J., Lukens, L., & Doebley, J. (1999). The limits of selection during maize domestication. *Nature*, *398*(6724), Article 6724. https://doi.org/10.1038/18435

Wang, Y., Liu, J., Huang, B., Xu, Y.-M., Li, J., Huang, L.-F., Lin, J., Zhang, J., Min, Q.-H., Yang, W.-M., & Wang, X.-Z. (2015). Mechanism of alternative splicing and its regulation (Review). *Biomedical Reports*, *3*(2), 152–158. https://doi.org/10.3892/br.2014.407

Watanabe, K., Breier, U., Hensel, G., Kumlehn, J., Schubert, I., & Reiss, B. (2016). Stable gene replacement in barley by targeted double-strand break induction. *Journal of Experimental Botany*, *67*(5), 1433–1445. https://doi.org/10.1093/jxb/erv537

Weber, E., Engler, C., Gruetzner, R., Werner, S., & Marillonnet, S. (2011). A Modular Cloning System for Standardized Assembly of Multigene Constructs. *PLOS ONE*, *6*(2), e16765. https://doi.org/10.1371/journal.pone.0016765

Wen, C., Zhao, W., Liu, W., Yang, L., Wang, Y., Liu, X., Xu, Y., Ren, H., Guo, Y., Li, C., Li, J., Weng, Y., & Zhang, X. (2019). CsTFL1 inhibits determinate growth and terminal flower formation through interaction with CsNOT2a in cucumber. *Development (Cambridge)*, *146*(14), dev180166. https://doi.org/10.1242/dev.180166

Whipple, C. J., Kebrom, T. H., Weber, A. L., Yang, F., Hall, D., Meeley, R., Schmidt, R., Doebley, J., Brutnell, T. P., & Jackson, D. P. (2011). Grassy tillers1 promotes apical dominance in maize and responds to Shade signals in the grasses. *Proceedings of the National Academy of Sciences of the United States of America*, *108*(33), E506–E512. https://doi.org/10.1073/pnas.1102819108

Winkelmolen, T., Colleoni, P., Moscou, M. J., Hoseinzadeh, P., Oldach, K., Schmidt, R. C., Immink, R. G. H., & van Esse, G. W. (2025). VULGARE ROW-TYPE SIX 5 binds to the promoter of tillering and floral homeotic genes to regulate their expression. *Plant Physiology*, kiaf309. https://doi.org/10.1093/plphys/kiaf309

Xie, Q., & Sparkes, D. L. (2021). Dissecting the trade-off of grain number and size in wheat. *Planta*, *254*(1), 3. https://doi.org/10.1007/s00425-021-03658-5

Yaffe, H., Buxdorf, K., Shapira, I., Ein-Gedi, S., Moyal-Ben Zvi, M., Fridman, E., Moshelion, M., & Levy, M. (2012). LogSpin: A simple, economical and fast method for RNA isolation from infected or healthy plants and other eukaryotic tissues. *BMC Research Notes*, *5*(1), 1–8. https://doi.org/10.1186/1756-0500-5-45/FIGURES/3

Ye, L., Wang, Y., Long, L., Luo, H., Shen, Q., Broughton, S., Wu, D., Shu, X., Dai, F., Li, C., & Zhang, G. (2019). A Trypsin Family Protein Gene Controls Tillering and Leaf Shape in Barley1. *Plant Physiology*, *181*(2), 701–713. https://doi.org/10.1104/pp.19.00717

Youssef, H. M., Eggert, K., Koppolu, R., Alqudah, A. M., Poursarebani, N., Fazeli, A., Sakuma, S., Tagiri, A., Rutten, T., Govind, G., Lundqvist, U., Graner, A., Komatsuda, T., Sreenivasulu, N., & Schnurbusch, T. (2017). VRS2 regulates hormone-mediated inflorescence patterning in barley. *Nature Genetics*, *49*(1), 157–161. https://doi.org/10.1038/ng.3717

Youssef, H. M., Mascher, M., Ayoub, M. A., Stein, N., Kilian, B., & Schnurbusch, T. (2017). Natural diversity of inflorescence architecture traces cryptic domestication genes in barley (Hordeum vulgare L.). *Genetic Resources and Crop Evolution*, *64*(5), 843–853. https://doi.org/10.1007/s10722-017-0504-6

Yuan, P., Usman, M., Liu, W., Adhikari, A., Zhang, C., Njiti, V., & Xia, Y. (2024). Advancements in Plant Gene Editing Technology: From Construct Design to Enhanced Transformation Efficiency. *Biotechnology Journal*, *19*(12), e202400457. https://doi.org/10.1002/biot.202400457

Yuan, Y., Ou, X., Yao, M., Wang, P., Li, C., Zhang, G., He, M., Li, H., Xu, X., Zhong, Z., Lu, Y., Lai, X., Zou, C., Shen, J., Zhang, T., Liu, D., Li, Y., Wang, H., Kong, D., & Liu, Q. (2025). GT1 and ZmHB13/VRL1 regulate flower sexual differentiation by modulating jasmonate biosynthesis and signaling in maize. *Plant Physiology*, *197*(3), kiaf075. https://doi.org/10.1093/plphys/kiaf075

Zažímalová, E., Murphy, A. S., Yang, H., Hoyerová, K., & Hošek, P. (2010). Auxin Transporters—Why So Many? *Cold Spring Harbor Perspectives in Biology*, *2*(3), a001552. https://doi.org/10.1101/cshperspect.a001552

Zhang, J., Mazur, E., Balla, J., Gallei, M., Kalousek, P., Medveďová, Z., Li, Y., Wang, Y., Prát, T., Vasileva, M., Reinöhl, V., Procházka, S., Halouzka, R., Tarkowski, P., Luschnig, C., Brewer, P. B., & Friml, J. (2020). Strigolactones inhibit auxin feedback on PIN-dependent auxin transport canalization. *Nature Communications*, *11*(1), 3508. https://doi.org/10.1038/s41467-020-17252-y

Zhang, R., Jia, G., & Diao, X. (2023). geneHapR: An R package for gene haplotypic statistics and visualization. *BMC Bioinformatics*, *24*(1), 199. https://doi.org/10.1186/s12859-023-05318-9

Zhang, S.-W., Li, C.-H., Cao, J., Zhang, Y.-C., Zhang, S.-Q., Xia, Y.-F., Sun, D.-Y., & Sun, Y. (2009). Altered Architecture and Enhanced Drought Tolerance in Rice via the Down-Regulation of Indole-3-Acetic Acid by TLD1/OsGH3.13 Activation. *Plant Physiology*, *151*(4), 1889–1901. https://doi.org/10.1104/pp.109.146803

Zhang, W., Li, H., Zhi, L., Su, Q., Liu, J., Ren, X., Meng, D., Zhang, N., Ji, J., Zhang, X., & Li, J. (2020). Functional markers developed from *TaGS3*, a negative regulator of grain weight and size, for marker-assisted selection in wheat. *The Crop Journal*, *8*(6), 943–952. https://doi.org/10.1016/j.cj.2020.03.003

Zhang, W., Tan, L., Sun, H., Zhao, X., Liu, F., Cai, H., Fu, Y., Sun, X., Gu, P., Zhu, Z., & Sun, C. (2019). Natural Variations at TIG1 Encoding a TCP Transcription Factor Contribute to Plant Architecture Domestication in Rice. *Molecular Plant*, *12*(8), 1075–1089. https://doi.org/10.1016/j.molp.2019.04.005

Zhang, Y., Li, Z., Zhang, Y., Lin, K., Peng, Y., Ye, L., Zhuang, Y., Wang, M., Xie, Y., Guo, J., Teng, W., Tong, Y., Zhang, W., Xue, Y., Lang, Z., & Zhang, Y. (2021). Evolutionary rewiring of the wheat transcriptional regulatory network by lineage-specific transposable elements. *Genome Research*, *31*(12), 2276–2289. https://doi.org/10.1101/gr.275658.121

Zhang, Y., Liu, T., Meyer, C. A., Eeckhoute, J., Johnson, D. S., Bernstein, B. E., Nussbaum, C., Myers, R. M., Brown, M., Li, W., & Shirley, X. S. (2008). Model-based analysis of ChIP-Seq (MACS). *Genome Biology*, *9*(9), 1–9. https://doi.org/10.1186/gb-2008-9-9-r137

Zhang, Y., Shen, C., Li, G., Shi, J., Yuan, Y., Ye, L., Song, Q., Shi, J., & Zhang, D. (2024). MADS1-regulated lemma and awn development benefits barley yield. *Nature Communications*, *15*(1), 301. https://doi.org/10.1038/s41467-023-44457-8

Zhang, Y., Shen, C., Shi, J., Shi, J., & Zhang, D. (2024). Boosting Triticeae crop grain yield by manipulating molecular modules to regulate inflorescence architecture: Insights and knowledge from other cereal crops. *Journal of Experimental Botany*, *75*(1), 17–35. https://doi.org/10.1093/jxb/erad386

Zhang, Y., Xu, Y., Nie, J., Chen, H., Qin, G., Wang, B., & Su, X.-D. (2023). DNA–TCP complex structures reveal a unique recognition mechanism for TCP transcription factor families. *Nucleic Acids Research*, *51*(1), 434–448. https://doi.org/10.1093/nar/gkac1171

Zhang, Z., Zhao, P., Wang, X., Wang, H., Zhai, Z., Zhao, X., Xing, L., Qi, Z., & Shang, Y. (2024). Identification and map-based cloning of long glume mutant gene lgm1 in barley. *Molecular Breeding*, *44*(1), 3. https://doi.org/10.1007/s11032-024-01448-x

Zhao, L., Tan, L., Zhu, Z., Xiao, L., Xie, D., & Sun, C. (2015). PAY1 improves plant architecture and enhances grain yield in rice. *The Plant Journal*, *83*(3), 528–536. https://doi.org/10.1111/tpj.12905

Zhong, J., van Esse, G. W., Bi, X., Lan, T., Walla, A., Sang, Q., Franzen, R., & von Korff, M. (2021). INTERMEDIUM-M encodes an HvAP2L-H5 ortholog and is required for inflorescence indeterminacy and spikelet determinacy in barley. *Proceedings of the National Academy of Sciences of the United States of America*, *118*(8). https://doi.org/10.1073/pnas.2011779118

Zhou, W., Shi, H., Wang, Z., Huang, Y., Ni, L., Chen, X., Liu, Y., Li, H., Li, C., & Liu, Y. (2024). Identification of highly repetitive barley enhancers with long-range regulation potential via STARR-seq. *Genomics, Proteomics & Bioinformatics*, qzae012. https://doi.org/10.1093/gpbjnl/qzae012

Zwirek, M., Waugh, R., & McKim, S. M. (2019). Interaction between row-type genes in barley controls meristem determinacy and reveals novel routes to improved grain. *New Phytologist*, *221*(4), 1950–1965. https://doi.org/10.1111/nph.15548



Appendices

A

Summary
Nederlandse samenvatting
Acknowledgements
Education statement
About the author

Summary

Plant architecture is a highly dynamic trait that can be influenced by many factors. Because of this, evolutionary adaptation created an immense variation in plant architecture across the plant kingdom. Also during domestication, several plant architectural traits were targeted to improve human usability of crops. Several important traits are tangled on a molecular level, meaning that changing one trait, often changes other traits as well. This is also the case in barley, where the transcription factor VRS5, regulates both tiller development and lateral spikelet development. Both of these processes are important yield related traits in barley, and their genetic connection makes it difficult to manipulate these traits independently. The main objective in this thesis was to provide molecular insights that can help untangle these traits, with the focus on VRS5.

As a transcription factor, VRS5 can directly bind to DNA and regulate the expression of downstream targets. Understanding what these targets are, can help to better understand how VRS5 exactly functions and regulates these different processes. In **Chapter 2**, we identified these direct targets in barley by combining two techniques. Using DNA-affinity purification followed by sequencing (DAP-seq), we identified the genome-wide binding sites of VRS5. Next to that, we compared gene expression in *vrs5* mutants to wild-type at four developmental stages using RNA sequencing. By combining the genes that are differentially expressed in *vrs5* and the loci where VRS5 binds, we obtained a set of direct VRS5 targets that are thus bound by and regulated by VRS5. We investigated four different developmental stages and therefore we could identify which of these targets mostly play a role early in development, and presumably in tillering, while others mostly play a role later in development, when the inflorescence is developing.

Next, we looked in more detail at VRS5 as a protein in **Chapter 3**. We found that in barley two different protein isoforms of VRS5 are formed; VRS5α and VRS5β. We wanted to know if these isoforms function differently, and by CRISPR mutagenesis we made mutations causing only one of the protein isoforms to be formed. After investigating these lines, we found that it is possible to uncouple the tillering from the row-type function. While complete knock-out lines of *vrs5* have both an increased number of tillers and six-rowed to intermediate spike phenotype, the *vrs5α* mutants only show increased tillering, but a two-rowed spike. We showed that these phenotypical differences are likely caused by differences in DNA binding of the isoforms in complex with another transcription factor, TB2.

One of the direct targets of VRS5 identified in **Chapter 2,** *VRS1* was already known as thus far the most downstream regulator of lateral spikelet development. Despite this role in such an agronomically important trait, little is known of the molecular function of VRS1. In **Chapter 4**, we identified the consensus DNA binding motif of VRS1, using DAP-seq. In combination with an already available RNA-seq dataset of a *VRS1* allele, we also identified some potential direct downstream targets of VRS1. One of these targets was *SOC1-like*, of which we made CRISPR mutants. These mutants showed significantly smaller lateral spikelets compared to WT. Analysis of natural variation in *SOC1-like* revealed that there has been a strong selection for a frameshift mutation of *SOC1-like* in six-rowed barleys.

Many of the experiments performed in this thesis would be impossible without having an efficient CRISPR based mutagenesis protocol. In **Chapter 5**, we showed how we greatly improved the editing efficiency of Cas9 in barley by using several methods shown to improve editing efficiency. With this improved system we were able to generate multiple knock-out lines and even double knock-outs in primary transformants already.

Finally, in **Chapter 6** I combined the obtained results and place them in a broader scientific perspective. I highlight the conserved function of VRS5 in regulating tillering, while some interesting VRS5 targets that might regulate lateral spikelet development are discussed. In conclusion, with the molecular insights provided in this thesis, I showed several potential ways to help untangle yield-related traits in barley, specifically via VRS5.

Nederlandse Samenvatting

Hoe een plant eruit ziet, oftewel plantenarchitectuur, kan heel erg veranderen en wordt beïnvloed door meerdere factoren en kan belangrijk zijn om te overleven in diens omgeving. Zo is er niet alleen verschil tussen soorten maar ook binnen dezelfde soort kan er veel verschil zitten. Tijdens evolutie is er zo een grote variatie aan verschillende planten en hoe ze eruit zien ontstaan. Toen mensen bepaalde plantensoorten gingen telen, werd er geselecteerd voor bepaalde eigenschappen in plantenarchitectuur om het gebruik voor de mens te verbeteren. Sommige van deze belangrijke eigenschappen zijn op een moleculair niveau aan elkaar gekoppeld. Dat betekent dat wanneer je de ene eigenschap wil sturen, je vaak ook andere eigenschappen mee verandert. Bij gerst is dit ook het geval, waarbij het aantal zijscheuten en rij-type, het aantal graankorrels per aar, door dezelfde transcriptiefactor gereguleerd wordt, namelijk VULGARE ROW-TYPE SIX 5 (VRS5). Beide eigenschappen zijn belangrijk voor de uiteindelijke opbrengst, en door deze genetische koppeling is het moeilijk om deze eigenschappen onafhankelijk van elkaar te sturen. Het overkoepelende doel in dit proefschrift is om op moleculair niveau beter te begrijpen hoe deze eigenschappen aan elkaar gekoppeld zijn, met de focus op VRS5.

VRS5 is een transcriptiefactor, dat betekent dat het de expressie van onderliggende genen kan reguleren door direct aan DNA te binden. Door te onderzoeken welke genen dit precies zijn, kunnen we beter begrijpen hoe VRS5 precies werkt en hoe het verschillende eigenschappen kan beïnvloeden. In **Hoofdstuk 2**, hebben we deze onderliggende genen geïdentificeerd door twee technieken te combineren. Door gebruik te maken van DNA-affinity purification gevolgd door sequencing (DAP-seq), hebben we over het hele gerstgenoom de locaties gevonden waar VRS5 bindt. Daarnaast hebben we de genexpressie vergeleken van wild-type planten en planten die een mutatie hebben in *VRS5*, oftewel *vrs5* mutanten, in vier verschillende ontwikkelingsstadia met RNA-sequencing. Door de verschillend gereguleerde genen in *vrs5* planten te combineren met de locaties in het genoom waar VRS5 bindt, hebben we een lijst met genen die zowel gebonden als gereguleerd worden door VRS5. Door dit in vier verschillende ontwikkelingsstadia te doen, konden we zien welke van deze onderliggende genen vooral vroeg in de ontwikkeling, en waarschijnlijk dus bij het maken van zijscheuten belangrijk zijn, terwijl andere, die vooral later in de ontwikkeling, en dus pas bij de ontwikkeling van de aar, belangrijk zijn.

Vervolgens hebben we in meer detail gekeken naar VRS5 als eiwit in **Hoofdstuk 3**. We hebben gevonden dat er twee verschillende VRS5 eiwitten gevormd kunnen worden; VRS5α en VRS5β. We wilden onderzoeken of deze verschillende

isoformen ook een anders functioneren. Door gebruik te maken van CRISPR mutagenese, hebben we een mutatie gemaakt waardoor er maar een van deze isoformen gevormd kan worden. We zagen dat in deze planten de koppeling tussen het vormen van zijscheuten en het rij-type verdwenen is. *vrs5* mutanten, waarbij geen enkel VRS5 eiwit gevormd kan worden, hebben zowel meer zijscheuten, als een aar met zes rijen graankorrels. *vrs5α* mutanten, waarbij alleen VRS5β gevormd kan worden, hebben meer zijscheuten, maar een aar met twee rijen graankorrels. We laten verder zien dat deze verschillen waarschijnlijk veroorzaakt worden door verschillen in de DNA-binding van de verschillende isoformen als ze een complex vormen met een andere transcriptiefactor, TB2.

Een van de direct onderliggende genen van VRS5 die we in **Hoofdstuk 2** geïdentificeerd hebben, VRS1, was in gerst al bekend als een gen dat rij-type reguleert. Hoewel rij-type een erg belangrijke agronomische eigenschap is voor gerst, is er moleculair erg weinig bekend over hoe VRS1 functioneert. In **Hoofdstuk 4**, hebben we aangetoond aan welke DNA-sequentie VRS1 kan binden als transcriptiefactor, door gebruik te maken van DAP-seq. In combinatie met bestaande genexpressiedata van een *VRS1* allel, hebben we ook mogelijke direct onderliggende genen van VRS1 geïdentificeerd. Een van deze genen is *SOC1-like*, waar we met CRISPR ook mutanten van hebben gemaakt. Deze mutanten hebben net als wild-type een twee-rijige aar, maar de laterale graankorrels in *soc1-like* mutanten zijn significant kleiner vergeleken met die van wild-type. Door natuurlijke variatie in de DNA-sequentie van *SOC1-like* te analyseren, zagen we dat er een sterke selectie is geweest voor een bepaalde mutatie in *SOC1-like* in zes-rijige gerst.

Veel van de experimenten die in dit proefschrift gedaan zijn, zouden onmogelijk zijn zonder een efficiënt CRISPR mutagenese protocol. In **Hoofdstuk 5** hebben we laten zien hoe we de efficiëntie van Cas9 in gerst hebben verbeterd door verschillende methodes te combineren. Met dit verbeterde systeem hebben we veel planten ontwikkeld met knock-out mutaties en zelfs knock-out mutaties van twee genen tegelijk, al in de primaire transformanten.

Uiteindelijk combineer ik in **Hoofdstuk 6** de behaalde resultaten en plaats ze samen in een breder wetenschappelijk perspectief. Ik benoem specifiek de geconserveerde functie van VRS5 in het reguleren van het maken van zijscheuten, terwijl ik sommige interessante direct onderliggende genen van VRS5 benoem die mogelijk de ontwikkeling van laterale graankorrels reguleren. Met de moleculaire inzichten uit dit proefschrift laat ik meerdere opties zien die helpen bij het ontkoppelen van verschillende opbrengsteigenschappen in gerst, specifiek via VRS5.

Acknowledgements

During the last few years I have got the help and guidance of some people and got the opportunity meet many new faces. My PhD journey would not be same without your help, guidance, or simply presence in the last couple of years.

First of all Wilma, thank you for being a great supervisor. I got to know you during my BSc Thesis. This was my first experience with doing science and working with barley, and it was amazing. At that time, I had never considered doing a PhD, but you planted the seed by saying: “But you are going to do a PhD, right?” A few years later, I saw the application for a position in your group and immediately applied, eventually resulting in this PhD Thesis. Your office door is always open and being able to just walk in for questions or ad hoc experiment planning was really nice. Not rarely one of these “quick questions” eventually resulted in hourlong brainstorm sessions.

Richard, you were very much involved in the start-up phase of my project and later you provided many useful view points and considerations that eventually led to this end result. I really appreciate our shared enthusiasm resulting in engaging discussions about the project or science in general. From you and Wilma, I learned a lot the past years, especially on how to present my work, both in writing, figures and speaking, which I am very grateful of.

Being part of the VIDI team was a great opportunity and provided close colleagues. The first year with Iris, and later with Pierangela. It was really nice that we were so closely involved in each others projects. Pierangela, you are an amazing colleague, scientist, cook, and friend. I liked our discussions and sharing the nice and less nice opportunities of working with barley. Marijke, the great amount of barley CRISPR mutants in this thesis is mainly because of you, which I am very grateful for. You took care of the transformations and tissue culture and eventually taught me how to do it. You taught me the tips, tricks and pitfalls of barley transformations. Next to that, I want to thank the scientists at the companies that are part of the VIDI team: Ralf-Christian, Parastoo, Klaus, and Monika. It was always encouraging to present my work for you. Your appreciation, questions, and suggestions, led to great discussions, insights and new experiments.

The flowering time group: Richard, Marian, Suze, Isabella, Qiqi, Hazel, Pierangela, Martijn, Marco, and Froukje. Even though I joined the flowering time group meetings only later in my project, these meetings were always my favorite. I really appreciated the informal and interactive nature of the meetings to discuss our projects, results, and plans.

My time in the office was always fun thanks to my amazing office mates: Peter, Joyce, Eline, Pierangela, Harald, Michiel, and Zifan. Our discussions about science, sports, existentialism, and dark humor as well as the “fifth screen” were always a nice distraction. It was an honor to be your mascot.

Next to that, I always liked working at the lab of Molecular Biology and that is thanks to all the colleagues that are or have been part of the lab. Thanks for your help, insights, conversations, and jokes.

During my PhD, I had to opportunity to supervise students during their BSc or MSc Theses. Nupur, Denis, Idil, Sjuul, Simon, and Uros, it was great to teach and supervise you. Your experiments and hard work provided great insights that helped shape this thesis.

Naast mijn werkomgeving zijn er ook heel veel personen daarbuiten die een grote rol hebben gespeeld in plezier, vertier en het ontwikkelen van mijn andere ambities. Juist dankzij jullie had ik een stok achter de deur om wel hard, maar niet te veel te werken.

Daan, je bent een dierbare vriend. We hebben heel wat samen gesport, sport gekeken, gegeten, muziek geluisterd en gelachen en ik hoop dat we dat ook nog jaren blijven doen. Bedankt dat je mijn verhalen over gerst, meristemen en DAP-seq aangehoord hebt.

Op maandag, dinsdag, en donderdag ga ik na het werk met heel veel plezier naar de atletiekbaan. Met een moe hoofd en een energiek lichaam, kon ik er op de training voor zorgen dat dit werd omgedraaid en de volgende dag weer met een frisse blik aanvangen. Daarom wil ik al mijn trainingsmaatjes bedanken met wie ik samen heb afgezien, maar vooral ook veel plezier heb gehad. In het bijzonder, Stijn, we kunnen uren kletsen en doordat we samen onze schema’s lopen, kan ik net dat tandje extra geven.

Anteun, door ons gedeeld optimisme ben ik altijd vrolijk als ik met jou gesproken heb. Ik vond onze lunchwandelingen verfrissend en het was heel fijn om met jou de leuke, bijzondere, en vervelende kanten van het doen van een PhD of de wetenschap in het algemeen te spreken. Het was een eer om jouw paranimf te zijn en ik ben heel blij dat je voor mij deze wederdienst wil bewijzen.

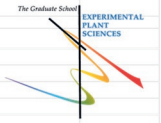
Mijn vrienden uit/van Limburg, Roy, Fleur, Tom, Bram, Elke, Marco, Job, Dion, Olaf, Ties en Joëlle: Het is altijd als vanouds met jullie, en ik zou jullie veel vaker willen zien.

Pap en mam, bedankt dat jullie mij altijd aangespoord hebben om te doen wat ik leuk vind en daar dan ook hard voor te werken. Jullie vertrouwen en steun heeft me altijd geholpen dit waar te maken.

Ilze, ondanks dat je mijn zusje bent, lijken onze persoonlijkheden misschien niet zoveel op elkaar. Toch hebben we onze eigen vorm van humor en gedeelde interesses. Met wat omwegen ben je ook nog net als ik in het lab beland. Je hebt een onwijs moeilijke en vervelende periode gehad, en wij daarom ook, maar ondanks dat bleef je positief en vol humor. Dat was en is nog steeds echt inspirerend.

Education statement

Education Statement of the Graduate School
Experimental Plant Sciences



Issued to: Ton Winkelmolen
Date: 12 June 2026
Group: Laboratory of Molecular Biology
University: Wageningen University & Research

1) Start-Up Phase	date	credits
► **First presentation of your project**		
Proposal Presentation	11 Feb 2022	1.5
► **Writing or rewriting a project proposal**		
Unbinding the DNA: The effect of changes in the binding sites of TCP transcription factors on barley shoot architecture and flowering time	Sep-Nov 2021	3.0
► **MSc courses**		
Subtotal Start-Up Phase		4.5

2) Scientific Exposure	date	credits
► **EPS PhD days**		
EPS PhD days 'Get2Gether', Soest (NL)	3 & 4 May 2022	0.6
EPS PhD days 'Get2Gether', Soest (NL)	1 & 2 May 2023	0.6
► **EPS theme symposia**		
EPS theme 1 symposium 'Developmental Biology of Plants', Wageningen (NL)	14 Jun 2022	0.3
EPS theme 4 symposium 'Genome Biology and Gene Regulation', Amsterdam (NL)	6 Dec 2022	0.3
EPS theme 4 symposium 'Genome Biology and Gene Regulation', Amsterdam (NL)	9 Oct 2024	0.3
► **National platform meetings**		
Annual Meeting 'Experimental Plant Sciences', Lunteren (NL)	11 & 12 Apr 2022	0.6
Annual Meeting 'Experimental Plant Sciences', Lunteren (NL)	17 & 18 Apr 2023	0.6
Annual Meeting 'Experimental Plant Sciences', Egmond aan Zee (NL)	8 & 9 Apr 2024	0.6
Annual Meeting 'Experimental Plant Sciences', Egmond aan Zee (NL)	14 & 15 Apr 2025	0.6
Dutch Chromatin Meeting, Amsterdam (NL)	3 Nov 2023	0.3
► **Seminars (series), workshops and symposia**		
EMBL-EBI Training Webinar: Methods for rare-variant association analysis	4 Jun 2022	0.1
EPSO Plant Science Seminar 25 - Epigenetics	21 Sep 2023	0.1
Plant Biotechnology For Agriculture of the XXI Century: "Gene regulatory networks at the shoot meristem that control floral transition in response to environmental cues"	23 Feb 2023	0.1
Plant Biotechnology For Agriculture of the XXI Century: "What is common in the control of meristem activity in land plants"	23 Feb 2023	0.1
Plant Biotechnology For Agriculture of the XXI Century: "Phenotypic plasticity in plants: adjusting flowering time when water is not enough"	24 Feb 2023	0.1
International Barley Hub seminar: "Recombining genomes and alleles of the wild for better adapted barley"	24 Feb 2022	0.1
International Barley Hub seminar: "GrainGenes Morex v3 and EoRNA"	17 Nov 2022	0.1
International Barley Hub seminar: "Barley inflorescence development under high temperatures and beyond"	23 Feb 2023	0.1
International Barley Hub seminar: International Barley Hub seminar: "Application of Genetic & Genomic Research in Cereals Breeding"	27 Mar 2023	0.1
International Barley Hub seminar: "Barley chromatin and regulation of gene expression"	8 Jun 2023	0.1
Internation Barley Hub seminar: International Barley Hub seminar: "Expanding the barley genome editing toolbox"	14 Sep 2023	0.1
Seminar: Francesca Turck "Polycomb-recruiting motifs in plants – a hard code for soft genetics?"	12 Apr 2024	0.1
Internation Barley Hub seminar: "PanBarlex – A Comprehensive Resource of Gene Annotations and Orthogroups of the Barley Pan-	30 May 2024	0.1
Seminar: Jocelyn Vreede "Modeling protein-DNA interactions: implications for gene regulation"	2 Oct 2024	0.1
Internation Barley Hub seminar: "Genetic basis of the awn development in barley"	3 Oct 2024	0.1
Seminar: Tobias Jores "Learning the grammar of plant regulatory DNA"	10 Oct 2024	0.1
Seminar: Olga Agata Oxholm "Smart crops: Improved Plants for Food Security and Pathogen Resistance"	25 Aug 2025	0.1
► **Seminar plus**		
► **International symposia and congresses**		
Workshop on Molecular Mechanisms Controlling Flowering, Palermo (IT)	16-20 Jun 2024	0.9
Barley Genome Net, Dundee (UK)	4 & 5 Feb 2025	0.6
Barley Away Days, Dunkeld (UK)	6 & 7 Feb 2025	0.6
► **Presentations**		
VIDI consortium first presentation	10 Mar 2022	1.0
Poster: "How do CYC/TB1 transcription factors in barley (Hordeum vulgare) regulate shoot architecture and in that way control yield?", Wageningen (NL)	13-15 Dec 2021	1.0
Poster: "VRS5 (HvTB1) binds to the promoter of tillering and row type genes in vitro to regulate their expression", Egmond aan zee (NL)	8 & 9 Apr 2024	1.0
Presentation: "The molecular regulation of inflorescence architecture and tillering in barley via VRS5 (HvTB1)", Egmond aan zee (NL)	9 Apr 2024	1.0
Presentation: "The molecular regulation of inflorescence architecture and tillering in barley via VRS5 (HvTB1)", Palermo (IT)	17 Jun 2024	1.0
Presentation: "The molecular regulation of inflorescence architecture and tillering in barley via VRS5 (HvTB1)", Dundee (UK)	4 Feb 2025	1.0
VIDI consortium final presentation	12 Feb 2025	1.0
► **Interviews**		
3rd year PhD interview with an EPS research theme coordinator	2 Jul 2024	0.7
► **Excursions**		
Subtotal Scientific Exposure		16.3

3) In-Depth Studies		date	credits
►	**Advanced scientific courses & workshops**		
	EPS course "Transcription Factors and Transcriptional Regulation"	13-15 Dec 2021	1.0
	EPS workshop "CRISPR/Cas"	13 & 14 Sep 2021	0.6
	EPS course "PLAZA - Functional Plant Bioinformatics"	25 & 26 Oct 2021	0.6
►	**Journal club**		
	Plant Developmental Biology (PDB) Journal club	2021-2025	3.0
►	**Individual research training**		
	Subtotal In-Depth Studies		5.2

4) Personal Development		date	credits
►	**General skill training courses**		
	EPS Introduction Course	1 Nov 2021	0.3
	WGS workshop "Start to supervise BSc & MSc thesis students"	3 Jun 2022	0.1
	Mindlab theatre performance on Social Safety	30 Nov 2022	0.2
	WGS course "Research Data Management Part 1-3"	14-28 Sep 2023	0.5
	WGS course "Scientific Writing"	2 Oct - 20 Nov 2023	2.0
	WGS course "Quarto"	1 & 8 Nov 2023	0.6
►	**Organisation of scientific meetings, PhD courses or outreach activities**		
►	**Membership of EPS PhD Council**		
	Subtotal Personal Development		3.7

5) Teaching & Supervision Duties		date	credits
►	**Courses**		
	Practical Biological Chemistry (BIC-10306)	2022	3.0
	Practical Biological Chemistry (BIC-10306)	2023	0.0
►	**Supervision of BSc/MSc projects**		
	Msc Thesis: "Understanding the genetic relationship of spike row gene VRS4 (HvRA2), and TCP transcription factor HvTB2 (COM1) and HvTB1-like in spike architecture/inflorescence architecture and determinacy in Barley"	2022	3.0
	Msc Thesis: "VRS5 downstream targets and conserved regions within its 10kb promoter"	2022	0.0
	Msc Thesis: "Exploring the molecular aspects of VRS1 transcriptional regulation"	2023	0.0
	Bsc Thesis: "Unveiling the molecular mechanism of VRS5 in spike development"	2024	0.0
	Msc Thesis: "VRS5 and the molecular basis for its role in row phenotype and tillering"	2024	0.0
	Msc Research Practice: "Determining downstream targets of the VRS1 gene in Hordeum vulgare"	2025	0.0
	Subtotal Teaching & Supervision Duties		6.0

TOTAL NUMBER OF CREDIT POINTS*		**35.7**

Herewith the Graduate School declares that the PhD candidate has complied with the educational requirements set by the Educational Committee of EPS with a minimum total of 30 ECTS credits.

** A credit represents a normative study load of 28 hours of study.*

About the author

Ton Winkelmolen was born on 1 September 1997 in the Netherlands. He grew up on the dairy farm of his parents in Limburg, which sparked his curiosity about biology, nature, and science in general at a young age. He went to Sint Ursula in Horn to get his Gymnasium diploma. Because of his broad interest in Biology, Chemistry, and Physics, he chose to go to Wageningen University for the BSc Molecular Life Sciences. After choosing the Minor Plant Biotechnology, he knew that he wanted to continue studying plants and stayed in Wageningen to do the MSc Plant Biotechnology. At the same time he started a summer/weekend job at the plant breeding company Nunhems, where he continued to work until finishing is MSc Plant Biotechnology. While doing both his BSc and MSc Thesis, he knew that doing research is something he loves and gets excited from. When he was notified that his former BSc Thesis supervisor had a PhD position, he didn't hesitate at all before applying. The result of that is presented in this Thesis.

Starting from October 2025, Ton went to the chair group of Plant Physiology in Wageningen as a postdoctoral researcher studying the molecular interaction between shading and salinity responses in rice.



Besides study and later working hours, Ton spends a lot of hours on the athletics track to train. Starting from a young age, he got to do all the athletics disciplines. At the age of 15 he started to focus mainly on hurdles and sprinting. Despite this focus, he cannot let go of the love for all the other disciplines, and does a decathlon once in a while.

You can contact Ton via:
ton.winkelmolen@wur.nl or
t.winkelmolen@gmail.com

The research described in this thesis was financially supported by Nederlandse organisatie voor Wetenschappelijk Onderzoek (NWO) VIDI grant “flowering time genes branching out” (project number 18366)

Financial support from Wageningen University for printing this thesis is gratefully acknowledged.

Cover design by: Ilze Winkelmolen
Printed by: proefschriftMaken

